



Wills, Lauren (2017) *SUMOylation of the B2AR influences receptor internalisation, desensitisation and downstream signalling*. PhD thesis.

<https://theses.gla.ac.uk/8564/>

Copyright and moral rights for this work are retained by the author

A copy can be downloaded for personal non-commercial research or study, without prior permission or charge

This work cannot be reproduced or quoted extensively from without first obtaining permission in writing from the author

The content must not be changed in any way or sold commercially in any format or medium without the formal permission of the author

When referring to this work, full bibliographic details including the author, title, awarding institution and date of the thesis must be given

Enlighten: Theses

<https://theses.gla.ac.uk/>
research-enlighten@glasgow.ac.uk

SUMOylation of the β_2 AR Influences Receptor Internalisation, Desensitisation and Downstream Signalling

Lauren Wills, MRes

This thesis is being submitted for the degree of
Doctor of Philosophy (Ph.D.)
in the Faculty of Medicine, University of Glasgow,
September 2017

BHF Cardiovascular Research Centre
Institute of Cardiovascular and Medical Sciences
College of Medical, Veterinary, and Life Sciences
University of Glasgow

© L. Wills

Author's Declaration

I declare this thesis has been written by myself and is a record of research performed by myself, with the exception of FRET assays which were performed by Bracy Fertig (PhD Student) at the University of Glasgow, Baillie laboratory group. Any contribution from others has been clearly referenced and reproduced with permission. This work has not been submitted previously for a higher degree and was supervised by Professor George S. Baillie and Dr Delyth Graham.

Acknowledgment

Firstly, I would like to thank my supervisors Professor George Baillie and Dr Delyth Graham for the support you have given me over the past three years. The opportunities you have given me are second to none and I will be eternally grateful. You have made my PhD an enjoyable experience which, in a way, I am sad to leave behind.

Thank you to Professor John Colyer and Dr Iain Manfield at Badrilla® for assisting me in the design and purification of the SUMO specific antibodies.

A very special thanks to the team of Professor Roger Hajjar at Mount Sinai for allowing me access to pig cardiac tissue, and the kindness you extended to me when I broke my wrist. Although unexpected for a laboratory placement, I did still enjoy the experience!

Many thanks to the various lab groups within Glasgow that have welcomed me to their team. To Aileen and Mike, thank you for providing me with cardiomyocytes and assisting me with virus transductions. To Professor Stuart Nicklin and team, thank you for assisting me with viral preparations. To Professor Graeme Milligan, Dr Brian Hudson and Laura Jenkins, the findings within this thesis would not have been possible without the support of you all, a massive thank you.

Thank you to the guys at the BHF office. You supported me through the writing of this thesis. As I paced the floor cursing the β_2 AR you always told me to keep going. Thank you for your encouragement. To the team at the Baillie office - including the Freeman group and Jane - thank you for making my PhD such a fun experience. Ella, you provided a different form of support, but possibly the most important of all. If you ever decide to break a bone, you know where I am!

Finally, I would like to thank my parents and David. To David, sadly now the unlimited holiday allowance may end (thanks George!) but I am looking forward to taking the next steps wherever they may be together. To my parents, not a day has passed over the past three years without encouragement from you both. It means everything.

Table of Contents

Author's Declaration	2
Acknowledgment	3
List of Figures	8
List of Tables.....	10
List of Abbreviations, Acronyms & Symbols	11
Oral presentations, publications and awards.....	17
Summary	18
Chapter 1 Introduction	20
1.1 The Cardiovascular System.....	21
1.1.1 Pulmonary and Systemic Circulation.....	21
1.1.2 The Anatomy of the Heart	21
1.1.3 Cardiac Cycle.....	22
1.1.4 Cardiac Conduction System	22
1.1.5 Excitation Contraction (EC) Coupling.....	22
1.2 Heart Failure (HF)	25
1.2.1 Definition of HF	25
1.2.2 Diagnosis and Classification of HF.....	25
1.2.3 The Cause of HF	26
1.2.4 Prevalence and Prognosis of HF	28
1.2.5 Management of HF.....	28
1.2.6 The Importance of Novel Cardiovascular Research to HF.....	32
1.3 The β_2 Adrenergic Receptor (β_2 AR)	35
1.3.1 Adrenergic Receptors	35
1.3.2 Crystal Structure of the β_2 AR	35
1.3.3 G Protein-Coupled Receptor (GPCR) Signal Transduction	41
1.3.4 β_2 AR Signalling	44
1.3.5 β_2 AR Signalling Regulation	47
1.3.6 β_2 AR Dimerisation	59
1.3.7 β_2 AR Gene Polymorphisms.....	60
1.3.8 Post-Translational Modifications (PTMs) of the β_2 AR.....	60
1.4 SUMOylation.....	62
1.4.1 The SUMO Paralogues	62
1.4.2 The SUMOylation Cascade	63
1.4.3 The SUMO Consensus Motif	68
1.4.4 Variation in the SUMO System	70
1.4.5 The Role of SUMOylation	70

1.4.6	SUMOylation of GPCRs	71
1.5	SUMOylation of SR Ca ²⁺ ATPase 2a (SERCA2a)	72
1.5.1	SERCA2a.....	72
1.5.2	SERCA2a Regulation	74
1.5.3	SERCA2a in HF.....	74
1.5.4	SERCA2a SUMOylation.....	75
1.5.5	Other SUMO-Susceptible Cardiac Signalling Proteins in HF.....	76
1.5.6	Inducing Protein SUMOylation	80
1.6	Aims and Hypothesis	81
1.6.1	Hypothesis	81
1.6.2	Aims	81
Chapter 2	General Materials and Methods.....	82
2.1	General Laboratory Practise	83
2.2	Cell Culture.....	84
2.2.1	HEK293 Cells	84
2.2.2	HEKB ₂ Cells	85
2.2.3	Cell Sub Culture.....	85
2.2.4	Cell Counting.....	86
2.2.5	Cryopreservation	86
2.3	Isolation of Plasmid DNA and Transient Transfection	87
2.3.1	Isolation of Plasmid DNA From E. coli	87
2.3.2	Transient Transfection of Plasmid DNA	89
2.4	Preparation of Cell Lysate.....	89
2.5	Protein Quantification by the Bradford Assay	90
2.6	Immunoblotting.....	90
2.6.1	Sample Preparation	91
2.6.2	SDS-PAGE (sodium dodecyl sulfate polyacrylamide gel electrophoresis)	91
2.6.3	Transfer	92
2.6.4	Detection	92
2.7	Peptide Array	94
2.7.1	Solid Phase Peptide Synthesis (SPPS)	94
2.7.2	Peptide Array - Overlay.....	97
2.7.3	Peptide Array - SUMOylation Assay	98
2.8	UniProt Sequence Analysis of β_2 AR.....	98
2.9	Immunoprecipitation (IP).....	98
2.10	ArrayScan High Content Analysis of Internalisation	99
2.11	Bioluminescence Resonance Energy Transfer (BRET)	100

2.12	Fluorescence Resonance Energy Transfer (FRET)	103
2.13	Radioligand Binding Studies	106
2.13.1	Cell Membrane Preparations	106
2.13.2	Saturation Ligand Binding.....	107
2.13.3	Competition Ligand Binding	109
2.14	Systemic Protein Affinity Strength Modulation (SPASM) Sensor	111
2.14.1	SPASM Sensor Protein Expression and Cell Preparation	113
2.15	Minimally Invasive TAC Pressure Overload Model in Mice	113
2.15.1	Ethical Approval.....	113
2.15.2	C57BL/6J Mice.....	114
2.15.3	Surgical Procedure	114
2.15.4	Transthoracic Echocardiography.....	117
2.15.5	Organ Harvesting	119
2.16	Histology.....	119
2.16.1	Picrosirius Red	120
2.16.2	Wheat Germ Agglutinin (WGA)	121
2.17	Tissue Homogenisation	121
2.18	Statistical Analysis	122
Chapter 3	Production of a SUMO- β_2 AR Specific Polyclonal Antibody	123
3.1	Introduction	124
3.1.1	Post-Translational Modification (PTM) Antibodies	124
3.2	Aims	126
3.3	Methods	127
3.3.1	Polyclonal Antibody Purification Overview	127
3.3.2	Epitope Design	127
3.3.3	Rabbit Immunisation Protocol	131
3.3.4	Immunoglobulin G (IgG) Isolation	133
3.3.5	Specific SUMO- β_2 AR IgG Isolation.....	135
3.3.6	Antibody Testing.....	139
3.4	Results	140
3.4.1	Identification of Key Amino Acid Residues Required for β_2 AR SUMOylation	140
3.4.2	Conservation of β_2 AR SUMOylation Lysines 232 and 235	143
3.4.3	Epitope Recognition Testing - Peptide Array	145
3.4.4	SUMO- β_2 AR Recognition in Cells	151
3.5	Discussion	154
Chapter 4	In Vitro SUMOylation of the β_2 AR.....	159

4.1	Introduction	160
4.1.1	Post-Translational Modifications (PTMs) of the β_2 AR	160
4.1.2	SUMOylation of the β_2 AR	160
4.2	Aims	162
4.2.1	HEKB β_2 Cell Line	163
4.2.2	SUMOylation of the β_2 AR In Vitro	167
4.2.3	Interaction between β_2 AR and SUMOylation Enzymes PIAS γ /UBC9	170
4.2.4	Influence of β_2 AR SUMOylation on Receptor Function.	175
4.3	Discussion	203
Chapter 5 Analysis of β_2 AR SUMOylation in Animal Models of Heart Failure (HF)		
	210	
5.1	Introduction	211
5.1.1	The Need for Animal Models of HF	211
5.1.2	Minimally Invasive TAC Pressure Overload HF Model in Mice.....	211
5.1.3	LAD Artery Balloon Occlusion Ischemic HF Model in Pigs	214
5.2	Aims	218
5.3	Results	219
5.3.1	Minimally Invasive TAC Pressure Overload Model in Mice.....	219
5.3.2	LAD Artery Balloon Occlusion Ischemic HF Model in Pigs	241
5.4	Discussion	247
Chapter 6 General Discussion.....		
	253	
6.1	The Susceptibility of the β_2 AR to SUMOylation.....	254
6.2	SUMO- β_2 AR Polyclonal Antibody Development	258
6.3	The Influence of β_2 AR SUMOylation on Receptor Signalling	259
6.4	SUMOylation of the β_2 AR in HF	261
6.5	Final Conclusion	263
Chapter 7 Appendix		
	264	
Chapter 8 References.....		
	265	

List of Figures

Figure 1.1 Excitation contraction (EC) coupling..	24
Figure 1.2 BAR-mediated PTMs of LTCC, troponin I and phospholamban..	34
Figure 1.3 Schematic diagram of the β_2 AR.	37
Figure 1.4 β_2 AR Ligand Binding Pocket.	40
Figure 1.5 G protein cycling..	43
Figure 1.6 Agonist-mediated β_2 AR activation.	46
Figure 1.7. β_2 AR desensitisation.....	50
Figure 1.8 β_2 AR internalisation.	52
Figure 1.9 β_2 AR resensitisation..	55
Figure 1.10 β_2 AR down-regulation..	58
Figure 1.11 The SUMOylation pathway.	64
Figure 1.12 SERCA2a affinity states..	73
Figure 1.13 SUMOylation of cardiac signalling proteins.....	77
Figure 2.1 Schematic of solid phase peptide synthesis.	96
Figure 2.2 Principle of BRET..	102
Figure 2.3 Principle of FRET.	105
Figure 2.4 Saturation ligand binding schematic.....	108
Figure 2.5 Competition ligand binding schematic.	110
Figure 2.6 Principle of SPASM sensor.	112
Figure 2.7. Minimally invasive TAC study timeline.	116
Figure 2.8 Transthoracic echocardiography parameters.....	118
Figure 3.1 Epitope design schematic.	130
Figure 3.2. Rabbit immunisation protocol.	132
Figure 3.3 IgG isolation.	134
Figure 3.4 Peptide affinity columns for isolation of specific SUMO- β_2 AR IgG....	137
Figure 3.5 Peptide affinity columns - affinity chromatography.	138
Figure 3.6 Lysines 232 and 235 are essential for SUMOylation of β_2 AR.....	142
Figure 3.7 β_2 AR SUMOylation sites are conserved between species.	144
Figure 3.8 Testing of SUMO-2/3- β_2 AR antibody - derived from rabbits 23 and 24.	146
Figure 3.9 Testing of SUMO-1- β_2 AR antibody - derived from rabbits 25 and 26.	147
Figure 3.10 Testing of SUMO- β_2 AR antibody - His-HRP antibody control.	148
Figure 3.11 Testing of SUMO-1- β_2 AR antibody from derived from rabbit 25 - blocking peptide.....	150
Figure 3.12 Testing of SUMO- β_2 AR specific antibody in cells.	153
Figure 4.1 Phosphorylation of β_2 AR-mediated by isoprenaline.	164
Figure 4.2 Increased activity of PKA-mediated by isoprenaline.	165
Figure 4.3 Phosphorylation of ERK mediated by isoprenaline.	166
Figure 4.4 Amplifying PIASy in HEK β_2 cells promotes SUMOylation of β_2 AR.	169
Figure 4.5. β_2 AR-PIASy interaction assessed by peptide array overlay.	172
Figure 4.6 β_2 AR-UBC9 interaction assessed by peptide array overlay.	173
Figure 4.7 β_2 AR-PIASy/UBC9 interaction sites identified near SUMOylation sites.	174
Figure 4.8. β_2 AR SUMOylation reduces isoprenaline-mediated PKA phosphorylation of β_2 AR.	177
Figure 4.9 β_2 AR SUMOylation reduces isoprenaline-mediated PKA cytosolic activity.....	178

Figure 4.10 β_2 AR SUMOylation reduces isoprenaline-mediated phosphorylation of ERK.	179
Figure 4.11 β_2 AR SUMOylation reduces isoprenaline-mediated reduction in total β_2 AR.	180
Figure 4.12 β_2 AR SUMOylation influence on isoprenaline-mediated GRK phosphorylation of β_2 AR is inconclusive.	181
Figure 4.13 β_2 AR SUMOylation delays receptor internalisation.	183
Figure 4.14 β_2 AR SUMOylation influence on receptor half-life is inconclusive. .	185
Figure 4.15 β_2 AR SUMOylation does not influence receptor ubiquitination at basal levels.	188
Figure 4.16 β_2 AR SUMOylation reduced isoprenaline-mediated receptor ubiquitination.	189
Figure 4.17 β_2 AR SUMOylation does not influence β_2 AR- β -arrestin interaction.	191
Figure 4.18 β_2 AR SUMOylation prolongs isoprenaline-mediated cellular levels of cAMP.	193
Figure 4.19 β_2 AR SUMOylation does not influence K_d or B_{max}	195
Figure 4.20 β_2 AR SUMOylation does not influence IC_{50}	197
Figure 4.21 Dose response SPASM sensor experiment - β_2 AR SUMOylation does not influence β_2 AR- G_s/G_i interaction.	200
Figure 4.22 Kinetics SPASM sensor experiment - β_2 AR SUMOylation does not influence β_2 AR- G_s/G_i interaction.	202
Figure 5.1 Location of aortic ligation during TAC surgery.	212
Figure 5.2 Location of the LAD artery for balloon occlusion.	216
Figure 5.3 Echocardiographic representative images and physical body measurements used to determine cardiac remodelling and function.	220
Figure 5.4 Cardiac function and remodelling assessed following TAC surgery. .	221
Figure 5.5 Left ventricular mass indices assessed following TAC surgery.	223
Figure 5.6 Heart weight is increased by TAC surgery.	225
Figure 5.7 TAC surgery does not influence body weight or tibia length.	227
Figure 5.8 TAC surgery does not influence other organs.	228
Figure 5.9 TAC surgery increases cardiomyocyte size.	231
Figure 5.10 TAC surgery increases cardiac fibrosis.	233
Figure 5.11 TAC surgery does not influence SUMO-2/3 expression.	235
Figure 5.12 TAC surgery influence on PIASy expression is inconclusive.	236
Figure 5.13 TAC surgery reduces UBC9 expression.	237
Figure 5.14 TAC surgery influence on SUMO-1 expression is inconclusive. .	238
Figure 5.15 TAC surgery does not influence SUMO- β_2 AR expression.	239
Figure 5.16 Testing of β_2 AR antibodies with cell lysate.	240
Figure 5.17 LAD artery balloon occlusion reduces SUMO-2/3 expression.	242
Figure 5.18 LAD artery balloon occlusion does not influence SUMO-1 expression. .	243
Figure 5.19 LAD artery balloon occlusion reduces PIASy expression.	244
Figure 5.20 LAD artery balloon occlusion increases SUMO- β_2 AR expression.	245
Figure 5.21 LAD artery balloon occlusion reduces UBC9 expression.	246
Figure 6.1 Post Translational Modifications and SUMO-Enzyme Interactions of the β_2 AR.	257

List of Tables

Table 1.1 NYHA HF classification scale.....	26
Table 1.2 AHA HF classification scale	26
Table 1.3 Management of HF	32
Table 1.4 G protein families	41
Table 2.1 Primary Antibodies.....	93
Table 2.2 Secondary Antibodies	94
Table 2.3 Processing sequence for Shandon Excelsior tissue processor	119
Table 2.4 De-paraffinisation and rehydration sequence.....	120
Table 3.1 Antigens for immunisation	128
Table 3.2 Rabbits immunised against SUMO-1 or SUMO-2/3- β_2 AR.....	129
Table 3.3 Affinity ligand peptides	135
Table 5.1 Echocardiographic data from RWT criterion animals	230

List of Abbreviations, Acronyms & Symbols

%	percent
°C	degrees celsius
2D	two dimensional
3D	three dimensional
AA1	amino acid 1
AA2	amino acid 2
AAV1	adeno-associated virus 1
AC	adenylyl cyclase
Ac	acetyl group
ACEi	angiotensin converting enzyme inhibitors
ADP	adenosine diphosphate
Adr	adrenaline
AHA	American Heart Association
AKAPs	A-kinase anchoring proteins
AMP	adenosine monophosphate
ANOVA	analysis of variance
AP-1	activator protein 1
AP-2	adaptor protein 2
AR	adrenergic receptor
ARB	angiotensin receptor blockers
ATP	adenosine triphosphate
AV	atrioventricular node
AWTd	anterior wall thickness during diastole
AWTs	anterior wall thickness during systole
BHF	British Heart Foundation
B _{max}	maximum binding sites
BRET	bioluminescence resonance energy transfer
BSA	bovine serum albumin
Ca ²⁺	calcium ions
CABG	coronary artery bypass graft
cAMP	cyclic adenosine monophosphate
CB1	cannabinoid receptor 1
CFP	cyan fluorescent protein
CGH-1	caenorhabditis elegans 1
cm	centimetres
CO ₂	carbon dioxide
CON	control
CRT	cardiac resynchronisation therapy
CRT-Ds	combination of both CRT and ICDs
cTNI	cardiac troponin I
CUPID	calcium upregulation by percutaneous administration of gene therapy in cardiac disease
DAPI	4', 6-diamidino-2-phenylindole

DESI	deSUMOylation isopeptidases
dH ₂ O	distilled water
DHA	dihydroalprenolol
DISC1	Disrupted in schizophrenia 1
DMEM	dulbecco's modified eagle's medium
DMF	dimethylformamide
DMSO	dimethyl sulfoxide
DNA	deoxyribonucleic acid
DPX	distyrene, plasticizer and xylene
E.coli	escherichia coli
E1/2	effector 1/2
EC	excitation contraction
EC ₅₀	[drug] that causes 50% of the maximal response
echo	echocardiography
ECL	enhanced chemiluminescence
EDTA	ethylenediaminetetraacetic acid
ELK1	ETS-like gene 1
EPAC	exchange protein activated by cAMP
ERK	extracellular signal regulated kinase
FBS	fetal bovine serum
Fmoc	9-fluorenylmethyloxycarbonyl
fmols	femtomoles
FRET	fluorescence resonance energy transfer
g	grams
G	gauge
G-pep	G protein peptide mimic
G418	geneticin
GAPDH	glyceraldehyde 3-phosphate dehydrogenase
GAPs	GTPase activating protein
GATA-2	gene for GATA binding protein 2
GDP	guanine diphosphate
GFP	green fluorescent protein
GI	gastrointestinal
GPCRs	G protein-coupled receptors
GRK	G protein receptor kinases
GST	glutathione S-transferase
GTP	guanine triphosphate
H ⁺	hydrogen ions
HA	hemagglutinin
HBSS	Hanks balanced salt solution
HCl	hydrochloride
HCSMs	hydrophobic cluster-dependent SUMO motifs
HDAC4	histone deacetylase 4
HDGF	hepatoma-derived growth factor
HEK	human embryonic kidney
HEPES-OH	4-(2-hydroxyethyl)-1-piperazineethanesulfonic acid

HF	heart failure
His	histidine tag
HPLC	high-performance liquid chromatography
HR	hour
HRP	horseradish peroxidase
IC ₅₀	[drug] causing 50% inhibition of competitor binding
ICDs	implantable cardioverter defibrillators
IgG	immunoglobulin G
IgM	immunoglobulin M
IκBα	inhibitor of kappa B alpha
IP	immunoprecipitation
IR	internal repeater
ISO	isoprenaline
K ⁺	potassium ions
kDa	kilodaltons
k _d	dissociation constant
kg	kilogram
K _i	inhibitor constant
KLH	keyhole limpet hemocyanin
KPA1	KRAB associated protein 1
L	ligand
LAD	left anterior descending
LB	lysogeny broth
LEF1	lymphoid enhancer factor 1
LG	L-glutamine
Log	logarithm
LTCC	l-type Ca ²⁺ channels
LV	left ventricle
LVEDD	LV end diastolic diameter
LVESD	LV end systolic diameter
M	molar
MAPK	mitogen-activated protein kinase
mBRET	milliBRET
MDM2	mouse double minute 2 homolog
mg	milligram
MgCl ₂	magnesium chloride
mGluR	metabotropic glutamate receptors
MI	myocardial infarction
min	minutes
ml	millilitre
mM	millimolar
mm	millimetre
mRNA	messenger ribonucleic acid
N HCl	acidified water
Na ₄ P ₂ O ₇	tetrasodium pyrophosphate
Na ⁺	sodium ions

NaCl	sodium chloride
NaF	sodium fluoride
NaHPO ₄	monosodium phosphate
NCX	Na ⁺ /Ca ²⁺ exchanger
NDSMs	negatively charged amino acid-dependent SUMO motifs
NEAA	non essential amino acids
NEDD4	neural precursor cell expressed developmentally down regulated protein 4
NEM	N-ethylmaleimide
NEMO	NF-kappa-B essential modulator
NF-κB	nuclear factor kappa-light-chain-enhancer of activated B cells
ng	nanogram
NLuc	nanoluc luciferase
nM	nanomolar
nm	nanometres
NSF	N-ethylmaleimide-sensitive factor
NYHA	New York Heart Association
P	phosphate group
P.I	preimmune
PP2A	phosphatase 2A
PTHr	parathyroid hormone receptor
PBS	phosphate buffered saline
Pc2	proprotein convertase 2
PDE	phosphodiesterase
PDSMs	phosphorylation-dependent SUMO motifs
PFA	paraformaldehyde
phosERK	phosphorylated ERK
phosPKA substrate	phosphorylated PKA substrate
phosβ2	phosphorylated β ₂ AR
Pi	inorganic phosphate
PIAS	protein inhibitor activated STAT
PKA	protein kinase A
PLB	phospholamban
pM	picomolar
PS	penicillin-streptomycin
PTM	post-translational modification
PWTd	posterior wall thickness during diastole
PWTs	posterior wall thickness during systole
RAAS	renin-angiotensin-aldosterone system
RanBP2	RAN binding protein 2
RanGAP1	Ran GTPase activating protein 1
RING	really interesting new gene
RIPA	radioimmunoprecipitation assay
RLuc	renilla luciferase
RNA	ribonucleic acid

RNase	ribonuclease
ROS	reactive oxygen species
rpm	rotations per minute
RWT	relative wall thickness
RyRs	ryanodine receptors
S	SUMO
SA	sinoatrial node
SAE1-SAE2	SUMO-1 activating enzyme subunits 1 and 2
SDS-PAGE	sodium dodecyl sulfate polyacrylamide gel electrophoresis
SEM	standard error of the mean
SENPs	sentrin specific proteases
SERCA2a	sarcoplasmic reticulum Ca ²⁺ ATPase
SIMs	SUMO interacting motifs
SNARE	soluble N-ethylmaleimide-sensitive factor activating protein receptor
Sp1	specificity protein 1
SpA	staphylococcal protein A
SPASM	systemic protein affinity strength modulation
SPPS	solid phase peptide synthesis
SP-RING	Siz/PIAS(SP)-RING
SR	sarcoplasmic reticulum
SRF	serum response factor
STAT	signal transduce and activator of transcription
Stx1A	syntaxin-1A
SUMO	small ubiquitin-like modifier
TAC	transverse aortic constriction
TBS-T	tris-buffered saline-tween20
TCEP	tris(2-carboxylethyl)phosphine)
TM	transmembrane domain
TNI	troponin
topors	TOP1 binding arginine/serine rich protein
TSH	thyroid stimulating hormone
Tris HCl	tris hydrochloride
U	ubiquitin
UBC9	ubiquitin carrier protein 9
UK	United Kingdom
USPL1	ubiquitin specific protease-like 1
V	volts
WGA	wheat germ agglutinin
WT	wildtype
X	times
YFP	yellow fluorescent protein
ZBTB1	zinc finger and BTB domain containing 1
α	alpha
α _{1A} AR	alpha 1A adrenergic receptor
β	beta

β_1 AR	beta 1 adrenergic receptor
β_2 AR	beta 2 adrenergic receptor
BAR	beta adrenoceptor
BARK	beta arrestin kinase
ϵ	epsilon
γ	gamma
μg	microgram
μl	microliter
μm	micrometre
μM	micromolar

Oral presentations, publications and awards

Abstract Publication: Poster Presentation

Wills, L; Munro, K; Ballantyne, M; Findlay, J; Graham, D; Baillie, G. S (2015). SUMOylation of essential cardiac signalling proteins: preliminary evidence, *Heart*, 101, A4. University of Glasgow British Society for Cardiovascular Research Autumn Meeting (Sept 2015).

Poster Presentation

Wills, L; Munro, K; Ballantyne, M; Findlay, J; Graham, D; Baillie, G. S (Nov 2014). SUMOylation of essential cardiac signalling proteins: preliminary evidence. DZHK (Deutsches Zentrum Fur Herz-Kreislauf-Forschung E.V) Symposium (Berlin).

Invited Presentation

University of Louisville (Kentucky, USA). SUMOylation of Essential Cardiac Signalling Proteins - The β_2 AR (August 2016)

Oral Presentation

British Heart Foundation Student Conference (Kings College, London). SUMOylation of Essential Cardiac Signalling Proteins - The β_2 AR (April 2017)

Awards

MVLS (Medical, Veterinary and Life Science) Institute Funding (DZHK Symposium, Berlin) - £350

Lister Bellahouston Scholarship (Mount Sinai Cardiovascular Research Centre, New York) - £1000

David Fleming Brown Scholarship (Mount Sinai Cardiovascular Research Centre, New York) - £500

Summary

The beta 2 adrenergic receptor (β_2 AR) is a GPCR that is susceptible to multiple post-translational modifications (PTMs) including phosphorylation, ubiquitination, palmitoylation and glycosylation, which can alter how the β_2 AR orchestrates downstream intracellular signals. Following the discovery of SUMOylation of the cardiac signalling protein SERCA2a, we hypothesised that the β_2 AR, which is also involved in cardiac signalling, may be a substrate for SUMOylation. This notion was supported by previous findings that five different GPCRs have been identified as susceptible to SUMOylation, including metabotropic glutamate receptors (mGluR), a cannabinoid receptor, a serotonin receptor and a receptor involved in basal cell carcinoma known as smo.

For the first time, we confirm the susceptibility of the β_2 AR to SUMOylation by identifying SUMO accepting lysines, interaction sites between the β_2 AR and the enzymes of the SUMOylation cascade, and the traditional “ghost” band, which is indicative of protein SUMOylation. SUMOylation has been shown to influence receptor signalling, and we now uncover a possible role for SUMOylation in β_2 AR signalling. I report that SUMOylation of the β_2 AR (mediated via overexpression of the E3 ligase PIASy) reduces β_2 AR phosphorylation by PKA altering the receptor driven phospho-ERK response, inhibits β_2 AR ubiquitination and degradation, and delays β_2 AR internalisation. These changes could be associated with steric effects of the bulky SUMO modification and ubiquitin-SUMOylation competition for available surface associated lysines.

With the importance of SUMOylation in multiple disease states (including cardiovascular disease, neurodegenerative disease and cancer), we worked in conjunction with the antibody production company Badrilla® to produce a SUMO-substrate specific antibody for a site within the third intracellular loop of the β_2 AR. The antibody we have produced is successful in recognising the SUMOylated form of the receptor in both cell and tissue lysate, making it the first antibody of its kind to be generated. In conjunction with the Hajjar group at Mount Sinai Cardiovascular Research Centre (New York, USA) we used the SUMO- β_2 AR specific antibody to assess the influence of the SUMO modification in two animal models of heart failure (HF); transverse aortic constriction (TAC) pressure overload HF model in mice and the left anterior descending (LAD) artery balloon occlusion

ischemic HF model in pigs. Prior work within the Hajjar group has revealed that SUMOylation of SERCA2a is reduced in HF, and restoring this modification to SERCA2a via SUMO-1 adeno-associated viral-mediated gene delivery is beneficial in restoring cardiac function. We hypothesised that SUMOylation of the β_2 AR would also be reduced in HF, however unexpectedly; the SUMOylated form of the β_2 AR was increased in the LAD artery balloon occlusion ischemic HF model in pigs.

The role of the β_2 AR in HF is unclear. There are studies which both report a cardio-protective and a cardio-toxic role of the receptor. To ascertain the role SUMOylation of the β_2 AR plays, *in vivo* studies promoting SUMOylation of the β_2 AR in the HF models described above will help to determine if enhanced SUMOylation of the receptor worsens the HF phenotype or prevents its development.

To conclude, we present the first evidence that the β_2 AR can be modified by SUMOylation, which acts to influence the receptors downstream signalling, desensitisation and degradation. We have designed a first-in-class SUMO- β_2 AR antibody - which paves the way for a panel of SUMO specific antibodies - and utilised it to assess SUMOylation of the β_2 AR in model cellular systems and animal models of HF. Similarly, to SERCA2a, SUMOylation does influence β_2 AR in the HF phenotype, although not a decrease in SUMOylation as was expected, but an increase. Future work in animal models promoting SUMOylation of the receptor is vital to assess the role of this highly novel post-translational modification of the β_2 AR.

Chapter 1 Introduction

1.1 The Cardiovascular System

The cardiovascular system - composed of the heart, veins and arteries - is responsible for providing the organs and tissues of the body with oxygenated blood. Following cardiac contraction, the heart expels blood into two vital circuits; the pulmonary and the systemic circuit (Campbell, et al., 2008).

1.1.1 Pulmonary and Systemic Circulation

The pulmonary circuit begins at the right ventricle with de-oxygenated blood being ejected into the pulmonary artery, where it passes to the lungs. Within the lungs, blood flows through the capillary beds, allowing gaseous exchange between the blood and the lungs - oxygen diffusing into the blood and carbon dioxide diffusing out of the blood. Oxygen-rich blood now returns to the left atrium via the pulmonary veins, where it will be sent to the systemic circuit. The systemic circuit begins with blood flowing from the left atrium into the left ventricle, where it is then ejected into the aorta. The aorta then branches off into smaller vessels providing blood supply to the heart itself, the upper body - head and arms - and the lower body - abdomen and lower limbs. Blood passes through the capillary beds of organs and tissues, allowing gaseous exchange. Within the systemic circuit, oxygen diffuses from the blood into organs and tissues, whereas carbon dioxide from metabolising organs and tissues diffuses into the blood. The oxygen-poor blood now returns to the right side of the heart via the superior and inferior vena cava, draining into the right atrium. This blood can pass to the right ventricle - beginning the pulmonary circuit once again (Campbell, et al., 2008).

1.1.2 The Anatomy of the Heart

The heart is composed of four chambers; two smaller chambers with relatively thin walls known as the atria, and two larger chambers with thicker walls known as the ventricles. In addition to the chambers, there are four valves present in the heart to prevent the back flow of blood; two atrioventricular valves which are located at the junction between the atria and the ventricle, and two semilunar valves, which are located at the junction between the ventricles and the arteries (Campbell, et al., 2008).

1.1.3 Cardiac Cycle

The cardiac cycle is a rhythmic cycle of contraction (systole) and relaxation (diastole), with contraction pumping blood from the heart and relaxation allowing chambers to fill. During relaxation, blood returning to the heart from the vena cava passes easily from the atria to the ventricles, through the atrioventricular valves, allowing ventricular filling. During systole, the remaining blood within the atria is pumped into the ventricles, immediately followed by the ventricles pumping blood through the semilunar valves, into both the pulmonary and systemic circulation (Campbell, et al., 2008).

1.1.4 Cardiac Conduction System

An organised rhythmic contraction of the heart requires adequate propagation of electrical impulses along the conduction pathway. To generate cardiac contraction, an electrical signal comes from the sinoatrial (SA) node - which is located in the wall of the right atrium - and travels through the heart via the electrical conduction system. Due to the location of the node, the signal first passes to the right atrium where it passes through the Bachman's bundle to the left atrium. From the right atrium, the signal passes to a second node known as the atrioventricular (AV) node. From this node, the electrical signal passes through the bundle of His and down the bundle branches, the right bundle branch depolarising the right ventricle and the left bundle branch depolarising both the left ventricle and the interventricular septum (Annderson, et al., 2009) (Renwick, et al., 1993).

1.1.5 Excitation Contraction (EC) Coupling

The sarcomere is the basic functional unit of the muscle within a myocyte. The contractile elements are firstly myosin, thick filaments with globular heads which have ATPase activity (enzymatic activity to catalyse the degradation of adenosine triphosphate (ATP) to adenosine diphosphate (ADP)), and secondly, actin, the thin filaments arranged as an alpha helix woven between myosin filaments. Regulatory elements include tropomyosin and troponin. Tropomyosin prevents the interaction between myosin globular heads and actin in the resting state. Troponin is a complex of three subunits (T, I and C) that sits along the actin filaments: troponin

T is responsible for mediating the interaction between troponin and the other contractile proteins tropomyosin and actin; troponin I is responsible for inhibiting the enzymatic capacity of myosin in the actin-myosin interaction; troponin C is the regulatory component which binds Ca^{2+} to allow regulation of contraction (Bers, 2002).

When electrical impulses pass through the conduction pathway this leads to depolarisation of the cardiomyocyte membrane. Following depolarisation, the L-type Ca^{2+} channels (LTCC) on the myocyte membrane open, allowing an initial influx of Ca^{2+} into the myocyte. This Ca^{2+} influx induces the opening of ryanodine receptors (RyRs) which are located on the surface of the sarcoplasmic reticulum (SR) - an intracellular Ca^{2+} store - allowing a much greater influx of Ca^{2+} into the cell interior. This is known as Ca^{2+} -induced- Ca^{2+} -release (Pathak, et al., 2005). The free Ca^{2+} is responsible for mediating cardiomyocyte contraction via the contractile proteins. The free Ca^{2+} binds to troponin C and induces a conformational change in troponin, such that troponin I exposes a site on actin that can now interact with the myosin ATPase of the myosin globular head. This interaction leads to ATP hydrolysis, which supplies the energy for the conformational change that occurs in the actin-myosin complex. This change promotes movement between the myosin globular heads and actin, such that the filaments slide past each other, shortening the length of the sarcomere. This leads to cardiomyocyte contraction (Ikonnikov & Yelle, 2016). Relaxation occurs when Ca^{2+} is released from troponin C, and the contractile proteins return to their resting state. Ca^{2+} is then either returned to the SR via the sarcoplasmic reticulum Ca^{2+} ATPase (SERCA2a) or expelled from the cell via membrane protein $\text{Na}^+/\text{Ca}^{2+}$ exchanger (NCX) (Figure 1.1) (Kawase & Hajjar, 2008).

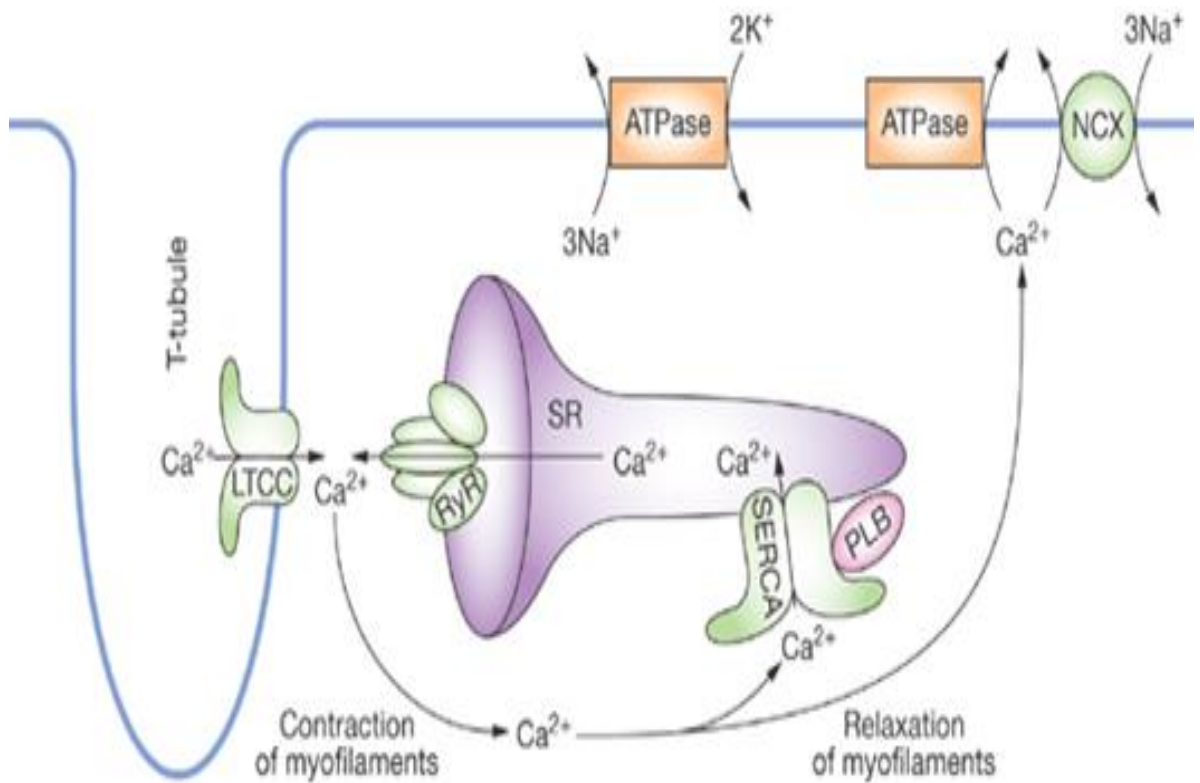


Figure 1.1 Excitation contraction (EC) coupling. Ca^{2+} enters the cell via the LTCC. This Ca^{2+} is responsible for inducing a conformational change in the RyR to induce Ca^{2+} release from the SR. This Ca^{2+} interacts with the contractile proteins to mediate cellular contraction. Following contraction relaxation occurs and Ca^{2+} is removed from the contractile proteins and removed from the cell interior either via SERCA2a or the NCX exchanger (Kawase & Hajjar, 2008). L-type Ca^{2+} channels (LTCC), ryanodine receptor (RyR), sarcoplasmic reticulum (SR), sarcoplasmic reticulum Ca^{2+} ATPase (SERCA2a), $\text{Na}^+/\text{Ca}^{2+}$ exchanger (NCX), Na^+/K^+ ATPase exchanger (ATPase), phospholamban (PLB).

1.2 Heart Failure (HF)

1.2.1 Definition of HF

Heart failure (HF) is often regarded as the inadequacy of cardiac output resulting in the metabolic needs of organs and tissues being unmet. This definition is mostly suited to describe patients who are admitted to hospital with salt and water retention or pulmonary oedema, but is less suited to patients suffering with chronic HF (Denolin, et al., 1983). When patients suffering from chronic HF are adequately treated they can have a normal resting cardiac output, as well as a normal left ventricular pressure, therefore their tissues' metabolic needs are met. At rest, these patients are described asymptomatic, however they will experience symptoms during exercise leading to their exercise capabilities being limited (Denolin, et al., 1983). The animal models that are utilised in this thesis (Chapter 5 - Analysis of β_2 AR SUMOylation in Animal Models of Heart Failure (HF)) were designed to resemble chronic HF; therefore, SUMOylation of the β_2 AR will be assessed in this disease state.

1.2.2 Diagnosis and Classification of HF

The characteristic symptoms of HF are not limited to this disease state. They include dyspnoea (shortness of breath), fatigue, oedema (water retention) in the legs/ankles/feet, irregular or fast heartbeat, and exercise limitation. The origin of these symptoms is not fully understood, but the severity of these symptoms correlates accurately with the extent of cardiac dysfunction (Cleland, et al., 2003) (Marantz, et al., 1988). The severity of symptoms allows HF patients to be classified on two specialised scales derived by two independent associations; the New York Heart Association (NYHA) and the American Heart Association (AHA). The NYHA scale originated in 1928 and was revised and widely accepted in 1964, categorising patients in groups I-IV (Table 1.1) (Marvin, 1964) (Miller-Davis, et al., 2006). The AHA scale originated in 1995 and proposed an additional classification which would complement the NYHA classification, categorising patients in groups A-D (Table 1.2) (Hunt, et al., 2005) (Williams, et al., 1995).

Table 1.1 NYHA HF classification scale

Class	Description
I	The patient suffers from cardiac disease but experiences no symptoms and no limitation to general physical activity.
II	The patient suffers from cardiac disease and experiences mild symptoms and slight limitation to general physical activity
III	The patient suffers from cardiac disease and experiences limitation in both minimal and general physical activity. The patient is only comfortable at rest.
IV	The patient suffers from cardiac disease and experiences severe physical activity limitation. The patient experiences symptoms even at rest and is mostly bedbound.

(Marvin, 1964).

Table 1.2 AHA HF classification scale

Class	Description
A	The patient displays no objective evidence of cardiovascular disease and experiences no symptoms or limitation to general physical activity
B	The patient displays objective evidence of cardiovascular disease and experiences mild symptoms and slight limitation to general physical activity. The patient is comfortable at rest.
C	The patient displays objective evidence of moderate cardiovascular disease and experiences marked limitation in minimal and general physical activity due to symptoms. The patient is only comfortable at rest.
D	The patient displays objective evidence of severe cardiovascular disease and experiences severe limitations in physical activity. The patient experiences symptoms even at rest.

(Williams, et al., 1995)

1.2.3 The Cause of HF

The classical causes of HF are the cardiovascular conditions which precede HF initiation. In Western countries, the most common cause of HF is coronary heart disease, which begins when plaque - a combination of fat, cholesterol and cellular waste products - builds up within the vasculature. When plaques become large enough, fragments can break off and these broken fragments are known as

thrombi. Thrombi can become lodged within the vasculature, and if this occurs in a coronary artery, it can lead to a myocardial infarction (MI) (Thygesen, et al., 2007). A blockage within a coronary artery will inhibit the artery from supplying the blood flow to the heart, with the extent of the inhibition being dependent upon the size of the thrombus. If the thrombus is large enough, then a healthy ventricle can become severely dysfunctional almost instantaneously due to massive myocardial ischaemia and subsequent necrosis of the myocardial tissue. If the blockage is successfully removed the tissue will be re-perfused, but this in itself can promote problems, as although re-perfusion saves viable myocytes it also accelerates the necrosis of injured myocytes and permits infarct scar growth (Simonis, et al., 2012). Those who have an elevated chance of plaque formation, have an elevated risk of MI, and consequently an elevated risk of HF. This includes individuals who suffer from hypertension, high cholesterol levels, high triglyceride levels, obesity, diabetes and high blood sugar levels, as well as the more traditional factors of age, smoking and genetics (Macon, et al., 2015).

Following an MI, the heart will attempt to function in the same manner as it did before the MI occurred, but with the scar tissue which was once viable myocardium inhibiting the function, the remaining myocardium must remodel to compensate for the loss of functional tissue. The left ventricle (LV) is the chamber which expels oxygenated blood to the body; hence, this chamber undergoes remodelling to maintain the cardiac output. Remodelling of the LV following an MI involves LV wall thinning at the infarct area, chamber dilation and compensatory hypertrophy via the lengthening of the non-infarcted areas. This remodelling will initially maintain the stroke volume - volume of blood pumped from the LV per heart beat - but over time these compensatory changes will become maladaptive, leading to increased wall stress and oxygen demand along with interstitial fibrosis, which results from elevated cardiac fibroblast proliferation and collagen synthesis in response to the growing myocardium (Diez, et al., 2007). With the build-up of collagen, the LV becomes stiffer, leading to decreased contractility which results in diastolic dysfunction (Cowie, et al., 2005) (Krayenbuehl, et al., 1989) (Heyman, et al., 2005) (Monrad, et al., 1988). This leads to the manifestation of HF symptoms where the heart is in a state of both LV systolic and diastolic dysfunction (Houser, et al., 2012) (Peske, 2004).

1.2.4 Prevalence and Prognosis of HF

HF impacts on healthcare systems worldwide. In 2015 the British Heart Foundation (BHF) estimated that over half a million people in the UK (about 1% of the UK population) were affected by HF (BHF, 2015), with more than 23-26 million people worldwide suffering from the disease. Furthermore, HF prevalence is rising (Roger, 2013) (Ambrosy, et al., 2014). Even although HF can be managed by multiple approaches, the prognosis is poor with average life expectancy approximately 3 years post diagnosis (Dickstein, et al., 2008). For patients with severe HF, more than half will die within a year (Cleveland, et al., 1999) (Stewart, et al., 2001).

1.2.5 Management of HF

Although there is no cure for HF, it can be managed by a number of multiple approaches ranging from lifestyle changes and pharmacological therapies to more extreme approaches such as implantable devices and cardiac surgery. These forms of management are summarised in Table 1.3.

1.2.5.1 Life Style Changes

Positive lifestyle changes concern diet and exercise. Patients suffering from HF are advised to participate in light exercise rather than heavy exercise. In 2012, a meta-analysis study identified that aerobic exercise training can reverse the LV remodelling that occurs in HF (Chen, et al., 2012). In relation to changes to diet, HF patients are often restricted to 2-3g of sodium per day. This dietary change is beneficial as HF causes patients to absorb an unnecessarily high level of sodium at the kidneys, and subsequently retain excessive water. This additional water retention will exacerbate the existing HF symptoms (Konerman & Hummel, 2014).

1.2.5.2 Pharmacological Therapies

Various pharmacological interventions are available for HF patients and the medications outlined here are by no means an exhaustive list (Table 1.3).

Diuretics promote the loss of fluid from the vasculature through urine. This counteracts the excessive water retention in HF patients and relieves the

associated symptoms, such as oedema in the legs/ankles/feet (Beckerman, 2016). Furthermore, if there is less volume within the vasculature then the pressure is lower. This leads to a lower LV afterload, i.e. the pressure the LV must develop to force blood out of the chamber - therefore lessening the stress on the LV walls (Houser, et al., 2012).

The elevated water retention in HF patients is partly due to excessive activation of the renin-angiotensin-aldosterone system (RAAS). This is a system which regulates plasma sodium concentration and arterial blood pressure (Selektor & Weber, 2008) (Schrier, 1990). When the volume of blood in the vasculature is low, the RAAS system is activated to promote reabsorption of sodium at the kidney, which leads to reabsorption of water. In patients with HF, the excessive activation of this system leads to heightened water reabsorption; therefore, medications which inhibit this system are beneficial. Angiotensin converting enzyme inhibitors (ACEi), angiotensin receptor blockers (ARBs) and aldosterone antagonists are all pharmacological interventions that inhibit the RAAS, and therefore reduce water reabsorption. As mentioned before for diuretics, less volume within the vasculature will lower the LV afterload. Both ACEi and ARBs can lower this further by promoting vessel dilation. This is another way of reducing the LV afterload, by reducing pressure in the vasculature (Dumitru, 2016).

In a similar fashion to the RAAS, the sympathetic nervous system activation is markedly higher in HF patients. This is one of two branches of the autonomic nervous system - parasympathetic and sympathetic - that is responsible for the "fight or flight" response mediated by the catecholamines adrenaline and noradrenaline (Selektor & Weber, 2008) (Schrier, 1990). The traditional response of the sympathetic nervous system begins with a stressful situation causing the hypothalamus in the brain to promote increased production of the catecholamines in the adrenal glands. Adrenaline and noradrenaline are released into the bloodstream where they travel in the blood to the adrenergic receptors (described further in section 1.3.1 - Adrenergic Receptors). Through these receptors catecholamines mediate their effects including increased heart rate and force, increased blood pressure, and an increased uptake/production of glucose to provide energy for metabolising muscles (Tank & Wong, 2015) (Chistiakov, Ashwell, Orekhov, & Bobryshev, 2015) (Thorp & Schlaich, 2015) (Konturek,

Konteruk, Pawlik, & Brzozowski, 2004). The symptoms of HF can be worsened by catecholamines and therefore it is beneficial to inhibit the body's response to these hormones. This can be done by inhibiting beta adrenoceptors (BAR) - a type of adrenergic receptor - using beta-blocker drugs. These drugs act antagonistically at these receptors and were first synthesized in 1958 by James Black (Black, et al., 1964). Although the initial increase in sympathetic nervous system activity during HF is beneficial as it compensates for left ventricular dysfunction, chronic adrenergic stimulation causes myocardial damage due to left ventricular remodeling and cardiomyocyte necrosis. Attenuation of this adrenergic stimulation is associated with improvement in survival (Manurung & Trisnohadi, 2007). Furthermore, these drugs can slow the heart rate giving the LV more time to fill correctly in an attempt to maintain an appropriate stroke volume (Pai & Hetherington, 2015).

A combination therapy of nitrate and the drug hydralazine can change vessel dilation and subsequently alter blood pressure. This method mediates both venous and arterial dilation, therefore reducing both cardiac preload - the degree of myocardial distension prior to contraction - and LV afterload. This reduction in pressure within the heart may reduce adverse cardiac remodelling by lowering cardiac wall stress (Colucci, 2016).

There are certain drugs which can also be administered in conjunction to the standard pharmacological therapies; two examples are digoxin and anticoagulants.

Digoxin is a cardiac glycoside which inhibits the $\text{Na}^+ \text{K}^+ \text{ATPase}$ pump on cardiomyocytes leading to elevated Na^+ concentration within the cell. This rise impacts the $\text{Na}^+ \text{Ca}^{2+}$ exchanger pump causing Ca^{2+} to rise as the elevated Na^+ is pumped out of the cell. The additional Ca^{2+} is now available to bind to troponin C mediating stronger contractions. In addition to this, digoxin can also promote parasympathetic nervous system activity. This system works in opposition to the sympathetic nervous system and, rather than increasing heart rate, the parasympathetic system acts to reduce heart rate (Campbell & MacDonald, 2003). Therefore, digoxin both increases the strength of the heart contraction, while lowering the heart rate, allowing additional filling time for the LV.

Anticoagulants are drugs which act to prevent the coagulation cascade. Activation of the coagulation cascade leads to the formation of blood clots, also known as thrombi when they form within the veins or arteries. As described above, a thrombus can be an initiating event which leads to MI and subsequent development of HF. In light of this, patients can be given anticoagulant drugs to reduce the risk of further thrombotic events (Dumitru, 2016).

1.2.5.3 Surgical Intervention

Often pharmacological and lifestyle changes are not enough to counteract the symptoms of HF and surgical intervention is necessary (Table 1.3).

HF is a dynamic process in which the myocardium is continuously adapting to try to maintain perfusion of the other organs and tissues in the body. The alterations to the myocardium can lead to discrepancies in the electrical conducting system of the heart. The SA node is the natural pacemaker of the heart. Cardiac contraction is initiated at this node and electrical signal passes through the remaining electrical conducting system (NIH, 2011). Any of these components can be damaged by HF. In these circumstances, electrophysiological intervention is available through the following implantable devices; pacemakers, cardiac resynchronisation therapy (CRT), implantable cardioverter defibrillators (ICDs), and a combination of both CRT and ICDs known as CRT-Ds (NHS, 2016). Pacemakers encourage the heart to beat at regular intervals if the origin of cardiac contraction is damaged by HF remodelling. CRT can be used to synchronise contractions between the right and left ventricle, as the remodelling process can result in deleterious alternate chamber contraction times. ICDs can be implanted as a pre-emptive measure, if the failing heart enters a state of fatal arrhythmia - which is possible if the conducting system is damaged by remodelling - the ICD can be triggered to restore normal rhythm. A combination of both ICDs and CRT is known as CRT-Ds, a device which can both synchronise ventricular contraction and restore normal rhythm if arrhythmia arises (AHA, 2016).

Surgical intervention can also be performed to restore the physical damage caused to the heart during the cardiac remodelling in HF. The development of HF can be initiated by a blockage in the arteries which supply the heart, and therefore revascularisation procedures can be used to restore the cardiac blood supply.

Coronary artery bypass graft (CABG) is an option if HF is initiated by coronary artery disease, in which a thrombus is lodged within a coronary artery and therefore the heart has a reduced blood supply and reduced function. Using arteries or veins taken from other parts of the body, the blood flow is re-routed around the blocked arteries, restoring cardiac perfusion. The valves of the heart can also be damaged by HF. These valves normally control the unidirectional flow of blood through the heart but in HF they can become leaky, as the muscles which normally tightly close them have become weakened. In other cases, the valves can become stiff and do not open properly. These valves can be replaced or repaired by prosthetic components to restore function (AHA, 2016). A more novel technique is ventricular restoration, in which a plastic model is used to reshape the heart. During HF, the shape of the heart can be lost due to remodelling and this alters the LV volume, which will directly impact on stroke volume. Ventricular restoration helps return the heart to its original shape. (Castelvecchio, et al., 2010) (BCBST, 2016). The final surgical intervention for end-stage HF is complete heart transplantation as the damaged heart is beyond repair by any other method.

Table 1.3 Management of HF

Lifestyle Changes	Pharmacological Intervention	Surgical Intervention	
		Electrical	Non-Electrical
Diet Exercise	Diuretics RAAS Drugs Beta Blockers Hydazaline & Nitrate Therapy Digoxin Anticoagulants	Pacemaker ICD CRT CRT-D	CABG Valve Repair/Replacement Ventricular Restoration Heart Transplant

1.2.6 The Importance of Novel Cardiovascular Research to HF

With the prognosis of HF being poor, research has been aimed at discovering alternate methods to tackle HF in terms of both new diagnostics and treatments. Cardiac function is assessed at a molecular level in both healthy and diseased states to identify essential cardiac contractile and signalling proteins which are

defective in HF and therefore could be novel therapeutic targets (Gomez, et al., 1997). One molecular mechanism which can compensate for loss of functionality during HF is modulation of protein activity via post-translational modification (PTM). Proteins can be modified in this manner at any point in their life cycle, ranging from directly after ribosomal translation, up until the protein relocates to a specific cellular compartment or tissue. This type of modulation can occur naturally to control heart rate, for example in the cardiomyocyte, beta adrenoceptor (BAR) activation by catecholamines promotes phosphorylation - a PTM in which a phosphate group is covalently linked to the target protein - of the L-type Ca^{2+} channel (LTCC), TNI and phospholamban (PLB). This causes increased Ca^{2+} entry into the cell via the LTCC allowing further Ca^{2+} release from the SR to promote contraction, desensitization of TNI to Ca^{2+} ions making the cell less susceptible to Ca^{2+} -mediated contraction (Bodor, et al., 2001), and reduced inhibitory action of PLB on SERCA2a resulting in more Ca^{2+} being removed from the cell cytosol and further inhibiting cardiac contraction. These actions on TNI and PLB combine to improve cardiac relaxation, which can often be inhibited in HF (MacLannan & Kranias, 2003). Therefore, catecholamine levels are elevated in HF to promote BAR stimulation, promote protein phosphorylation, and promote optimum relaxation following an enhanced contraction (Figure 1.2) (Kaumann, et al., 1999).

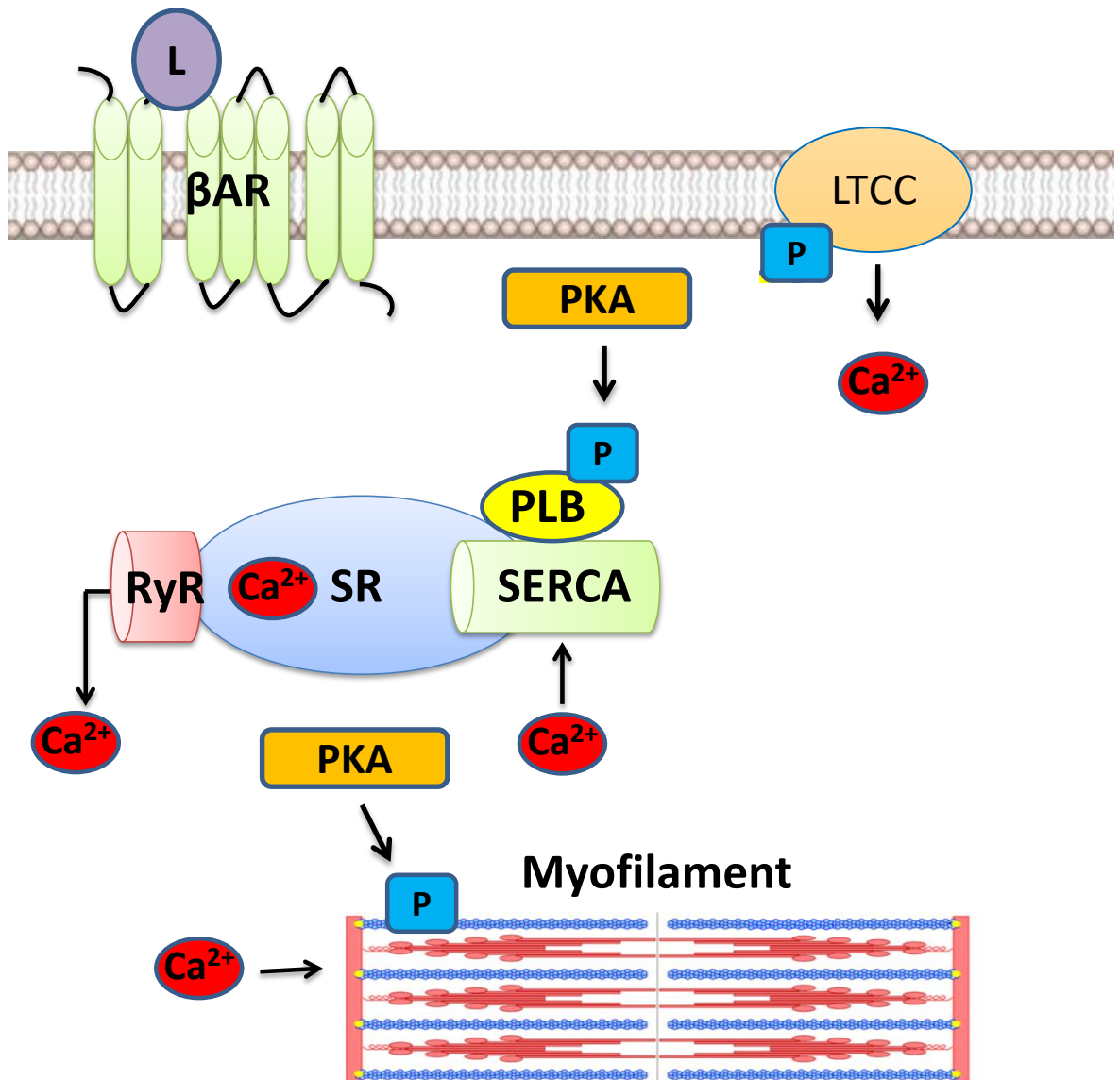


Figure 1.2 BAR-mediated PTMs of LTCC, troponin I and phospholamban. Activation of BAR by ligand mediates phosphorylation of LTCC, TNI and PLB by PKA. This causes an increased Ca²⁺ entry into the cell via LTCC, desensitization of TNI to Ca²⁺ ions and reduced inhibitory action of PLB on SERCA2a. BAR (beta adrenoceptor), RyR (ryanodine receptor), SR (sarcoplasmic reticulum), SERCA (sarcoplasmic reticulum Ca²⁺ ATPase), PLB (phospholamban), P (phosphate group) L (ligand), PKA (protein kinase A) LTCC (L-type Ca²⁺ channel).

1.3 The β_2 Adrenergic Receptor (β_2 AR)

1.3.1 Adrenergic Receptors

Raymond Alquist believed that the cardiovascular effects of catecholamines - increased blood pressure and heart rate - were explained by two distinct sets of receptors, the α and β receptors (Wenger & Greenbaum, 1984). It is now accepted that there are three types of adrenergic receptor: α_1 , α_2 and β . All adrenergic receptor subtypes are G protein-coupled receptors (GPCRs): the α_1 family (α_{1A} , α_{1B}) couple to the G_o protein to modulate phospholipase C; the α_2 family (α_{2A} , α_{2B} , and α_{2C}) couple to the G_i protein to inhibit adenylyl cyclase; and the β family (β_1 , β_2 , and β_3) couple to the G_s protein to stimulate adenylyl cyclase. The receptors share similar features including a single polypeptide chain ranging from 400 to greater than 500 residues in length, amino- and carboxy-terminal regions, three extracellular and three intracellular loops, and seven transmembrane stretches. The carboxy-terminal differs between families to allow interaction with the respective G proteins - the α_2 and β families have shorter C-termini than the α_1 family, which requires a longer sequence to interact with G_o (Strosberg, 1993). The adrenergic receptors are located throughout the body however, they can be found abundantly in specific tissue types: α_{1A} in the arteries, α_{1B} in the heart, α_2 family in the brain, β_1 in the heart, β_2 in the heart and the lungs, and β_3 in fat tissue (Molinoff, 1984). The focus of this thesis is the β_2 adrenergic receptor (β_2 AR) in the heart.

In addition to both the β_1 AR and β_2 AR being located in the heart, they also share other similarities with approximately 54% structural homology: their N-terminals are susceptible to glycosylation; their C-terminals can be phosphorylated by two kinases, namely PKA and GRK; and a disulphide bond between their second and third extracellular loop is essential for receptor activity. These properties will be discussed further for the β_2 AR, the focus of this thesis (Coman, et al., 2009).

1.3.2 Crystal Structure of the β_2 AR

The gene for the human β_2 AR, ADRB2 is located on the long arm of chromosome 5q31 and codes for a gene of approximately 1200 base pairs. This gene codes for the β_2 AR which is composed of 413 amino acid residues totalling approximately

46500 Daltons in weight (Kobilka, et al., 1987). The receptor belongs to a family known as G protein-coupled receptors (GPCRs), which consist of seven transmembrane spanning alpha helices, with three extracellular loops, and three intracellular loops, with one being the amino-terminus and carboxy-terminus, respectively (Qing, et al., 1997) (Figure 1.3).

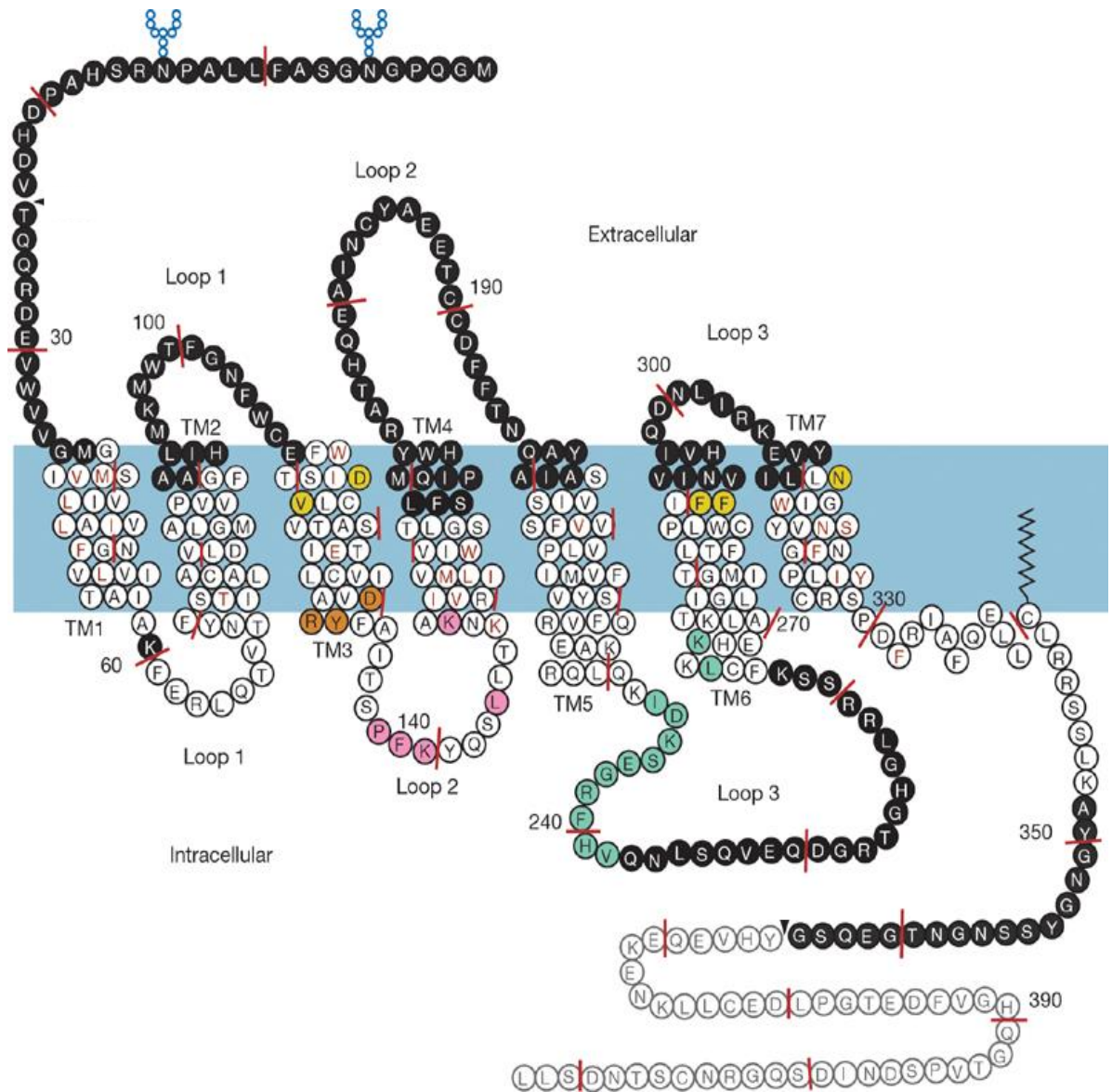


Figure 1.3 Schematic diagram of the β_2 AR. β_2 AR consists of seven transmembrane spanning alpha helices, with three extracellular loops, and three intracellular loops, with one being the amino-terminus and carboxy-terminus, respectively. Image from (Rasmussen, et al., 2007). The differing amino acid colouring represents a key for the crystallography studies described by Rasmussen et al (2007) but as this diagram is being used here to illustrate general modular structure the specifics are not required in this instance. TM (transmembrane domain). Amino acid abbreviations in appendix.

The amino acid sequence of a protein is not enough to relate shape to definitive function - for this, high-resolution crystal structures are vital. The three-dimensional (3D) structure allows visualisation of the spatial characteristics of each individual amino acid, and therefore can be used to predict sites of protein-protein interactions, in addition to assessing ligand binding pockets for pharmacological intervention. In the GPCR field, rhodopsin - a light sensitive receptor found within the retina - was the first receptor to be crystallised (Palczewski, et al., 2000). The elucidation of the crystal structure of rhodopsin made it feasible to predict the structures of other similar GPCRs, such as the β_2 AR, by using the rhodopsin coordinates as a template. It is prudent to note that although the template is useful to predict related GPCR structures, it is difficult to assess the changes of predicted structures such as the β_2 AR when bound to its agonist, as rhodopsin covalently binds its ligand 11-cis-retinal (Cherevoz, et al., 2007) (Rasmussen, et al., 2007) (Rosenbaum, et al., 2007) and this is markedly different to the ligand binding mode of the β_2 AR.

The crystal structure of the β_2 AR revealed that the receptor is composed of seven transmembrane helices, in addition to two additional helical segments. One of these segments is known as helix 8 and exists in other rhodopsin-like GPCRs (Katragadda, et al., 2004), whereas the other is a shorter helix - not present in the rhodopsin template - which is found in the middle of the second extracellular loop. Helix 8 has been shown to interact with transmembrane domain 1 to play a role in β_2 AR homodimer formation and in the delivery of functional β_2 AR complexes to the plasma membrane (Parmar, et al., 2016). The shorter helix has been shown to work in conjunction with a pair of disulphide bridges to promote ligand binding (Warne, et al., 2008). The crystal structure also revealed that the N-terminus (residues 1-28), the majority of the C-terminus (residues 343-365), and a stretch of 26 amino acids in the third intracellular loop are disordered (Cherevoz, et al., 2007) (Rasmussen, et al., 2011). It is thought that disordered areas must be unfolded to perform their functions, or they only fold when the β_2 AR interacts with other proteins or become post-translationally modified (Gunasekaran, et al., 2003) (Wright & Dyson, 2015).

1.3.2.1 β_2 AR Ligand Binding Pocket

The ligand binding site on the receptor is a narrow and deep cleft, located approximately one third of the way into the hydrophobic core of the β_2 AR. At this site, interactions between the amino acid residues on the β_2 AR and functional groups on the ligand promote ligand binding. These interactions were assessed using the ligand isoprenaline - the agonist used within this thesis to stimulate the β_2 AR - but other ligands will interact with the β_2 AR slightly differently dependent upon their molecular structure (Bang & Choi, 2015). There are specific residues which are important for ligand binding including aspartate residue 113 in domain III; serine residues 203 and 207 in domain V and asparagine residue 293 in domain VI (Liggett, 2002) (Strader, et al., 1988) (Strader, et al., 1989) (Wieland, et al., 1996) (Figure 1.4). Aspartate 113 forms an ion pair with the amino nitrogen on the ligand (Strader, et al., 1988); serines 203 and 207 interact with the hydroxyl groups on the phenyl ring of the ligand (Strader, et al., 1989); the asparagine 293 binds to the β -hydroxy group in the ligand (Wieland, et al., 1996). Following agonist binding, the receptor undergoes a conformational change. Initially transmembrane domain (TM) 5 moves inwards, resulting in TM6 to move outwards. This outwards swing is the largest change in receptor confirmation. The movement by TM6 mediates an outward movement of TM5, and an inward movement of both TM3 and TM7 to accommodate the β_2 AR- G_s protein interaction (Rasmussen, et al., 2011) (Rasmussen, et al., 2011) (Bang & Choi, 2015).

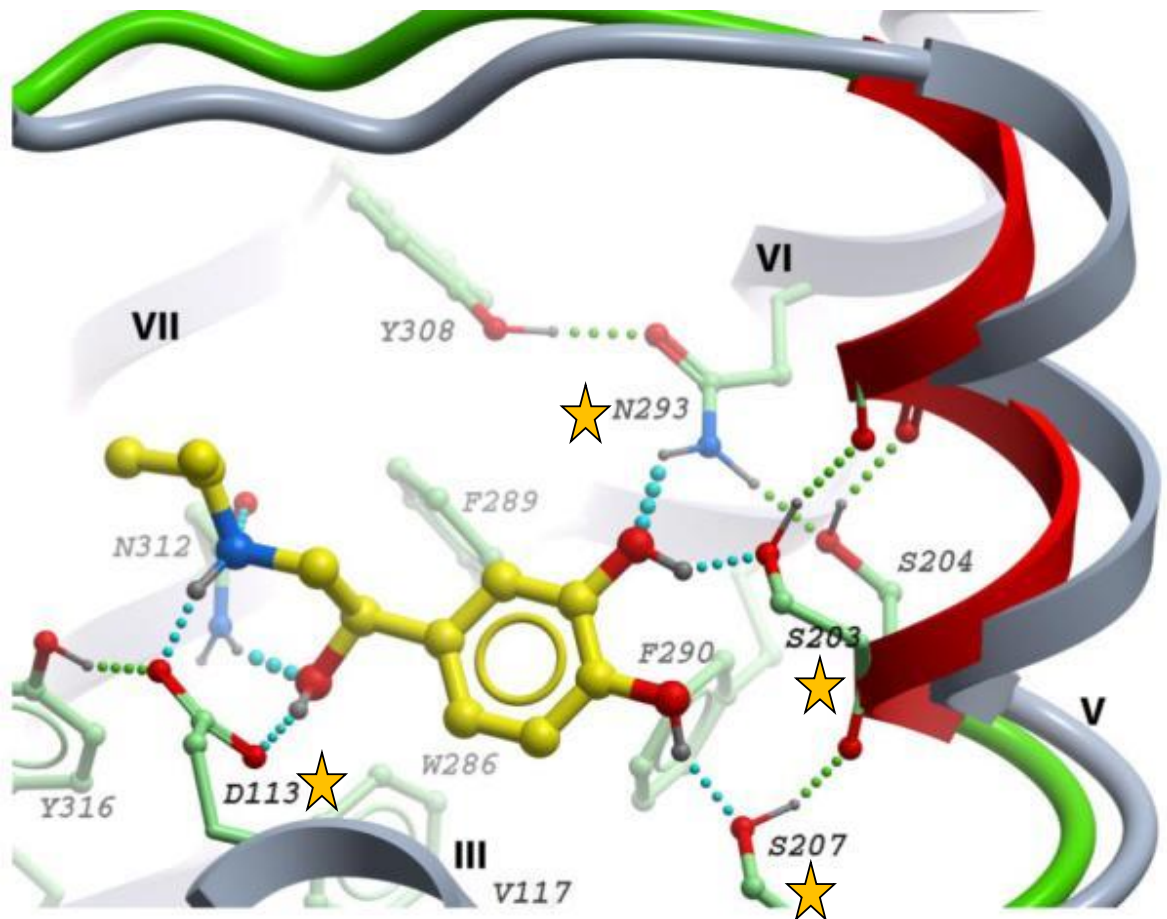


Figure 1.4 β_2 AR Ligand Binding Pocket. Residues which are important for ligand binding (highlighted by yellow star) include aspartate 113 (domain III), serines 203 and 207 (domain V) and asparagine 293 (domain VI). Aspartate 113 forms an ion pair with the amino nitrogen on the ligand, serines 203 and 207 interact with the hydroxyl groups on the phenyl ring of the ligand, and asparagine 293 binds to the β -hydroxy group in the ligand. Protein model shown as grey backbone, flexible backbone shown as green, extracellular portion shown as red, rigid side chains are grey sticks with grey carbon atom ball, flexible side chains are green sticks with green carbon atom ball, predicted ligand positioning in yellow with yellow carbon atom ball, hydrogen bonds between ligand and receptor represented by chain of cyan balls, intracellular hydrogen bonds imperative in formation of binding site represented by chain of green balls, hydrogen acceptors are blue sticks with blue ball. Amino acid abbreviations in appendix (Katritch, et al., 2009).

1.3.3 G Protein-Coupled Receptor (GPCR) Signal Transduction

The β_2 AR is a GPCR and following activation by agonist, GPCRs mediate signal transduction via G proteins. These proteins are part of the GTPase super family of enzymes which have intrinsic ability to hydrolyse the guanyl nucleotide guanine diphosphate (GDP) to guanine triphosphate (GTP). The G proteins can be divided into four subfamilies; G_s , $G_{i/o}$, $G_{q/11}$ and $G_{12/13}$ (Table 1.4). G proteins have three subunits; α , β , γ which are each encoded by a separate gene selected from 16 G_α , 6 G_β and 12 G_γ genes, respectively (Downes & Gautam, 1999). The G_α subunit is receptor specific, with the C-terminus of the subunit containing the receptor recognition domain. This G_α subunit can switch between an inactive and active conformation to mediate the signal transduction of GPCRs (Tesmer, et al., 1997). The β_2 AR mediates signal transduction via the G_s protein, with the capability to switch to the G_i protein (Daaka, et al., 1997).

Table 1.4 G protein families

Family	Members	Function
G_s	G_s and G_{olf}	Activate adenylyl cyclase (AC)
$G_{i/o}$	G_{i1} , G_{i2} , G_{i3} , G_{o1} , G_{o2} , G_z , G_{t1} , G_{t2} , and G_{gust}	Inhibit adenylyl cyclase (AC)
$G_{q/11}$	G_q , G_{11} , G_{14} , and $G_{15/16}$	Activate phospholipase C
$G_{12/13}$	G_{12} and G_{13}	Activate Rho guanine nucleotide exchange factors, Na^+ - H^+ exchanges and phospholipase- ϵ

(Riobi & Manning, 2005).

1.3.3.1 G Protein Cycling

When the GPCR is inactive, it is coupled to the inactive GDP-bound G_α subunit of the G protein. In this state, it has a high affinity for agonist. Upon agonist binding, the GPCR undergoes a conformational change which causes the G_α subunit to exchange GDP for GTP. This guanyl nucleotide change from GDP to GTP reduces the affinity of the receptor for the agonist, therefore increasing the probability of agonist dissociation. This results in a limitation in G protein activation. Another action mediated by the switch from GDP to GTP is the G_α subunit dissociating from the G_β and G_γ subunits. These subunits - G_β and G_γ - remain associated with the plasma membrane via prenylation at the G_γ subunit. G_α subunit and $G_\beta G_\gamma$ subunit

complex are capable of activating effectors to generate an intracellular second messenger and a physiological response. To return the system to the resting state, the intrinsic GTPase activity of the G protein is activated by a GTPase activating protein (GAPs). GAPs can be part of the signal transduction pathway which has been activated by initial agonist binding to the GPCR. The intrinsic GTPase activity means the G protein mediates the hydrolysis of the γ phosphate of GTP into GDP and an inorganic phosphate. The system is now reset with G_{β} G_{γ} subunit complex binding to the G_{α} subunit-GDP to allow for further agonist activation (Figure 1.5) (Billington & Penn, 2003) (Hamm, 1998) (Tuteja, 2009).

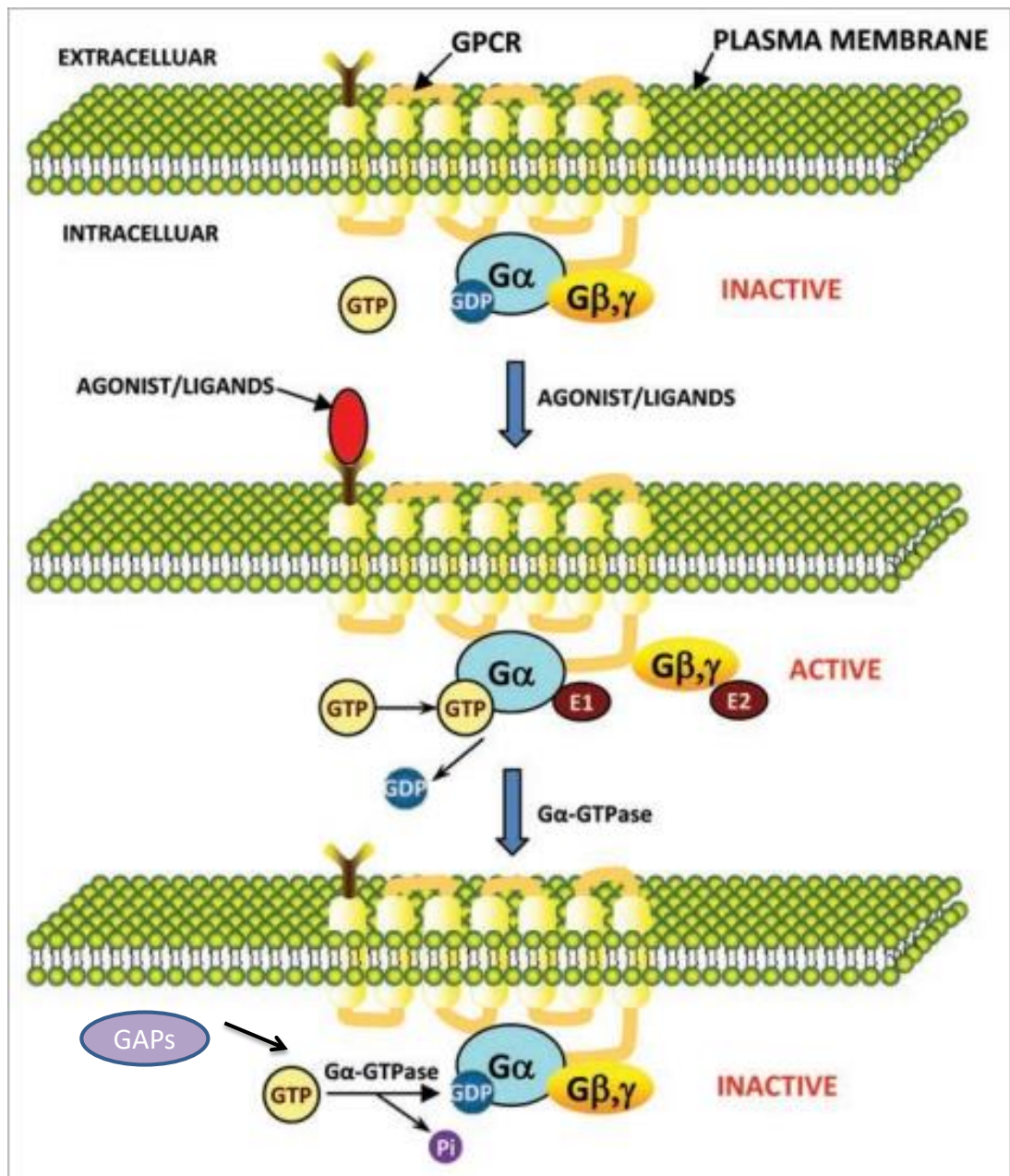


Figure 1.5 G protein cycling. Upon agonist binding to GPCR it undergoes a conformational change and the $G\alpha$ subunit switches GDP for GTP. The $G\alpha$ subunit now dissociates from $G\beta$ $G\gamma$ subunit complex. $G\beta$ $G\gamma$ complex remains associated with the plasma membrane via prenylation at the $G\gamma$ subunit. The free subunits can activate effectors to mediate intracellular effects. The system returns to its original state when the intrinsic GTPase activity of the G protein is activated by GAPs resulting in the hydrolysis of the γ phosphate of GTP into GDP and an inorganic phosphate. GPCR (G protein-coupled receptor), GTP (guanosine triphosphate), GDP (guanosine diphosphate), E1/2 (effector 1/2), GAPs (GTPase activating protein), Pi (inorganic phosphate) (Tuteja, 2009).

1.3.4 β_2 AR Signalling

1.3.4.1 Agonist-Mediated β_2 AR Activation

Upon agonist binding, the β_2 AR mediates activation of adenylyl cyclase (AC) via the stimulatory G protein (G_s) (Figure 1.6). The ratio β_2 AR : G_s : AC is approximately 1 : 100 : 3 therefore receptor activation of G_s is considered the most critical event for signal amplification (Alousi, et al., 1991) (Ostrom, et al., 2000).

The majority of AC isoforms are membrane bound, however a soluble isoform also exists. The AC enzyme contains two cytosolic catalytic and two integral membrane domains, with each domain containing six transmembrane alpha helices (Tang & Gilman, 1992) (Tesmer, et al., 1997). The cytosolic catalytic domains possess specific binding sites for G protein subunits and when the G_α subunit of the G_s protein stimulates the catalytic domains, this initiates the conversion of ATP to cyclic adenosine monophosphate (cAMP) - the intracellular second messenger which can go on to activate multiple targets, one of which is protein kinase A (PKA) (Figure 1.6). This occurs within milliseconds/seconds of receptor stimulation (Hein, et al., 2006) (Violin, et al., 2008).

PKA is a cAMP-dependent kinase that can phosphorylate a large number of proteins - on serine or threonine residues - leading to tailored physiological responses. PKA is a cytosolic protein therefore, it must be localised to the vicinity of the β_2 AR. Spatial compartmentation of the β_2 AR and PKA is achieved by PKA anchoring to scaffold proteins known as A-kinase anchoring proteins (AKAPs) (Chen & Malbon, 2009) (Fan, et al., 2001). AKAPs bind to the regulatory subunits of PKA and limit the pool of PKA to the vicinity of the β_2 AR (Wang, et al., 2006). PKA activation is the most common mechanism by which the β_2 AR signals, but it can also mediate effects via G_i proteins, which oppose G_s and acts to inhibit AC (Figure 1.6) (Daaka, et al., 1997). This occurs because the β_2 AR itself is a target for PKA phosphorylation. The consensus sequences for PKA-mediated phosphorylation fall within the C-terminus of intracellular loop 3 (serines 261 and 262) and in the proximal cytoplasmic tail (serines 345 and 346), but the former is the preferred substrate (Bouvier, et al., 1989). Direct phosphorylation of the β_2 AR by PKA results in reduced coupling between the β_2 AR and G_s , switching it to G_i , with a mutant

β_2 AR lacking these phospho-sites incapable of signalling via G_i (Hausdorff, et al., 1989) (Strulovici, et al., 1984) (Daaka, et al., 1997). In the active state the G_{α} -GTP subunit of G_i dissociates from the $G_{\beta}G_{\gamma}$ subunit complex and these free $G_{\beta}G_{\gamma}$ subunits mediate activation of the mitogen-activated protein kinase (MAPK) signalling pathways, such as extracellular signal regulated kinase (ERK) (Figure 1.6).

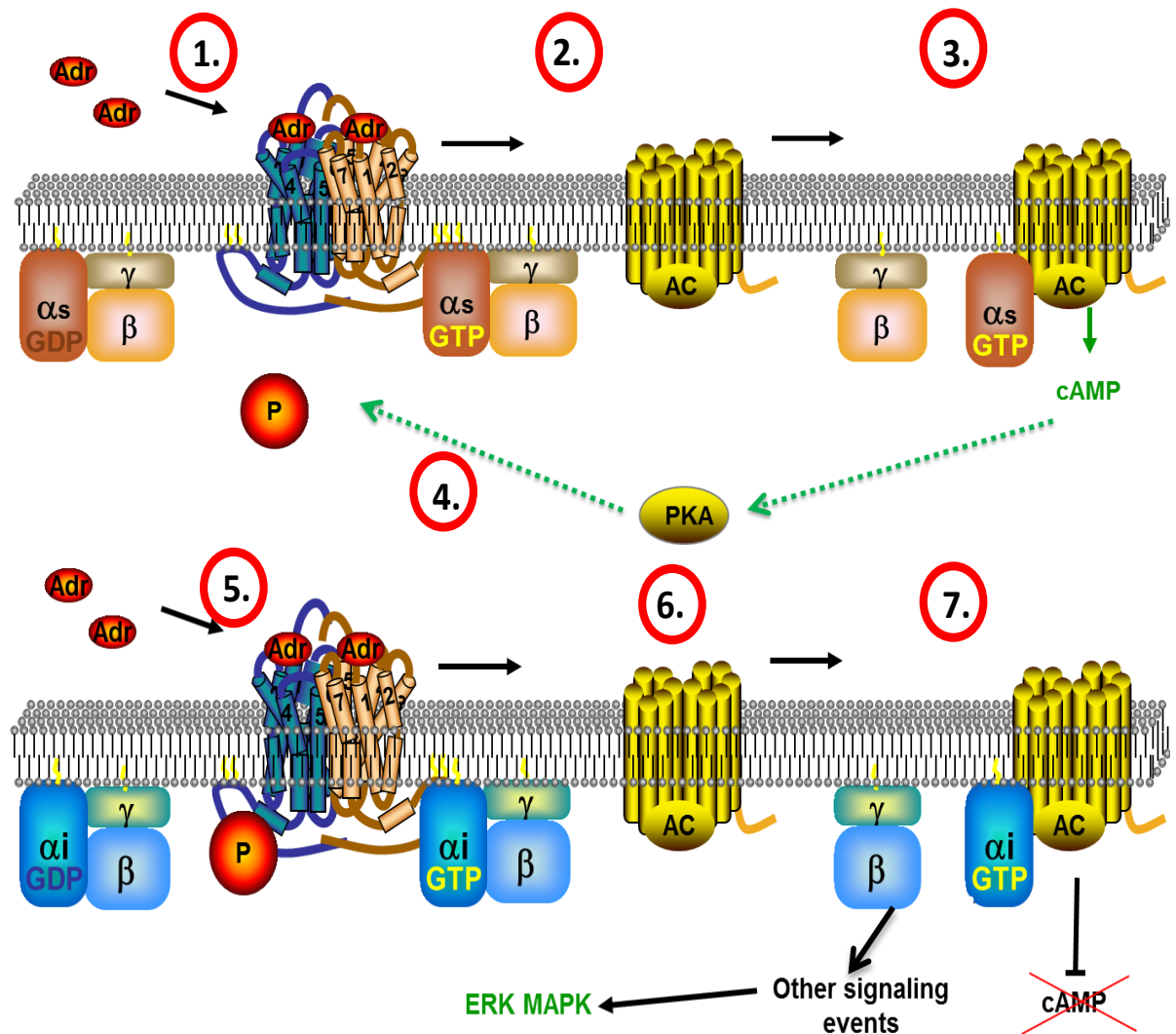


Figure 1.6 Agonist-mediated β_2 AR activation. Upon agonist binding (1) the β_2 AR activates AC via the G_s protein (2). AC initiates the conversion of ATP to cAMP (3). cAMP is the intracellular second messenger which can go on to activate multiple targets, one of which is PKA. The β_2 AR is a target for PKA (4). This PTM of the β_2 AR results in reduced coupling between the β_2 AR and G_s , and switches it to G_i (5). In the active state, the G_{α} -GTP subunit of G_i dissociates from the G_{β} G_{γ} subunits. G_{α} mediates inhibition of AC (6&7) and the free G_{β} G_{γ} subunits mediate activation of the MAPK signalling pathway such as ERK (7). β_2 AR (beta 2 adrenergic receptor), Adr (adrenaline), GDP (guanosine diphosphate), GTP (guanosine triphosphate), AC (adenylyl cyclase), PKA (protein kinase A), cAMP (cyclic adenosine monophosphate), P (phosphate), ERK MAPK (extracellular signal regulated kinase mitogen-activated protein kinase).

1.3.5 β_2 AR Signalling Regulation

Receptor signalling is subject to regulatory mechanisms to prevent constant signalling in response to continuous agonist exposure. Cells mediate this by regulating the expression, localisation and activity of all signalling molecules involved. Common mechanisms directly related to the receptor include desensitisation, resensitisation and down-regulation.

1.3.5.1 β_2 AR Desensitisation

Desensitisation acts as a safety device to prevent the over stimulation of receptors by excessive agonist stimulation. The extent of desensitisation depends upon the degree and duration of the β_2 AR agonist response. There are two types of desensitisation; homologous and heterologous. Homologous desensitisation occurs via direct agonist stimulation of the β_2 AR, whereas heterologous desensitisation occurs when the receptor becomes desensitised even without agonist occupancy (Litalien & Beaulieu, 2011).

For homologous desensitisation, the β_2 AR is agonist-occupied leading to the following: phosphorylation of the receptor by both G protein receptor kinases (GRK) family members and PKA; β -arrestin recruitment, and uncoupling of receptors from the G_s protein. As mentioned above, PKA can phosphorylate the receptor leading to a switch from G_s to G_i signalling (Figure 1.6). This occurs within seconds of agonist binding (Yuan, et al., 1994). This acts as a method of desensitisation as regardless of agonist occupancy, the receptor will not allow further cAMP production via the G_s pathway. Additionally, as the G_s pathway stimulates AC, the G_i pathway inhibits AC; therefore the combination of both AC inhibition and functional uncoupling from G_s will inhibit the β_2 AR-mediated cAMP signal (Daaka, et al., 1997).

The β_2 AR can be phosphorylated by GRKs and, similarly to PKA phosphorylation of the receptor, this also occurs within seconds of agonist binding (Figure 1.7). The first of these kinases was discovered during the studies comparing the β_2 AR with the rhodopsin receptor, and was initially named BARK (Benovic, et al., 1987). After this, other GRKs were identified and BARK was renamed GRK2. GRK isoforms are capable of phosphorylating the β_2 AR at multiple residues within the C-terminus

of the receptor including serines 355, 356, 364 and threonine 360 (Vaughan, et al., 2006) (Nobles, et al., 2011). This phosphorylation initiates the recruitment of the scaffold protein β -arrestin1/2 to the membrane (Krasel, et al., 2005) (Figure 1.6). A scaffold protein often acts to bring other proteins into close proximity allowing specific protein-protein interactions to occur. Although PKA phosphorylation of the β_2 AR reduces coupling between the receptor and G_s - it does not promote β -arrestin binding or internalisation, unlike GRK phosphorylation (Billington & Penn, 2003). Another difference between PKA and GRK-mediated phosphorylation is that PKA-mediated phosphorylation does not require agonist occupancy, whereas GRK-mediated phosphorylation is agonist-dependent (Nobles, et al., 2011).

The scaffold protein β -arrestin binding to the receptor sterically uncouples the β_2 AR from the G_α subunit of G_s protein therefore preventing further cAMP production via the agonist-dependent G_s pathway. This occurs within a minute following agonist treatment (Violin, et al., 2008) (Oakley, et al., 2000). Krasel et al (2005) identified that both subtypes of β -arrestins (1 and 2) are capable of binding to the β_2 AR but studies in knockout mice have identified that β -arrestin 2 has a higher affinity for the receptor than β -arrestin 1 (Kohout, et al., 2001). The affinity of β -arrestin for the receptor is dependent upon two factors; agonist occupancy and phosphorylation (Violin, et al., 2006). Phosphorylation of serines 355, 356 and 364 - which are susceptible to GRK agonist-mediated phosphorylation - in the cytoplasmic tail of the β_2 AR are crucial for β -arrestin- β_2 AR interaction (Vaughan, et al., 2006). β -arrestin also plays an additional role in β_2 AR desensitisation by acting as a protein scaffold to either mediate arrestin-biased signalling pathways, or to inhibit the existent G_s signal.

In addition to sterically uncoupling the β_2 AR from the G_α subunit of G_s protein, another desensitising function of β -arrestin is that it recruits phosphodiesterase 4 (PDE4) to activated receptors (Perry, et al., 2002) (Figure 1.7). This enzyme acts to hydrolyse locally generated cAMP to 5'-AMP. Hence, the recruitment of arrestin-PDE4 complex dually desensitises by concomitantly uncoupling G_s signalling and promoting degradation of the second messenger cAMP. Multiple isoforms of cAMP PDEs have been identified (Rabe, et al., 1993) and are known to degrade cAMP to 5'-AMP. The expression of specific isoforms of cAMP PDEs is

induced by an increase in intracellular cAMP, which is initiated by β_2 AR activation and serves as a means of termination of signal, by reducing cAMP and therefore reducing PKA activity.

Furthermore, in addition to inhibiting G_s signalling, β -arrestin can initiate alternate signalling cascades by selectively scaffolding signalling cascade components including small GTP binding proteins and members of the MAPK cascade (Lefkowitz, et al., 2006) (Lefkowitz & Shenoy, 2005). This was first observed for the non-receptor tyrosine kinase Src. Following agonist stimulation of the β_2 AR, arrestin mediates the formation of a complex which consists of arrestin, β_2 AR and Src. This complex has been shown to be essential in β_2 AR-mediated ERK1/2 activation (Luttrell, et al., 1999).

Heterologous desensitisation occurs when the receptor becomes desensitised without agonist occupancy. This can occur via other GPCRs signalling pathways stimulating proteins that are involved in the β_2 AR signalling pathway. For example, other GPCRs which mediate their effects via G_s , such as the histamine H2 receptor, can go on to mediate phosphorylation of the β_2 AR via cAMP elevation and subsequent increase in PKA activity (Johnson, 1998) (Hill, et al., 1997). This type of modulation means the β_2 AR can be influenced by steroid hormones, inflammatory mediators and other agents (Pelaia & Marsico, 1994).

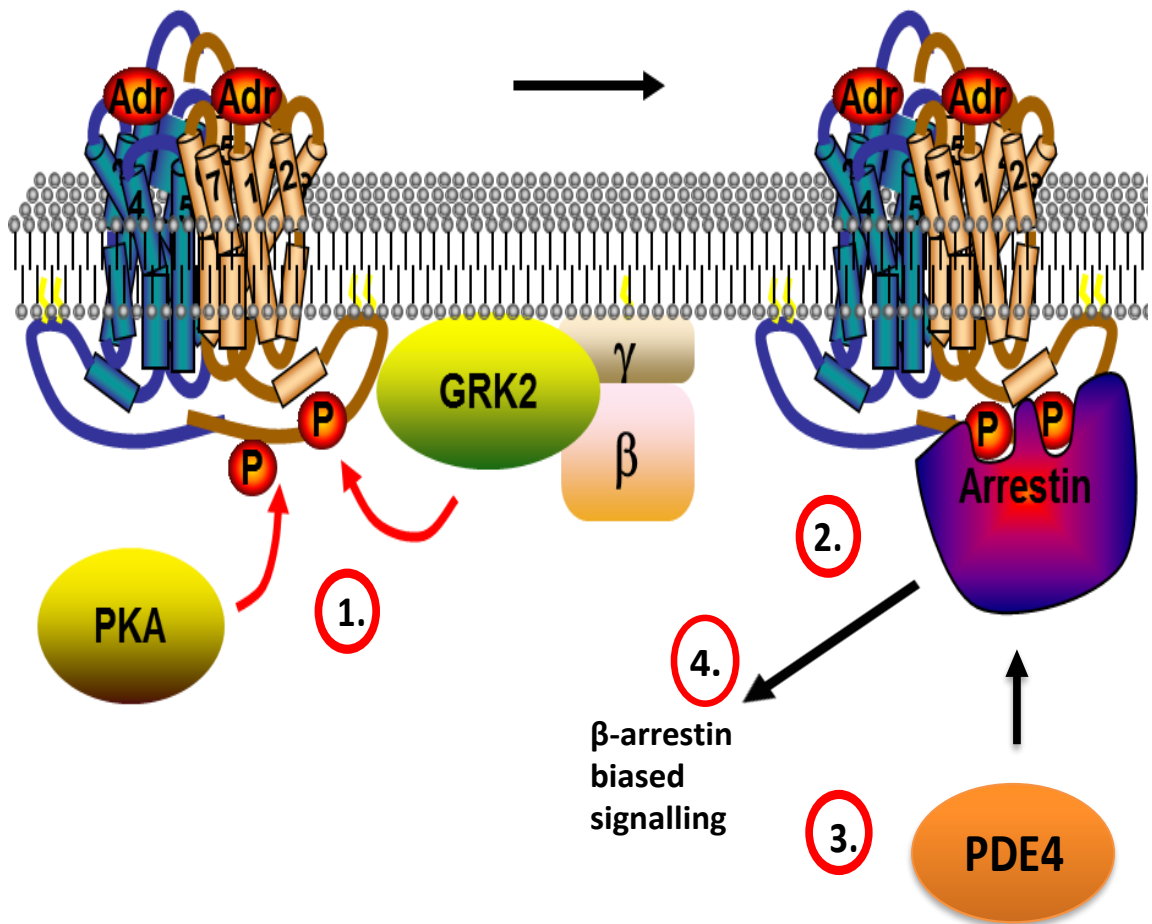


Figure 1.7. β_2 AR desensitisation. β_2 AR is susceptible to phosphorylation by both GRK and PKA. Phosphorylation functionally uncouples the receptor from G_s (1). GRK sites of phosphorylation have been shown to be vital for β -arrestin- β_2 AR interaction (2). β -arrestin brings phosphodiesterase 4 (PDE4) into the receptors environment to metabolise locally generated cAMP and terminate the effects of receptor signalling via the G_s protein (3). β -arrestin can mediate biased signalling (4). Adr (adrenaline), PKA (protein kinase A), P (phosphate), GRK2 (G protein-coupled receptor kinase), PDE4 (phosphodiesterase 4).

1.3.5.2 β_2 AR Internalisation

When the β_2 AR is either phosphorylated by PKA or interacting with β -arrestin following GRK phosphorylation, the receptor is functionally uncoupled from G_s . The next step is for the cell to physically remove the β_2 AR from the cell surface. This is termed internalisation and occurs within approximately three minutes of receptor agonist stimulation (Morrison, et al., 1996). When the receptor is internalised, it is moved away from the cell surface and localised within endosomal compartments, which are formed from endocytosis of plasma membrane fragments that contain the embedded β_2 AR (Kallal, et al., 1998) (Figure 1.8). When β -arrestin translocates to the receptor in response to agonist stimulation and subsequent GRK phosphorylation, it not only co-localises with the β_2 AR, but also with clathrin - the major structural component of the coated pits formed during membrane endocytosis (Goodman, et al., 1996) (Figure 1.8). The arrestin-receptor complex then interacts with the adaptor protein 2 (AP-2) of clathrin, initiating the formation of the clathrin coated endosome (Laporte, et al., 2000) in which the receptor is contained. The interaction between β -arrestin and the β_2 AR is a prerequisite for the receptor internalisation, as internalisation was prevented in β -arrestin knockout mouse embryonic fibroblast cells (Kohout, et al., 2001). An additional requirement for internalisation is β -arrestin ubiquitination - a PTM in which a small ubiquitin protein is covalently attached to a lysine on the target protein (Shenoy, et al., 2001) (Figure 1.8). Ubiquitination of arrestin is encouraged by the scaffold forming a complex with mouse double minute 2 homolog (MDM2) - an ubiquitin E3 ligase (Ferguson, et al., 1996) (Wang, et al., 2003). The ubiquitin E3 ligase is the final enzyme in the ubiquitination pathway which underpins the specificity of ubiquitin ligation to a specific lysine residue on the target protein. Although the MDM2- β -arrestin interaction occurs prior to membrane co-localisation with the β_2 AR, it is thought the arrestin only becomes ubiquitinated when it interacts with the β_2 AR, as this changes arrestin conformation exposing the susceptible lysine residues (Shenoy, et al., 2008).

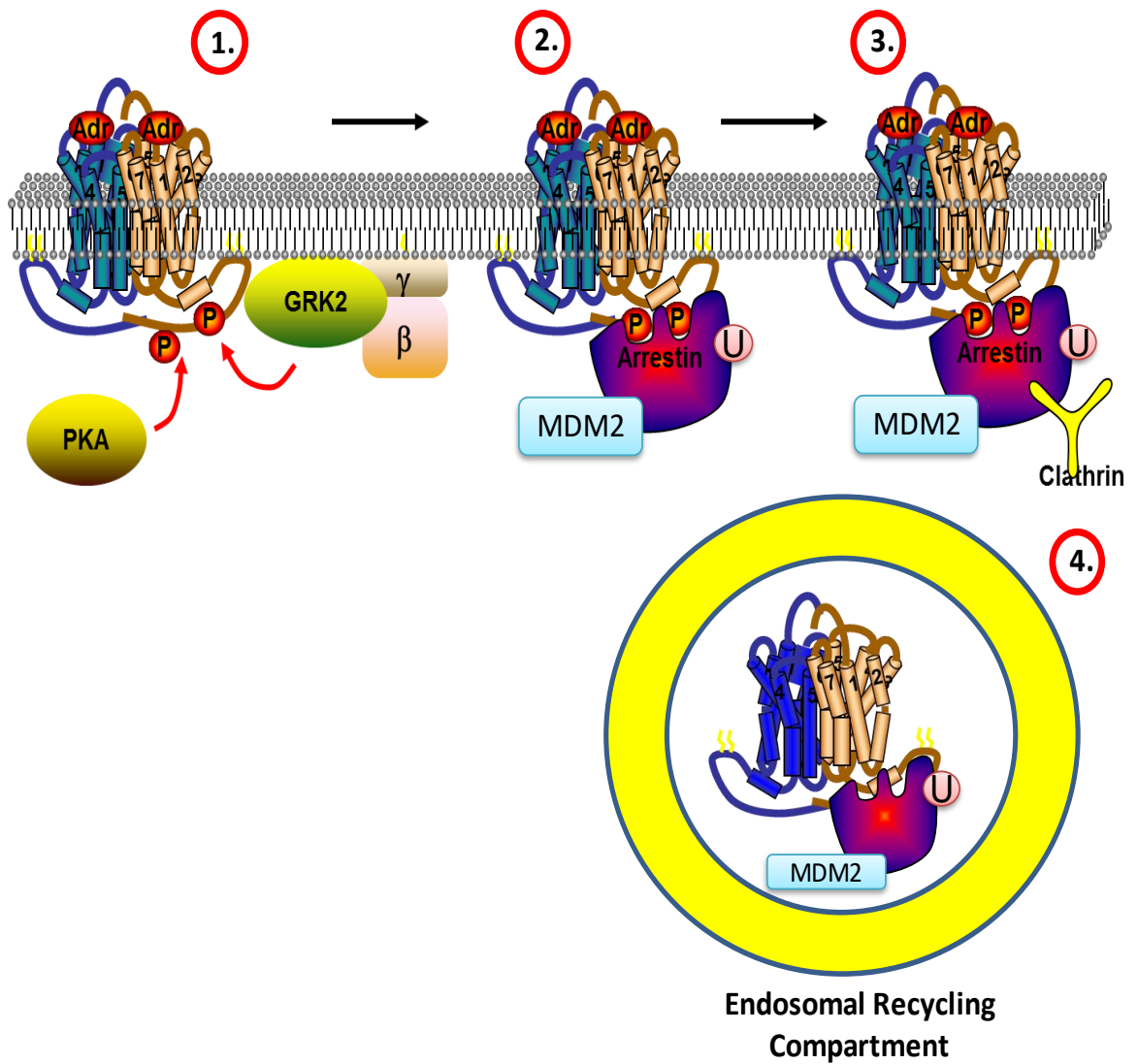


Figure 1.8 β_2 AR internalisation. β_2 AR is phosphorylated by PKA/GRK (1) and interacts with β -arrestin to functionally uncouple the receptor from G_s (2). β -arrestin is associated with scaffold proteins such as E3 ligase MDM2 and clathrin. β -arrestin ubiquitination occurs when the interaction between β_2 AR- β -arrestin changes the conformation of β -arrestin making it susceptible to ubiquitination (2). β -arrestin also interacts with clathrin, initiating the formation of the clathrin coated endosome in which the receptor is contained (3&4). β_2 AR (beta 2 adrenergic receptor), Adr (adrenaline), PKA (protein kinase A), P (phosphate), GRK2 (G protein-coupled receptor kinase), MDM2 (mouse double minute 2 homolog), U (ubiquitin).

1.3.5.3 β_2 AR Resensitisation

Internalisation of the receptor is vital for preventing excessive receptor response via G_s (Freedman & Lefkowitz, 1996) in the presence of prolonged agonist exposure, but this is not its only purpose. Within the endosomal compartments the receptor can be dephosphorylated by the phosphatase 2A enzyme, and recycled back to the plasma membrane where the receptor appears in a resensitised state capable of signalling once again in response to agonist (Pipping, et al., 1995) (Barak, et al., 1997) (Krueger, et al., 1997) (Figure 1.9). Internalisation is therefore vital for resensitisation as otherwise phosphatase 2A would not have access to the receptor. An additional protein which is important to this process is N-ethylmaleimide-sensitive factor (NSF) (Figure 1.9). This is an enzyme which is involved in membrane fusion processes (Furst, et al., 2003). The β_2 AR has been shown to interact with NSF, and this interaction is vital for recycling of the receptor to the cell surface (Cong, et al., 2001). This resensitisation is a rapid process with receptors being rapidly recycled to the surface within approximately 8 minutes of being internalised (Pipping, et al., 1995) (Zhang, et al., 1997) (Morrison, et al., 1996) (Hertel & Staehelin, 1983).

A novel role for internalisation is now known; namely endosomal signalling. Traditionally GPCRs signalling via G_s produced cAMP via activation of AC at the cell membrane, however it is now known that G_s -GPCRs can also initiate cAMP generation from within the endosomal compartments. This has been studied for the thyroid stimulating hormone (TSH) receptor in which a complex of G_s , AC and the receptor itself was internalised allowing continuation of cAMP production. Additionally, the signals generated by cAMP produced at the endosome differed from those generated by cAMP at the cell membrane (Calebiro, et al., 2009). A similar situation has been observed for the GPCR parathyroid hormone receptor (PTHr), in which alternate agonists mediate either signalling from the endosomal compartment or at the membrane surface. This can explain how different agonists, with a common receptor, can mediate distinct cellular outcomes (Ferrandon, et al., 2009). There is now evidence for endosomal signalling by the β_2 AR. Irannejad et al (2013) revealed that in HEK293 cells isoprenaline promoted cAMP production at the plasma membrane via the β_2 AR as expected, but also in the early endosome. Furthermore, inhibition of endocytosis led to a reduction in cAMP production mediated via the β_2 AR (Irannejad, et al., 2013). This group

propose that $\beta_2\text{AR-G}_s$ coupling occurs in the early endosome, promoting a discrete phase of cAMP production (Irannejad & Von Zastrow, 2014).

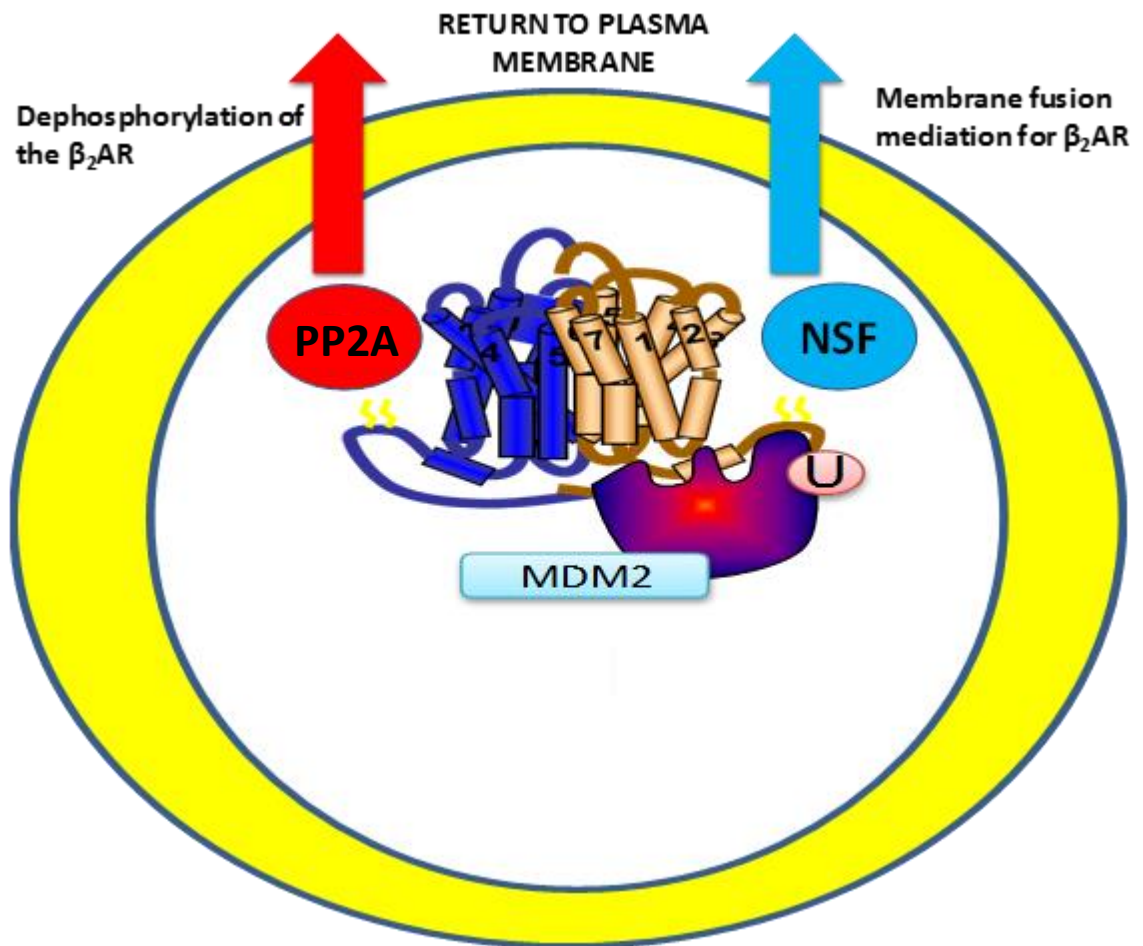


Figure 1.9 β_2 AR resensitisation. Within endosomal compartments the β_2 AR can be dephosphorylated by PP2A and recycled back to the plasma membrane where it appears in a resensitised state capable to respond to agonist again. The β_2 AR has been show to interact with NSF for recycling of the β_2 AR to the cell surface. PP2A (phosphatase 2A), β_2 AR (beta 2 adrenergic receptor), NSF (N-ethylmaleimide-sensitive factor), U (ubiquitin), MDM2 (mouse double minute 2 homolog).

1.3.5.4 β_2 AR Down-Regulation

Although internalisation of the β_2 AR is necessary for recycling of the receptor back to the plasma membrane, this is not the only fate for internalised β_2 AR. These receptors can be degraded leading to a permanent reduction in receptor density, thus diminishing β_2 AR responsiveness to subsequent exposure of ligand (Moore, et al., 1999) (Futter, et al., 1996). The two common methods of protein degradation are via lysosomal or proteasomal degradation. Lysosomes are membrane-enclosed organelles that contain an array of digestive enzymes including several proteases. These act to degrade all kinds of biomolecules including proteins, carbohydrates, nucleic acids, lipids and cellular debris (Cooper, 2000). In contrast, proteasomes are cylindrical protein complexes that only degrade proteins which have been marked for degradation by the PTM ubiquitination (Naujokat & Hoffman, 2002).

In the presence of a proteasomal inhibitor (MG132), ubiquitinated proteins accumulate, indicative of a lack of protein degradation at the proteasome. Shenoy et al (2001) identified that in the presence of MG132, the degradation of the β_2 AR-mediated by isoprenaline was inhibited. However, even without proteasomal inhibition, the ubiquitinated form of the β_2 AR was identified, suggesting that the ubiquitinated β_2 AR was not an immediate target for proteasomal proteases (Shenoy, et al., 2001). Although 26S proteasomes often degrade ubiquitinated substrates, it has recently become clear that they also play roles in targeting ubiquitinated membrane proteins to lysosomes (Yu & Malek, 2000). In support of this, Moore et al (1999) showed that the internalised β_2 AR can be targeted to lysosomes via transport by the endosomal compartments. Ubiquitination of the receptor still plays a role in mediating degradation at lysosomes as a β_2 AR mutant which lacked lysine residues could be internalised but was not degraded. The enzyme MDM2 which mediates β -arrestin ubiquitination can also mediate receptor ubiquitination. However, ubiquitination of the receptor and subsequent degradation can occur in the absence of MDM2. This implied that the receptor could be ubiquitinated by an alternative E3 ligase, namely neural precursor cell expressed developmentally down-regulated protein 4 (NEDD4) (Shenoy, et al., 2008). Shenoy et al (2008) identified that β -arrestin2 recruits NEDD4 to the receptor- β -arrestin complex within the endosome, dependent upon specific conformational changes in β -arrestin2 when held by the activated β_2 AR. The Shenoy group hypothesised that NEDD4 displaces MDM2 (Figure 1.10). Thus β -

arrestin binds at least two E3 ubiquitin ligases; MDM2 which mediates β -arrestin ubiquitination and regulates the initial step of receptor endocytosis, and NEDD4 which mediates receptor ubiquitination, within the endosome, that targets receptors to lysosomal compartments. The process of down-regulation occurs after approximately 6 hours of agonist stimulation (Moore, et al., 1999).

Following down-regulation of the β_2 AR, transcription at the gene level and post-translational conversion of mRNA (molecules which direct ribosomal production of the protein) to protein is now required to restore the membrane complement of β_2 AR. In addition to prolonged agonist stimulation mediating down-regulation of the β_2 AR receptor protein from the membrane surface, a decrease in the expression of β_2 AR mRNA levels has also been reported in several cell lines, therefore inhibiting the synthesis of further receptors during periods of high agonist exposure (Bouvier, et al., 1989) (Hadcock, et al., 1989). However, even with reduced synthesis, the existent β_2 ARs have a half-life of up to approximately 30 hours (Mahan & Insel, 1986) (Fraser & Venter, 1980) therefore receptor degradation is imperative during high levels of agonist exposure.

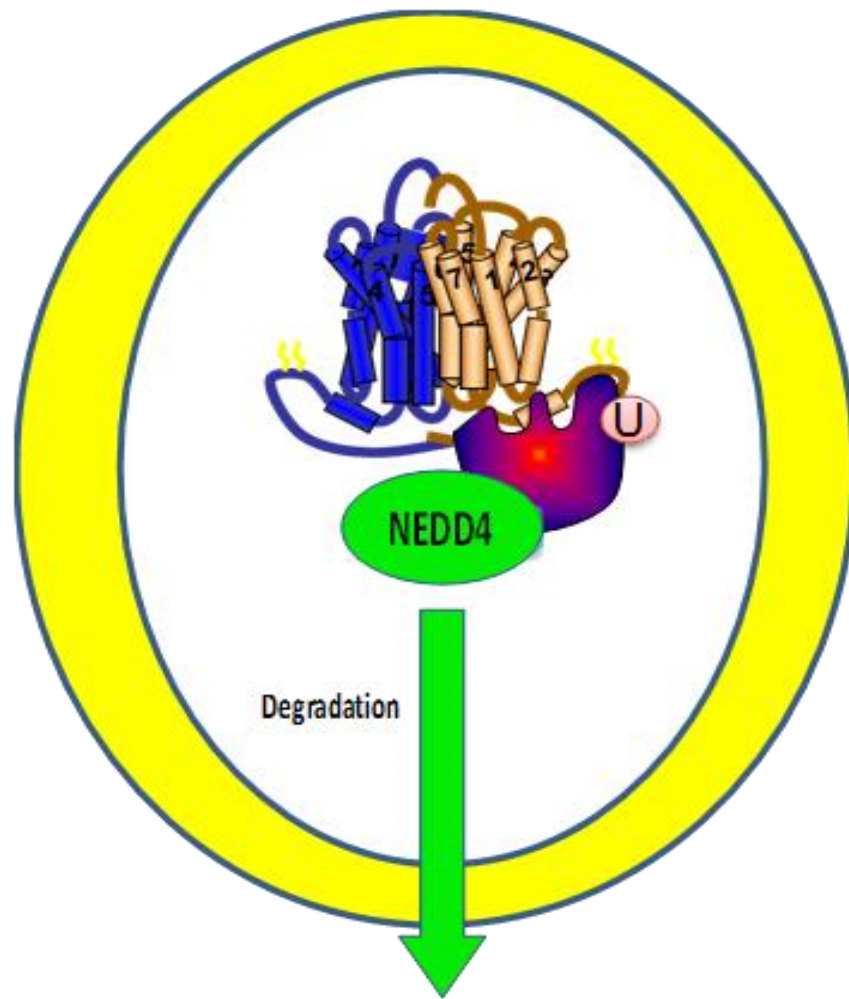


Figure 1.10 β_2 AR down-regulation. For down-regulation β -arrestin2 recruits NEDD4 to the receptor- β -arrestin complex within the endosome. NEDD4 displaces MDM2 and acts to ubiquitinate the receptor within the endosome. This targets receptors to lysosomal compartments for down-regulation. β_2 AR (beta 2 adrenergic receptor), U (ubiquitin), NEDD4 (neural precursor cell expressed developmentally down regulated protein 4).

1.3.6 β_2 AR Dimerisation

The capability of β_2 AR to form dimers (a complex of two proteins) and oligomers (complex of three proteins or more) is uncertain. Conflicting reports both support (Calebiro, et al., 2013) (Angers, et al., 2000) (Mercier, et al., 2002) and refute (Kawano, et al., 2013) (Felce, et al., 2014) this notion. The uncertainty is believed to come from the methods used to study interactions between integral membrane proteins, as biochemical methods are not appropriate to assess interactions between transmembrane proteins. For this reason, biophysical methods that can be applied to receptors in living cells have been utilised such as BRET (see Chapter 2 - General Materials and Methods). The following discusses dimer relationships that have been reported to occur (Lan, et al., 2015).

1.3.6.1 Homodimerisation

Homodimerisation occurs when two identical receptors form a complex. It has been identified that the β_2 AR forms a homodimer in HEK293 cells and agonists can interact with the homodimers at the cell surface (Angres, et al., 2000). It is believed these homodimers are formed during endoplasmic reticulum processing or trafficking to cell surfaces (Salahpour, et al., 2004). It has been reported that prevention of homodimerisation results in reduced β_2 AR signalling, suggesting that dimer formation is important for normal function (Hebert, et al., 1996).

1.3.6.2 Heterodimerisation

Heterodimerisation occurs when two distinct receptor types form a complex. The β_2 AR has been shown to form heterodimers with both the β_1 AR and α_{1A} adrenergic receptor (α_{1A} AR) (Mercier, et al., 2002) (Lavoie, et al., 2002) (Uberti, et al., 2005). These dimers mediate different receptor characteristics. The formation of the α_{1A} AR- β_2 AR dimer promotes cell surface expression of the α_{1A} AR, whereas formation of the β_1 AR- β_2 AR dimer inhibits β_2 AR internalisation. This reduction in internalisation results in the β_2 AR behaving in a manner characteristic of the β_1 AR. In addition, the β_1 AR- β_2 AR dimer inhibits the β_2 AR from activating the G_i pathway (Lavoie, et al., 2002). A third dimer has also been identified to exist between the β_2 AR and the prostanoid EP1 receptor (McGraw, et al., 2006). Formation of this

dimer allows the EP1 receptor to influence β_2 AR signalling - activation of EP1 receptor results in a loss of isoproterenol-mediated relaxation in murine airway smooth muscle cells. It is believed this effect is steric, and influences the β_2 AR coupling to G_s . Activation of the prostanoid EP1 receptor had no direct physiological action itself, thus it was suggested that the EP1 receptor only functions in conjunction with the β_2 AR to form a signalling unit in airway smooth muscle cells (McGraw, et al., 2006).

1.3.7 β_2 AR Gene Polymorphisms

The β_2 AR gene is polymorphic which means it can exhibit multiple genetic variants. Initially 9 polymorphisms were identified (Reihause, et al., 1993), but it has now been discovered that 49 polymorphisms exist (Hawkins, et al., 2006). Only 4 single nucleotide polymorphisms in the coding region of the receptor - at codons 16, 27, 34 and 164 - result in amino acid changes and therefore may influence function. Several mechanisms by which polymorphisms of the β_2 AR might influence the function of the receptor were proposed. Polymorphisms at codon 34 may influence receptor expression at the translational level (McGraw, et al., 1998). A rare polymorphism at amino acid position 164 (Thr to Ile) influences the ability of the receptor to bind agonist and couple to G protein (Green, et al., 1993). N terminal polymorphisms at amino acid positions 16 and 27 are thought to affect receptor down-regulation (Green, et al., 1995) (Green, et al., 1994).

1.3.8 Post-Translational Modifications (PTMs) of the β_2 AR

PTMs play an important role in the function of the β_2 AR such as phosphorylation initiating the switch from G_s to G_i , as well as β -arrestin binding, and ubiquitination being vital for receptor down-regulation. However, there are other PTMs which are also of importance.

1.3.8.1 Glycosylation of the β_2 AR

The β_2 AR has been shown to undergo both N- and O- linked glycosylation, a PTM in which a carbohydrate group is attached to a hydroxyl or another functional group on a protein (Rands, et al., 1990) (Benya, et al., 2000) (Sadeghi & Birnbaumer, 1999). There are three sites on the human β_2 AR which are susceptible

to glycosylation; asparagines 6, 15 (found within the N-terminus) and 187 (found within extracellular loop 2) (Rands, et al., 1990) (Li, et al., 2017) (Mialet-Perez, et al., 2004). In 1990, Rands et al identified that mutagenesis of sites 6 and 15 resulted in impaired β_2 AR membrane insertion, while Mialet-Perez et al (2004) identified that lack of glycosylation at site 187 results in receptors which do not down regulate due to the lack of lysosomal sorting. This is in conflict with reports from Li et al (2017) who found that N-glycosylation of the β_2 AR does not affect membrane insertion. The Li group report that deletion of sites 6 and 15 resulted in decreased cAMP accumulation, β -arrestin2 recruitment, receptor internalisation and receptor dimer formation. They did not find any impact of site 187 deletion on receptor expression, G protein-dependent signalling, β -arrestin recruitment, receptor internalisation or receptor dimerisation (Li, et al., 2017). Further work is needed to confirm the role of β_2 AR glycosylation.

1.3.8.2 Palmitoylation of the β_2 AR

The β_2 AR has been shown to undergo palmitoylation at cysteine 341 (Ovchinnikov, et al., 1988). This is a PTM in which fatty acids such as palmitic acid are attached to cysteine residues. If this cysteine is mutated to a serine it results in a reduced ability of the β_2 AR to stimulate AC in an agonist-dependent manner - suggesting palmitoylation at this site may be required for adequate G_s - β_2 AR coupling. This mutated form of the receptor also has an impaired ability to form a high affinity state for agonist - characteristic of an uncoupled form of the receptor (De Lean, et al., 1980) (O'Dowd, et al., 1988). Palmitoylation at this site has also been shown to influence phosphorylation and desensitisation of the β_2 AR (Moffett, et al., 2001). Moffett et al (2001) propose that agonist stimulation of the β_2 AR mediates depalmitoylation of cysteine 341 which releases the cytoplasmic tail of the β_2 AR from the plasma membrane. Serines 345 and 346 are now exposed for phosphorylation by PKA which initiates phosphorylation of the downstream serines by GRK2.

1.4 SUMOylation

SUMOylation is a PTM in which a small SUMO (small ubiquitin-like modifier) protein is covalently linked to a lysine residue on the substrate protein. Much like other PTMs, this SUMO modification can act to regulate protein-protein interactions, intracellular localisation or directly change the activity of the target protein (Gareau & Lima, 2010).

1.4.1 The SUMO Paralogues

The SUMO protein family was discovered approximately 15 years ago with mammalian cells expressing three main isoforms; SUMO-1, SUMO-2 and SUMO-3. SUMO-2 and SUMO-3 share 97% similarity, only differing at 3 residues in the N-terminus, and therefore are often termed SUMO-2/3 as biological applications such as antibodies cannot distinguish between them (Varadaraj, et al., 2014). In contrast, the SUMO-1 isoform shares only 50% sequence identity with the SUMO-2/3 isoform (Hay, 2013). The presence of a SUMO-4 isoform has been identified but the mRNA for this molecule is only found within the kidneys, dendritic cells and macrophages, whereas SUMO-1 and SUMO-2/3 exist universally in all human tissue (Varadaraj, et al., 2014) (Bohren, et al., 2004).

There are important differences between the SUMO paralogues, including isoform preference, abundance, subcellular localisation and chain formation. Certain target proteins display preference for a specific SUMO isoform, whereas other proteins will form covalent linkage with any SUMO isoform (Vertegaal, et al., 2006). However, since SUMO-2/3 is more abundant in cells than SUMO-1, it is probable the majority of protein SUMOylation is mediated via SUMO-2/3 (Saitoh & Hinchey, 2000). The SUMO isoforms can also show different subcellular localisation patterns. Compartmentalisation of proteins can define which isoform will be available for SUMOylation, for example SUMO-1 has been shown to uniquely localise to the nucleoli, nuclear envelope and cytoplasmic foci, and therefore would be the dominant paralogue mediating substrate SUMOylation within these locations. Additionally, compartmentalisation of the SUMO paralogues has been shown to be influenced by cell cycle - with SUMO-1 and SUMO-2/3 co-localising with chromosomes at different points of the cycle (Ayaydin & Dasso, 2004) (Zhang, et al., 2008). SUMOylation mimics ubiquitination in two ways; firstly, the

conjugation of both SUMO and ubiquitin occurs on a lysine residue, and secondly much like poly-ubiquitination, in which a target protein is ubiquitinated by multiple ubiquitin molecules, poly-SUMOylation can also occur. This can either involve multiple individual lysines within a protein being conjugated to one SUMO protein, or individual lysines being SUMOylated by a chain of SUMO proteins. Chain formation is only possible for the SUMO-2/3 paralogue as both isoforms 2 and 3 contain a single conserved acceptor lysine at position 11 which allows linkage to a second SUMO protein (Bylebyl, et al., 2003) (Tatham, et al., 2001) (Ulrich, 2008). As SUMO-1 does not have this lysine residue it cannot act as a link in a SUMO chain, however it may act as a chain terminator at the end of a series of SUMO-2/3 proteins (Matic, et al., 2008). It is possible, that in a similar manner to poly-ubiquitination, the differing chain lengths in poly-SUMOylation may alter the fate of the protein (Wang & Dasso, 2009).

1.4.2 The SUMOylation Cascade

SUMOylation of proteins occurs via an enzymatic cascade which terminates with the covalent linkage of SUMO to a target protein via an isopeptide bond (Figure 1.11).

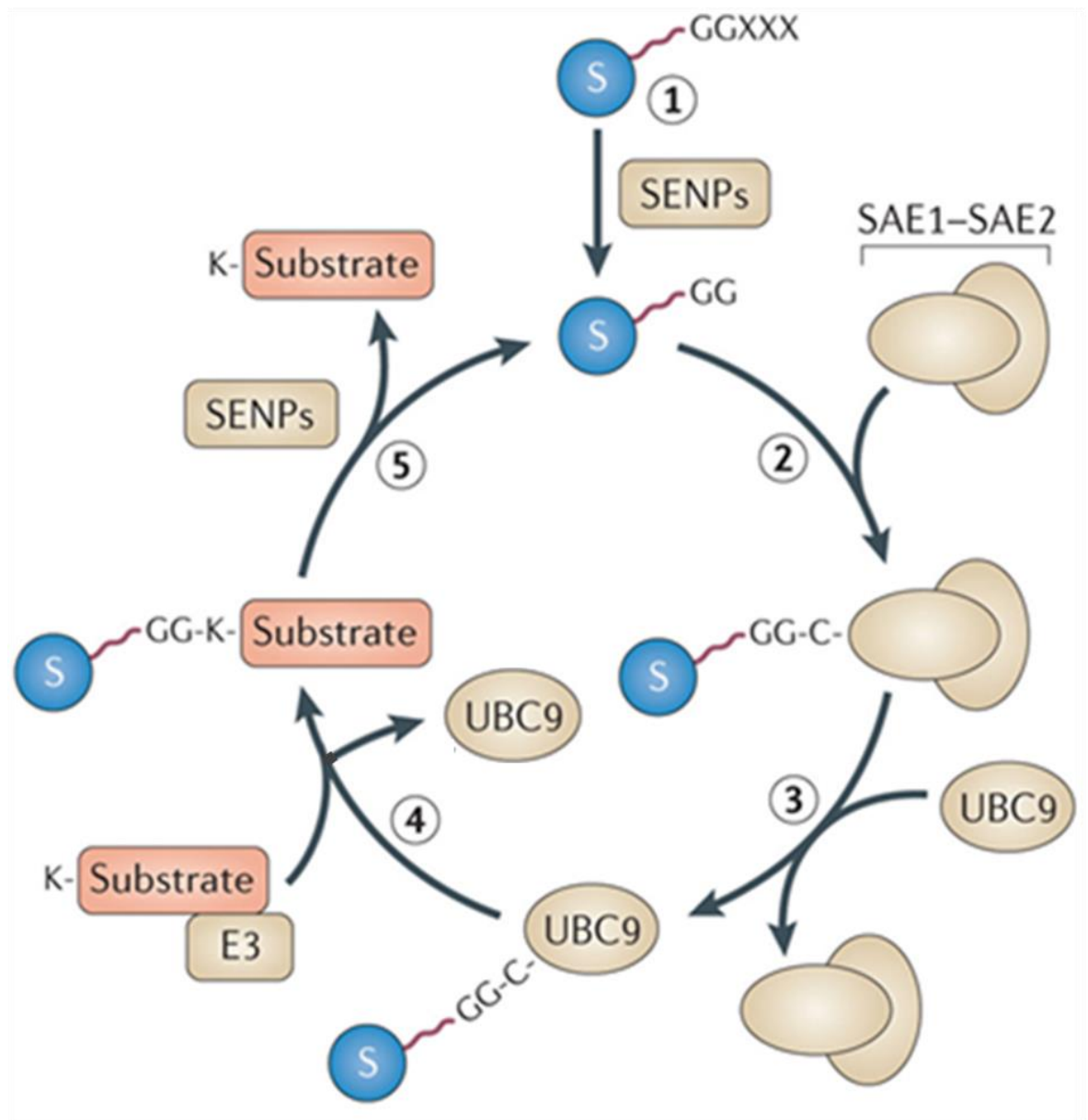


Figure 1.11 The SUMOylation pathway. The immature SUMO is processed into the mature form by SENPs, which cleave the SUMO carboxyl-terminus to reveal a Gly-Gly motif, which is essential for all subsequent steps of the SUMO cycle (1). Mature SUMO is activated by SAE1-SAE2 heterodimer (2). Activated SUMO is transferred to the catalytic cysteine of UBC9 (3). UBC9 catalyses the conjugation of SUMO to lysine residues in target proteins, either independently or in conjunction with a SUMO E3 ligase (4). SENPs can cleave SUMO from target substrates, thus releasing an unmodified target and free SUMO, which can re-enter the SUMOylation cycle (5). S (SUMO), SENPs (sentratin specific proteases), SAE1-SAE2 (SUMO-1 activating enzyme subunits 1 and 2), UBC9 (ubiquitin carrier protein 9), E3 (SUMO E3 ligase). Amino acid abbreviations in appendix.

1.4.2.1 SUMO Specific Proteases

The SUMO cascade begins with SUMO proteins which are translated as immature precursors being converted to the mature form. The proteases responsible for this are known as SENPs (sentrin specific proteases) and they act to expose a C-terminal glycine-glycine on the SUMO isoform that is essential for the formation of the isopeptide bond between the acceptor lysine on the substrate and SUMO. Furthermore, the conversion to the mature form means the SUMO protein can interact with the next enzyme of the cascade; the E1 SUMO activating enzyme (Hannoun, et al., 2010).

1.4.2.2 The SUMO E1 Activating Enzyme

The E1 SUMO activating enzyme is a complex formed by a heterodimer of SUMO-1 activating enzyme subunits 1 and 2 (SAE1 and SAE2). This complex is responsible for promoting the adenylation of the SUMO protein. This is the process by which an AMP molecule is added to the side chain on the SUMO protein in an ATP-dependent manner. This results in the formation of a thioester conjugate between the E1 SUMO activating enzyme and SUMO, in which the thiol group at cysteine 173 on the E1 SUMO activating enzyme, conjugates to the C-terminus of the SUMO protein (Desterro, et al., 1999). In this complex, adenylated SUMO can be transferred to ubiquitin carrier 9 (UBC9), the SUMO E2 conjugating enzyme.

1.4.2.3 UBC9

UBC9 is the only E2 conjugating enzyme that exists for SUMOylation and is highly related to the E2 conjugating enzymes of the ubiquitin pathway (Johnson & Blobel, 1997) (Hayashi, et al., 2002) (Jones, et al., 2002) (Desterro, et al., 1997). A second thioester conjugate is now formed between SUMO and UBC9, which is capable of interacting directly with certain SUMO target proteins to transfer SUMO to the substrate protein's acceptor lysine residue via an isopeptide bond. However, in many cases UBC9-mediated transfer is not capable of promoting substrate SUMOylation. This can be due to a lack of interaction between the target protein and UBC9. In these cases, a further step is required which is mediated by E3 ligases which act as a bridge to bring UBC9 and SUMO substrate proteins together (Henley, et al., 2014).

1.4.2.4 E3 Ligases

SUMO E3 ligases facilitate the conjugation of most substrates to SUMO under physiological conditions (Meulmeester, et al., 2008). These E3 ligases can act via two mechanisms. One mechanism is via recruiting the E2-SUMO thioester and the SUMO target protein into a complex to promote interaction, whereas the second mechanism involves stimulating the ability of UBC9 to discharge the SUMO protein (Gareau & Lima, 2010). SUMO E3 ligases which have been identified include SP-RING type, IR E3 ligases and a number of other proteins which have potential E3 SUMO ligase activity. These four other potential E3 ligases include: histone deacetylase 4 (HDAC4), an enzyme which is involved in removing acetyl groups from histones (Haberland, et al., 2009); proprotein convertase 2 (Pc2), an enzyme which converts immature proteins of neuroendocrine peptides to the mature form (Seidah & Prat, 2012); KRAB associated protein 1 (KPA1), a scaffold protein involved in chromatin remodelling (Chang, et al., 2009); and topoisomerase I-binding arginine/serine-rich protein (topors), a E3 ligase of the ubiquitin system (Hartz, 2005). In this thesis, the focus will be on the E3 ligase PIASy and therefore the HDAC4, Pc2, KPA1 and topors will not be further discussed.

The first type of E3 ligase is the SP-RING type ligases. These are named for containing a Siz/PIAS (SP)-RING (really interesting new gene) finger-like domain. Siz proteins are found within yeast whereas PIAS proteins are found within mammals. The RING domain is characteristic of the E3 ligase enzymes of the ubiquitin pathway, that function by binding a pair of zinc atoms in a distinctive cross arrangement involving cysteine and histidine residues. The SP-RING type of the SUMO pathway E3 ligases is believed to function in the same manner as those of the ubiquitin pathway; however, it lacks two of the cysteines which are conserved in the classic RING domain (Hochstrasser, 2001).

In mammalian cells, there are five members of the PIAS (protein inhibitor activated STAT) family of E3 ligases; PIAS1, PIASx α , PIASx β , PIAS3 and PIASy. These proteins display a high similarity in amino acid sequence (Shuai & Liu, 2005). Originally these PIAS proteins were identified to be involved in transcription regulation as they are inhibitors of STAT (signal transduce and activator of transcription) proteins, but later they were found to function as SUMO E3 ligases (Nishida & Yasuda, 2002) (Rogers, et al., 2003) (Kotaja, et al., 2002). The PIAS

proteins have shown SUMO substrate preference. Gocke et al (2005) reported that PIAS1 and PIASx β can facilitate SUMOylation of a broader range of substrates than PIAS γ (Gocke, et al., 2005). Additionally, the PIAS proteins also display isoform preference. PIAS γ prefers to facilitate the modification of LEF1 (lymphoid enhancer factor 1) and GATA-2 by SUMO-2, not SUMO-1, even though the proteins can be modified by both isoforms (Sachdev, et al., 2001) (Chun, et al., 2003). Facilitation of SUMOylation by the PIAS proteins requires three domains to recruit UBC9-SUMO thioester and the substrate into a complex; the C-terminal domain which interacts with the SUMO protein; the SP-RING domain which interacts with UBC9; and an area within the N-terminal known as the PINIT domain that interacts with the substrate (Duval, et al., 2003) (Yunus & Lima, 2009) (Hochstrasser, 2001).

The second type of E3 ligase is the IR E3 ligase. To date the only ligase of this type identified is the RAN binding protein 2 (RanBP2), a member of the nucleoporin family which form the nuclear pore. This ligase contains two internal repeater (IR) domains, named IR1 and IR2, and both are required for SUMO E3 ligase activity (Gareau, et al., 2012). RanBP2 binds to the UBC9-SUMO thioester, altering the thioester conformation to promote the discharge of SUMO (Reverter & Lima, 2005).

1.4.2.5 The SUMO Deconjugation System

Much like other PTMs SUMOylation can be reversed - a process termed deSUMOylation. This results in an unmodified substrate protein and a free SUMO protein which can be utilised for further protein SUMOylation. As SUMO is linked to the substrate via an isopeptide bond, enzymes with isopeptidase activity are essential to this process (Wang & Dasso, 2009) (Doerks, et al., 2002) (Seeler & Dejean, 2003). In mammals, there are 9 enzymes capable of mediating deconjugation of SUMO; 6 types of sentrin specific proteases (SENPs) (SENPS 1, 2, 3, 5, 6, and 7), 2 types of deSUMOylation isopeptidases (DESI1 and DESI2), and ubiquitin specific protease-like 1 (USPL1) (Henley, et al., 2014) (Hickey, et al., 2012). In a similar fashion to the SUMO paralogues, the SENP members can be distinct in their subcellular localisation as well as with which SUMO isoform they would prefer to deconjugate from the target protein (Gareau & Lima, 2010). For example SENP1 has been shown to be mostly present in the nucleoplasm (Gong,

et al., 2000) (Mukhopadhyay, et al., 2006) (Shen, et al., 2009), as well as showing slight preference for deconjugating SUMO-1 (Shen, et al., 2006).

1.4.3 The SUMO Consensus Motif

Unlike ubiquitination where any surface associated lysine can be modified, the acceptor lysine of the SUMOylation motif is found within a consensus motif γ KxE/D (where γ is a large hydrophobic residue often consisting of 3-4 aliphatic (straight chains of carbon atoms) residues, K is the lysine SUMO acceptor, x is any residue, and D/E an acidic residue) (Hay, 2005) (Rodriguez, et al., 2001) (Bernier-Villamor, et al., 2002). These residues directly interact with UBC9 and thus play a crucial role in regulating the stability of interactions between the enzyme and the target protein (Sampson, et al., 2001). The acceptor lysine within the motif slots into a hydrophobic groove on UBC9, while electrostatic interactions and hydrogen bonding occur between the residues surrounding the lysine and UBC9 (Lin, et al., 2002) (Bernier-Villamor, et al., 2002). The consensus motif is believed to play a role in the preference of proteins to certain SUMO isoforms. It is believed this could be down to the arrangement of hydrophobic and acidic residues. For example, protein conjugation to SUMO-1 and not with SUMO-2 can be attributed to the clusters of negatively charged amino acids at the C-terminus to the hydrophobic core (Kerscher, 2007).

1.4.3.1 Additional Elements of the SUMO Consensus Motif

In addition to this canonical consensus motif, longer sequences that include both SUMO consensus motifs and additional elements have been identified in certain SUMO substrates. These include phosphorylation-dependent SUMO motifs (PDSMs), negatively charged amino acid-dependent SUMO motifs (NDSMs), hydrophobic cluster-dependent SUMO motifs (HCSMs) and inverted SUMO motifs.

For PDSMs, substrates have a phosphorylation site adjacent to the SUMO site which can influence substrate susceptibility to SUMOylation. This was first identified in heat shock factors, in which stress-induced phosphorylation, resulted in increased levels of SUMO modification (Hietakangas, et al., 2003). In contrast, phosphorylation can also negatively regulate SUMO modification. For example, phosphorylation of ELK1 (transcription factor which regulates early gene

expression) results in a reduction in ELK1 SUMO modification (Yang, et al., 2003). NDSMs occur where negatively charged amino acid residues are located immediately downstream of the SUMO consensus motif (Yang, et al., 2006). ELK1 SUMOylation is also subject to control by NDSMs, since mutation of the negatively charged residues C-terminal to the consensus sequence inhibited the SUMOylation of the protein (Yang, et al., 2006). Both NDSM and PDSM SUMO consensus motifs are believed to mediate their effects by interacting with lysine residues on UBC9 (Mohideen, et al., 2009) (Yang, et al., 2006). In HCSMs, the hydrophobic cluster N-terminal to the SUMO consensus motif acts to enhance SUMOylation via promotion of interactions with UBC9. This has been demonstrated for RanGAP1 (GTPase activator) and ZBTB1 (transcriptional repressor) (Matic, et al., 2010). For inverted motifs, the consensus motif is reversed (Impens, et al., 2014).

1.4.3.2 SUMO Interacting Motifs (SIMs)

On SUMO substrates, SUMO interacting motifs (SIMs) are important in mediating non-covalent interactions with SUMO (Kerscher, 2007). SIMs contain a short stretch of hydrophobic amino acids which are flanked by acidic residues. When the target interacts with SUMO, the SIM adopts a conformation that promotes this interaction using a hydrophobic pocket on the SUMO surface (Reverter & Lima, 2005) (Song, et al., 2005). SIMs can be found in a wide variety of proteins including those of the SUMO pathway such as the PIAS family members (Kerscher, 2007) (Perry, et al., 2008). Three SIMs have been identified in the PIAS_γ C terminus and are required for full E3 ligase activity of the enzyme (Kaur, et al., 2017).

1.4.3.3 Alternative Lysine Modifications

The PTMs SUMOylation and ubiquitination both occur on lysine residues and this can sometimes be observed on the same lysine residue of a substrate. IκBα - a protein involved in DNA transcription - can be modified by ubiquitin and SUMO on the same lysine residue (Desterro, et al., 1998). In this case, SUMO modification was shown to inhibit phosphorylation-induced ubiquitination and subsequent proteasomal degradation of the protein (Desterro, et al., 1998). This has also been identified for other proteins: MDM2 (an E3 ubiquitin ligase) is stabilised by SUMOylation at lysine 446 but ubiquitination at this same lysine mediates degradation (Meek & Knippschild, 2003); NEMO (an inhibitor of nuclear factor

kappa B) accumulates in the nucleus when SUMOylated at lysines 277 and 309, whereas ubiquitination at these sites mediates translocation to the cytoplasm (Huang, et al., 2003); axin (a signalling component of the Wnt pathway) and RNA helicases p68 and p72 (involved in RNA metabolism) have increased stability when they are SUMOylated due to the inhibition of ubiquitination (Kim, et al., 2008) (Mooney, et al., 2010).

1.4.4 Variation in the SUMO System

The SUMO system can vary dependent on the expression levels or activities of enzymes within the pathways, as well as in response to altered intercellular environment. For example, there is an overall increase in SUMO conjugation in response to heat shock and both high levels of oxidative stress and ethanol stress (Saitoh & Hinchev, 2000) (Zhou, et al., 2004).

1.4.5 The Role of SUMOylation

SUMOylation was initially identified as having a role in nuclear biology. SUMO was shown to mediate subcellular targetting including nucleocytoplasmic trafficking (Pichler & Melchior, 2002) and orientating substrates to mitotic spindles and kinetochores in dividing cells (Joseph, et al., 2002). SUMO has also been shown to play a role in the regulation of transcription factor activity by trafficking the modified factor to the appropriate subcellular compartment, and directly influencing transcriptional activity (Seeler & Dejean, 2003). Further biological roles for SUMO include DNA repair and replication regulation (Hoege, et al., 2002), and regulation of chromosome dynamics (Apionishev, et al., 2001) (Bachant, et al., 2002). There is a large and growing number of SUMO substrates, and this demonstrates a previously unexpected diversity of physiological processes affected by this modification (Hay, 2013) (Hay, 2005).

A role for SUMO in the gastrointestinal (GI) tract is supported by the discovery that a UBC9 knockout in the GI tract of adult mice leads to disruption of the intestinal stem cells causing death within six days (Demarque, et al., 2011). SUMOylation has also been implicated in cancer as increased levels of SUMO-E1 activating enzyme, UBC9 and SUMO isopeptidases correlate with tumour development, tumour grade and metastasis (Bettermann, et al., 2012) (Bawa-Khalfe & Yeh,

2010). SUMO has also been shown to play a role in cardiovascular disease with SUMO-1 levels being reduced in HF, and SUMO-1 overexpression markedly improving cardiac function (Kho, et al., 2011). Neurodegenerative diseases such as Huntington's Disease and Alzheimer's Disease (Henley, et al., 2014) (Subramaniam, et al., 2009) (Dorval & Fraser, 2006) can also be influenced by SUMOylation, as SUMO can modulate synapse formation, spine morphogenesis, neurotransmission and synaptic plasticity. Some infections have also been shown to impact the SUMO system, for example *Listeria monocytogenes* - a pathogen responsible for the human food-borne disease listeriosis - affects the stability of the SUMO E1 activating enzyme and UBC9, therefore altering the SUMO pathway (Ribet, et al., 2010).

1.4.6 SUMOylation of GPCRs

To date there are only 5 GPCRs which are identified as substrates for SUMOylation; these include metabotropic glutamate receptors (mGluR), a cannabinoid receptor, a serotonin receptor and a receptor involved in basal cell carcinoma known as smo. mGluR8b was identified to have affinity with PIAS1 and PIAS3 *in vitro*, with PIAS1 enhancing the SUMOylation of the receptor in HEK293 cells with no function defined as of yet (Tang, et al., 2005) (Dutting, et al., 2011). mGluR7 is conjugated to SUMO-2 *in vitro*, with deSUMOylation shown to promote receptor internalisation (Wilkinson & Henley, 2011) (Choi, et al., 2015). For the cannabinoid receptor 1 (CB₁) (Gowran, et al., 2009) and the 5-HT_{1A} serotonin receptor (Li & Muma, 2013) SUMOylation influenced receptor trafficking. For the most recently discovered GPCR shown to be susceptible to SUMOylation, smo, SUMOylation was shown to stabilise the protein preventing degradation (Zhang, et al., 2017).

1.5 SUMOylation of SR Ca²⁺ ATPase 2a (SERCA2a)

1.5.1 SERCA2a

SERCA2a is a protein pump which is found on the surface of the SR within cardiac myocytes that plays a vital role in cardiac contraction. Cardiac contraction is triggered via a depolarisation event which leads to the opening of the LTCC allowing Ca²⁺ to enter the cell and stimulate the RyR on the surface of the SR. Activation of the RyR leads to a release of Ca²⁺ from the SR into the cytosol (Bers, 2002), which initiates cardiac contraction via binding to troponin C. Cardiomyocyte contraction cannot continue indefinitely, and must be terminated - this is pertinent to the role of SERCA2a. SERCA2a removes Ca²⁺ transporting it back to the SR to lower cytosolic Ca²⁺ levels, and therefore terminate contraction (Shannon & Bers, 2004).

SERCA2a exists in two structural states dependent upon the protein's affinity for Ca²⁺; E1 and E2 (Figure 1.12). In the E1 state the Ca²⁺ binding sites have high Ca²⁺ affinity and are open to the cytoplasm, whereas in the E2 state the binding affinity for Ca²⁺ is lower, with the sites facing in towards the SR lumen (Toyoshima & Mizutani, 2004) (Toyoshima, et al., 2000). In the E1 confirmation, two cytosolic Ca²⁺ bind to the separate high affinity sites within the transmembrane domain, followed by ATP binding to the cytosolic domain. When ATP is hydrolysed to ADP, this leads to the phosphorylation of Asp351 residue of SERCA2a (Toyoshima & Mizutani, 2004). As this occurs, the pump changes confirmation from E1 to E2 resulting in the Ca²⁺ being transported across the membrane and released into the lumen of the SR. As the Ca²⁺ ions are deposited in the SR, there is partial exchange of protons at these residues. This leads to a favourable environment for dephosphorylation of SERCA2a. This deactivates the luminal Ca²⁺ binding sites and reactivates the cytosolic Ca²⁺ binding sites, while shifting the confirmation of the protein back to E1 (Olesen, et al., 2004).

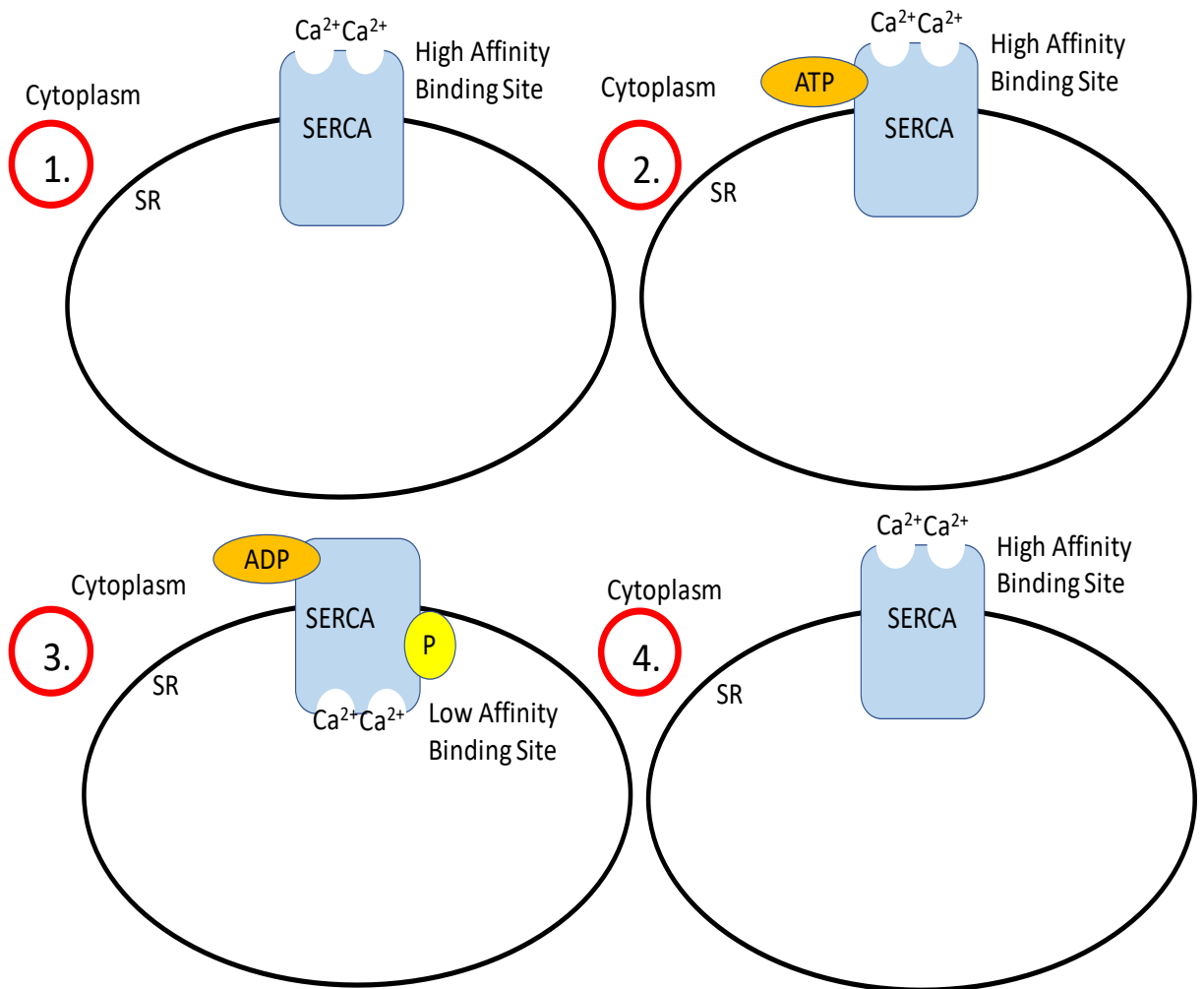


Figure 1.12 SERCA2a affinity states. SERCA2a exists in two structural states; high and low affinity. The high affinity binding state Ca²⁺ sites are open to the cytoplasm (1). High affinity state binds Ca²⁺ and ATP (2). When ATP binds and is hydrolysed to ADP this leads to phosphorylation of SERCA2a. This changes conformation of SERCA2a passing Ca²⁺ through to the lumen of the SR with low affinity binding sites and Ca²⁺ is released (3). The cycle is complete when SERCA2a is dephosphorylated shifting confirmation back to high affinity for Ca²⁺ (4). SR (sarcoplasmic reticulum), ADP (adenosine diphosphate), ATP (adenosine triphosphate), P (phosphate) SERCA (sarcoplasmic reticulum Ca²⁺ ATPase).

1.5.2 SERCA2a Regulation

SERCA2a is the most abundant isoform within the heart. The activity of the pump is specifically regulated by the integral SR membrane protein phospholamban (PLB). PLB is susceptible to phosphorylation by multiple different kinases including PKA, Ca²⁺ calmodulin-dependent kinase and Ca²⁺ phospholipid-dependent protein kinase (Kranias & Solaro, 1982) (Le Peuch, et al., 1980) (Simmerman, et al., 1986), however it interacts with SERCA2a in the unphosphorylated form. This interaction lowers the affinity of SERCA2a for Ca²⁺ by structurally altering the Ca²⁺ transport site in the E1 state, therefore reducing transport of Ca²⁺ to the SR pump (Asahi, et al., 2003) (Chen, et al., 2005) (Koss & Kranias, 1996) (Espinoza-Fonesca, et al., 2015). Phosphorylation of PLB acts to release the inhibitory effect of PLB on SERCA2a leading to an increase in SERCA2a activity (Kadambi & Kranias, 1997). The inhibitory effects of PLB are restored through dephosphorylation by SR associated phosphatases (Kranias, 1985). Although PLB is the main mechanism by which SERCA2a is regulated, other mechanisms do exist including sarcolipin-mediated inhibition. This protein acts in the same manner as PLB to mediate SERCA2a inhibition at the Ca²⁺ transport site in the E1 state (Espinoza-Fonesca, et al., 2015).

1.5.3 SERCA2a in HF

A decrease in SERCA2a protein expression has been described by many groups in the pathogenesis of HF. As a consequence, there is a limitation to cardiac relaxation as Ca²⁺ remains elevated within the cytosol, and subsequent contractions are weaker due to the depleted SR Ca²⁺ store (Beuckelmann, et al., 1995) (Hasenfuss, et al., 1999) (Schmidt, et al., 1998) (Schwinger, et al., 1995). An increase in SERCA2a expression in rat neonatal cardiomyocytes was shown to promote cardiac contraction (Hajjar, et al., 1997). The results obtained with reconstitution of SERCA2a *in vitro* have been reproduced *in vivo* and have demonstrated a significant improvement of cardiac contractility in an aortic banding model of HF (Miyamoto, et al., 2000). The first clinical trial of SERCA2a gene therapy in humans; the CUPID (calcium upregulation by percutaneous administration of gene therapy in cardiac disease) trial was conducted to examine the effect of restoring SERCA2a expression in HF patients via AAV1 (adeno-associated virus 1)-SERCA2a. This demonstrated improvements in patients with HF

resulting in reduced HF symptoms, increased exercise capacity, reduced HF biomarker expression and improved LV function (Jaski, et al., 2009). These findings supported the initiation of the phase-2 double-blind, placebo controlled portion of this study, but unfortunately restoring SERCA2a via AAV1-SERCA2a did not improve the clinical outcomes for patients with HF in comparison to placebo control. Patients receiving AAV1-SERCA2a did not demonstrate a prolonged time to recurrent events - regarded as hospital admission or ambulatory treatment relating to HF - in comparison to placebo control (Greenberg, et al., 2014) (Greenberg, et al., 2016).

1.5.4 SERCA2a SUMOylation

In 2011, Kho et al discovered that the cardiac signalling protein SERCA2a is modified by SUMO-1. The group identified that as well as SERCA2a being decreased in the pathogenesis of HF that also SUMO-1 and SUMO-SERCA2a was also reduced. The group went on to prove that restoring SUMO-1 expression via adenoviral gene transfer is beneficial as it improves cardiac function and also stabilizes heart weight to body weight ratio - indicative of reduced hypertrophic response. Furthermore, this transfer causes SERCA2a levels, which are normally reduced in HF, to remain elevated in the animal model (Kho, et al., 2011) (Tilemann, et al., 2013).

Multiple reasons have been speculated as to why SUMO-1 restoration is beneficial in HF. Firstly, SUMO-1 prevented poly-ubiquitination of SERCA2a as SUMO-1 modification and ubiquitination appear to occur at the same lysine residues 480 and 585 (Kho, et al., 2011). This therefore prevents SERCA2a from being targeted to the 26S proteasome for degradation. This competitive relationship between ubiquitination and SUMOylation has been observed for other proteins described in section 1.4.3.3 - Alternative Lys Modifications. Secondly, SUMOylation can act to influence cardiac transcription factors, such as serum response factor (SRF) (Matsuzaki, et al., 2003) and specificity protein 1 (Sp1) which is associated with SERCA2a promoters (Tilemann, et al., 2013). SUMOylation of SRF can lead to an activation of genes for contractile proteins, such as SERCA2a, therefore promoting SERCA2a expression (Wang & Schwartz, 2010), whereas Sp1 levels which are normally reduced in HF were restored following SUMO-1 gene transfer, also promoting SERCA2a expression (Tilemann, et al., 2013). Thirdly, SUMO-1 has been

shown to abrogate the damage of reactive oxygen species (ROS) formation, which is often elevated in HF (Lee, et al., 2014) by inhibiting nitric oxidase activity - an enzyme responsible for ROS production (Pandey, et al., 2011).

Recently the Hajjar group have identified a small molecule, N106, which promotes SUMOylation of SERCA2a by directly activating the SUMO E1 activating enzyme (Kho, et al., 2015). In a mouse model of HF, this molecule improves ventricular function. Additionally, although the enhancement in the SUMOylation pathway is often associated with cancer (Lee & Thorgeirsson, 2004) (Kessler, et al., 2012) the small molecule N106 mediated no such effects and may serve as a potential therapeutic strategy for HF treatment (Kho, et al., 2015).

1.5.5 Other SUMO-Susceptible Cardiac Signalling Proteins in HF

There are more than 1000 SUMO substrates known in nature (Hay, 2013) - supporting the notion, that SERCA2a may not be the only cardiac protein susceptible to SUMOylation. Using sp2.0 SUMOylation site identification software (GPS-SUMO, Guangzhou, China) the Baillie group (University of Glasgow, unpublished work) identified putative SUMOylation sites on the β_2 AR, RyR, LTCC, cTNI and myosin binding protein C (Figure 1.13). This software identifies possible SUMOylation sites by examining lysines residues and their surrounding amino acids. To validate these putative SUMOylation sites 15 mer peptides which contained potential SUMO conjugation motifs were synthesized as peptide arrays (Frank, 2002) and then SUMOylated using an *in vitro* assay (described in Chapter 2 - General Materials and Methods) (Figure 1.13). This confirmed that SERCA2a is not the only cardiac signalling protein susceptible to SUMOylation and therefore modification of the other proteins by SUMOylation may also be important in HF. The following proteins are speculated to have SUMOylation sites: RyR (positions 833, 841, 1572, 3413, 4385, 4265, 4601), β_2 AR (positions 60, 227 and 235), LTCC (position 1621), myosin binding protein C (position 543 and 1816), and cTNI (position 177 and 178) (Figure 1.13).

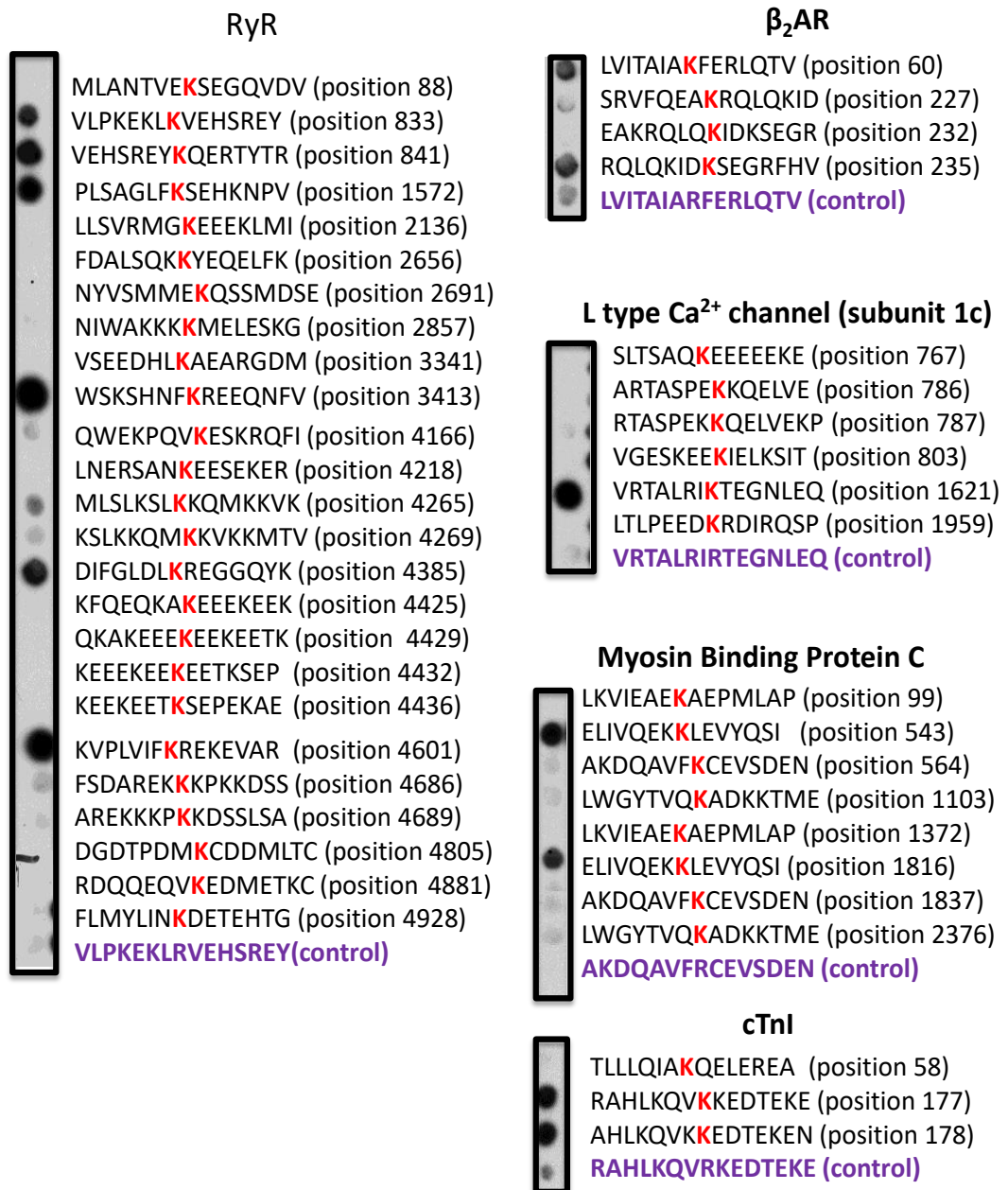


Figure 1.13 SUMOylation of cardiac signalling proteins. Using sequence analysis, the Baillie group have identified putative SUMOylation sites on the β₂AR, RyR, LTCC, cTNI and myosin binding protein C. To validate these putative SUMOylation sites 15 mer peptides which contained potential SUMO conjugation motifs were synthesized as peptide arrays (Frank, 2002) and then SUMOylated using an *in vitro* assay. β₂AR (beta 2 adrenergic receptor), RyR (ryanodine receptor), LTCC (L-type Ca²⁺channel), cTNI (cardiac troponin I). Amino acid abbreviations in appendix.

1.5.5.1 RyR

The RyR protein mediates the release of Ca^{2+} from the SR and this Ca^{2+} is vital for mediating cardiomyocyte contraction. The receptor is susceptible to phosphorylation (Lokuta, et al., 1995) and it has been suggested that in HF the receptor can become hyper-phosphorylated resulting in it leaking Ca^{2+} ions continuously (Marks, 2000). This leads to depletion of the SR Ca^{2+} store and therefore subsequent cardiac contractions are weaker (Eisner & Trafford, 2002).

1.5.5.2 LTCC

The LTCC allows for the initial Ca^{2+} influx following the initiation of cardiac contraction. This small influx of Ca^{2+} stimulates the RyR to release a much greater volume of Ca^{2+} from the SR which mediates contraction at the myofilament. In HF, single LTCC's display elevated activity, but this was not observed when the current through the channels was measured from whole cell preparations (Schroder, et al., 1998). This discrepancy could be explained if the cardiomyocytes displayed fewer channels in HF but no changes were observed in channel density. Schroder et al (1998) proposed that the increased channel activity in HF could be caused by increased PKA-mediated phosphorylation of the α_{1c} subunit of LTCC (Bodi, et al., 2005).

1.5.5.3 Myosin binding protein C

Myosin binding protein C is a thick filament accessory protein that inhibits the cross-bridge cycling of actin and myosin, therefore inhibiting contraction. Upon phosphorylation, myosin binding protein C releases the inhibitory effect, and therefore the rate of cross-bridge cycling is accelerated (Tong, et al., 2008). Rosas et al (2015) identified that inhibition of the PKA-mediated phosphorylation of myosin binding protein C led to reduced myocardial relaxation - a phenotype associated with HF (Rosas, et al., 2015).

1.5.5.4 cTNI

Troponin is the protein within cardiac myocytes which regulates Ca^{2+} -mediated contraction. It has been shown that elevation of troponin within serum correlates with adverse outcomes in HF (Kociol, et al., 2010). It is not fully understood why

troponin levels are elevated in HF but the cardiac conditions such as volume/pressure overload, increased wall stress and elevated inflammation lead to an increase in myocyte apoptosis, autophagy, proteolysis and membrane permeability. The enhanced membrane permeability leads to an increased volume of circulating cTNI (Wettersten & Maisel, 2015) (Francis, et al., 1995) (Januzzi, et al., 2012). In addition to acting as a biomarker, troponin I also has a functional role in HF. When intracellular Ca^{2+} concentration is low, troponin I binds to actin, mediating an interaction between tropomyosin and actin which sterically hinders cross-bridge attachment of actin and myosin. A rise in Ca^{2+} allows troponin C and troponin I to bind, allowing tropomyosin to interact further with the actin filaments, leading to actin and myosin cross-bridge cycling (Day, et al., 2007). During HF, the sensitivity of troponin C to Ca^{2+} is increased - believed in part to be due to decreased phosphorylation of troponin I, the regulatory subunit (Day, et al., 2007). In HF, the density of $\beta_1\text{AR}$ (Bristow, et al., 1993) (Daaka, et al., 1997) is reduced, and this is believed to be responsible for less PKA-mediated phosphorylation on troponin I (Metzger & Westfall, 2004).

1.5.5.5 $\beta_2\text{AR}$

In ventricular myocytes both $\beta_1\text{AR}$ and $\beta_2\text{AR}$ mediate cAMP signalling, however only the $\beta_1\text{AR}$ is capable of initiating PKA-mediated phosphorylation of phospholamban and troponin I (Xiao, 2001), inducing cardiomyocyte hypertrophy (Engelhardt, et al., 1999) and promoting cardiomyocyte apoptosis (Communal, et al., 1999). The difference in the outcome following receptor stimulation can in part be attributed to receptor localisation. The surface of cardiomyocytes consists of domes and troughs with the T tubules found in the base of the troughs stretching into the myocyte centre (Ibrahim, et al., 2010). Nikolaev et al (2010) identified that in healthy cardiomyocytes, $\beta_2\text{AR}$ are exclusively localised to T-tubules whereas $\beta_1\text{AR}$ are present in both the domes and T-tubules (Nikolaev, et al., 2010). In addition to receptor location, spatial compartmentation within the cell can influence the outcome of receptor stimulation. Following $\beta_1\text{AR}$ stimulation for example, cAMP is propagated throughout the entire cell whereas $\beta_2\text{AR}$ stimulation leads to locally confined cAMP production at the T-tubules (Nikolaev, et al., 2006). This cAMP confinement is mediated by PKA-stimulated PDE4 activity which degrades cAMP before it can spread throughout the cytosol, and AKAP anchoring of PKA subunits to within the direct vicinity of the $\beta_2\text{AR}$ (Fischmeister, et al., 2006).

Cardiac disease can act to influence both receptor localisation and spatial compartmentation within the cell. In HF, myocytes display an extensive loss of T-tubules (Lyon, et al., 2009) which encourages the β_2 AR to redistribute to non-tubular areas such as the domes, which in healthy cells are predominantly occupied by β_1 AR (Nikolaev, et al., 2010). With this positioning, the β_2 AR can now stimulate cAMP production, which is capable of propagating throughout the cytosol (Nikolaev, et al., 2010). In addition to alternate localisation of the β_2 AR, spatial compartmentation of PKA is also abolished due to the lack of AKAP-PKA interaction during HF (Zakhary, et al., 2000). This further encourages cAMP propagation throughout the cell, as PDE4 is not activated by PKA to degrade local cAMP pools. Therefore in HF, the β_2 AR signals would be expected to manifest in a similar manner to that of the β_1 AR, contributing to initiating PKA-mediated phosphorylation of phospholamban and troponin I (Xiao, 2001), inducing cardiomyocyte hypertrophy (Engelhardt, et al., 1999) and promoting cardiomyocyte apoptosis (Communal, et al., 1999). This would contribute to the HF phenotype (del Monte, et al., 1993) (Dorn, et al., 1999).

In contrast, numerous studies indicate a cardio-protective role for the β_2 AR: in isolated myocytes β_2 AR stimulation protects against stress-induced apoptosis (Chelsey, et al., 2000); in a rat model of myocardial infarction-induced HF, selective activation of the β_2 AR improves cardiac performance and reduces apoptosis (Ahmet, et al., 2004); and in HF there is enhanced signalling of β_2 AR via the inhibitory G_i protein, which attenuates the positive inotropic effects of β_1 AR stimulation and activates cardio-protective signalling pathways (Bohm, et al., 1994) (Chelsey, et al., 2000) (Feldman, et al., 1988) (Zhu, et al., 2001).

1.5.6 Inducing Protein SUMOylation

Kho et al (2011) identified that SERCA2a is a substrate for SUMOylation. To SUMOylate this protein *in vitro* they used the HEK293 cell line to overexpress SERCA2a in conjunction with SUMO-1 and UBC9. This approach of upregulating SUMOylation cascade components has been utilised by other groups. For LIN-1, - a DNA binding transcription factor - SUMOylation was promoted in yeast cells via overexpression of SUMO-1 (Leight, et al., 2005). For LEF1, - a nuclear mediator of Wnt signalling - SUMOylation was promoted by overexpression of PIAS γ in HEK293T cells (Sachdev, et al., 2001).

1.6 Aims and Hypothesis

1.6.1 Hypothesis

This thesis focuses on the SUMOylation of the β_2 AR, a modification that has not previously been described. It is hypothesised that SUMOylation of the β_2 AR can occur and that this modification may alter downstream signalling of the receptor. We also hypothesise that as in the case of SUMO-SERCA2a, that SUMOylation of the receptor protects it from degradation during HF.

1.6.2 Aims

The aims for this thesis are as follows;

1. Validation of SUMO sites in the β_2 AR using peptide array
2. Design, generation and validation of a SUMO- β_2 AR specific polyclonal antibody
3. Promotion of β_2 AR SUMOylation in the HEKB₂ cell line to assess the influence of receptor SUMOylation on downstream signalling
4. Assessment of β_2 AR SUMOylation in small and large animal models of HF

Chapter 2 General Materials and Methods

2.1 General Laboratory Practise

Laboratory equipment and reagents were of the highest commercially available grades purchased from Sigma-Aldrich (Sigma-Aldrich, Dorset, UK) unless otherwise stated. Hazardous reagents were handled as described in the Control of Substances Hazardous to Health regulations. A laboratory coat and non-latex powder-free gloves were worn during all procedures.

Laboratory glassware was cleaned in Decon 75 detergent (Decon Laboratories Ltd, East Sussex, UK), rinsed with distilled water (dH₂O) and dried at 37°C. Otherwise, sterile disposable plastic ware was used, including 0.5 and 1.5ml microcentrifuge tubes (Greiner Bio-one, Stonehouse, UK), 15 and 50ml centrifuge tubes (Corning, Birmingham, UK), and also 5 and 20ml 'universal' containers (Sterilin, Newport, UK). Laboratory-ware and liquids requiring sterilisation were autoclaved in a Classic Prestige Medical autoclave (Prestige Medical, Blackburn, UK). Reagents were weighed using a Mettler Toledo balance (sensitive to 0.01g) (Mettler Toledo, Ohio, USA), or a Sartorius CP124S balance (sensitive to 0.0001g) (Sartorius, Bradford, UK). Solutions were pH'd using a Mettler Toledo Seven Easy digital pH meter (Mettler Toledo, Ohio, USA) calibrated with pH 4.0, 7.0 and 10.0 prepared from buffer tablets (Sigma-Aldrich, Dorset, UK). Volumes from 0.1 to 1000µl were dispensed with Gilson Medical Instruments pipettes. Volumes from 1 to 25ml were measured with sterile disposable pipettes (Corning, Birmingham, UK) and a Gilson battery-powered pipetting aid (Gilson Medical Instruments, Wisconsin, USA). Autoclaved dH₂O was used to prepare aqueous solutions unless otherwise indicated, and a Stuart Scientific hotplate/stirrer (Stuart Scientific, Staffordshire, UK) was used to aid dissolving and mixing. Vortexing was carried out using a Fisons Scientific Equipment Whirlimixer (Fisons Scientific, London, UK). Centrifugation for samples up to 1.5ml was performed at 4-20°C in a table top Sigma-Aldrich 1-14K microcentrifuge (Sigma-Aldrich, Dorset, UK), while larger sample volumes were centrifuged in a ThermoFisher Scientific Cl31 multispeed (ThermoFisher Scientific, Paisley, UK), compatible with 15 and 50ml centrifuge tubes, and 20ml 'universal' tubes. For ultracentrifugation, a Beckman Coulter Optima L-80 XP ultracentrifuge (Beckman Coulter, High Wycombe, UK) was used. A Grant OLS200 water bath (Grant Instruments, Cambridgeshire, UK) was used for experiments

requiring incubations from 37 to 90°C, and a Techne DRI-BLOCK DB2A heating block (Teche, Staffordshire, UK) was used for temperatures up to 100°C.

2.2 Cell Culture

All cell culture procedures were carried out in a class II hoods (ThermoFisher Scientific, Paisley, UK) using standard aseptic techniques and sterile instruments via autoclaving. All culture reagents were supplied by Gibco (ThermoFisher Scientific, Paisley, UK) unless stated otherwise. The tissue culture flasks, dishes and pipettes were supplied by Corning (Sigma-Aldrich, Dorset, UK). All cultures were examined regularly under a phase contrast inverted microscope (Leitz Diavert, Berlin, Germany).

2.2.1 HEK293 Cells

HEK293 cells were originally derived from human embryonic kidney (HEK) cells and are used for their ease of culture and transfection. HEK293 cells were cultured in growth medium consisting of Dulbecco's Modified Eagle's Medium (DMEM) supplemented with 10% fetal bovine serum (FBS), 1% penicillin-streptomycin (PS), 1% L-glutamine (LG) and 1% non-essential amino acids (NEAA) at 37°C in humidified air with 5% CO₂.

HEK293 cells were used in two results chapters of this thesis;

- Chapter 3 - Production of a SUMO-β₂AR Specific Polyclonal Antibody. These cells were used in the antibody testing phase to prove the SUMO-β₂AR antibody could detect the β₂AR overexpressed in HEKβ₂ cells, with HEK293 cells which lack the overexpressed β₂AR used as control.
- Chapter 4 - *In Vitro* SUMOylation of the β₂AR. These cells were used in BRET (bioluminescence resonance energy transfer) and SPASM (systemic protein affinity strength modulation) sensor experiments to determine the influence of β₂AR SUMOylation on receptor function. These cells were also used as a control to HEKβ₂ cells, as they contain no overexpressed β₂AR.

2.2.2 HEK β_2 Cells

HEK β_2 cells are a stable HEK293 cell line which overexpresses the GFP/FLAG-tagged form of the β_2 AR. GFP is a green fluorescent protein meaning the receptor can be visualised in these cells using fluorescent microscopy. FLAG is an 8 amino acid tag commonly used to tag proteins. Generation and maintenance of this cell line is described elsewhere (McLean & Milligan, 2000) (Mclean, et al., 1999). These cells were maintained and passaged in the same manner as HEK293 cells. HEK β_2 cells contain an extra component of geneticin G418 (Sigma-Aldrich, Dorset, UK) in the growth medium at 0.5mg/ml. This antibiotic prevents growth of HEK293 cells, which do not express the GFP/FLAG-tagged β_2 AR.

HEK β_2 cells were used in all results chapters of this thesis;

- Chapter 3 - Production of a SUMO- β_2 AR Specific Polyclonal Antibody. HEK β_2 cells were used in the antibody testing phase to prove the SUMO- β_2 AR antibody could detect the β_2 AR stably transfected in the HEK β_2 cell line.
- Chapter 4 - *In Vitro* SUMOylation of the β_2 AR. HEK β_2 cells were used to determine the influence of β_2 AR SUMOylation on receptor function in a range of techniques including drug stimulation and subsequent immunoblotting, immunoprecipitation, peptide array overlay, ArrayScan internalisation assay, FRET (fluorescence resonance energy transfer) and radioligand binding studies.
- Chapter 5 - Analysis of β_2 AR SUMOylation in Animal Models of HF. HEK β_2 cell lysate was used as an antibody positive control for immunoblotting when protein detection proved problematic in animal tissue lysate.

2.2.3 Cell Sub Culture

The cells were passaged at approximately 90% confluency. For cell passage, growth medium was removed and the cells were washed in sterile phosphate buffered saline (PBS) to remove traces of media. The PBS was then removed and the cells were treated with 5ml trypsin-EDTA solution per 75cm² culture flasks of

cells to dissociate the cell monolayer for 5 minutes at 37°C. Growth medium was added to neutralise the trypsin-EDTA solution, and then cells and media were collected and subject to centrifugation at 10,000rpm for 3 minutes at room temperature to isolate the cell pellet. The supernatant was removed, without disturbing the cell pellet, which was then resuspended in fresh growth media and re-plated according to the requirement.

2.2.4 Cell Counting

Cells were counted with a Bright Line Haemocytometer (Sigma-Aldrich, Dorset, UK). 10µl of a cell suspension was pipetted under a cover slip onto the grid, using a light microscope; the number of viable cells in each 1mm corner square was counted and averaged. Cells crossing the bottom or right-hand edge of any square were not counted. The average number of cells in each 1mm square was derived, and then multiplied by 10⁴ to give the number of cells per ml in the suspension. The subsequent concentration of cells per ml can be determined using the following calculation:

$$\text{Cell number / ml} = \text{average cell count per square} \times 10^4 \times \text{original volume}$$

The calculated cell concentration (cells/ml) was then used for seeding cells at the desired density.

2.2.5 Cryopreservation

For cryopreserving the cells, the cell pellet was prepared as described in 2.2.3 - Cell Subculture. The pellet was resuspended in 10% dimethyl sulfoxide (DMSO) diluted in a 50/50 mix of growth medium and FBS. DMSO is a cryoprotectant which protects the cells from damage during the freezing procedure. The cell containing media was aliquoted into cryovials - small tubes designed for cryopreservation - which were placed into a freezing container filled with 100% isopropanol and placed into a -80°C freezer for 24 hours. This method allowed cells to freeze slowly, preventing rupture initiated by rapid freezing. After 24 hours, frozen cells were transferred to liquid nitrogen tanks for long term storage.

To recover cells from liquid nitrogen, cells were defrosted within the cryovial in a water bath at 37°C. The cell suspension was then mixed with approximately 10ml of appropriate cell culture medium and centrifuged at 10,000rpm for 3 minutes at room temperature to remove residual DMSO. This ensures successful cell growth, as cells do not grow well in media containing DMSO. The cell pellet was then resuspended in cell culture medium and incubated at 37°C and 5% CO₂ for further culturing.

2.3 Isolation of Plasmid DNA and Transient Transfection

Transient transfection is a method of introducing a foreign gene into a cell. The transiently transfected cells will express the foreign gene but will not incorporate it into their genome, therefore it will not be replicated. These cells will express the transfected gene for several days, but after which the foreign gene is lost through cell division (Smith, 2013). Transient transfection can be encouraged by the use of chemical reagents - one such reagent is Lipofectamine LTX (ThermoFisher Scientific, Paisley, UK). Lipofectamine LTX is a liposomal transfection reagent, which means it processes the DNA of the foreign gene into liposomes which fuse with cell membranes and release DNA into the cell interior by endocytosis (Felgner, et al., 1987). This method is necessary to allow the negatively charged nucleic acids to pass through the negatively charged plasma membrane, as the membrane would normally repel the negative charge.

Isolation of PIASy HA-tagged DNA and transient transfection was used in this thesis to promote SUMOylation of the β_2 AR in both Chapter 3 - Production of a SUMO- β_2 AR Specific Polyclonal Antibody and Chapter 4 - *In Vitro* SUMOylation of the β_2 AR. For control, cells were treated with empty transfection reagent. These are known as mock transfected cells.

2.3.1 Isolation of Plasmid DNA From E. coli

The only plasmid DNA used in multiple chapters (Chapter 3 - Production of a SUMO- β_2 AR Specific Polyclonal Antibody and Chapter 4 - *In Vitro* SUMOylation of the β_2 AR) of this thesis was PIASy with an HA tag. The HA (hemagglutinin) tag is derived from the human influenza virus HA protein (ThermofisherScientific, 2017).

This tag allows determination of PIASy HA transfection success by immunoblotting for the HA tag.

A scraping was taken from a PIASy HA tag *E. coli* bacterial glycerol stock (a stock of bacterial cells which express the PIASy HA plasmid vector) using a sterile pipette and grown in 250ml of sterile lysogeny broth (LB) media (2.5g tryptone, 1.25g yeast extract, 2.5g NaCl, 250ml of dH₂O, sterilised via autoclave and cooled before use) containing appropriate antibiotic overnight at 37°C in an orbital shaker (Cole Parmer, London, UK). The antibiotic for PIASy HA was ampicillin 500µg/ml. This means that all bacterial cells which did not display the resistance gene for ampicillin - which is encoded within the PIASy HA plasmid vector - were unable to grow. This allowed bacterial cells which expressed the PIASy HA tag plasmid vector to multiply uninhibited.

Plasmid DNA was isolated using the QIAGEN Maxiprep Kit (QIAGEN, Manchester, UK) according to the manufacturers' instructions. The DNA was then eluted with sterile dH₂O and stored at -20°C for long term storage. Plasmid DNA other than PIASy which was used within this thesis was provided by the laboratory of Professor Graeme Milligan at the University of Glasgow.

2.3.1.1 Storage of Plasmid DNA as Glycerol Stocks

For plasmid storage, 900µl of bacterial cell culture was mixed with 900µl of 30% glycerol solution, to give a final glycerol concentration of 15%. The glycerol was sterilised by autoclaving, prior to use. The glycerol stock was snap frozen using dry ice and stored at -80°C. Glycerol stocks were never unfrozen and remained on dry ice throughout use. Scrapings from the frozen stock were enough for isolation of plasmid DNA via Maxiprep.

2.3.1.2 Quantification of DNA Concentration

The concentration of purified DNA was determined using Nanodrop 3300 spectrophotometer (ThermoFisher Scientific, Paisley, UK) following manufacturer instruction. Absorbance wavelength was set at 260nm and 280nm, and the A₂₆₀ : A₂₈₀ ratio determines the purity of the nucleic acid extract. The ratio of A₂₆₀ : A₂₈₀ ideally should be between 2 - 2.3 and a lower reading may indicate organic

solvent contamination in the preparation. Values above 400ng/ μ l were deemed suitable for future transient transfection experiments.

2.3.2 Transient Transfection of Plasmid DNA

Cells were plated the day before transient transfection for 60-80% confluency on day of transfection. Plasmid DNA used in the present study was transiently transfected into cells using Lipofectamine LTX according to manufacturers' instructions and OPTIMEM (ThermoFisher Scientific, Paisley, UK). OPTIMEM is reduced serum media which is used during liposomal transfection methods, as serum can reduce transfection efficiency. Cells were incubated for a minimum of 24 hours to allow sufficient protein expression. As control, mock transfected cells were treated with empty transfection reagent.

2.4 Preparation of Cell Lysate

To assess cellular contents, it is essential to lyse the cells - a process in which individual cellular proteins are isolated from the intact cells. Using detergent-based lysis buffers the cell membranes are disrupted allowing cell contents to leak free. 3T3 lysis buffer (25mM HEPES-OH, pH 7.5, 50mM NaCl, 10% glycerol, 1% triton, 50mM NaF, 30mM Na₄P₂O₇, 5mM EDTA) was used for cell lysates, unless stated otherwise in chapter specific methods. This buffer contains triton which is a detergent for disrupting the membranes. The buffer was supplemented with protease cocktail inhibitor tablets (Roche, West Sussex, UK), phos-stop tablets (Roche, West Sussex, UK) and 25mM NEM (N-ethylmaleimide) (Sigma-Aldrich, Dorset, UK). The protease cocktail inhibitor tablets inhibit a broad spectrum of proteases which would normally break down proteins, phos-stop tablets inhibit phosphatases which prevents phosphorylated proteins from becoming de-phosphorylated, and NEM inhibits enzymes which promote de-SUMOylation.

Lysates were obtained by harvesting cells at 4°C. Cells were first washed in ice cold PBS then lysed using 250 μ l of supplemented 3T3 lysis buffer. The cell lysate was centrifuged at 13,000rpm for 10 minutes at 4°C. The supernatant lysate was removed and kept. The cell lysates were snap frozen on dry ice and stored at -80°C until required. The protein concentration in the supernatant was analysed by the Bradford method (Bradford, 1976).

2.5 Protein Quantification by the Bradford Assay

The concentration of protein in cell lysates was determined using the Bradford method (Bradford, 1976). The Bradford assay determines the concentration of a protein sample based on an absorbance shift of the dye Coomassie Brilliant Blue G-250. Protein assays were performed in clear 96 well plates. Each protein sample of unknown concentration was diluted 1 : 100 in sterile dH₂O, 2 μ l sample 198 μ l dH₂O. 50 μ l of each sample was added to 3 consecutive wells in a clear 96 well plate for testing in triplicate. Known BSA concentrations between 0 and 5 μ g were prepared and also tested in triplicate to generate a standard curve. Bradford reagent (Bio-Rad, Hertfordshire, UK) was diluted 1 : 5 in sterile dH₂O, and 200 μ l of diluted reagent was added per well. Samples and standards were analysed with a 595nm filter on an Anthos 2010 plate reader (Biochrom, Cambridge, UK) using ADAP software (Biochrom, Cambridge, UK). Protein concentrations were calculated using a curve derived from the BSA standard values, and adjusted for sample dilution.

2.6 Immunoblotting

Immunoblotting is a technique widely used to assess proteins which are present within cell lysate. Cell lysates are prepared for separation by gel electrophoresis, followed by transfer to nitrocellulose membranes. Once the proteins which were present in cell lysate are captured within membranes, the membranes are incubated overnight with a primary antibody. This antibody has been designed to recognise the desired target protein, and therefore will bind like an antibody-to-antigen. With the primary antibody bound to the target protein, a secondary antibody incubation step is required. This secondary antibody is designed to recognise the primary antibody based upon the animal in which the primary antibody was raised. For example, if the primary antibody was raised in a rabbit, then a rabbit secondary antibody would be required. The secondary antibody can then be detected by various visualisation methods allowing quantification of the target protein.

Immunoblotting was used in all results chapters of this thesis;

- Chapter 3 - Production of a SUMO-B₂AR Specific Polyclonal Antibody. Immunoblotting was used to assess the function of the novel SUMO-B₂AR antibody.
- Chapter 4 - *In Vitro* SUMOylation of the B₂AR. Immunoblotting was used in multiple experiments including assessment of protein content in cellular lysates following drug treatments, assessment of immunoprecipitation experiments, and assessment of successful PIASy HA transfection.
- Chapter 5 - Analysis of B₂AR SUMOylation in Animal Models of HF. Immunoblotting was used to assess protein content of heart tissue lysates.

2.6.1 Sample Preparation

Protein samples were denatured and reduced for gel electrophoresis by diluting in 5x laemmli protein sample buffer (Bio-Rad, Hertfordshire, UK) and boiling for 5 minutes to denature the protein. Denaturing is the process by which proteins lose their higher structure which exists in their native state. This higher structure includes hydrogen bonding, three-dimensional shape and protein subunit arrangement. The negative charge on the amino acids is not neutralised in denaturing, and therefore allows the protein to be separated by gel electrophoresis (Mahmood & Yang, 2012). Tracking dye bromophenol blue was also present in the sample buffer to visualise samples passing through the gel.

2.6.2 SDS-PAGE (sodium dodecyl sulfate polyacrylamide gel electrophoresis)

From protein samples, 15µg of protein per well was loaded directly onto SDS-PAGE precast gels (NuPAGE ® 4-12% Bis-Tris gel, ThermoFisher Scientific, Paisley, UK). These gels consist of a 4% low acrylamide density stacker gel and a 4-12% acrylamide gradient running gel. The stacker gel is porous and therefore separates proteins poorly, but as the samples progress to the running section of the gel, the pores become much narrower. This leads to protein separation dependent on size, as the smaller proteins will travel easily and hence more quickly through the gel versus the larger proteins (Mahmood & Yang, 2012). Gels were immersed in

NuPAGE[®] MES (for <50kDa proteins) or MOPS (for >50kDa proteins) SDS Running Buffer (ThermoFisher Scientific, Paisley, UK) in the Xcell[®] SureLock MiniCell system (ThermoFisher Scientific, Paisley, UK). 1.5µl of Bio-Rad Precision Plus Protein Standard (Bio-Rad, Hertfordshire, UK) was added to the first well of each gel. This is a pre-stained marker which gives a scale to aid analysis of protein molecular weight. Gels were ran at 200V until the samples reached gel bottom, indicative by the blue bromophenol dye colouring, allowing maximum protein separation.

2.6.3 Transfer

Following electrophoresis, the gel was transferred onto a 0.2µm pore size nitrocellulose membrane (ThermoFisher Scientific, Paisley, UK). Transfer buffer was prepared by diluting 20X NuPAGE[®] Transfer Buffer (ThermoFisher Scientific, Paisley, UK) in 20% methanol in dH₂O. The membrane was soaked in transfer buffer briefly along with sponges and filter papers. The gel was removed from electrophoresis cassette and placed on top of two sponges and two pieces of filter paper within an Xcell[®] II Blot Module (ThermoFisher Scientific, Paisley, UK). The membrane was placed on top of the gel with care taken to avoid bubbles. Then a further two pieces of filter paper and two sponges were added on top of the gel. The blot module was then placed into the transfer tank and filled with transfer buffer. The membrane must face the anode to allow proteins to migrate from the gel to the membrane. Current was applied at 30V for 90 minutes.

2.6.4 Detection

Following transfer, the membranes were blocked in 5% Marvel/TBS-T (marvel milk powder in 1X TBS-T, 20mM Tris-HCl, pH 7.6, 150mM NaCl, 0.1% Tween20) for 40 minutes to 1 hour with gentle shaking to block unspecific antibody binding sites. For detection of phosphorylated proteins, phos-block (Cambridge Bioscience, Cambridge, UK) was used in place of marvel, as marvel milk contains casein, which is a phospho-protein, and therefore would interfere with antibodies which are designed to detect a phosphorylated protein, leading to unspecific binding (Mahmood & Yang, 2012). Following blocking, the membrane is incubated with the appropriate primary antibody (Table 2.1) at the appropriate dilution made up in blocking buffer at 4°C overnight. The following morning the membranes were

washed 3 times for 5 minutes in 1X TBS-T. Licor Alexa-Fluor conjugated secondary antibodies (Licor Odyssey, Nebraska, USA) (Table 2.2) were added in blocking buffer at 1 : 5000 dilution and incubated for 1 hour at room temperature. Membranes were washed as before then visualised. Bound antibody was detected by Licor Odyssey scanner (Licor Odyssey, Nebraska, USA) which detects the fluorescence within the secondary antibody. Densitometry of the image was performed using Odyssey software (Licor Odyssey, Nebraska, USA). The level of a particular protein in a sample was always measured relative to the level of a 'housekeeping' protein, namely glyceraldehyde-3-phosphate dehydrogenase (GAPDH).

Table 2.1 Primary Antibodies

Name	Supplier	Catalogue Number	Dilution
His-HRP	Abcam	ab1187	1:5000
GFP	Abcam	ab6556	1:1000
HA	Cell Signalling	2367	1:1000
GAPDH	Abcam	ab8245	1:1000
Phos β_2 AR (PKA) 345-346	Santa Cruz	sc-16718	1:1000
Phos PKA Substrate	Cell Signalling	9621	1:1000
Phos ERK	Cell Signalling	9101	1:1000
ERK	Cell Signalling	9102	1:1000
UBC9	Santa Cruz	sc-271057	1:1000
Phos β_2 AR (GRK) 355-356	Santa Cruz	sc-16719	1:1000
Ubiquitin K48	Abcam	ab140601	1:1000
SUMO-2/3	Abcam	ab22654	1:1000
SUMO-1	Abcam	ab11672	1:1000
PIASy	Abcam	ab58416	1:1000
β_2 AR	Thermofisher	PA5-18423	1:1000
β_2 AR	Santa Cruz	Sc-569	1:1000

Table 2.2 Secondary Antibodies

Name	Supplier	Catalogue Number	Dilution
IRDye® 800 Goat anti-Rabbit IgG	Licor	P/N 925-32211	1:5000
IRDye® 680 Donkey anti-Mouse IgG	Licor	P/N 925-68022	1:5000
Anti-rabbit IgG HRP-linked Antibody	Cell Signalling	7074	1:1000-5000
Anti-mouse IgG HRP-linked Antibody	Cell Signalling	7076	1:1000-5000

2.7 Peptide Array

The peptide array technique involves the spotting of sequences of amino acids as various spots on a cellulose membrane support. In this thesis, this technique has been used in two different ways;

- Chapter 3 - Production of a SUMO- β_2 AR Specific Polyclonal Antibody. Peptide arrays were used to determine the ability of the SUMO- β_2 AR antibody to recognise the epitope against which it was raised.
- Chapter 4 - *In Vitro* SUMOylation of the β_2 AR. Peptide arrays were used to determine the points of interaction between the SUMOylation enzymes UBC9 and PIAS γ with the β_2 AR.

2.7.1 Solid Phase Peptide Synthesis (SPPS)

The standard method for synthesizing peptides is solid phase peptide synthesis (SPPS). Peptides are synthesised by the coupling of the carboxyl group on one amino acid to the amino group on another. Since peptides have side chain functional groups which could interact with carboxyl or amino groups, these functional groups must be chemically protected during synthesis. An important protection group is Fmoc (9-fluorenylmethyloxycarbonyl), which protects the

amino group from interaction with carboxyl groups. This is important as it isolates only the carboxyl group on the amino acid for further interaction, meaning interactions can be chosen and not random.

An example of the coupling of two amino acids (Figure 2.1) (SigmaAldrich, 2017) could occur as follows;

1. Amino acid 1 (AA1) could be coupled to a solid resin support via its carboxyl group, while its amino group is protected by Fmoc. This resin is the solid support which the chain of peptides can be built upon.
2. Amino acid 2 (AA2) has its amino group protected by Fmoc, but its carboxyl group must be activated before coupling to AA1 can occur. Activation means the carboxyl group becomes more susceptible to nucleophilic attack by the amino group on AA1.
3. Before the amino group on AA1 can attack the activated carboxyl group the Fmoc group which protects the amino group on AA1 must be removed. Fmoc can be removed using the base piperidine in DMF (dimethylformamide).
4. Coupling can then occur with the carboxyl group from AA2 and amino group from AA1. This chain can continue to be built upon in a similar manner by unblocking appropriate groups.
5. The final steps involve removing additional protecting groups from side chains and cleaving the peptide from resin.

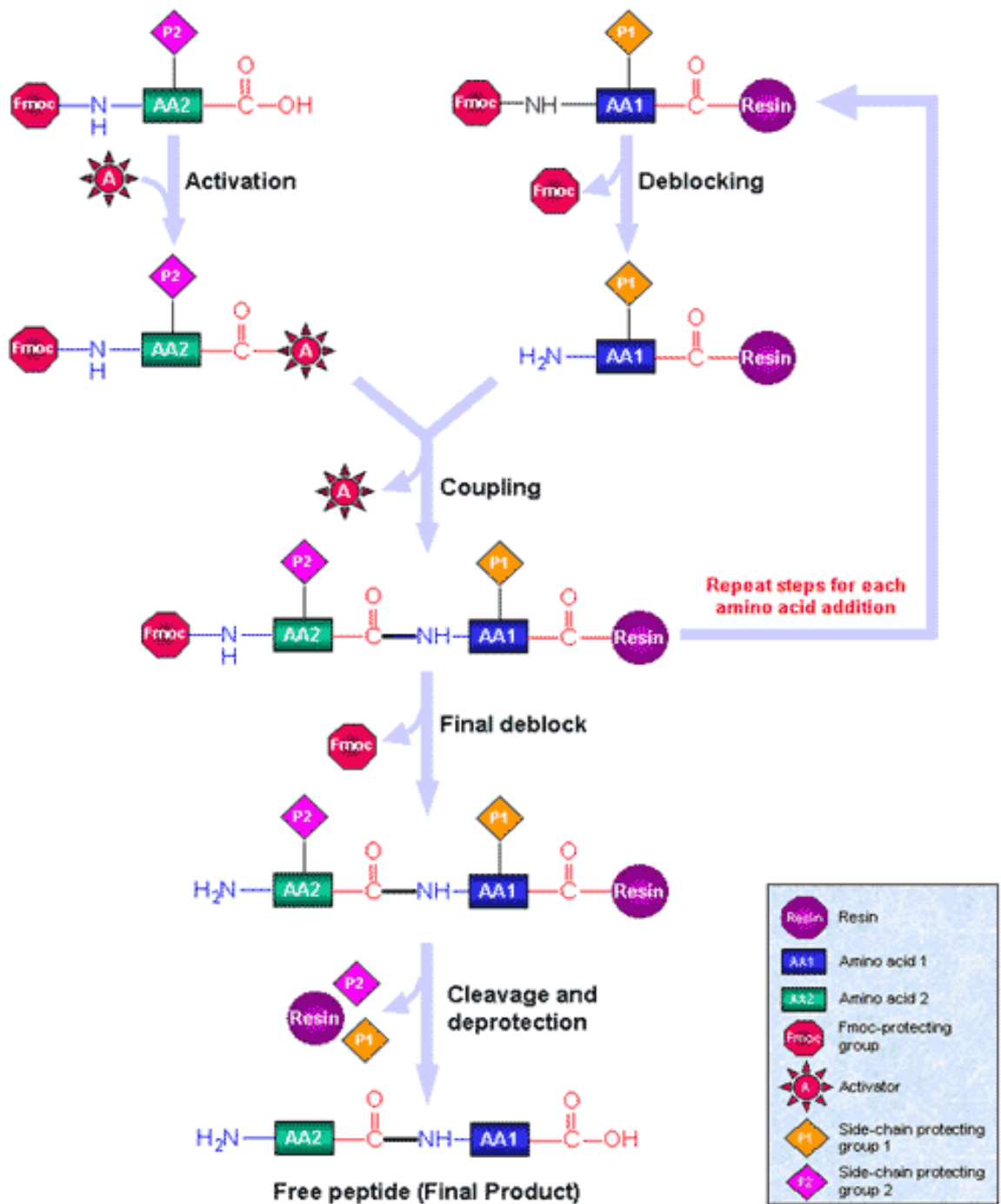


Figure 2.1 Schematic of solid phase peptide synthesis. AA1 coupled to a solid resin support via carboxyl group, while amino group is protected by Fmoc. AA2 amino group protected by Fmoc, but carboxyl group must be activated before coupling to AA1 can occur. Fmoc removed from AA1. Coupling can then occur with the carboxyl group from AA2 and amino group from AA1. The final steps involve removing additional protecting groups (P1 and P2) from side chains and cleaving the peptide from resin (SigmaAldrich, 2017). AA1 (amino acid 1), AA2 (amino acid 2), A (activator), P1 (protecting group 1), P2 (protecting group 2) Fmoc (9-fluorenylmethyloxycarbonyl).

The peptide arrays used within this thesis were synthesized on either Whatman 50 cellulose membranes (Sigma-Aldrich, Dorset, UK), or on cellulose membranes immobilised on glass slides (Intavis, Köln, Germany) by automatic spot synthesis using Autospot Robot ASS 222 (Intavis, Köln, Germany) (Frank, 2002). Either a domain within a protein, or the full-length protein can be spotted as overlapping 25-mer or shorter peptides, each shifted by 5 amino acids to increase the reliability of the screen.

2.7.2 Peptide Array – Overlay

Cellulose membrane peptide arrays spotted with the amino acid sequence of the β_2 AR were used to elucidate interactions between β_2 AR and enzymes of the SUMOylation cascade, UBC9 and PIAS γ (Chapter 4 - *In Vitro* SUMOylation of the β_2 AR).

The array was bathed in 100% ethanol for 30 seconds and then equilibrated in 1X TBS-T for 10 minutes before blocking in 5% TBS-T/phospho-block (Cambridge Bioscience, Cambridge, UK) to prevent unspecific binding for 2 hours. The array was then incubated with 400-1000 μ g/ μ l of HEK β_2 lysate overexpressing the enzyme of interest - either UBC9 or PIAS γ - in 1% TBS-T/phospho-block at 4°C overnight. As control, standard HEK β_2 lysate, in which no enzyme was overexpressed, was incubated on a separate array to determine unspecific binding, and treated exactly the same as the PIAS γ /UBC9 lysate array. The following morning arrays were washed 3 times in 1X TBS-T for 10 minutes and incubated in 1% TBS-T/phospho-block with primary antibody (specific for the enzyme of interest) (Table 2.1) overnight at 4°C. The following morning, arrays were then washed three times in 1X TBS-T and the appropriate secondary antibody (Table 2.2) was applied at the appropriate dilution in 1% TBS-T/phospho-block at room temperature for 1 hour. After a further 3 washes the array was exposed to Pierce ® ECL (enhanced chemiluminescence) western blotting substrate (ThermoFisher Scientific, Paisley, UK). The array was then placed in a developing cassette for developing in the dark room with X-OMAT (Kodak, London, UK). X-ray film (Kodak, London, UK) was placed in the cassette alongside the array for various exposure times before development in the X-OMAT.

2.7.3 Peptide Array – SUMOylation Assay

Glass slide cellulose membrane peptide arrays were spotted with truncations of the epitope against which the SUMO- β_2 AR antibody was raised, to allow SUMO- β_2 AR antibody specificity testing (Chapter 3 - Production of a SUMO- β_2 AR Specific Polyclonal Antibody). The array was blocked in 5% BSA (bovine serum albumin) in 1X TBS-T for 1 hour at room temperature with gentle rocking. SUMO kit (Enzo Life Sciences, Exeter UK) was used to SUMOylate peptide array. The kit contains purified recombinant His (histidine) tagged human SUMO-1, SUMO-2, SUMO-3 proteins, activating E1 enzyme, E2 enzyme, and ATP (required co factor for SUMO conjugation). This kit provides a means of generating SUMOylated proteins *in vitro*, by covalent linkage of the carboxy-terminal of SUMO-1, -2 or -3 to specific lysine residues on the target protein via isopeptide bonds. A reaction mixture was prepared with all the above kit components and made up to 1ml with sterile PBS. The array was incubated at 37°C for 60 min with the SUMO reaction mixture. The array was then washed three times in 1X TBS-T for 5 minutes followed by probing with His-HRP conjugated antibody (Table 2.1) 1 : 5000 dilution overnight at 4°C to allow detection of SUMOylation. This antibody is capable of detecting SUMOylation, as it identifies the His tag on the SUMO paralogues. Slides are then washed 3 times for 5 minutes in 1X TBS-T. The array was developed via ECL as described for array in section 2.7.2 “Peptide Array Overlay”.

2.8 UniProt Sequence Analysis of β_2 AR

To assess the aptness of the SUMOylation sites within the β_2 AR identified by the Baillie lab using peptide array (Figure 1.13, Chapter 1 - Introduction), a comparison was made with a SUMO-site finding algorithm, sp2.0 SUMOylation site identification software (GPS-SUMO, Guangzhou, China). The four identified sites (60, 227, 232 and 235) were examined in the following species; human, rat, mouse, rhesus monkey, cow. This was completed using the UniProt website (www.uniprot.org).

2.9 Immunoprecipitation (IP)

To assess the influence of SUMOylation on β_2 AR ubiquitination the extent of ubiquitination was assessed using immunoprecipitation (IP). This allowed

evaluation of the interaction between the β_2 AR and ubiquitin proteins. Following cell lysis and determination of protein concentration, samples were equilibrated to 400 μ g/ μ l in 3T3 lysis buffer per IP. A “mock” IP involving antibody conjugate beads (ThermoFisher, Paisley, UK) which will not bind to the target molecule within the lysate was completed alongside the test IP (antibody conjugate beads which will bind the target molecule) to act as a control. 100 μ l of IP beads or mock IP beads were added to an eppendorf and then beads were washed twice with 500 μ l of 3T3 lysis buffer via brief centrifugation. Supernatant was removed leaving beads alone, which were diluted with 100 μ l of 3T3 lysis buffer and vortex mixed to provide both mock IP and IP bead stock. 75 μ l of the appropriate bead stock was added to the appropriate lysate, both a mock set of lysate (incubated with mock beads) and an IP set of lysate (incubated with test beads). Beads and samples were incubated for 1-2 hours at 4°C with end over end rotation to allow proteins within the lysate to bind to the beads. Beads were then washed twice via brief centrifugation with 500 μ l of 3T3 lysis buffer. Supernatant was removed and 100 μ l of 5x lammeli sample buffer (Bio-rad, Hertfordshire, UK) was added to the beads then heated to 90°C for 5 minutes. This caused bound proteins to denature releasing them from the beads. Proteins that associated with the immunopurified subject protein were detected via immunoblotting.

2.10 ArrayScan High Content Analysis of Internalisation

The ArrayScan system was used to determine the influence of β_2 AR SUMOylation on isoprenaline-mediated receptor internalisation. The ArrayScan® (Cellomics, Pittsburgh, USA) is a microtiter plate imaging system that allows both cellular and subcellular quantification of fluorescence in cells. Within the HEK β_2 cell line (McLean & Milligan, 2000) (Mclean, et al., 1999) (described in section 2.2.2 - HEK β_2 Cells) the β_2 AR is GFP labelled, and therefore isoprenaline-mediated internalisation of the β_2 AR was visualised as fluorescent green spots enclosed within the cell. An algorithm has been developed that identifies and collects information about these spots, allowing quantification of the internalisation process (Conway, et al., 1999).

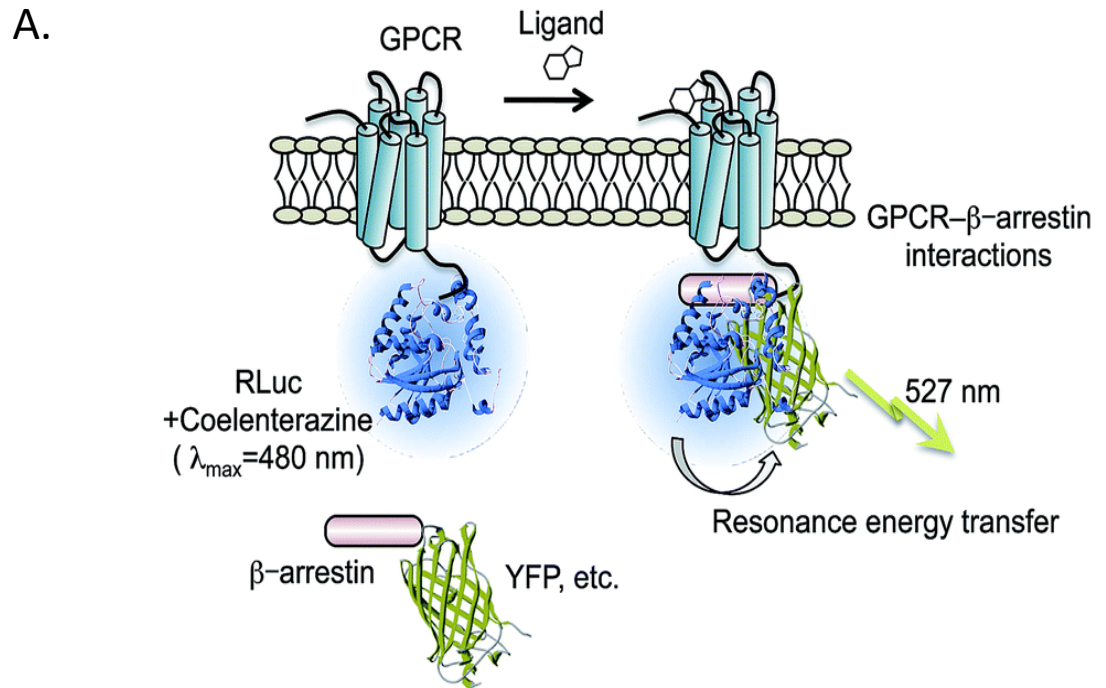
HEK β_2 cells were seeded into a poly-D-lysine (1:20 dilution in phosphate buffered saline (PBS), 40 μ l/well) coated 96 well plate at a density of 35,000 cells/well. HEK β_2 cells were subject to this assay with prior mock transfection with empty

transfection reagent or transfection with the E3 ligase PIAS γ , which promotes SUMOylation of the β_2 AR (Figure 4.4) (described in section 2.3.2 - Transient Transfection of Plasmid DNA). After 24 hours, cells were washed 2X with Hanks balanced salt solution (HBSS) and incubated with 10 μ M isoprenaline for the following time points: - 10, 20, 40, 60, 90 minutes. Cells were then washed 3X with PBS and fixed with 4% paraformaldehyde (PFA)/PBS. Cells were then incubated for 30 minutes with 10 μ g/ml Hoechst nuclear stain (ThermoFisher, Paisley, UK) which binds to nucleic acids at 37°C. Images were acquired immediately by using a Cellomics ArrayScan II high content imager and internalised receptors were quantified by using the proprietary algorithm designed to identify the number of endosomal recycling compartments per cell (Conway, et al., 1999).

2.11 Bioluminescence Resonance Energy Transfer (BRET)

The bioluminescence resonance energy transfer (BRET) assay was used to determine the influence of β_2 AR SUMOylation on the relationship between the β_2 AR and β -arrestin. BRET is similar to FRET and was originally discovered in marine organisms. This is a naturally occurring non-radiative energy transfer from a donor enzyme to a suitable acceptor molecule after substrate oxidation. Renilla luciferase (RLuc), isolated from the sea pansy *Renilla reniformis*, is traditionally used as a bioluminescence donor in conjugation with a fluorescent acceptor, which for this work is YFP (yellow fluorescent protein) (Ward & Cormier, 1979). This enzyme generates bioluminescence through oxidation of its substrate coelenterazine-h, and thus excites the fluorescence acceptor YFP. BRET was used to determine if the SUMOylation of the β_2 AR influenced the interaction between the receptor and β -arrestin. The constructs used for this project were kindly provided by Professor Graeme Milligan of University of Glasgow. The β_2 AR was attached to RLuc and β -arrestin was attached to YFP. Binding of isoprenaline to β_2 AR induces recruitment of β -arrestin to the receptor. The interaction brings RLuc and YFP into close proximity, therefore bioluminescent resonance energy transfer occurs in the presence of co-elentrazine h (Figure 2.2A) (Hattori & Ozawa, 2015). The effectiveness of energy transfer between RLuc and YFP is demonstrated in the ratio of acceptor energy emission relative to the donor emission. This is also referred to as the BRET ratio and is a degree for proximity

of YFP to RLuc. For this project, the BRET ratio was monitored in the presence of increasing concentrations of isoprenaline, RLuc emitting at 480nm and YFP at 527nm (Figure 2.2B) (Hattori & Ozawa, 2015).



B.

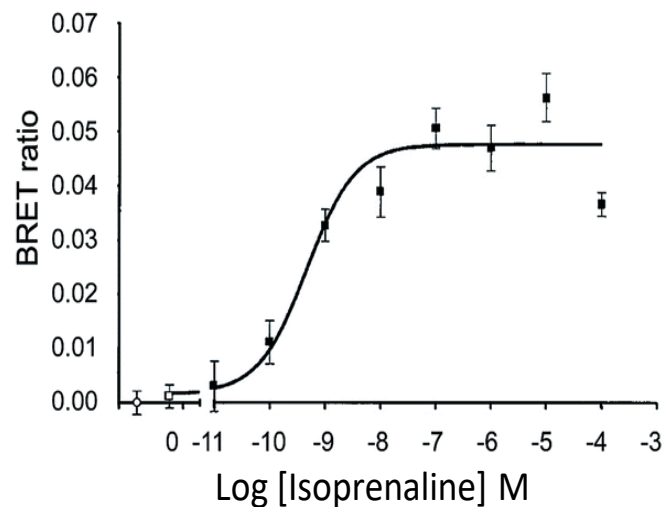


Figure 2.2 Principle of BRET. (A) β_2 AR attached to RLuc, β -arrestin attached to YFP. Binding of isoprenaline to β_2 AR induces recruitment of β -arrestin to β_2 AR. The interaction brings RLuc and YFP into close proximity therefore bioluminescent resonance energy transfer occurs. (B) BRET ratio can be monitored in the presence of increasing concentrations of isoprenaline, RLuc emitting at 480nm and YFP at 527nm. At higher concentrations, greater BRET will be observed (Hattori & Ozawa, 2015). BRET (bioluminescence resonance energy transfer) YFP (yellow fluorescent protein), RLuc (renilla luciferase), GPCR (G protein-coupled receptor).

HEK293 cells were transfected with β_2 AR tagged with YFP and β -arrestin2 tagged with RLuc 6 (Lorenz, et al., 1991) (ratio 4:1) in addition to mock transfection with empty transfection reagent or transfection with the E3 ligase PIASy, which promotes SUMOylation of the β_2 AR (Figure 4.4) (described in section 2.3.2 - Transient Transfection of Plasmid DNA). An additional transfection was performed with only the RLuc construct to measure background from RLuc alone. From 10cm dishes, cells were seeded into a poly-D-lysine (1 : 20 dilution in phosphate buffered saline (PBS), 40 μ l/well) coated 96 well plate at a density of 50,000 cells/well. After 24 hours, cells were washed 2X with HBSS and 5mM coelentrazine-h (Promega, Southampton, UK) was added. Cells were incubated in darkness for 10 min at 37°C before addition of isoprenaline (1 μ M-10 μ M). Cells were incubated for a further 5 min at 37°C before reading on a Mithras LB940 plate reader (Berthold Technology, Bad Wildbad, Germany), that allows sequential reading of emission signals detected at 480nm and 527nm, for RLuc and YFP, respectively. Net BRET was defined as the 527nm : 480nm ratio of cells co-expressing RLuc and YFP minus the BRET ratio of cells expressing only the RLuc construct in the same experiment. This value was multiplied by 1000 to obtain mBRET units. This gives a degree of proximity of YFP to RLuc in response to isoprenaline concentration allowing quantification of the relationship between β_2 AR- β -arrestin.

2.12 Fluorescence Resonance Energy Transfer (FRET)

Fluorescence resonance energy transfer (FRET) was used to determine how long after β_2 AR isoprenaline-mediated stimulation the cAMP levels within the cell interior remain elevated, and if SUMOylation of the β_2 AR influences this timeframe. FRET is a non-radiative process of energy transfer from an excited donor fluorophore to an acceptor fluorophore. This phenomenon can only occur when the two fluorophores are in close proximity to one another. This technique has been exploited to generate genetically-encoded sensors to visualise cAMP dynamics in intact living cells (Zaccolo, et al., 2000). A FRET-based indicator of cAMP is usually composed of a cAMP-binding domain and the cyan and yellow variants of the green fluorescent protein, CFP and YFP respectively. Excitation of CFP, by 430nm wavelength, results in the transfer of excited state energy to YFP, which will emit a signal at 545nm. Both emissions from CFP (480nm) and YFP

(545nm) are collected for analysis. Binding of cAMP to the sensor induces a conformational change which alters the distance between the two fluorophores thereby affecting the energy transfer between them. When this occurs only the CFP emission (480nm) is detected as no energy is transferred to YFP. FRET changes can be expressed as changes in the ratio between CFP emission (480 nm)/YFP emission (545 nm) (Figure 2.3). Changes in FRET can be used in real-time imaging experiments as variations in FRET efficiency correlates with changes in cAMP intracellular concentration. An elevation in cAMP binding to the FRET probe results in less FRET from CFP to YFP therefore the ratio will be reduced.

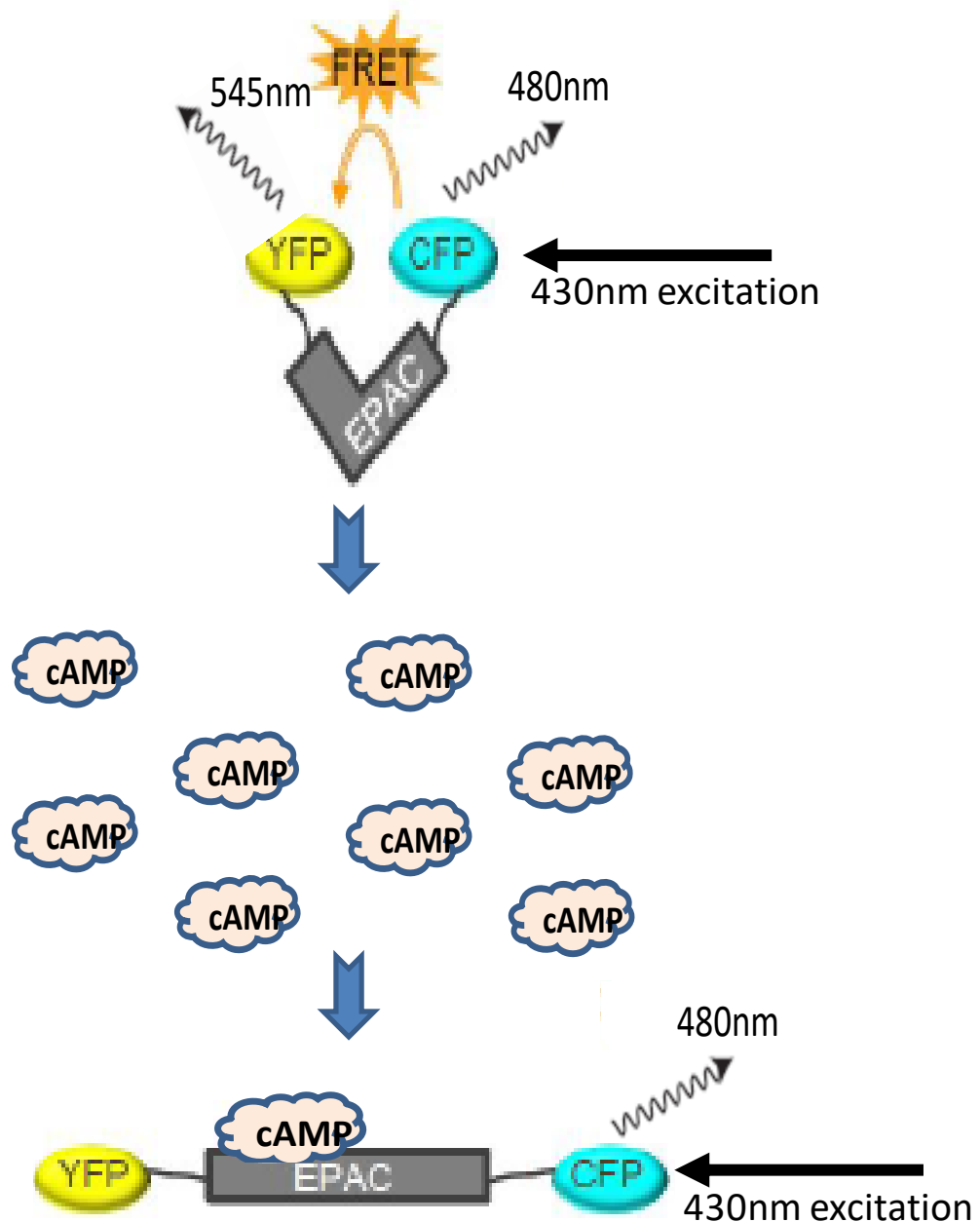


Figure 2.3 Principle of FRET. Excitation of CFP (430 nm) results in the transfer of energy to YFP (emitting a signal at 545 nm). Binding of cAMP to the sensor induces a conformational change which alters the distance between the two fluorophores, thereby affecting the energy transfer between them. When this occurs only the CFP emission (480nm) is detected if the wavelength selected for excitation is 430nm as this excites only the CFP donor and no energy is transferred to YFP. FRET changes can be expressed as changes in the ratio between CFP emission (480 nm)/YFP emission (545 nm). Image adapted from original in the thesis of Dr Ashleigh Fields “Local cAMP signalling and phosphodiesterase activity in an *in vitro* model of cardiac hypertrophy” <http://theses.gla.ac.uk/4755/>. CFP (cyan fluorescent protein), YFP (yellow fluorescent protein), FRET (fluorescence resonance energy transfer), EPAC (exchange protein activated by cAMP), cAMP (cyclic adenosine monophosphate).

HEKB₂ cells were seeded onto glass coverslips at a density of 700,000 cells per coverslip. Targeted FRET sensor - EPAC cAMPs-1 which is a cytosolic cAMP sensor - was transiently transfected in addition to mock transfection with empty transfection reagent or transfection with the E3 ligase PIASy, which promotes SUMOylation of the β_2 AR (Figure 4.4) (described in section 2.3.2 - Transient Transfection of Plasmid DNA). Cells were imaged 24-48 hours following transfection. Cells were stimulated in real time with 1nM isoprenaline on an Olympus IX71 inverted microscope with a 100x oil immersion objective (Zeiss, London, UK) in the presence of 10 μ M rolipram. Rolipram was used to inhibit phosphodiesterase-4 (PDE-4) as this enzyme will normally degrade cAMP. The sample was exposed to excitation at 430nm, and CFP and YFP signals acquired. FRET changes were measured following background subtraction by dividing the intensity of emissions at 480nm and 545nm, to give a FRET ratio.

2.13 Radioligand Binding Studies

Radioligand binding studies were used to determine if the SUMOylated β_2 AR interacts differently with ligand. These studies provided information on the interaction between the β_2 AR and both radioligand and isoprenaline.

2.13.1 Cell Membrane Preparations

Cell membrane preparations were used to isolate the β_2 AR. Pellets of cells were frozen at -80°C for a minimum of 1 hour, thawed, and re-suspended in ice-cold 10 mM Tris, 0.1 mM EDTA, pH 7.4 (Tris-EDTA buffer) supplemented with complete protease inhibitors cocktail (Roche, West Sussex, UK) and N-ethylmaleimide (NEM) (25mM) (Sigma-Aldrich, Dorset, UK) to inhibit deSUMOylation. Cells were homogenized on ice by 40 strokes of a glass-on-Teflon homogenizer followed by centrifugation at 1000g for 5 minutes at 4°C to remove unbroken cells and nuclei. The supernatant fraction was removed and passed through a 25-gauge needle 10X before being transferred to ultracentrifuge tubes and subjected to centrifugation at 50,000 x g for 45 minutes at 4°C . The resulting pellets were re-suspended in ice-cold Tris-EDTA buffer. Protein concentration was assessed via Bradford assay (described in section 2.5 - Protein Quantification by the Bradford Assay) and membranes were stored at -80°C until required. The membrane preparations

were prepared from HEK β_2 cells which had been mock transfected with empty transfection reagent or transfected with the E3 ligase PIASy, which promotes SUMOylation of the β_2 AR (Figure 4.4) (described in section 2.3.2 - Transient Transfection of Plasmid DNA).

2.13.2 Saturation Ligand Binding

Saturation radioligand binding studies are performed using several concentrations of a radioligand to allow determination of the dissociation constant (K_d) and the number of binding sites in the assay (B_{max}) for the radioligand. K_d is indicative of the receptor affinity for the radioligand - it is the concentration at which the ligand binds to half of its binding sites, the ligand's affinity for the receptor is small when its K_d is large. Conversely, ligands with a high affinity have small K_d values. The B_{max} is representative of the number of binding sites in the assay for the radioligand - indicative of receptor density (Figure 2.4) (Hein, et al., 2005). Saturation binding isotherms were established after the addition of 5 μ g of membrane protein both with and without the SUMOylated form of the β_2 AR - mediated via PIASy transfection - to assay buffer (TEM: Tris 75mM, EDTA 1mM, MgCl₂ 12.5mM) containing varying concentrations of ³H-dihydroalprenolol (DHA) (Tocris, Bristol, UK) (0.1nM-10nM). This is a common radioligand used to assess BARs. Nonspecific binding was determined in the presence of 50 μ M propranolol (BAR antagonist). Reactions were incubated for 60 min at 25 $^{\circ}$ C, and bound ligand was separated from free by vacuum filtration through GF/C filters (Brandel Inc., Gaithersburg, Maryland). The filters were washed 2X with PBS, and bound ligand was estimated by liquid scintillation counting. For this the filters are mixed with a scintillator solution, which will fluoresce upon interaction with a particle emitted by radioactive decay - meaning it has been irradiated by the sample. The light emitted in response to this irradiation is taken as a measure of the amount of radioactivity in the sample (Diagnostics, 2004). This allowed determination if SUMOylation of the β_2 AR influences the receptor K_d or B_{max} for the radioligand.

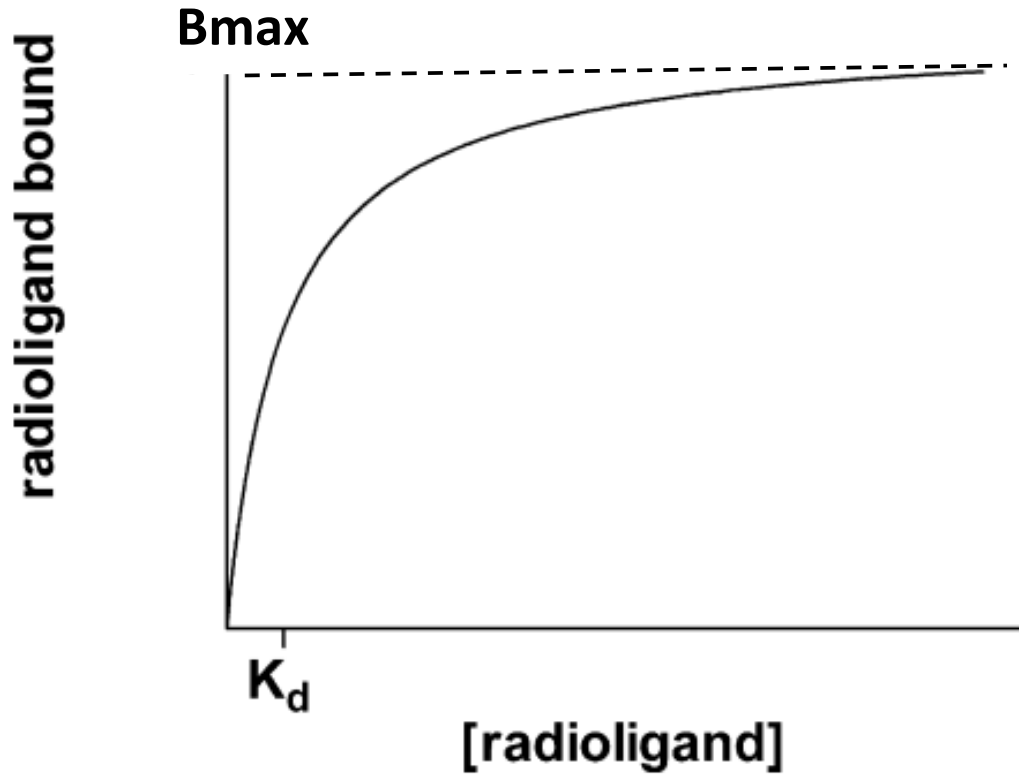


Figure 2.4 Saturation ligand binding schematic. K_d is indicative of the receptor affinity for the radioligand - it is the concentration at which the ligand binds to half its binding sites. The B_{max} is representative of the number of binding sites in the assay for the radioligand - indicative of receptor density (Hein, et al., 2005).

2.13.3 Competition Ligand Binding

To assess the interaction between the β_2 AR and isoprenaline in both its SUMOylated and non SUMOylated format a competition binding assay was used. A single concentration of radioligand, ^3H -DHA (Tocris, Bristol, UK), competes for receptor site occupation with multiple concentrations of a non-radioactively labelled compound, isoprenaline. Competition studies primarily yield the concentration of the inhibitor causing 50% inhibition of radioligand binding (IC_{50}), which can be converted into the inhibitor constant (K_i) using appropriate equations (Figure 2.5) (Hein, et al., 2005). Saturation binding isotherms were established after the addition of $5\mu\text{g}$ of membrane protein both with and without the SUMOylated form of the β_2 AR - mediated via PIASy transfection - to assay buffer (TEM: Tris 75mM, EDTA 1mM, MgCl_2 12.5mM) containing 0.7nM ^3H -DHA. Nonspecific binding was determined in the presence of $50\mu\text{M}$ propranolol. The radioligand ^3H -DHA was competed for receptor occupation with isoprenaline (1nM - $100\mu\text{M}$). Reactions were incubated for 60 min at 25°C , and bound ligand was separated from free by vacuum filtration through GF/C filters (Brandel Inc., Gaithersburg, Maryland). The filters were washed 2X with PBS, and bound ligand was estimated by liquid scintillation counting. This allowed us to determine if SUMOylation of the β_2 AR influences its interaction with isoprenaline, the ligand used within our studies to promote β_2 AR signalling.

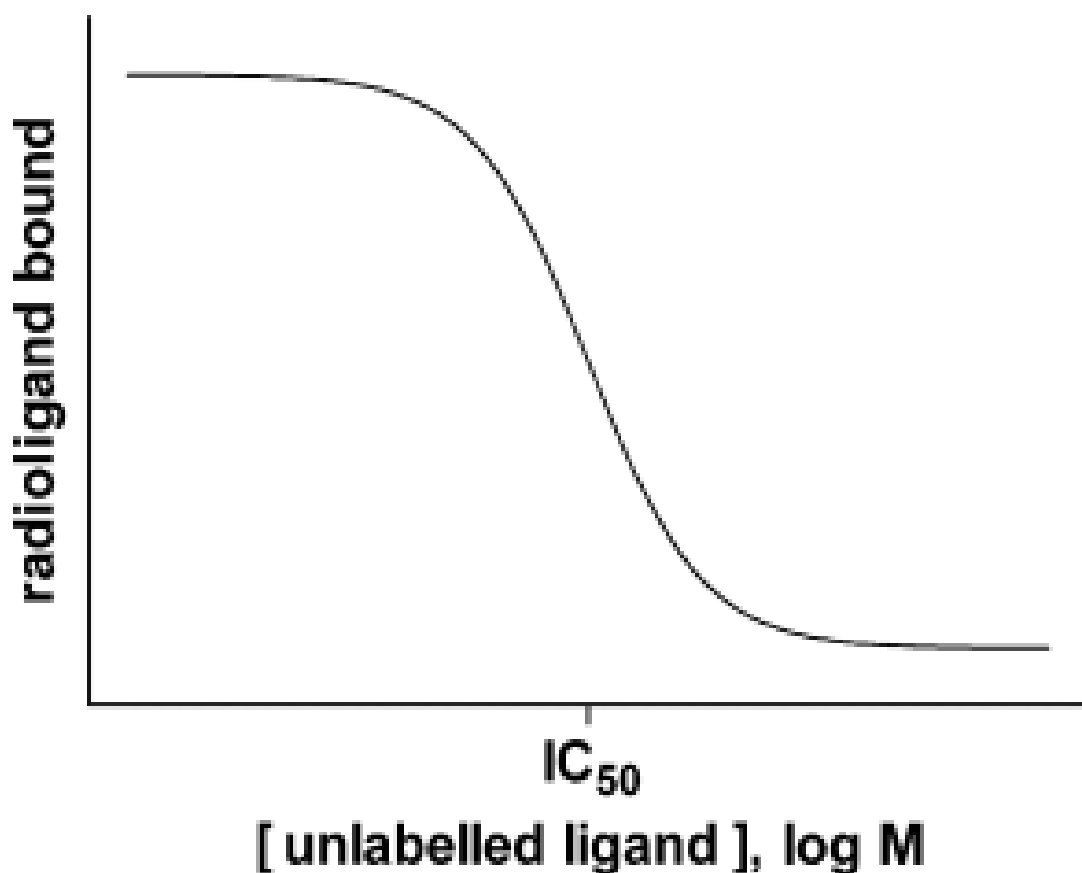


Figure 2.5 Competition ligand binding schematic. A single concentration of radioligand is competed for by multiple concentrations of a non-radioactively labelled compounds, namely isoprenaline. Competition studies primarily yield the concentration of the inhibitor causing 50% inhibition of radioligand binding (IC_{50}), which can be converted into the inhibitor constant of the inhibitor (K_i) using appropriate equations (Hein, et al., 2005).

2.14 Systemic Protein Affinity Strength Modulation (SPASM) Sensor

The Systemic Protein Affinity Strength Modulation (SPASM) sensor was used to determine the influence of β_2 AR SUMOylation on the interaction between the β_2 AR and different G proteins. The SPASM sensors used in this project were BRET sensors which are based on a recently developed technique that involves the fusion of a native peptide from the C-terminus of a G_α subunit to the C-terminus of the intact GPCR (Sivaramakrishnan & Spudich, 2011). Upon activation of the GPCR, the C terminus of the G_α subunit slots itself into a cytosolic groove on the GPCR (Choe, et al., 2011) (Rasmussen, et al., 2011) (Chung, et al., 2011). Therefore, mimicking this peptide will allow the mimic to slot into this same area on the GPCR as the native C-terminus of the G_α subunit. For our work, SPASM sensors within a Flp-In T-Rex[®] HEK293 system were used to investigate the relationship between G_s - β_2 AR and G_i - β_2 AR. These cells were kindly provided by Dr Brian Hudson from the group of Professor Graeme Milligan of University of Glasgow. This system allows induction of the gene for the G_s - β_2 AR and G_i - β_2 AR sensors by the addition of doxycycline (Ward, et al., 2011). Each SPASM sensor contains, from N to C-terminus: a GPCR joined to mCitrine (BRET acceptor); ER/K linker which is a polypeptide motif joining acceptor to donor; a peptide which is designed for $G_{i\alpha}$ or $G_{s\alpha}$ subunit (G-pep) joined to NLuc (BRET donor). When the β_2 AR is stimulated with isoprenaline the G peptide mimic will interact with the GPCR giving BRET signal due to interaction between mCitrine and NLuc (Figure 2.6).

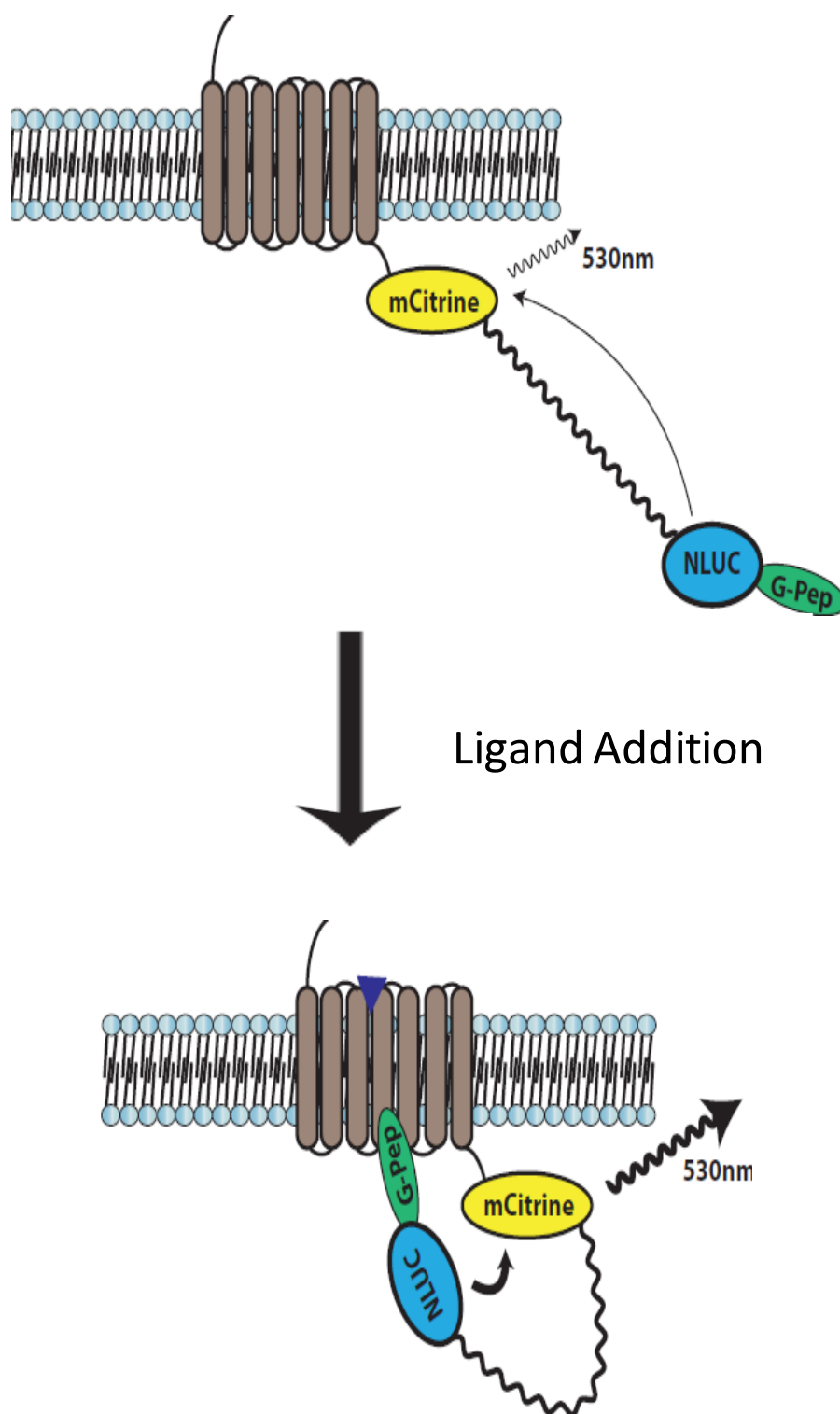


Figure 2.6 Principle of SPASM sensor. When the β_2 AR is stimulated with isoprenaline (ligand addition) the G-pep will interact with the GPCR giving BRET signal seen with stimulation by agonist in a dose-dependent manner. Image designed by Dr Brian Hudson of University of Glasgow. NLuc (NanoLuc Luciferase).

2.14.1 SPASM Sensor Protein Expression and Cell Preparation

HEK293 Flp-In T-Rex[®] cells (ThermoFisher, Paisley, UK) which stably expressed either G_i - β_2 AR or G_s - β_2 AR SPASM sensors were cultured in culture medium and incubated at 37°C in DMEM 41695 with 10% fetal bovine serum, 1% penicillin/streptomycin. Cells were plated into 10cm dishes and both sets of SPASM sensor cells were either mock transfected with empty transfection reagent or transfected with the E3 ligase PIAS γ , which promotes SUMOylation of the β_2 AR (Figure 4.4) (described in section 2.3.2 - Transient Transfection of Plasmid DNA). 24 hours later the plate was coated with poly-D-lysine (1 : 20 dilution in phosphate buffered saline (PBS), 40 μ l/well) at a density of 40,000 cells/well. The medium was refreshed to contain 1 μ g/ml doxacycline to promote induction of the gene for the G_s - β_2 AR and G_i - β_2 AR sensors. 24 hours later cells were washed with twice with HBSS and Nanoglo luciferase (Promega, Wisconsin, USA) substrate was added to the cells and incubated for 10 minutes. Isoprenaline was then added for 10 minutes for either concentration response experiments (1pM-10 μ M), or kinetics experiments (10 μ M). Cells were read either on PheraStar FS (kinetics) (BMG LabTech, Buck, UK) or Clariostar (concentration response) (BMG LabTech, Buck, UK) that allows sequential reading of emission signals detected at 485nm and 530nm, for NLuc and mCitrine, respectively. Net BRET was defined as the 530nm : 485nm ratio of cells co-expressing NLuc and mCitrine. This gives a degree of proximity of NLuc and mCitrine in response to isoprenaline concentration, allowing quantification of the relationship between β_2 AR and the respective G protein-dependent upon with set of Flp-In T-Rex[®] cells were being assessed, G_s - β_2 AR and G_i - β_2 AR.

2.15 Minimally Invasive TAC Pressure Overload Model in Mice

2.15.1 Ethical Approval

Animal experiments were performed in accordance with the UK Animals (Scientific Procedures) Act 1986. These experiments were approved by institutional ethical review committees and conducted under authority of project licenses held at the University of Glasgow.

2.15.2 C57BL/6J Mice

C57BL/6J mice (25-30 g) were purchased from Harlan (Bicester, UK) and group housed in standard conditions of a 12h-12h light-dark cycle with ad libitum feeding (Rat and Mouse Chow, Special Diet Services, Witham, UK) and water. Only male mice were used for these experiments.

2.15.3 Surgical Procedure

The surgical protocol was an adaptation of the minimally invasive TAC technique described by Martin et al (2012). Mice were anaesthetized in a perspex chamber with 3% isofluorane in oxygen delivered at 2 l minute⁻¹ for induction. After 2-3 minutes, mice were placed supine on a heating pad - to maintain body temperature at 37°C - and visualised under an operating microscope (Zeiss, Stuttgart, Germany). Anaesthesia was maintained at 1.5% isofluorane in 1 l minute⁻¹ oxygen via a specially designed facemask which orients the animal in an optimal surgical position. Fur was removed from the neck and upper chest area using hair removal cream (Veet ®) and the area was wiped with betadine to prevent infection at the surgical site. A sterile adhesive patch (Tegaderm, 3M, Warks) was placed over the surgical area to aid in preventing infection. A small horizontal 1cm skin incision was made at the level of the suprasternal notch, allowing location of the trachea. Using the trachea for anatomical placement the thymus was located and retracted allowing location of the aortic arch. A 5-0 silk suture was snared with a hooked needle and passed under the aortic arch before tying between brachiocephalic and left carotid artery (Figure 5.1). This hooked needle had been blunted under a surgical microscope to prevent any damage to the blood vessels when passing under the arch. A 27G needle was used to control the tightness of the suture by laying the needle alongside the aortic arch during the suture tying. Following aortic arch ligation, the skin was sutured and the animal was left to recover in a heated box until fully conscious. SHAM operated animals were subjected to the same procedure, with the exception of the aortic arch ligation. In these animals, the hooked needle was passed underneath the aortic arch and then removed. Immediately after surgery, 0.5ml saline was administered subcutaneously if necessary due to blood loss. Rimadyl (carprofen) - a non-steroidal anti-inflammatory drug - was administered post-surgery for

analgesia, at a dose of 5mg/kg. Animals were housed individually following surgery for 8 weeks to allow subsequent cardiac remodelling (Figure 2.7).

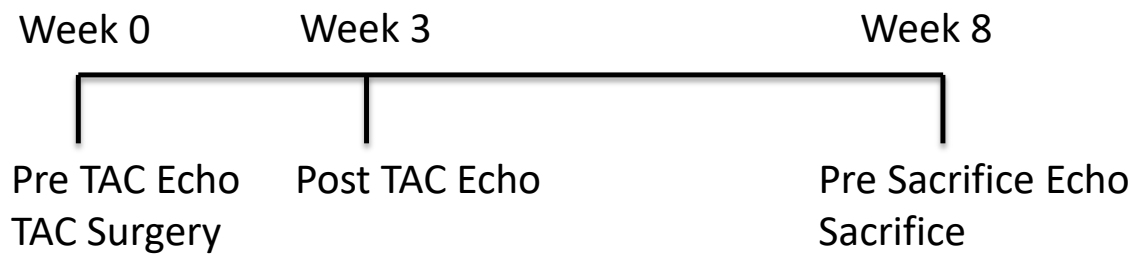


Figure 2.7. Minimally invasive TAC study timeline. Animals underwent pre-TAC transthoracic echocardiography to assess baseline cardiac function prior to TAC surgery. At 3 weeks, cardiac function was assessed again by transthoracic echocardiography. At 8 weeks, cardiac function was assessed a final time and then animals were sacrificed. TAC (transverse aortic constriction), Echo (echocardiography).

2.15.4 Transthoracic Echocardiography

Transthoracic echocardiographic assessment of LV function was performed both 3 and 8 weeks after surgery, as well as before surgery (Figure 2.7). Animals were anaesthetized with isoflurane and oxygen as described for surgical procedure (section 2.15.3 - Surgical Procedure). Two-dimensional short-axis views and M-mode images of the LV were recorded at the level of the papillary muscle using a Siemens Acuson Sequoia 512 ultrasound machine and a 15L8 probe set to a frequency of 14Hz (Siemens, Surrey, UK). The measurements taken include LV end systolic diameter (LVESD), LV end diastolic diameter (LVEDD), posterior wall thickness during systole (PWTs), posterior wall thickness during diastole (PWTd), anterior wall thickness during systole (AWTs), anterior wall thickness during diastole (AWTd). An average of 3 measurements of each variable was taken from each image (Figure 2.8). At the time of echocardiography both body weight and tibia length were also recorded.

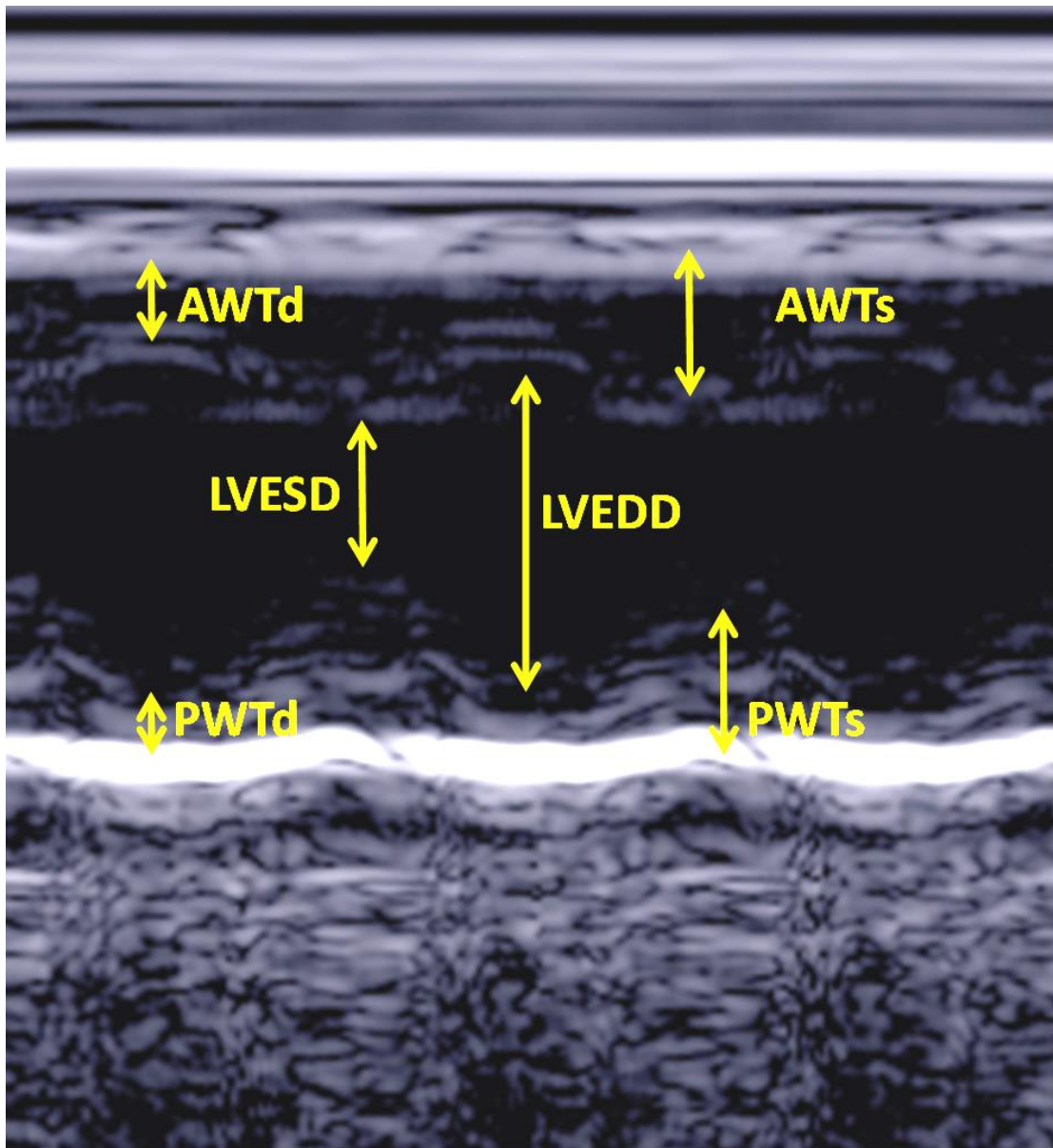


Figure 2.8 Transthoracic echocardiography parameters. Animals underwent transthoracic echocardiography to assess cardiac function. The measurements taken include LVESD, LVEDD, PWTs, PWTd, AWTs, AWTd. LVESD (LV end systolic diameter), LVEDD (LV end diastolic diameter), PWTs (posterior wall thickness during systole), PWTd (posterior wall thickness during diastole), AWTs (anterior wall thickness during systole), AWTd (anterior wall thickness during diastole).

2.15.5 Organ Harvesting

Mice were anaesthetised with isoflurane and oxygen as described above for surgical procedure (section 2.15.3 - Surgical Procedure) only maintenance remained at 5% isoflurane in oxygen delivered at 2 l min⁻¹ as the animals were non-recovery. Mice were immobilised on a surgical pad before a vertical incision was made to expose the internal organs. Mice were culled via exsanguination, with blood being drawn from the LV. Aorta, heart, lungs, epididymal fat, kidneys, brain and plasma were then collected. Samples for protein analysis were snap frozen in liquid nitrogen, while samples reserved for immunohistochemistry were placed in 4% paraformaldehyde overnight before being transferred to 50% ethanol. At the time of sacrifice, both body weight and tibia length were also recorded.

2.16 Histology

Paraformaldehyde treated tissue was transferred into Shandon biopsy cassettes (ThermoFisher Scientific, Paisley, UK) and then processed in a Shandon Excelsior tissue processor (ThermoFisher Scientific, Paisley, UK) (Table 2.3).

Table 2.3 Processing sequence for Shandon Excelsior tissue processor

Solvent	Time (minutes)
70% Ethanol	30
95% Ethanol	30
100% Ethanol	30
100% Ethanol	30
100% Ethanol	45
100% Ethanol	45
100% Ethanol	60
Xylene	30
Xylene	30
Xylene	30
Paraffin Wax	30
Paraffin Wax	30
Paraffin Wax	45

After infiltration in wax, the tissue was embedded on a Shandon Histocentre 3 (ThermoFisher Scientific, Paisley, UK). For sectioning, heart tissue blocks were chilled overnight in the freezer and then sectioned on a Shandon Finesse 325 microtome (ThermoFisher Scientific, Paisley, UK). Initially, tissue blocks were

sectioned at 15µm until the entire cardiac section could be visualised, from which point on 5µm sections were taken for staining. After cutting, sections were transferred to a 40°C waterbath to remove wrinkles before mounting on Tissue-Tek silanized microscope slides (Sakura Finetek, Thatcham, UK) and placing at 60°C overnight to dry. Prior to histological staining, sections were de-paraffinised and re-hydrated by passing through histoclear and an alcohol gradient (Table 2.4).

Table 2.4 De-paraffinisation and rehydration sequence

Solution	Time (minutes)
Histoclear	7
Histoclear	7
100% Ethanol	7
90% Ethanol	7
70% Ethanol	7
Water	5

2.16.1 Picrosirius Red

Picrosirius red is used to assess collagen deposition. This stain consists of a solution of yellow picric acid and sirius red. With picric acid being small and hydrophobic, whereas sirius acid being large and hydrophilic, the acids penetrate the fixed tissue at different rates. This leads to the collagenous tissue staining bright red, and the remaining tissue staining yellow.

Sections were de-paraffinised and re-hydrated, as described previously (Table 2.4) After re-hydration, sections were placed into Weigert's haematoxylin (TCS Bioscience, Buckingham, UK) for 10 minutes to stain the nuclei before washing in running tap water for 10 minutes. Slides were then stained in a 0.1 % sirius red solution in saturated picric acid (Picrosirius red (F3BA)) (Sigma-Aldrich, Dorset, UK) in the dark for 90 minutes. Slides were washed in 2 changes of 0.01 N HCl (acidified water) by submerging 3 times before de-hydration in 2 changes of 100 % ethanol for 3 minutes and 2 changes in histoclear for 7 minutes. Sections were then mounted in DPX mountant (Sigma-Aldrich, Dorset, UK) and dried overnight at room temperature. Slides were imaged on Life Technologies EVOS microscope (ThermoFisher Scientific, Paisley, UK). 10 images were taken per slide for quantification by Image J (NIH, Maryland, USA).

2.16.2 Wheat Germ Agglutinin (WGA)

Wheat Germ Agglutinin (WGA) is a plant lectin found in *Triticum vulgare* (wheat), which binds to sugars with N-acetylglucosamine and N-acetylneuraminic acid residues. These residues are found in membrane glycoproteins, including those of the cardiomyocyte membrane (Wright, 1984). Therefore, fluorescently labelled WGA staining can be used to visualise the cardiomyocyte membrane (Savio-Gamilberti, et al., 2008) (Tsukamoto, et al., 2013) (Bueno, et al., 2000).

Sections were de-paraffinised and re-hydrated as described previously (Table 2.4) before sodium citrate-mediated antigen retrieval. This is an essential step, as during fixation methylene bridges are formed which cross link proteins and mask antigenic sites. The sodium citrate retrieval process breaks these bridges and exposes the antigenic sites, allowing for antibodies to bind (Abcam, 2017). Retrieval involves boiling the slides for 10 minutes in a pre-heated sodium citrate solution, and then allowing them to cool for 20 minutes to give time for antigen refolding. Slides were then washed in running tap water for 5 minutes followed by 5 minutes in PBS. Sections were blocked in PBS with 1 % BSA and 5 % goat serum (VectorLabs, Peterborough, UK) for 1 hour at room temperature, before being incubated with 10 µg/mL Alexa Fluor 555 conjugated WGA (ThermoFisher Scientific, Paisley, UK) prepared in the blocking solution for 1 hour. WGA allowed visualisation of the cell membrane. Following incubation, sections were washed twice in PBS for 5 minutes and mounted in Prolong Gold+DAPI (ThermoFisher Scientific, Paisley, UK). DAPI is a nuclear stain which allows visualisation of the nucleus in the cardiomyocytes. Slides were protected from light and allowed to dry overnight prior to imaging by epifluorescence confocal microscopy. 10 images were taken per slide, and were analysed in Image J (NIH, Maryland, USA) to assess cardiomyocyte cross-sectional area. All cardiomyocytes were measured per image.

2.17 Tissue Homogenisation

Tissue homogenisation is similar to preparation of cell lysate, where the tissue must be broken down to release cellular contents. Both cardiac tissue samples from the mouse TAC surgical study and LAD artery balloon occlusion pigs, kindly provided by the Hajjar group, were prepared in this manner to allow assessment

of proteins via immunoblotting. 50mg of tissue was placed in a 2ml RNase free tube alongside 5mm stainless steel beads (QIAGEN, Manchester, UK). 700µl of RIPA buffer (Sigma-Aldrich, Dorset, UK) substituted with appropriate inhibitors; protease cocktail inhibitor (Roche, West Sussex, UK), phos-stop tablets (Roche, West Sussex, UK) and 25mM N-ethylmaleimide (NEM) (Sigma-Aldrich, Dorset, UK) was added to the tubes and the tubes were then placed in the homogenizer (QIAGEN, Manchester, UK). The protease cocktail inhibitor tablets inhibited a broad spectrum of proteases which would normally break down proteins, phos-stop tablets inhibited phosphatases which prevented phosphorylated proteins from becoming de-phosphorylated, and NEM inhibited enzymes which promote de-SUMOylation. The tubes were pulsed for 45 seconds with a 3 minute rest period in between to prevent excess heat. This was repeated 3 times. After homogenisation samples were centrifuged for 12 minutes at 13,000rpm at 4°C. The supernatant was collected and subject to protein quantification by Bradford assay (described in section 2.5 - Protein Quantification by the Bradford Assay). Samples were assessed via immunoblotting (described in section 2.6 - Immunoblotting).

2.18 Statistical Analysis

Data are expressed as mean \pm standard error of the mean (SEM) unless otherwise stated. Statistical analysis was performed using GraphPad Prism Version 6 (GraphPad Prism, California, USA). For comparisons of a continuous variable between 2 experimental groups, paired and unpaired Student's t-tests were applied as appropriate. For statistical comparisons in data sets with more than two groups, repeated measures analysis of variance (ANOVA) was applied, followed by the Dunnett's or Tukey's post-tests, comparing all samples groups against a designated control group or for comparisons between the groups. For the majority of data derived from immunoblotting raw data was normalised and expressed as a percentage of control values. In each instance, statistical significance was denoted as follows; * when $p < 0.05$, ** when $p < 0.01$, *** when $p < 0.001$, **** when $p < 0.0001$.

Chapter 3 Production of a SUMO- β_2 AR Specific Polyclonal Antibody

3.1 Introduction

3.1.1 Post-Translational Modification (PTM) Antibodies

A post-translational modification (PTM) is a chemical change experienced by a protein as a result of the covalent attachment of functional groups or smaller proteins. This can occur at any point within the life cycle of a protein ranging from directly after ribosomal translation up until the protein has relocated to a specific cellular location. These chemical changes can alter the structure of the protein and therefore can impact on protein stability, activity, localisation and protein-protein interactions (Rockland-Inc, 2017). As discussed in Chapter 1 - Introduction, the β_2 AR, is subject to various PTMs including phosphorylation, glycosylation, palmitoylation, and ubiquitination (Rands, et al., 1990) (Sadeghi & Birnbaumer, 1999) (Ovchinnikov, et al., 1988) (Benovic, et al., 1987) (Daaka, et al., 1997) (Hausdorff, et al., 1989) (Vaughan, et al., 2006) (Shenoy, et al., 2001). Since PTMs play a key role in regulating both function and activity of proteins in response to environmental stimuli, they are important determinants of cellular signalling, and therefore it is imperative to have biochemical techniques which allow us to quantify these modifications.

Developing antibodies that specifically recognise the PTM modified residue and the surrounding amino acids within a protein, but not the non-modified sequence is an advancing area (Arur & Schedl, 2014) (Hattori, et al., 2013). This type of antibody is challenging to generate, but multiple companies now produce highly specific PTM antibodies that can be used in a wide range of *in vitro* and *in vivo* studies. The most common PTM examined via specific antibodies is phosphorylation - a PTM in which a phosphate group is added to either a serine, threonine or tyrosine residue by a kinase (Rockland-Inc, 2017). Many companies offer a diverse range of phospho-specific antibodies that successfully detect the phospho-modified sequence with great precision but this is not true for the other mentioned PTMs such as ubiquitination, palmitoylation, glycosylation, and the focus of our work SUMOylation.

3.1.1.1 SUMO Specific Antibody Development

This thesis concentrates on SUMOylation of the β_2 AR, in which a small SUMO protein is covalently linked to a lysine residue on the substrate. The Baillie group confirmed putative SUMOylation sites on the β_2 AR using both software sequence analysis and peptide array (Figure 1.13, Chapter 1 - Introduction). Traditional identification of SUMOylation is mediated via the presence of a “ghost” band - a band which is apparent via immunoblotting at approximately 12-25kDa larger than the original protein band - indicative of the addition of the SUMO molecule. Although the SUMO protein itself only has an approximate weight of 11kDa - often larger shift sizes are observed due to the formation of SUMO chains, in which multiple SUMO molecules are added to either one lysine residue as a chain, or multiple lysine residues throughout the protein (Park-Sarge & Sarge, 2005). These band shifts are not always easily observed next to the non-modified protein therefore we aimed to develop a SUMO-site specific antibody for the β_2 AR. To produce such an antibody, we worked in conjunction with cardiovascular life science company Badrilla ® (Badrilla, Leeds, UK) to produce a panel of novel SUMO-specific antibodies against modified cardiac signalling proteins, starting with the β_2 AR. To my knowledge, this is the first time a SUMO-site specific antibody has been successfully raised.

3.2 Aims

We aimed to:

1. Validate the SUMOylation site at lysine 235 using peptide array
2. Develop a polyclonal antibody which specifically identifies the SUMOylated form of the β_2 AR
3. Validate the specificity of the SUMO- β_2 AR antibody to the epitope against which it was raised
4. Determine the capability of the SUMO- β_2 AR antibody to detect the SUMOylated form of the β_2 AR in cell and tissue samples

3.3 Methods

General materials and methods can be found in Chapter 2 - General Materials and Methods. The methods discussed below are specific to this chapter. In addition to these methods, immunoblotting was used (previously described in Chapter 2 - General Materials and Methods). Immunoblotting was used to assess protein expression.

3.3.1 Polyclonal Antibody Purification Overview

The first step in polyclonal antibody production is to design an antigen for injection into an animal. The second step is to choose a host animal for antibody production. The choice of animal is based on two factors; 1) the volume of antibody required to be produced, as a larger animal will produce a greater volume of antibody, and 2) the phylogenetic link between the immunised animal and the source of the antigen, as a more distant phylogenetic relationship will lead to a more immunogenic antigen. After primary immunisation and additional booster injections, the blood was collected and centrifuged to remove both blood cells and clotting factors. In serum, 1% of the total antibody population consists of antibodies specific to the antigen used for animal immunisation (Uhlen & Ponten, 2005). To isolate this 1% there are various purification strategies, one of which is affinity chromatography. The principles of affinity chromatography depend on the reversible interaction between a binding protein - the antibody - and a ligand - the antigen. One of these interacting molecules can be coupled to a solid support, known as an affinity chromatography column. When sera containing antibodies is passed through a column which has been packed with antigen, the antibodies become bound on the column via numerous non-covalent interactions including van der Waals forces, ionic bonds, hydrogen bonds and/or hydrophobic interactions. Antibodies can then be eluted by changing buffer conditions such as pH, ionic strength or polarity, to disrupt the interaction between antibody and column (GEHealthcare, 2014).

3.3.2 Epitope Design

Although the initial data (Figure 1.13) indicates the lysines at 60 and 235 to be the dominant SUMOylation sites, this may not reflect the case in real life due to

the proximity of position 60 to the cell membrane, as this lysine emerges from the membrane into the first intracellular loop. In this position, access of SUMO machinery to this site may prove problematic. Further analysis utilising alanine scans reveals that both lysines 232 and 235 are susceptible to SUMOylation (Figure 3.6). For this reason, the SUMO-specific antibody epitope was designed against the first site in the sequence, 232. However, we do not expect the antibody to be capable to distinguish between SUMO conjugation on lysines which are only 3 amino acids apart.

The epitope, which is the antigen for immunisation, is chemically synthesised via standard solid phase methodology and purified by preparative reversed phase high-performance liquid chromatography (HPLC) (Anderson, et al., 1984). The peptide epitope was attached covalently to an immunogenic carrier protein, which in this case was keyhole limpet hemocyanin (KLH), a mollusc protein, to promote a more immunogenic response. A cysteine next to the acetyl (Ac) group on the antigen epitope was incorporated into the sequence and used for carrier protein attachment.

The peptides in Table 3.1 are the antigens which were used to immunise rabbits. The antigens are a partial sequence of the β_2 AR with lysine 232 modified by either SUMO-1 or SUMO-2/3. Two rabbits were injected with the upper peptide against the SUMO-1 modified antigen and two injected with the lower peptide against the SUMO-2/3 modified antigen (Table 3.2).

Table 3.1 Antigens for immunisation

SUMO-1- β_2 AR	KRQLQK (GGTQEY)IDKSEGRF
SUMO-2/3- β_2 AR	KRQLQK(GGTQQ)IDKSEGRF

Amino acid abbreviations in appendix.

Table 3.2 Rabbits immunised against SUMO-1 or SUMO-2/3- β_2 AR

RABBIT 23	SUMO-2/3- β_2 AR
RABBIT 24	SUMO-2/3- β_2 AR
RABBIT 25	SUMO-1- β_2 AR
RABBIT 26	SUMO-1- β_2 AR

Amino acid abbreviations in appendix.

The epitope consists of partial sequence of receptor **KRQLQKIDKSEGRF** with covalent attachment of either SUMO-1 or SUMO-2/3 sequences, **YQEQTGG** or **QQQTGG**, respectively at lysine 232 (Figure 3.1A). The epitope was designed with the intention to detect the interaction point between β_2 AR and the SUMO protein, as opposed to either SUMO or β_2 AR alone (Figure 3.1B).

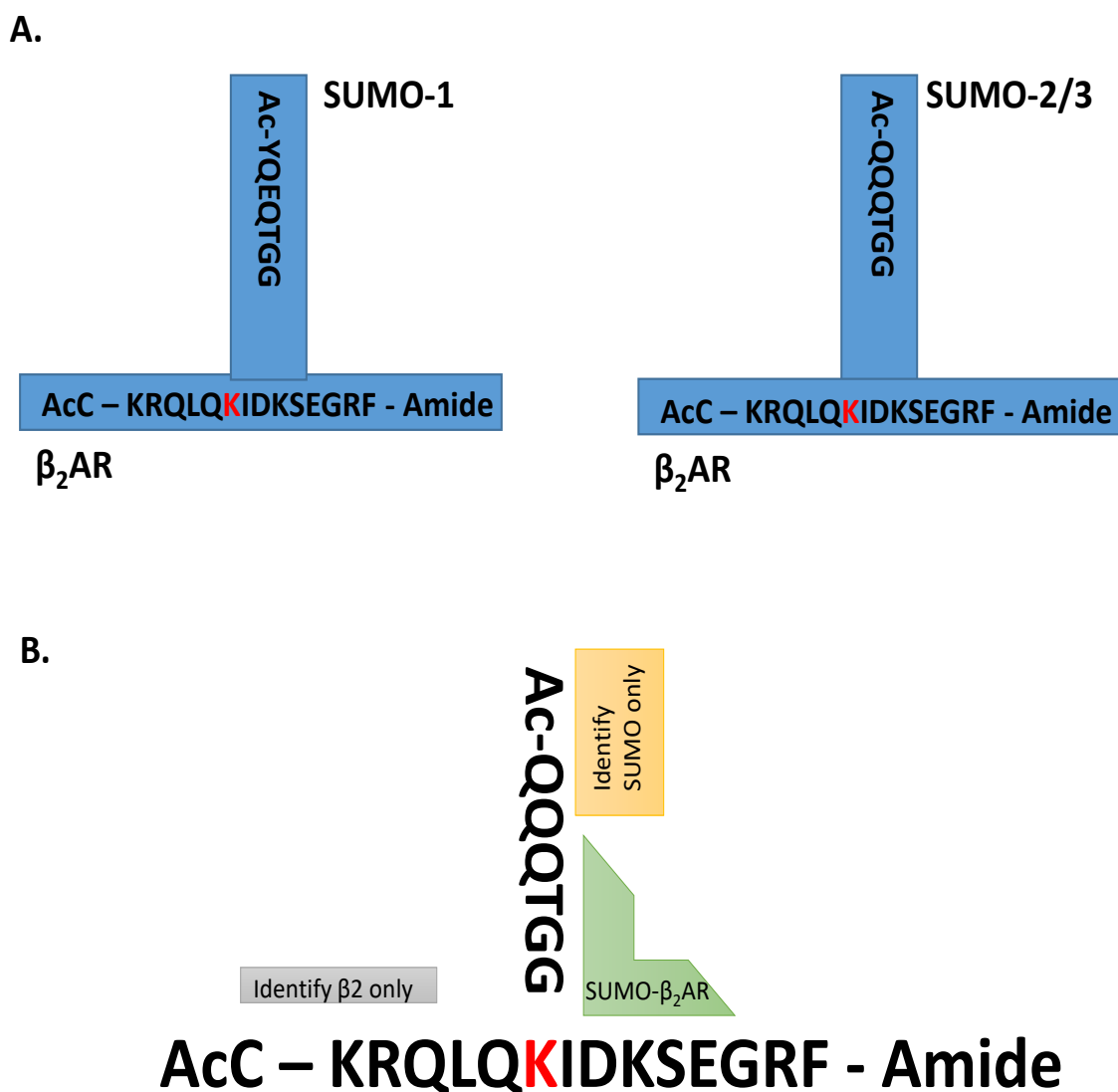


Figure 3.1 Epitope design schematic. (A) Epitope used for rabbit immunisation against SUMOylated β_2 AR. Consisted of partial sequence of β_2 AR KRQLQKIDKSEGRF with addition of either SUMO-1 or SUMO-2/3 sequences, YQEQTGG or QQQTGG, respectively. (B) Our antibody was designed to detect the interaction point between β_2 AR and SUMO not β_2 AR only or SUMO only. Amino acid abbreviations in appendix.

3.3.3 Rabbit Immunisation Protocol

Rabbits received an initial immunisation via intradermal injection. After this, at monthly intervals, the animals underwent further antigen booster injections (Figure 3.2). The initial immunisation promotes production of immunoglobulin M (IgM) by B cells, which is the first antibody to be produced in response to first-time antigen exposure (Alberts, et al., 2002). Booster injections promote a switch from the production of IgM to immunoglobulin G (IgG), the most dominant immunoglobulin found within the circulation, making up 75% of serum antibodies in humans (Alberts, et al., 2002). These bleeds contained the IgG against the injected antigens, but combined with a mixture of other blood proteins. To isolate the antibodies against SUMO- β_2 AR, the contaminating serum proteins and non-specific antibodies were removed by affinity chromatography.

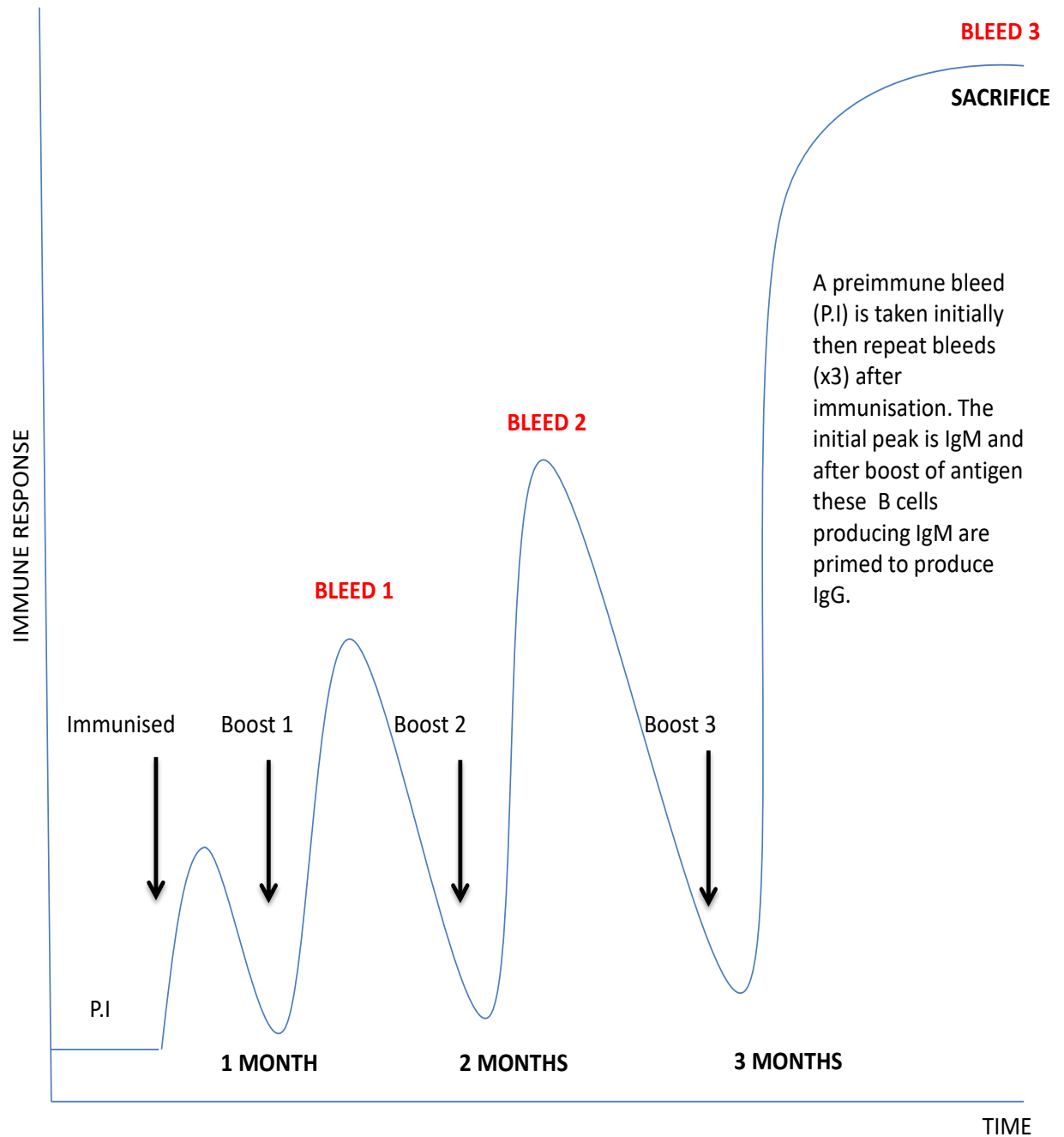


Figure 3.2. Rabbit immunisation protocol. A pre-immune bleed was taken initially prior to injection with antigen. After immunisation, a boost injection was given at monthly intervals. Bleeds were taken from the rabbit after each boost. The final bleed was larger in volume since the animal was sacrificed via exsanguination. The initial peak prior to boost 1 was IgM response to antigen, but after boost 1 this switches to IgG. IgM (immunoglobulin M), IgG (immunoglobulin G), P.I (pre-immune).

3.3.4 Immunoglobulin G (IgG) Isolation

The blood samples were dialysed with binding buffer (20mM NaHPO₄, 150mM NaCl pH 7) and left at 4°C overnight. The dialysed serum was passed through the AKTA chromatography system (GE Healthcare, Buckinghamshire, UK) using a protein A epoxy activated sepharose 6B column (GE Healthcare, Buckinghamshire, UK). Staphylococcal protein A (SpA), is a naturally occurring protein found in the cell wall of staphylococcus aureus which has affinity for IgG, and therefore, is often used in antibody purification (Hjelm, et al., 1972). Approximately 5ml of dialysed serum was passed through the column using AKTA affinity chromatography equipment in one load, as excess of 5ml compromised function of the column. All IgG was bound to the protein A column with non-IgG passing through the column as “flow through”. The column was then washed and IgG was eluted using low pH eluting buffer (100mM glycine HCl pH 3) which disrupted the interaction between the column and IgG. The eluted product was collected in 2ml segments and monitored by UV absorption at 280nm, with the output displayed graphically (Figure 3.3). This allowed identification of the segments containing IgG. The segments containing IgG for further purification ranged from B2 to B12 (Figure 3.3). These segments were then pooled for treatment with neutralisation buffer (1.0M Tris HCl pH9) to prevent damage from the acidic low eluting pH. Further chromatographic procedures were required to isolate IgG which identified SUMOylated B₂AR antigen from the complete pool of IgG.

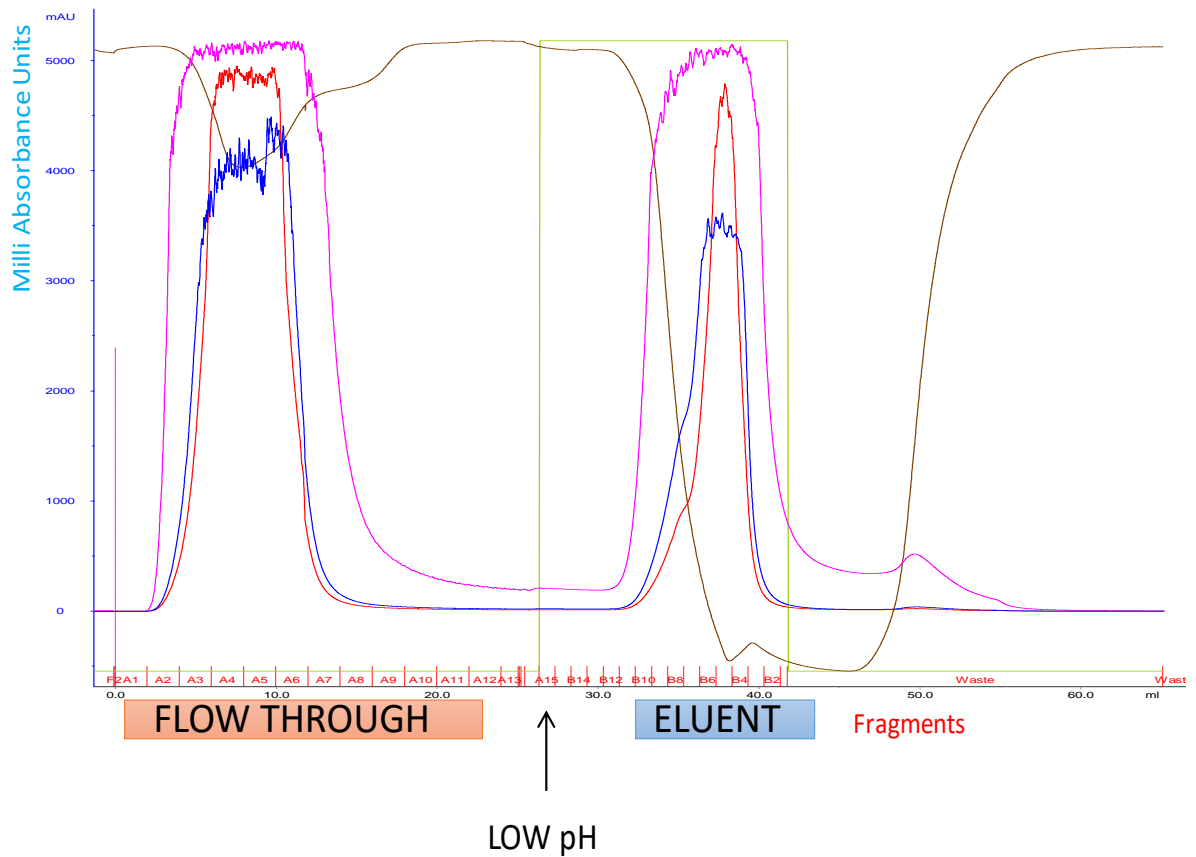


Figure 3.3 IgG isolation. 5ml of dialysed serum purified via affinity chromatography on protein A epoxy activated sepharose 6B column. Large pink peak represents the 280 UV absorption (amino acid detection) by the initial “flow through” material which does not bind to column. Low pH was applied to elute bound fraction producing the second pink peak. This peak indicates segments which contain the eluent; B2-B12. The eluent contained all IgG from the sera. Blue peak absorbance 280nm. Pink peak absorbance at 280nm. Red peak absorbance 260nm. Brown peak representative of conductivity. Green peak representative of concentration.

3.3.5 Specific SUMO- β_2 AR IgG Isolation

Following total IgG isolation, IgG which specifically recognised the SUMOylated form of the β_2 AR was isolated. The specific SUMO- β_2 AR IgG was isolated from the pool of IgG using custom peptide affinity columns. For these columns, the affinity ligand that is immobilised on the column is custom designed. To immobilise affinity ligand on the columns, 1.2g of freeze dried sepharose powder (GE Healthcare, Buckinghamshire, UK) was suspended in dH₂O giving matrix volume of 3.6ml. This was washed via 500 x g centrifugation for 60 seconds. The affinity ligands which were peptides either recognising β_2 -SUMO-1/ β_2 -SUMO-2/3 or β_2 alone (Table 3.3) were dissolved in coupling buffer (phosphate buffered saline) to a concentration of 0.5mg-10mg/ml and reduced using TCEP (tris(2-carboxylethyl)phosphine)) before addition to the matrix.

Table 3.3 Affinity ligand peptides

SUMO-1- β_2 AR	KRQLQK (GGTQEQY)IDKSEGRF
SUMO-2/3- β_2 AR	KRQLQK(GGTQQQ)IDKSEGRF
β_2 AR alone	KRQLQKIDKSEGRF

Amino acid abbreviations in appendix.

The columns were known as column 1) designed to recognise SUMO- β_2 AR either against the SUMO-2/3 or SUMO-1 paralogue dependent upon which rabbit sera was being purified, and column 2) designed to recognise β_2 AR alone (Figure 3.4). The IgG binding to column 1 included IgG specific for β_2 AR, SUMO- β_2 AR and SUMO. The reason IgG against SUMO and β_2 AR could interact with this column, as well as IgG against SUMO- β_2 AR, is due to epitope design - it is probable that the column had enough points of interaction with both these types of IgG that an interaction is feasible, even although it is not completely specific like IgG against SUMO- β_2 AR. Total IgG was loaded onto column 1 using a peristaltic pump. This column was then slotted into position on the AKTA chromatography equipment and the eluent obtained. This eluent was of value as it contained IgG which can bind SUMO, SUMO- β_2 AR and β_2 AR, separated from the total portion of IgG (Figure 3.5A). To isolate the SUMO and SUMO- β_2 AR IgG from the β_2 AR IgG, column 2 was used. The eluent was passed down column 2 which recognised IgG specific for β_2 AR alone. Here the

fraction that was retained was the flow through, as it contained the bulk of SUMO-B₂AR IgG which was not masked by B₂AR alone IgG (Figure 3.5B).

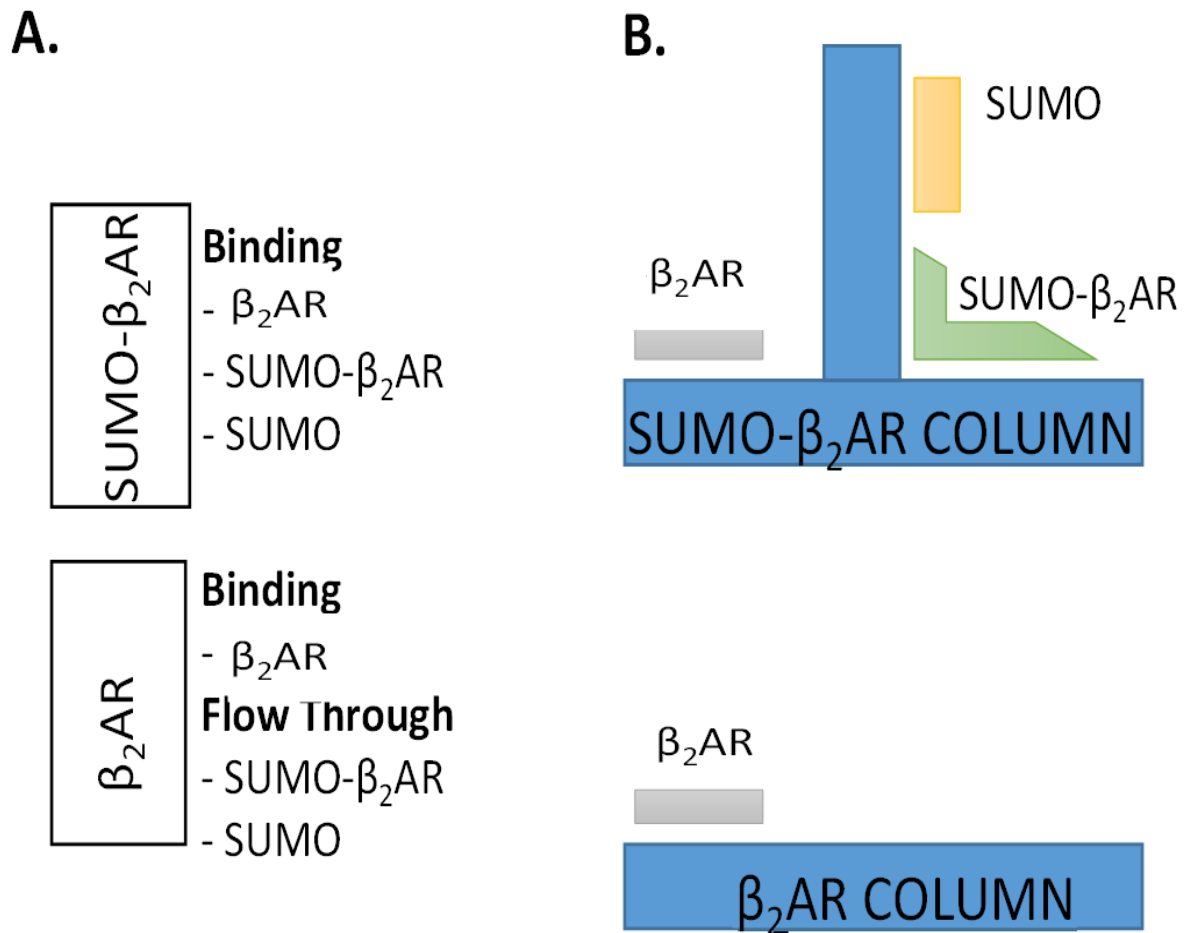
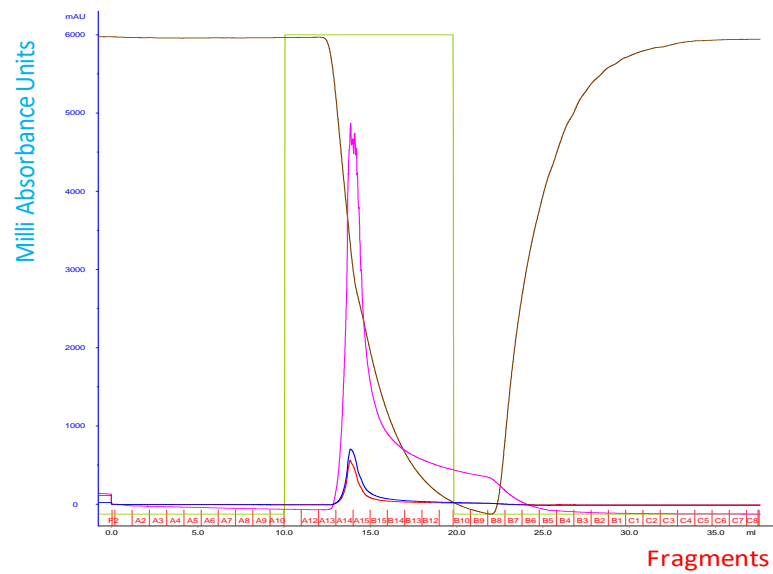


Figure 3.4 Peptide affinity columns for isolation of specific SUMO- β_2 AR IgG. (A) Total IgG was applied to column 1 which recognised SUMO- β_2 AR. This bound IgG specific for β_2 AR, SUMO- β_2 AR and SUMO. The eluent from this column was passed down column 2 which recognised β_2 AR alone. This column would interact with IgG for β_2 AR alone and therefore our flow through contained IgG which recognised SUMO- β_2 AR and SUMO (B) Peptides similar to epitope were used to produce columns and schematic identifies anticipated IgG-column interactions.

A.



B.

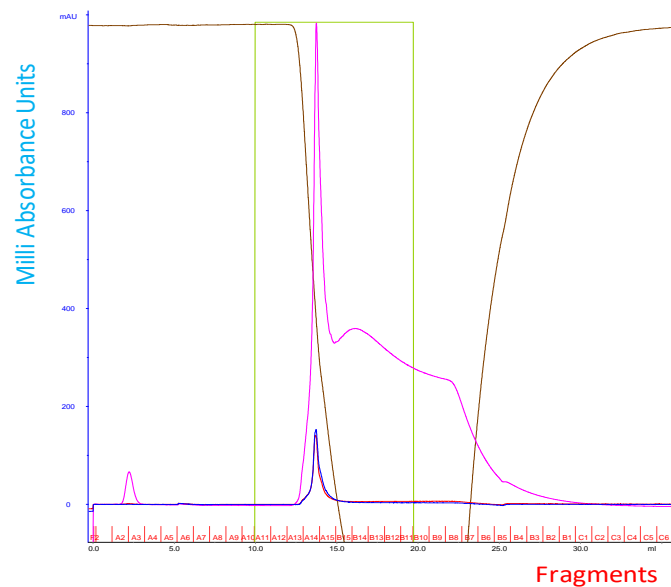


Figure 3.5 Peptide affinity columns - affinity chromatography. (A) SUMO- β_2 AR column. Eluent loaded onto the column using a peristaltic pump. Eluent processed via AKTA affinity chromatography equipment producing pink peak. This eluent was of value as it contains IgG which can bind SUMO, SUMO- β_2 AR and β_2 AR. **(B) β_2 AR column.** Eluent from SUMO- β_2 AR column was passed down this column. The important area was the flow through as the pink peak contained β_2 AR alone IgG. Flow through contained IgG against SUMO- β_2 AR which was not swamped by IgG against β_2 AR alone. Blue peak absorbance 280nm. Pink peak absorbance at 280nm. Red peak absorbance 260nm. Brown peak representative of conductivity. Green peak representative of concentration.

3.3.6 Antibody Testing

We tested the custom antibodies described above for the ability:

- 1) To specifically recognise the SUMOylated epitope against which it was raised
- 2) To detect the SUMOylated form of the β_2 AR in cell and tissue samples

To evaluate the success of these antibodies in recognising their epitope, a peptide array SUMOylation assay was used (described in Chapter 2 - General Materials and Methods). The procedure was followed as before, with four sets of slides consisting of truncated versions of the antigen epitope which were: -

- 1) Pre-SUMOylated and probed with commercially available His HRP conjugated antibody detecting SUMOylation promoted by an *in vitro* SUMOylation kit, which modifies with a His-SUMO protein
- 2) Pre-SUMOylated and probed with novel SUMO-antibodies developed in conjunction with Badrilla ®
- 3) Pre-SUMOylated and probed with novel SUMO-antibodies developed in conjunction with Badrilla ® after a pre-incubation with an unSUMOylated “blocking” peptide of the full length unSUMOylated epitope
- 4) UnSUMOylated and treated with antibodies either His-HRP conjugated or novel SUMO- β_2 AR antibodies to identify that *in vitro* SUMOylation has been successful.

The antibody was then tested in cell and tissue lysate samples via immunoblot analysis (described in Chapter 2 - General Materials and Methods).

3.4 Results

3.4.1 Identification of Key Amino Acid Residues Required for β_2 AR SUMOylation

The Baillie group identified four possible SUMOylation sites on the β_2 AR using sp2.0 SUMOylation site identification software at positions 60, 227, 232 and 235. Following further validation, the two most robustly SUMOylated lysines were at position 60 and position 235 (Figure 1.13, Chapter 1 - Introduction). As mentioned in section 3.3.2 - Epitope Design although, the lysine found at position 60 was susceptible to SUMOylation using an *in vitro* peptide array technique; this may not reflect the case in real life because of its proximity to the cell membrane. Therefore, the aim was to identify the SUMO-susceptibility of site 235. Due to the close proximity of lysines 232 and 235, both were mutated for alanine scanning peptide arrays.

Peptide array slides consisting of the sequence of the proposed cardiac SUMOylation site plus alanine scans of the sequence were developed. The slides were SUMOylated using an *in vitro* SUMOylation kit, which consists of the enzymes essential for SUMOylation and SUMO paralogues 1, 2 and 3 which are His tagged. This tag allows visualisation of SUMOylation using the His-HRP antibody. Peptide array data suggests that the receptor can be SUMOylated at two non-consensus lysines - 232 and 235. In both cases, mutation of lysine to alanine results in a 75% reduction in β_2 AR SUMOylation in comparison to native control peptide (Figure 3.6) (N=3) (* $p < 0.05$). Control coomassie stained slides demonstrated that the slides contained equal amounts of peptide spots (Figure 3.6) and control non-SUMOylated slides identified that the SUMOylation process was successful as the His-HRP antibody did not detect SUMOylation on these control arrays (Figure 3.6). It is notable that both lysines 235 and 232 are required for maximal SUMOylation, as substitution of either attenuates the signal significantly. Earlier data had suggested that 235 was the single non-consensus SUMO site. This probably stems from the close proximity of lysines as SUMOylation of one site alone is difficult to visualise in a peptide array format that uses 25-mer peptides. As discussed in section 3.3.2 - Epitope Design, SUMO-specific antibody epitope was designed against the first site in the sequence, 232. However, we do not expect the

antibody to be capable to distinguish between SUMO conjugation on lysines which are only 3 amino acids apart.

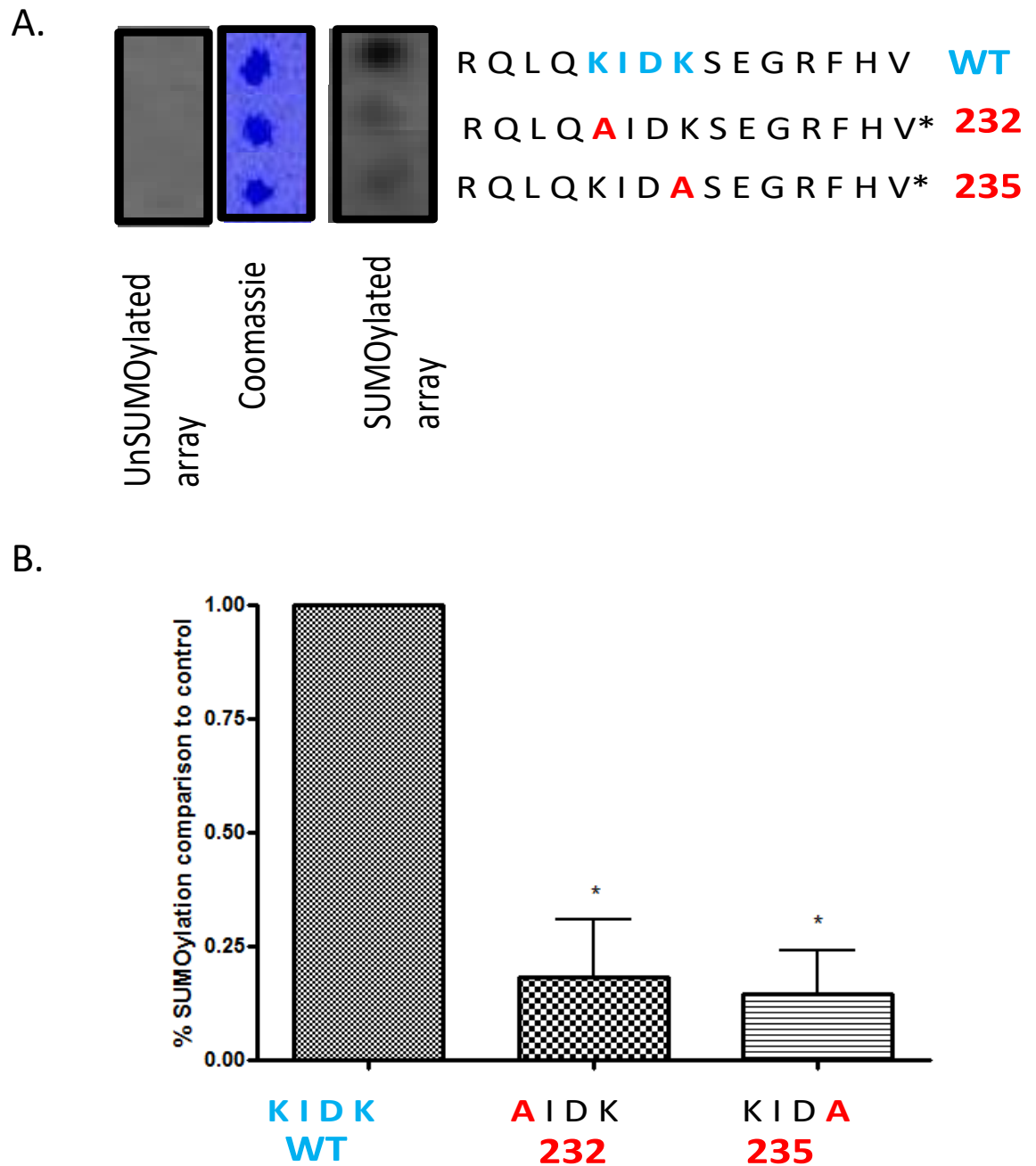


Figure 3.6 Lysines 232 and 235 are essential for SUMOylation of β_2 AR. (A&B) β_2 AR peptide arrays contained wild type sequences and alanine substitutions of crucial lysine residues 232 and 235. These were SUMOylated *in vitro*. Mutation of essential residues resulted in significant ablation of SUMO modification in β_2 AR. Control coomassie slides demonstrated that the slides contained peptide spots. Non-SUMOylated slides identified that the SUMOylation process was successful as the His-HRP antibody did not detect SUMOylation on this array (N=3) (* p <0.05). Primary concentration 1 : 5000. (A) Representative peptide array spots shown. Amino acid abbreviations in appendix.

3.4.2 Conservation of β_2 AR SUMOylation Lysines 232 and 235

Another way to emphasize the importance of the SUMO consensus motif is via examination of motif conservation throughout various species as was done for SERCA2a (Kho, et al., 2011). Through comparison of the SUMOylation sites of SERCA2a Kho et al examined the conservation of lysine 480 and 585 in mouse, rat, pig and human showing conservation of the sequence in all species. Often sequences of amino acids which play a functional role are conserved throughout multiple species. Indeed, the β_2 AR SUMOylation sites at position 60, 227, 232 and 235 which were identified from the sp2.0 SUMOylation site identification software are conserved throughout human, rat, mouse, rhesus monkey and cow (Figure 3.7).

Position 60 (consensus)

HUMAN	LVITAI AKFER LQTV
RAT	LVITAI AKFER LQTV
MOUSE	LVITAI AKFER LQTV
RHESUS MONKEY	LVITAI AKFER LQTV
COW	LVITAI AKFER LQTV

Position 232 (non consensus)

HUMAN	EAKRQLQ K IDKSEGR
RAT	VAKRQLQ K IDKSEGR
MOUSE	VAKRQLQ K IDKSEGR
RHESUS MONKEY	EAKRQLQ K IDKSEGR
COW	VAKRQLQ K IDKSEGR

Position 227 (non consensus)

HUMAN	SRVFQEA K RQLQKID
RAT	SRVFQVA K RQLQKID
MOUSE	SRVFQVA K RQLQKID
RHESUS MONKEY	SRVFQEA K RQLQKID
COW	SRVFQVA K RQLQKID

Position 235 (non consensus)

HUMAN	RQLQKID K SEGRFHV
RAT	RQLQKID K SEGRFHV
MOUSE	RQLQKID K SEGRFHV
RHESUS MONKEY	RQLQKID K SEGRFHV
COW	RQLQKID K SEGRFHV

Figure 3.7 β_2 AR SUMOylation sites are conserved between species. β_2 AR SUMOylation sites 60 (consensus) and 227, 232 and 235 (non-consensus) are conserved throughout species. Amino acid abbreviations in appendix.

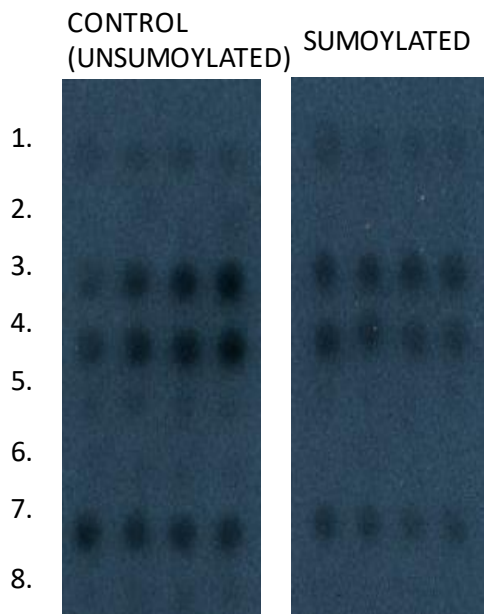
3.4.3 Epitope Recognition Testing – Peptide Array

All antibodies produced at Badrilla ® were shown to be non-specific for the SUMOylated epitope as they recognised the non SUMOylated β_2 AR sequence as well as the SUMOylated epitope (Figure 3.8 and 3.9) (N=3). For control experiments to confirm successful array SUMOylation, antigen epitope arrays, both SUMOylated and unSUMOylated, were incubated with the His tag antibody which detects SUMOylation mediated via the *in vitro* SUMOylation kit (Figure 3.10) (N=3). This provided evidence of successful *in vitro* SUMOylation. These findings confirmed the commercial antibody can decipher between the SUMOylated and non SUMOylated epitopes but the 4 custom antibodies cannot.

Rabbit 23

A.

1. VSFYVPLVIMVFVYSRVFQEAKR**QL**
2. VPLVIMVFVYSRVFQEAK**RQLQKID**
3. VVYSRVFQEAKR**QLQKIDKSEGRF**
4. VFQEAKR**QLQKIDKSEGRF**HVQ-NLS
5. KR**QLQKIDKSEGRF**HVQ-NLSQVEQD
6. **QKIDKSEGRF**HVQ-NLSQVEQDGRGTG
7. **SEGRF**HVQ-NLSQVEQDGRGTGHGLRR
8. HVQ-NLSQVEQDGRGTGHGLRRSSKFC



Rabbit 24

B.

1. VSFYVPLVIMVFVYSRVFQEAKR**QL**
2. VPLVIMVFVYSRVFQEAK**RQLQKID**
3. VVYSRVFQEAKR**QLQKIDKSEGRF**
4. VFQEAKR**QLQKIDKSEGRF**HVQ-NLS
5. KR**QLQKIDKSEGRF**HVQ-NLSQVEQD
6. **QKIDKSEGRF**HVQ-NLSQVEQDGRGTG
7. **SEGRF**HVQ-NLSQVEQDGRGTGHGLRR
8. HVQ-NLSQVEQDGRGTGHGLRRSSKFC

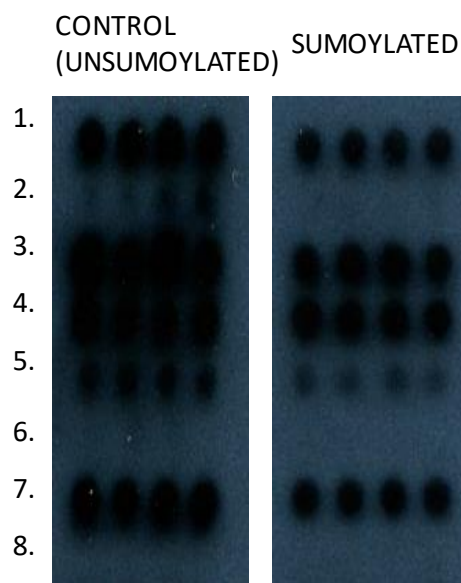
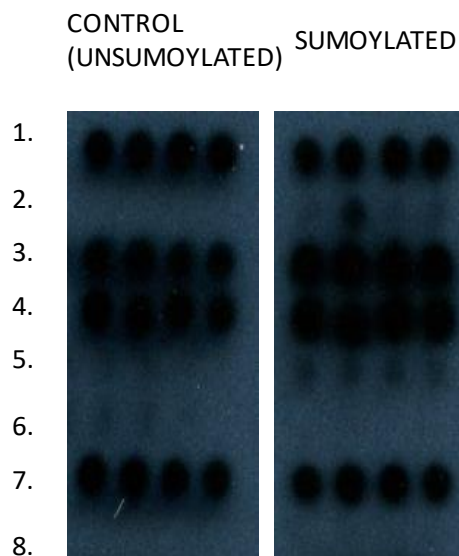


Figure 3.8 Testing of SUMO-2/3- β_2 AR antibody - derived from rabbits 23 and 24. SUMO- β_2 AR antibody from rabbit 23 (A) and 24 (B). Peptide array slides consisting of truncations of epitope highlighted in red. Peptide arrays SUMOylated via ENZO *in vitro* SUMOylation kit per manufacturers' instruction. Control array does not undergo *in vitro* SUMOylation therefore remains unSUMOylated. Antibody incubated overnight on both control and SUMOylated slide (N=3). Primary concentration 1 : 500, secondary concentration 1 : 1000. Representative peptide array spots shown. Amino acid abbreviations in appendix.

Rabbit 25

A.

1. VSFYVPLVIMVFVYSRVFQEAQRQL
2. VPLVIMVFVYSRVFQEAQRQLQKID
3. VFVYSRVFQEAQRQLQKIDKSEGRF
4. VFQEAQRQLQKIDKSEGRFHVQNLS
5. KRQLQKIDKSEGRFHVQNLSQVEQD
6. QKIDKSEGRFHVQNLSQVEQDGRTG
7. SEGRFHVQNLSQVEQDGRTGHGLRR
8. HVQNLSQVEQDGRTGHGLRRSSKFC



Rabbit 26

B.

1. VSFYVPLVIMVFVYSRVFQEAQRQL
2. VPLVIMVFVYSRVFQEAQRQLQKID
3. VFVYSRVFQEAQRQLQKIDKSEGRF
4. VFQEAQRQLQKIDKSEGRFHVQNLS
5. KRQLQKIDKSEGRFHVQNLSQVEQD
6. QKIDKSEGRFHVQNLSQVEQDGRTG
7. SEGRFHVQNLSQVEQDGRTGHGLRR
8. HVQNLSQVEQDGRTGHGLRRSSKFC

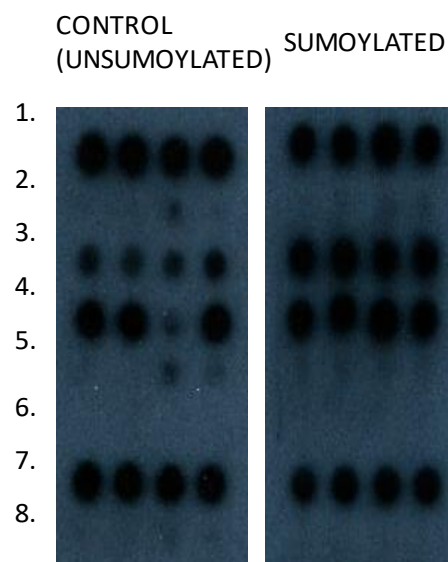


Figure 3.9 Testing of SUMO-1- β_2 AR antibody - derived from rabbits 25 and 26. SUMO- β_2 AR antibody from rabbits 25 (A) and 26 (B). Peptide array slides consisting of truncations of epitope highlighted in red. Peptide arrays SUMOylated via ENZO *in vitro* SUMOylation kit per manufacturers' instruction. Control array does not undergo *in vitro* SUMOylation therefore remains unSUMOylated. Antibody incubated overnight on both control and SUMOylated slide (N=3). Primary concentration 1 : 500, secondary concentration 1 : 1000. Representative peptide array spots shown. Amino acid abbreviations in appendix.

His-HRP Antibody Control

1. VSFYVPLVIMVFVYSRVFQEAKR~~QL~~
2. VPLVIMVFVYSRVFQEAKR~~QLQKID~~
3. VFVYSRVFQEAKR~~QLQKIDKSEGRF~~
4. VFQEAKR~~QLQKIDKSEGRF~~HVQ-NLS
5. KR~~QLQKIDKSEGRF~~HVQ-NLSQVEQD
6. ~~QKIDKSEGRF~~HVQ-NLSQVEQDGRGTG
7. ~~SEGRF~~HVQ-NLSQVEQDGRGTGHGLRR
8. HVQ-NLSQVEQDGRGTGHGLRRSSKFC

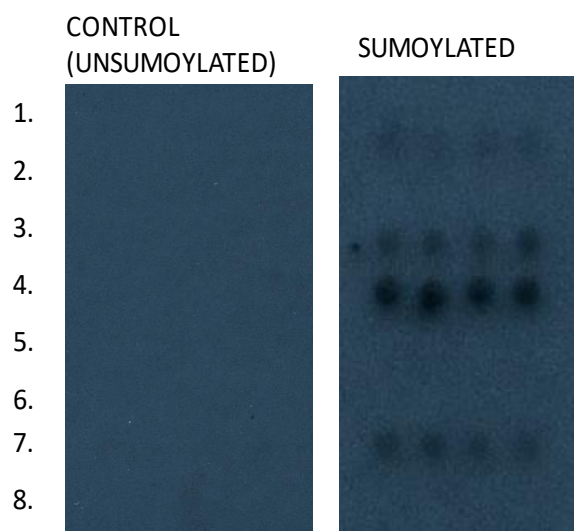


Figure 3.10 Testing of SUMO- β_2 AR antibody - His-HRP antibody control. Peptide array slides consisting of truncations of epitope highlighted in red. Peptide arrays SUMOylated via ENZO *in vitro* SUMOylation kit per manufacturers' instructions. Control array does not undergo *in vitro* SUMOylation therefore remains unSUMOylated. His-HRP Antibody incubated overnight on both control and SUMOylated slide (N=3). Primary concentration 1 : 5000. Representative peptide array spots shown. Amino acid abbreviations in appendix.

As all the custom designed SUMOylation-specific antibodies recognised the unmodified form of the β_2 AR, the testing process was redesigned to include pre-incubation (for approximately 1 hour) of the antibody with 10 μ M blocking peptide of the full length unSUMOylated epitope peptide (KRQLQKIDKSEGRF) prior to incubation with peptide arrays. For this, we selected 1 from the 4 rabbit antibody sets; rabbit 25. This decision was made on the basis that rabbits 23 and 24 showed excessive non-specific binding of the unSUMOylated slides compared to the SUMOylated slides. Rabbit 26 derived antibody showed high variability in the control slide in comparison to other animals - therefore the rabbit selected for further testing was rabbit 25 - as the antibody derived from the sera of this animal showed a similar profile in both the SUMOylated and non SUMOylated slides. This technique proved successful in quenching unspecific binding leading to recognition of the SUMOylated epitope alone (Figure 3.11) (N=3). This represents the first time a SUMOylated epitope has been recognised specifically using immunoblot-peptide array technique, validating the antibody derived from rabbit 25 sera for further testing.

Rabbit 25

1. VSFYVPLVIMVFVYSRVFQEAKRQL
2. VPLVIMVFVYSRVFQEAKRQLQKID
3. VFVYSRVFQEAKRQLQKIDKSEGRF
4. VFQEAKRQLQKIDKSEGRFHVQNLS
5. KRQLQKIDKSEGRFHVQNLSQVEQD
6. QKIDKSEGRFHVQNLSQVEQDGRGTG
7. SEGRFHVQNLSQVEQDGRGTGHGLRR
8. HVQNLSQVEQDGRGTGHGLRRSSKFC

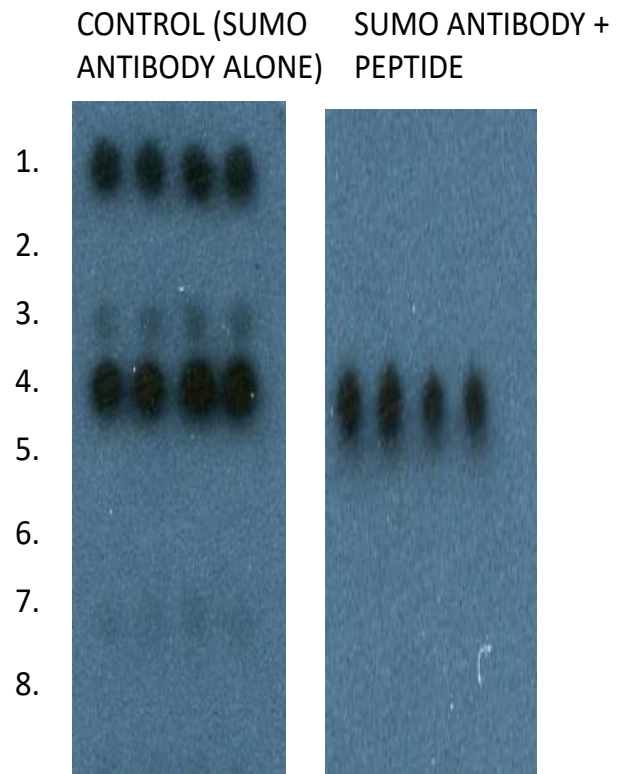


Figure 3.11 Testing of SUMO-1- β_2 AR antibody from derived from rabbit 25 - blocking peptide. Peptide array slides consisting of truncations of epitope highlighted in red. Peptide arrays SUMOylated via ENZO *in vitro* SUMOylation kit per manufacturers' instruction. Control array does not undergo *in vitro* SUMOylation therefore remains unSUMOylated. Antibody incubated overnight on both control and SUMOylated slide after 1 hour pre incubation with 10 μ M non-SUMOylated epitope blocking peptide (N=3). Primary concentration 1 : 500, secondary concentration 1 : 1000. Representative peptide array spots shown. Amino acid abbreviations in appendix.

3.4.4 SUMO- β_2 AR Recognition in Cells

In Chapter 4 - *In Vitro* SUMOylation of the β_2 AR, I have shown that the E3 ligase PIAS γ - the final enzyme of the SUMOylation cascade - plays an important role in the SUMOylation of the β_2 AR. Many of the findings within this thesis are based on this premise. For further evidence to support the notion that PIAS γ mediates SUMOylation we wished to use the SUMO- β_2 AR specific antibody to determine if the SUMOylated form of the β_2 AR could be identified in cells, which overexpress PIAS γ and the β_2 AR.

To examine the SUMOylation of the β_2 AR *in vitro* in the presence of PIAS γ , the HEK β_2 cell line was used. This is a stable HEK293 cell line which stably overexpresses the GFP/FLAG-tagged form of the β_2 AR (McLean & Milligan, 2000) (McLean, et al., 1999). These cells were either transiently transfected with PIAS γ -HA tagged DNA constructs or mock transfected with empty transfection reagent. PIAS γ expression was confirmed via the expression of the HA tag (panel 4). Standard HEK293 cell lysate was probed using SUMO- β_2 AR antibody to provide evidence that the antibody was specific for the β_2 AR in the HEK β_2 stable cell line. GFP antibody identified the β_2 AR present within the HEK β_2 cell lysate but not in HEK293 cell lysate (panel 5). GAPDH was used as a loading control (panel 3).

In agreement with the peptide array validation (Figure 3.8 - 3.11) above, SUMO- β_2 AR antibody (without prior incubation with blocking peptide) was capable of detecting the receptor specifically within the HEK β_2 cell line (both with and without PIAS γ expression) but not in native HEK293 cell lysate (panel 1). After 1 hour pre-incubation of the SUMO- β_2 AR antibody with blocking peptide, the SUMO- β_2 AR antibody selectively identifies the SUMOylated form of the β_2 AR which is promoted via overexpression of the E3 ligase PIAS γ (panel 2) (Figure 3.12) (N=3).

However, there are two important points to consider. Firstly, in the HEK β_2 lane (lanes 1 and 2) (panel 2) the SUMO- β_2 AR antibody still detects what would appear to be unSUMOylated β_2 AR, when the intention of the blocking peptide is to prevent unSUMOylated receptor detection. We cannot rule out unspecific binding to another protein of similar molecular weight, or the blocking peptide incubation time and/or concentration is not sufficient to abolish antibody-receptor interaction. Another option to consider is the antibody could be detecting

endogenous levels of β_2 AR SUMOylation, which we would expect to be lesser in lanes 1 and 2 (panel 2) when compared to HEK β_2 +PIAS γ lanes 3 and 4 (panel 2). This seems the more probable option as the HEK293 lane alone should account for any unspecific binding from proteins existing with the HEK cell lysate (lane 5 and 6), and no bands are apparent in these lanes. Secondly, the SUMOylated- β_2 AR band does not appear to be presenting at a 12-25kDa shift from the original 75kDa β_2 AR band, indicative of SUMOylation. However, as the upper molecular markers of the gel present closely together (see panel 5, 75kDa and 100kDa), it would be important to run the gel for longer leading to increased separation between higher molecular weights. This would allow determination of the band shift that may be present. This is the first time a SUMO-site specific antibody has been reported to monitor SUMOylation of a protein using cellular lysates, and the first validation that the β_2 AR gets modified by SUMO.

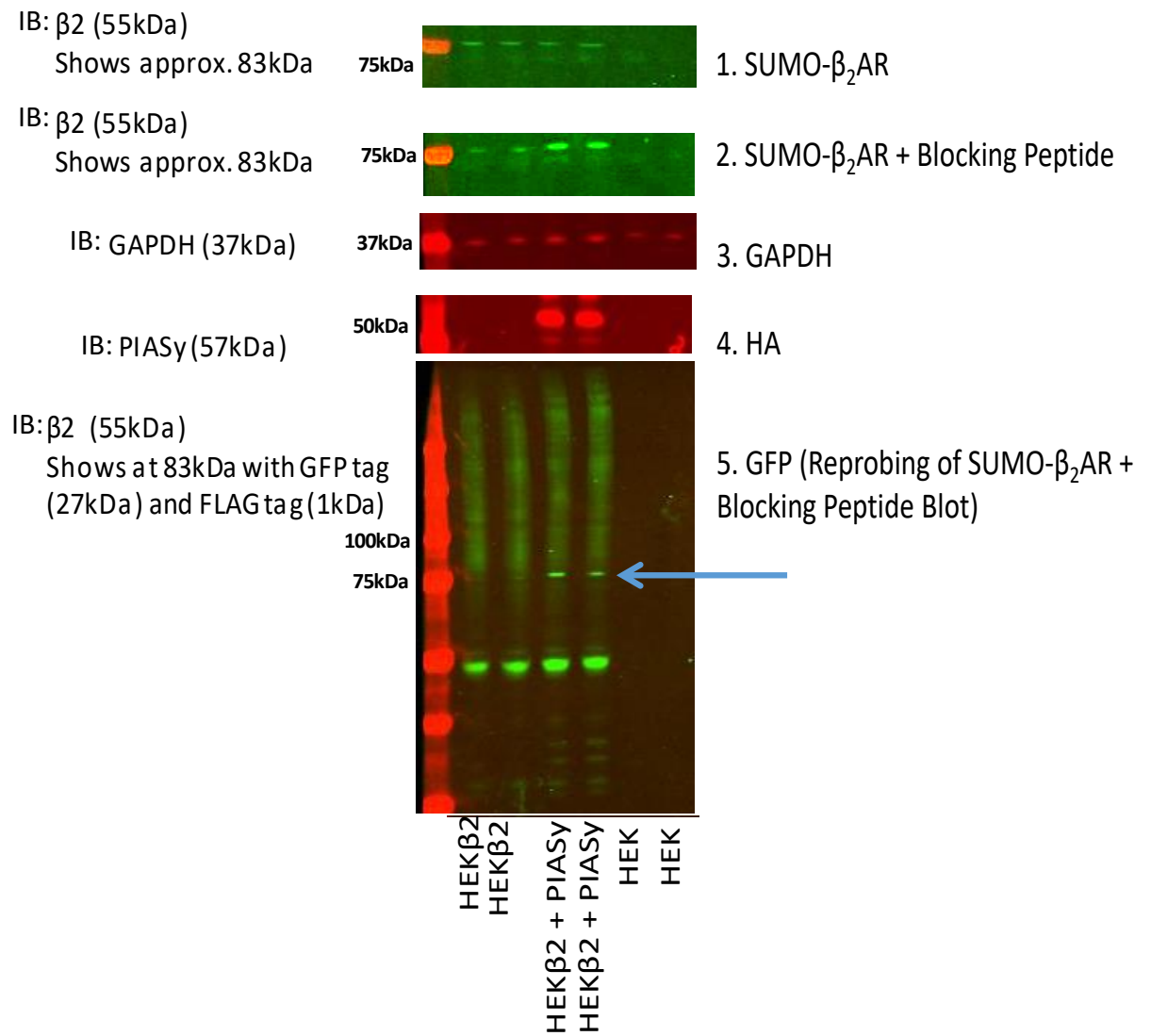


Figure 3.12 Testing of SUMO- β_2 AR specific antibody in cells. PIASy used to promote SUMOylation of the β_2 AR. With SUMO- β_2 AR antibody alone antibody detected all forms of receptor as opposed to only SUMOylated forms (panel 1). SUMO- β_2 AR antibody detected SUMOylated form of the β_2 AR in the presence of blocking peptide, however protein detection in lanes 1&2 and band shift in lanes 3&4 remain to be confirmed (panel 2). GAPDH identified protein in all lanes (panel 3). HA identified expression of PIASy indicating transfection success (panel 4). GFP identified β_2 AR receptor presence in the cells, blue arrow indicative of re-probing of blot from panel 2 (panel 5) (N=3). Representative blots are shown.

3.5 Discussion

As eluded to above, the β_2 AR is subject to various PTMs. Since these modifications play a key role in regulating protein function or activity in response to environmental stimuli, they are important determinants of cellular signalling (Rands, et al., 1990) (Sadeghi & Birnbaumer, 1999) (Ovchinnikov, et al., 1988) (Benovic, et al., 1987) (Daaka, et al., 1997) (Hausdorff, et al., 1989) (Vaughan, et al., 2006) (Shenoy, et al., 2001). Hence, it is imperative to have biochemical techniques which allow us to quantify these modifications. I aimed to develop an antibody which would recognise the SUMOylated form of the β_2 AR. This is novel on two counts as firstly, it is previously unknown that the β_2 AR can be SUMOylated and secondly, a SUMO-site specific antibody has never before been reported on. The data here shows that the β_2 AR can be SUMOylated at lysines 232 and 235, and that the novel SUMO- β_2 AR antibody is capable of 1) identifying the epitope against which it was raised and 2) identifies the SUMOylated form of the β_2 AR in cell and tissue samples.

PTM antibodies of the β_2 AR have been utilised in the past to assess β_2 AR phosphorylation at distinct sites. As discussed in Chapter 1 - Introduction, the β_2 AR is susceptible to phosphorylation by PKA and GRK, therefore antibodies are commercially available which decipher between post-translational modification by these kinases. Shenoy et al (2006) utilised antibodies from Santa Cruz Biotechnology; phospho- β_2 AR at serines 345/346 (PKA-mediated phosphorylation) and phospho- β_2 AR at serines 355/356 (GRK-mediated phosphorylation). This group utilised the phospho- β_2 AR serines 345/346 antibody to confirm the susceptibility of a β_2 AR mutant to PKA phosphorylation. This mutant was functionally uncoupled from G_s , therefore did not produce cAMP elevation in response to isoprenaline, and via PTM antibody detection, it was confirmed the mutant was unable to be phosphorylated by PKA. This same group used the partner phospho β_2 AR antibody by Santa Cruz - serines 355/356 - to reveal that the same β_2 AR mutant, although unsusceptible to PKA-mediated phosphorylation, was subject to phosphorylation in the presence of GRK5/6 but not GRK2. This work exposed the fact that the β_2 AR can induce activation of the ERK MAPK in a β -arrestin-dependent manner, that is independent of the PKA-mediated G_s to G_i switch (Shenoy, et al., 2006)

In the quest to understand how PTMs impinge on cellular signalling processes, the advancement in site-specific PTM antibodies has been rapid in the last 10 years. For example, Hattori et al (2013) recently produced a novel PTM antibody against methylated histones and Arur and Schedl (2014) reported that 4 rounds of affinity chromatography purification were required to produce a phospho-specific antibody which was not available commercially for the RNA helicase, CGH-1. In contrast to the work presented in this chapter, when the phospho-CGH-1 specific antibody was shown to be ineffective in determining between phosphorylated and unmodified protein, the antibody was subject to further rounds of affinity purification. This continued until the antibody was capable of identifying only the phospho-modified form of the RNA helicase and not the non-modified form. This would have been a suitable alternative to the blocking peptide testing procedure used here, however the suitable equipment was within Badrilla® at Leeds University and the testing procedure was completed within the University of Glasgow, where the blocking peptide was readily available, and therefore was the first option to be assessed. By quenching unspecific total protein binding using pre-incubation with a full-length epitope blocking peptide, the antibody described in this chapter was proven to be capable of detecting the SUMOylated form of the β_2 AR in a specific fashion.

However, two features of the antibody remain to be solved; unspecific binding and the expected SUMO band shift. Although the antibody is selectively identifying the SUMOylated form of the β_2 AR promoted via overexpression of PIAS γ , the binding in HEK β_2 cells alone lanes implies that the antibody is possibly detecting endogenous levels of β_2 AR SUMOylation, or the unSUMOylated receptor is still being detected by the antibody. We believe the possibility of unspecific binding to another protein of a similar molecular weight is unlikely, as the HEK293 lysate should account for the antibody binding to proteins within the HEK β_2 cell line which are not the β_2 AR, and no bands are present in these lanes. Furthermore, SUMOylation is traditionally associated with a 12-25kDa ghost band shift which is not apparent in Figure 3.12 as both the SUMO- β_2 AR band and the β_2 AR band present between the 75kDa and 100kDa markers, which are spaced closely together. Further antibody validation should involve repeating these experiments with longer gel running times to promote further protein separation at these higher molecular weights.

There are different SUMO paralogues which can be conjugated to a substrate protein to mediate SUMOylation; SUMO-1 or SUMO-2/3 (Hay, 2013) (Varadaraj, et al., 2014). Although the immunisation peptide for rabbit 25 was designed to produce an antibody against SUMO-1- β_2 AR, the testing procedure involved using an *in vitro* SUMOylation kit, which mediated SUMO modification by SUMO-1 and SUMO-2/3 equally. I did not determine whether the custom antibody is capable of deciphering between different SUMO paralogues that modify the β_2 AR. The “TGG” residue of SUMO-1 and SUMO-2/3 is the same, and this is the area which is important for the bond between SUMO and the essential lysine. Therefore, as the desired sequence for identification was the link between the β_2 AR and SUMO this made it complex to produce an antibody which is specific for the SUMO-1- β_2 AR and SUMO-2/3- β_2 AR, when the areas which distinguish SUMO-1 and SUMO-2/3 from each other are not those which are directly involved with the lysine interaction. For the purpose of our work we did not intend to decipher between the forms and therefore testing was stopped at the stages described here, but it would be possible to determine the specificity of the antibody by using similar techniques of *in vitro* SUMOylated arrays using only one SUMO paralogue at a time. If the antibody purified from rabbit 25 was specific for the SUMO-1- β_2 AR form then continuation of the testing procedure for all other samples may have produced a panel of antibodies which could distinguish between the SUMO paralogue responsible for SUMO modification of the β_2 AR.

As mentioned in Chapter 1 - Introduction, SUMOylation shares similarities with the PTM ubiquitination. Both SUMOylation and ubiquitination can form chains of SUMO and ubiquitin molecules, respectively. Similarly to poly-SUMO chains, a poly-ubiquitin chain is formed when the lysine residue on the ubiquitin is linked to the carboxy-terminal of another ubiquitin. This linkage can be mediated by different lysines within ubiquitin, two of which are K48 and K63. K48 linked chains mainly target proteins for proteasomal degradation and K63 linked chains regulate protein function, subcellular localisation or protein-protein interactions (Komander, 2009). Commercial antibodies are available which distinguish between these poly-ubiquitin chains. During the assessment of proteasomal phosphorylation, the K48 poly-ubiquitin chain antibody was used to assess a build-up in poly-ubiquitinated proteins, giving an indication of proteasome activity (Guo, et al., 2016). The K63 poly-ubiquitin chain antibody has also been used to

assess the reduction of K63 poly-ubiquitin chain formation in yeast *Saccharomyces cerevisiae* in states of oxidative stress (Silva, Finley, & Vogel, 2015). This is a similar approach which could be utilised for poly-SUMO chains to reveal the purpose of these chain formations.

In addition to differing SUMO paralogues which can mediate SUMOylation, there are also different sites within the β_2 AR which can be subject to SUMO modification. The custom SUMO- β_2 AR antibody was designed to detect SUMOylation at lysine 232 on the β_2 AR. Alternative lysines which can be SUMOylated include 227 and 235 (Figure 1.13, Chapter 1 - Introduction), which are close to our lysine of interest. Due to the close proximity of the three lysines (227, 232 and 235) it is probable that the antibody may also be detecting SUMOylation at those sites. Further work with β_2 AR mutant peptide arrays with mutations at these neighbouring lysines may reveal a new level of antibody specificity, but various points of contact required between antibody and epitope recognition would even make this challenging to determine, as single lysine mutation may not be enough to prevent antibody detection of epitope.

Further research into the role of individual SUMO sites is important, as specific antibodies could be used to determine the functional output of specific lysine SUMOylation. For example, it is known when PKA phosphorylates the β_2 AR this mediates a switch in signalling from G_s to G_i , therefore antibodies are designed which detect phosphorylation by this kinase alone (Daaka, et al., 1997). In a similar manner, it would be important to identify if SUMOylation of specific lysines initiated tailored signalling changes, and therefore antibodies could be designed to examine this. Another alternative, is the design of an epitope which is based upon the consensus motif γ KxE/D (where γ is a large hydrophobic residue often consisting of 3-4 aliphatic residues, K is the lysine SUMO acceptor and x is any residue, D/E an acidic residue) (Hay, 2005) (Rodriguez, et al., 2001) (Bernier-Villamor, et al., 2002). The drawback with this work lies with the fact that some lysines which can be SUMOylated lie out with a consensus motif, and therefore SUMOylation at these sites would be undetected by an antibody designed in this manner (Impens, et al., 2014).

In conclusion, I have developed an antibody to recognise the SUMOylated form of the β_2 AR which is the first of its kind. I have proven this antibody is capable of 1)

identifying the SUMOylated epitope against which it was raised and 2) identifying the SUMOylated form of the β_2 AR promoted via PIAS γ transfection. This provides evidence to support our prior conclusion that PIAS γ promotes SUMOylation of the β_2 AR. We will use this important new reagent to probe β_2 AR SUMOylation in Chapter 5 - Analysis of β_2 AR SUMOylation in Animal Models of HF.

Chapter 4 *In Vitro* SUMOylation of the β_2 AR

4.1 Introduction

4.1.1 Post-Translational Modifications (PTMs) of the β_2 AR

Like many GPCRs, the β_2 AR is susceptible to multiple post-translational modifications (PTMs), which can alter how the β_2 AR orchestrates downstream intracellular signals. The β_2 AR can transduce signals via stimulatory G protein (G_s) to activate adenylyl cyclase (AC). AC catalyses the conversion of adenosine triphosphate (ATP) to cyclic adenosine monophosphate (cAMP), which then activates cAMP effectors such as protein kinase A (PKA) (Hausdorff, et al., 1989) (Strulovici, et al., 1984). PKA can phosphorylate a large number of proteins leading to tailored physiological responses. This is the most common mechanism by which the β_2 AR signals, but it can also mediate effects through G_i proteins which, have an opposite inhibitory influence on AC (Daaka, et al., 1997). The switch between G_s and G_i signalling is mediated by direct PKA-mediated phosphorylation of β_2 AR. Other PTMs have also been shown to play a role in β_2 AR signalling namely ubiquitination, palmitoylation and glycosylation. β_2 AR ubiquitination tags the receptor for degradation by the 26S proteasome and is therefore vital for receptor down-regulation in response to excessive agonist exposure (Shenoy, et al., 2001); glycosylation has been shown to be involved in β_2 AR internalisation (Rands, et al., 1990); palmitoylation promotes the interaction between G_s and the β_2 AR allowing AC activation (O'Dowd, et al., 1989).

4.1.2 SUMOylation of the β_2 AR

SUMOylation is a PTM much like ubiquitination in which a small SUMO protein is covalently linked to a lysine residue on the substrate protein (Hay, 2005). SUMOylation can occur on either a lysine within a consensus motif or a non-consensus lysine. This consensus motif consists of γ KxE/D (where γ is a large hydrophobic residue often consisting of 3-4 aliphatic residues, K is the lysine SUMO acceptor and x is any residue, D/E an acidic residue) (Hay, 2005) (Rodriguez, et al., 2001) (Bernier-Villamor, et al., 2002).

To date there are five GPCRs which are identified as substrates for SUMOylation; metabotropic glutamate receptors, a cannabinoid receptor, a serotonin receptor and smo (Tang, et al., 2005) (Dutting, et al., 2011) (Gowran, et al., 2009) (Li &

Muma, 2013) (Zhang, et al., 2017). In addition to GPCRs, other cardiac signalling proteins have also been shown to be susceptible to SUMOylation, such as SERCA2a. SERCA2a has been shown to be modified by SUMO-1, resulting in preserved ATPase activity of the protein (Kho, et al., 2011) (Tilemann, et al., 2013).

The purpose of this chapter is to assess the outcome of β_2 AR SUMOylation using *in vitro* functional signalling assays.

4.2 Aims

I hypothesise that SUMOylation of the β_2 AR influences receptor signalling and stability. The aims of this chapter are the following: -

- 1) Promote β_2 AR SUMOylation in the HEK β_2 cell line by overexpressing a SUMO E3 ligase, namely PIAS γ , to allow a model in which to probe function of the modification
- 2) Determine the influence of β_2 AR SUMOylation on receptor signalling in the model HEK β_2 cell line using a variety of *in vitro* functional signalling assays

4.2.1 HEK β_2 Cell Line

To monitor the effects of β_2 AR SUMOylation on receptor signalling *in vitro*, the HEK β_2 cell line was used. This is a stable HEK293 cell line which stably overexpresses the GFP/FLAG-tagged form of the β_2 AR (McLean & Milligan, 2000) (Mclean, et al., 1999). The stable expression of the receptor within this cell line allows us to examine the influence of SUMOylation on β_2 AR signalling as HEK β_2 is a robust and proven model for examining cellular effects of β_2 AR signalling (Bolger, et al., 2006) (Baillie, et al., 2003) (Perry, et al., 2002) .

Initial experiments using isoprenaline were undertaken to ensure the HEK β_2 cells were responding as expected upon activation of the β_2 AR. HEK β_2 cells were stimulated with 10 μ M isoprenaline for 5 and 10 minutes, and as expected I observed a 50% increase in PKA-mediated phosphorylation of the β_2 AR by PKA by (Figure 4.1) (N=4) (*p<0.05) and an approximate 1-fold increase in PKA-mediated phosphorylation of other target proteins (Figure 4.2) (N=4) (**p<0.01)(*p<0.05) as measured using a phospho-PKA consensus site antibody. Also, as expected, isoprenaline treatment promoted a 4-fold increase in phosphorylation of ERK MAP kinase (Figure 4.3) (N=4) (p=0.058/p=0.0550) in comparison to control. Previous work had shown that PKA-mediated phosphorylation of the β_2 AR by PKA switches G_s to G_i signalling to promote the increase in active ERK (Daaka, et al., 1997). All of these results indicated the β_2 AR was functional in the stable cell line.

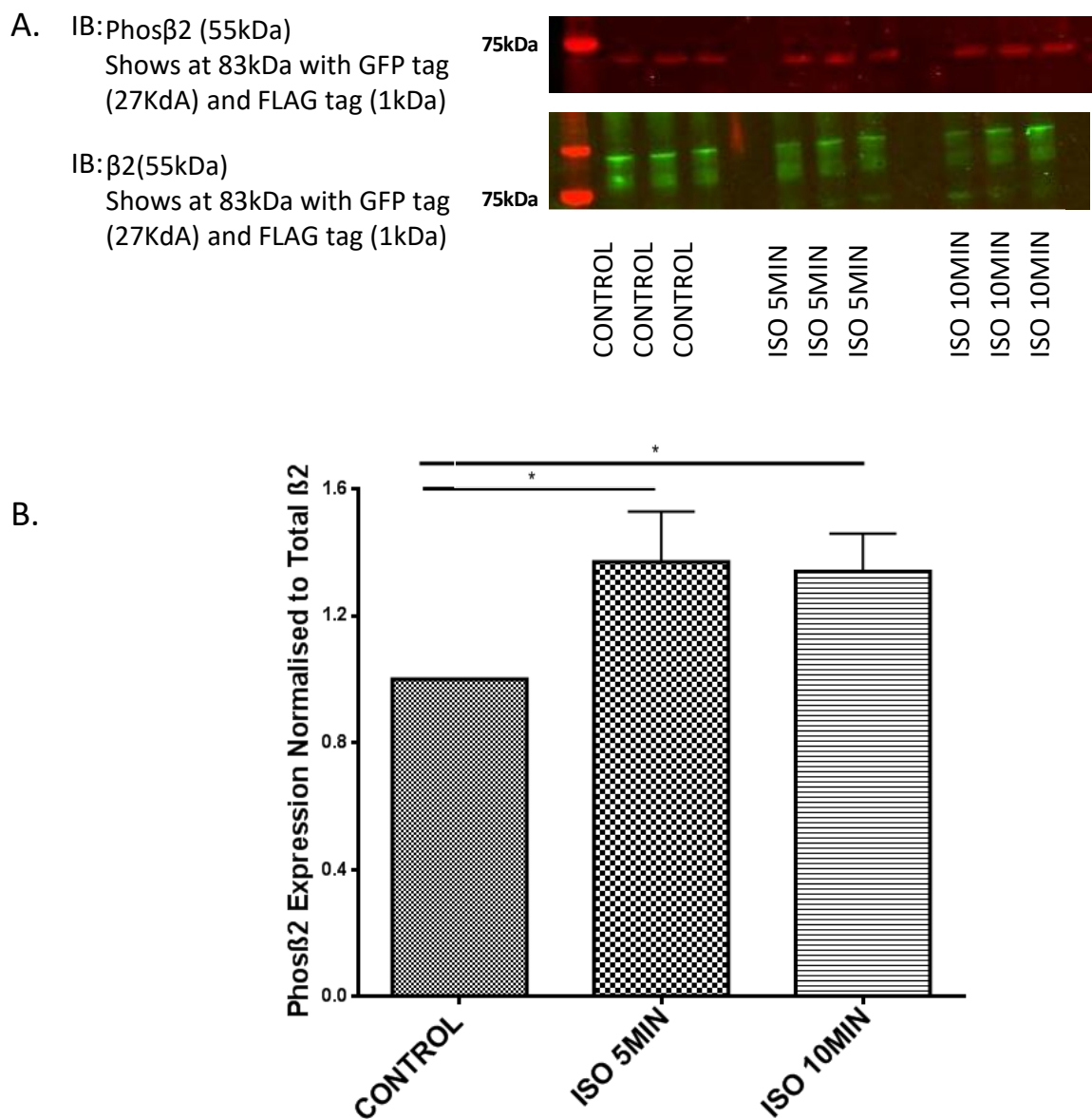


Figure 4.1 Phosphorylation of β_2 AR-mediated by isoprenaline. (A&B) HEK β_2 cells were stimulated with 10 μ M isoprenaline (ISO) for 5 and 10 minutes. This significantly increased phosphorylation of the β_2 AR by PKA in comparison to control (N=4) (* p <0.05). Primary concentration 1 : 1000, secondary concentration 1 : 5000. (A) Representative blots shown.

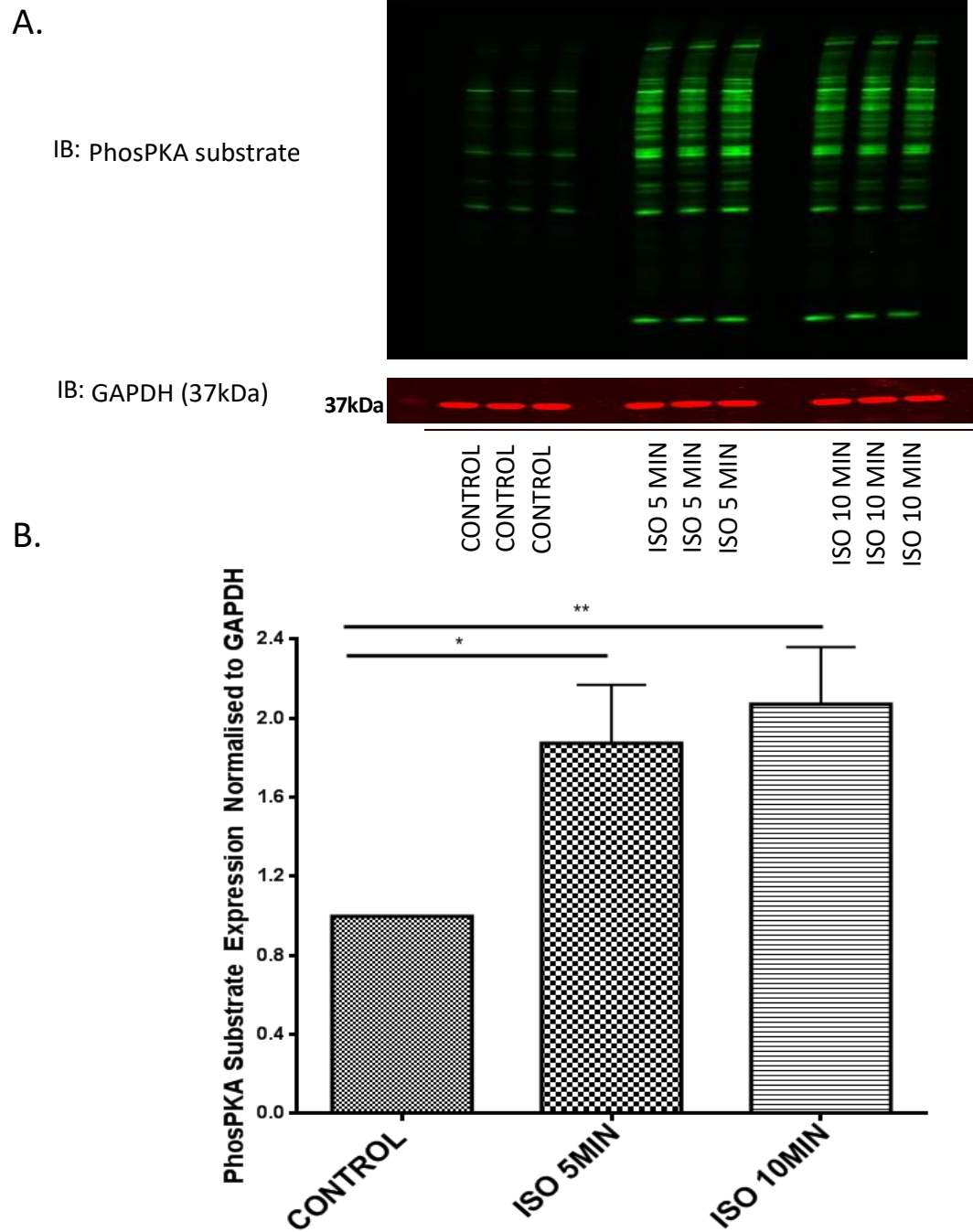


Figure 4.2 Increased activity of PKA-mediated by isoprenaline. (A&B) HEK β_2 cells were stimulated with 10 μ M isoprenaline (ISO) for 5 and 10 minutes. This significantly increased activity of protein kinase A (PKA) to phosphorylate substrates in comparison to control (N=4) (*p<0.05) (**p<0.01). Primary concentration 1 : 5000, secondary concentration 1 : 1000. **(A)** Representative blots shown.

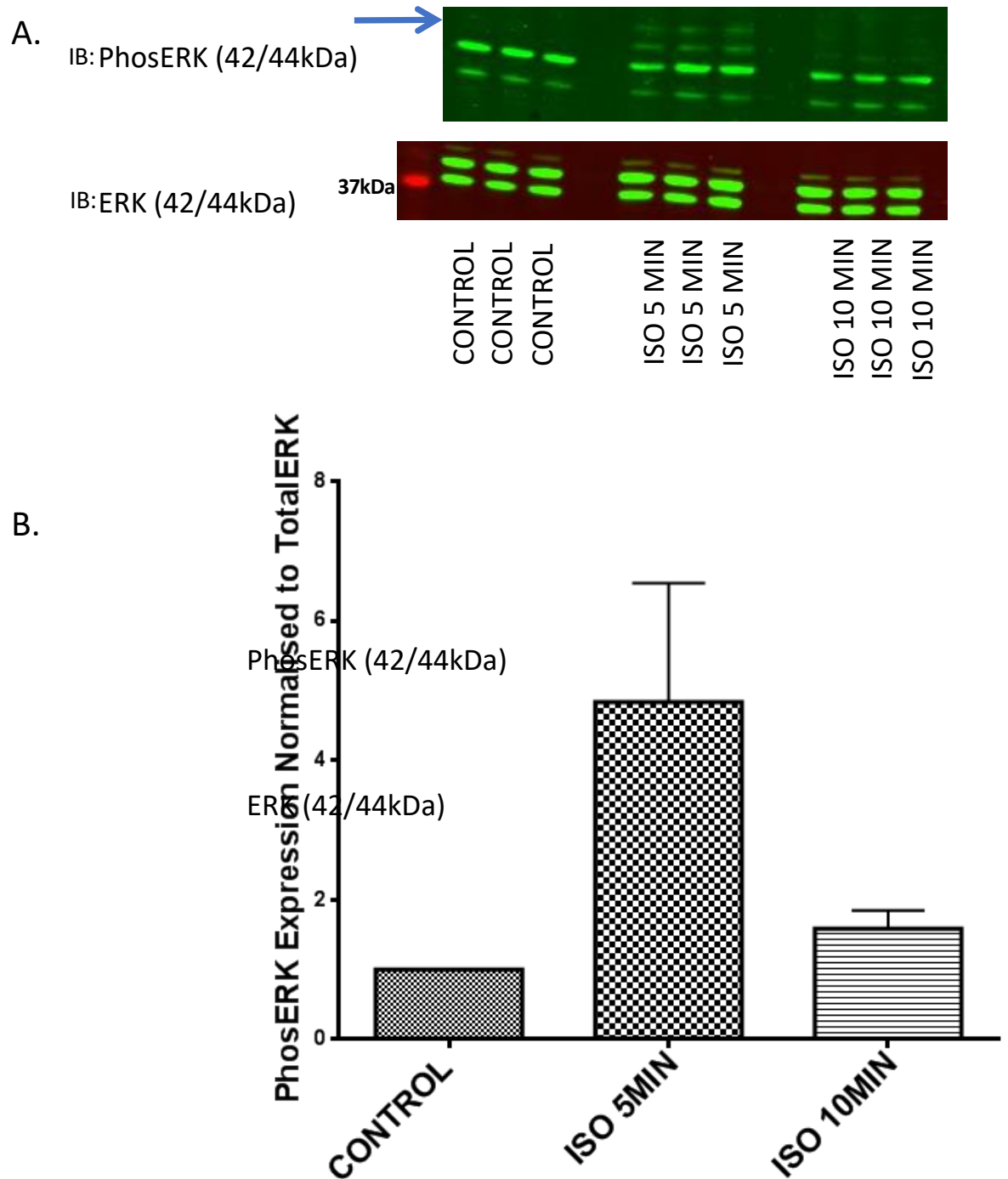


Figure 4.3 Phosphorylation of ERK mediated by isoprenaline. (A&B) HEKB₂ cells were stimulated with 10 μ M isoprenaline (ISO) for 5 and 10 minutes. This showed a trend to increase phosphorylation of ERK in comparison to control (N=4) (control vs 5 min $p=0.0558$ control vs 10 min $p=0.0550$). Primary concentration 1 : 1000, secondary concentration 1 : 5000. (A) Blue arrow indicative of quantification lanes. Representative blots shown.

4.2.2 SUMOylation of the β_2 AR *In Vitro*

Following validation of β_2 AR signalling in the HEK β_2 cell line, the next step was to promote SUMOylation of the β_2 AR within these cells and evaluate whether this modification altered signalling. To induce SUMOylation of the β_2 AR, PIAS γ was transiently transfected into HEK β_2 cells. PIAS γ is a SUMO E3 ligase, a family of enzymes which facilitates the conjugation of SUMO to substrates (Meulmeester, et al., 2008). Often the E2 enzyme UBC9 alone can be enough to encourage protein SUMOylation but many proteins require additional enzymatic support by E3 ligases which add fidelity to the process - one of which is PIAS γ (Yunus & Lima, 2009). Therefore, over-expression of PIAS γ was utilised as a route to increase the probability that the β_2 AR would be SUMOylated.

In optimising PIAS γ transfection into HEK β_2 cells, proof of successful transfection was shown by immunoblotting for the presence of the HA tag on PIAS γ (Figure 4.4A). At maximal PIAS γ expression, there was a trend for β_2 AR expression (analysed via GFP tag expression) to be enhanced 1-fold when normalised to GAPDH control (Figure 4.4B) (N=3) (p=0.0709). Traditional identification of SUMOylation is mediated via the presence of a “ghost” band - a band which is apparent via immunoblotting at approximately 12-25kDa larger than the original protein - indicative of covalent attachment of the SUMO protein. Although the SUMO protein itself only has an approximate weight of 11kDa - often larger shift sizes are observed due to the formation of SUMO chains, in which multiple SUMO molecules are added to either one lysine residue as chains, or multiple lysine residues throughout the protein (Park-Sarge & Sarge, 2005). Following PIAS γ expression a “ghost” band is observed above the β_2 AR, which I believe to be the SUMOylated form of the β_2 AR (Figure 4.4A). At maximal PIAS γ expression there is a significant 1-fold increase in the SUMO- β_2 AR band shift when normalised to GAPDH control (Figure 4.4C) (N=3) (*p<0.05). Detection of this ghost band and its increase in line with PIAS γ expression suggests the discovery of a means by which to enhance SUMO modification of the β_2 AR. Increased β_2 AR expression following PIAS γ expression may also suggest that SUMOylation of the β_2 AR may prevent degradation of the receptor. SUMOylation of other proteins on lysine residues known to be ubiquitination sites can protect such proteins from degradation by the proteasome (Desterro, et al., 1998) (Meek & Knippschild, 2003) (Kim, et al.,

2008) (Mooney, et al., 2010). To my knowledge, this work is the first to support the notion that the B₂AR can be directly modified by SUMOylation.

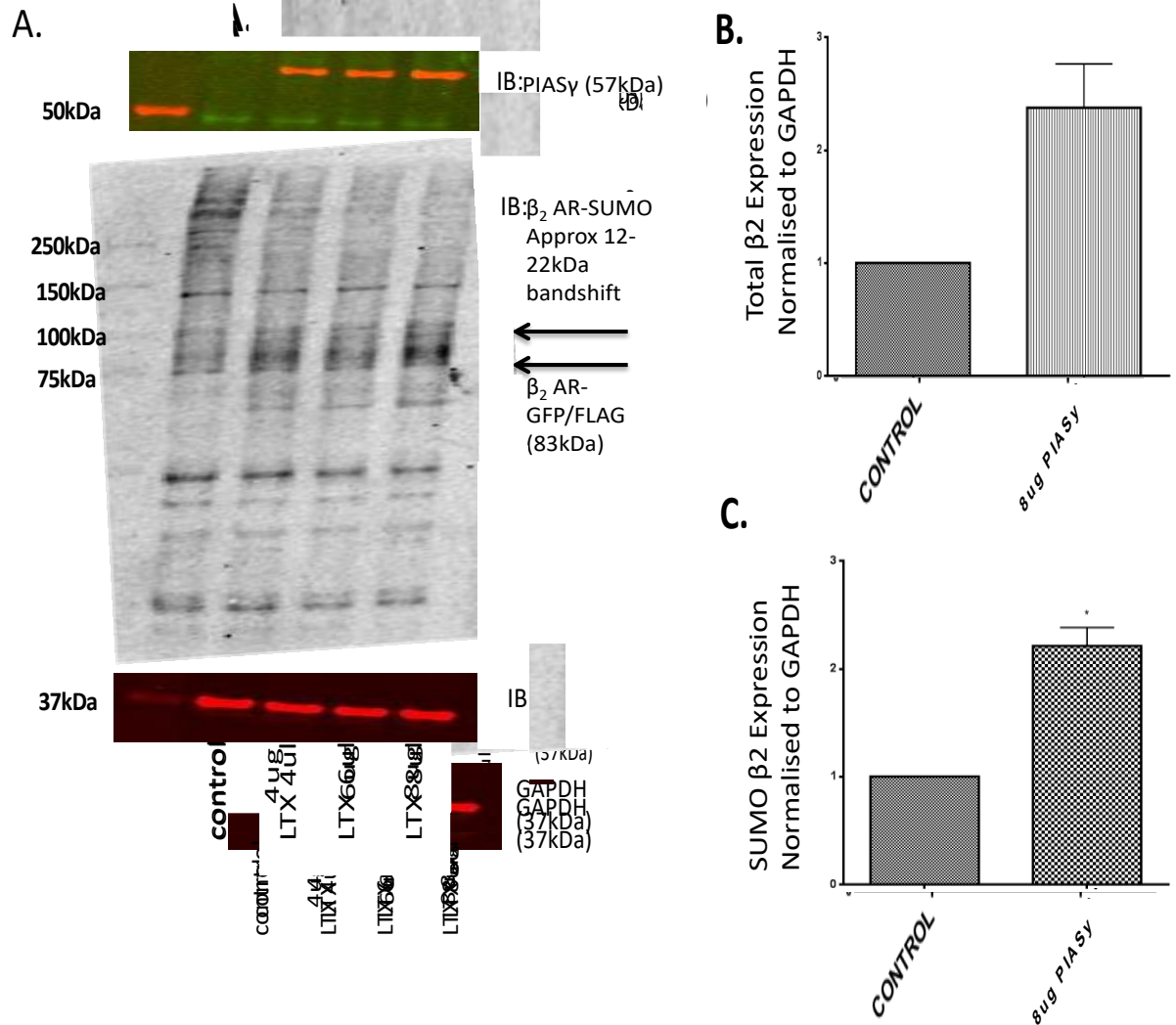


Figure 4.4 Amplifying PIASy in HEK293 cells promotes SUMOylation of β_2 AR. (A&C) HEK293 cell transfection with PIASy (E3 ligase) provokes SUMO band shift which could be indicative of SUMOylation of β_2 AR (N=3) (* $p < 0.05$). (A&B) In addition to band shift, promotion of SUMOylation appears to enhance expression of β_2 AR (N=3) ($p = 0.0709$). Primary concentration 1 : 1000, secondary concentration 1 : 5000. (A) Representative blots shown.

4.2.3 Interaction between β_2 AR and SUMOylation Enzymes PIAS γ /UBC9

Although overexpression of PIAS γ mediates a band shift indicative of SUMOylation of the β_2 AR, further evidence is required to support this hypothesis. To this end, the putative interaction between the β_2 AR and the enzymes involved in the SUMOylation cascade, namely PIAS γ and UBC9, were examined using peptide array overlay.

4.2.3.1 Peptide Array Overlay Assessment of β_2 AR-PIAS γ /UBC9 Interaction

The peptide array overlay can predict the regions of interaction between the proteins down to the amino acid level. The interaction between the receptor and SUMOylation enzymes was examined by overlaying cellular lysate prepared from cells overexpressing the desired enzyme onto peptide arrays corresponding to the intra-cellular portions of the β_2 AR. Interaction sites were identified using overnight incubation with appropriate antibody and ECL detection the following day. HA-tag antibody was used to identify the interaction points between PIAS γ and β_2 AR since PIAS γ was HA tagged, whereas UBC9 had no tag and therefore a UBC9 antibody raised against UBC9 protein was used. The latter antibody produced more non-specific sites due to direct interaction with peptide array peptides (Figure 4.6).

Putative interaction sites between PIAS γ and β_2 AR were detected at three different areas within the receptor; intracellular loop 2 (spot 2), intracellular loop 3 (spots 3, 4, 6, 8 and 9) and the cytoplasmic tail (spots 13 and 20) (Figure 4.5) (Figure 4.7) (N=1). Interaction sites between UBC9 and β_2 AR occurred at two different areas within the receptor; intracellular loop 3 (spots 4 and 6), and cytoplasmic tail (spots 12, 22 and 23) (Figure 4.6) (Figure 4.7) (N=1). As expected interactions with both enzymes occurred near the identified SUMO sites, 232 and 235 within the third intracellular loop, as traditionally these enzymes mediate their interactions via the amino acids which surround the SUMO consensus motif (Bernier-Villamor, et al., 2002) (Duval, et al., 2003) (Yunus & Lima, 2009) (Hochstrasser, 2001). The interactions found within the other areas of the β_2 AR could imply that further SUMOylation sites exist within the receptor that have not been recognised by the sequence analysis prediction software or that there is a

more extensive binding of UBC9 with β_2 AR than was previously imagined. For future work, immunoprecipitations and visualisation of β_2 AR and SUMOylation enzymes co-localisation using microscopy should be done to verify the interaction. Sites of interaction could be verified by undertaking IP experiments with mutants of the β_2 AR that contain substitutions shown to ablate interactions between the enzymes and the receptor (Figure 4.5 & 4.6). The UBC9 overlay on β_2 AR peptide array should also be completed with a tag expression construct of the enzyme to compensate for unspecific binding.

In conclusion, the data suggest that interactions exist between vital SUMOylation enzymes and β_2 AR, a conclusion that supports the identification of SUMO modification of the β_2 AR for the first time.

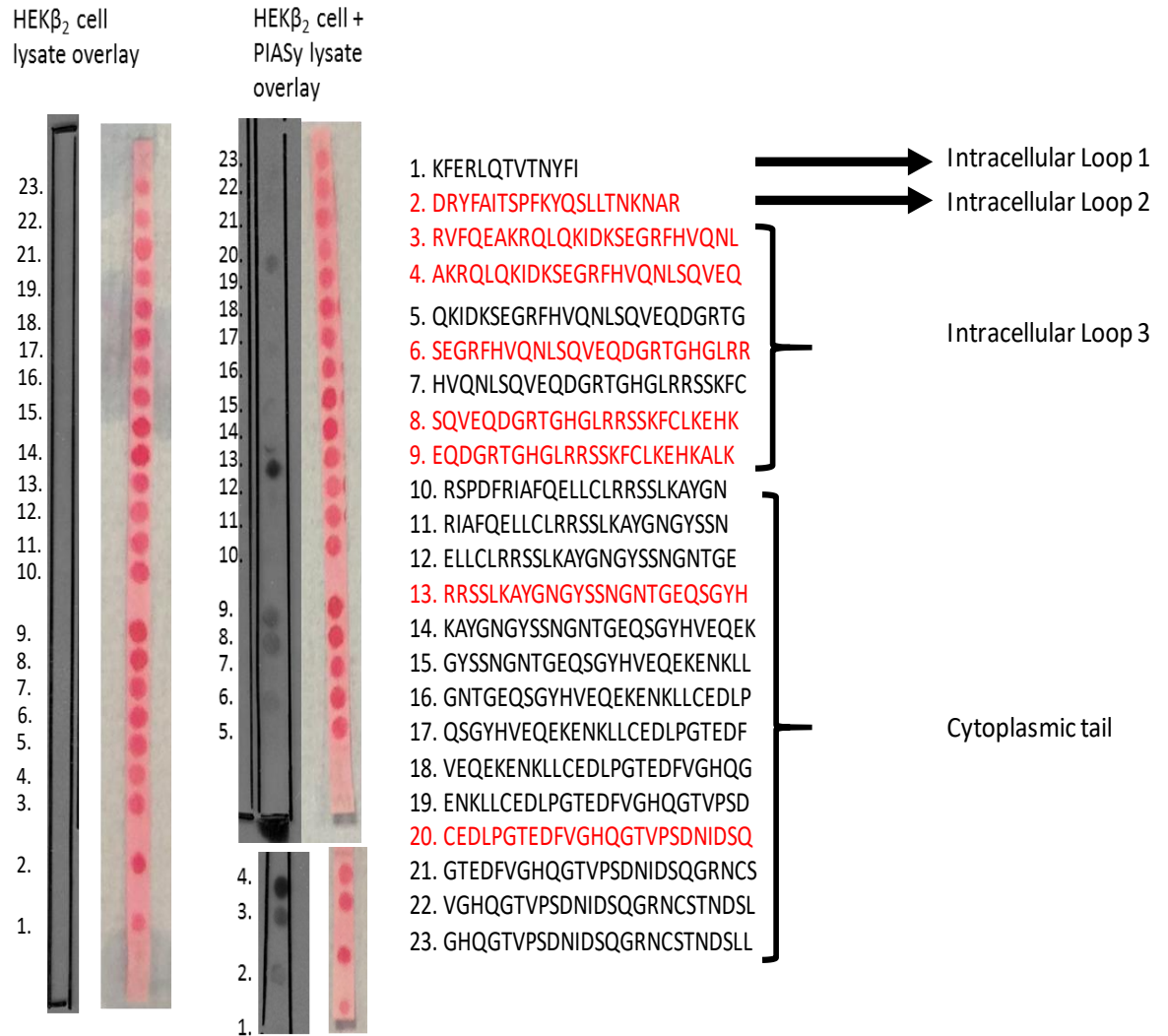


Figure 4.5. β_2 AR-PIASy interaction assessed by peptide array overlay. β_2 AR peptide array on cellulose incubated overnight with either HEK β_2 lysate or HEK β_2 lysate overexpressed with PIASy. Following overnight incubation with appropriate antibody and ECL detection the following day, the point of interaction was identified with black spots. The text is displayed in red for the positive back spots (N=1). Ponceau identifies all spots within array as control. Primary concentration 1 : 1000, secondary concentration 1 : 1000. Amino acid abbreviations in appendix.

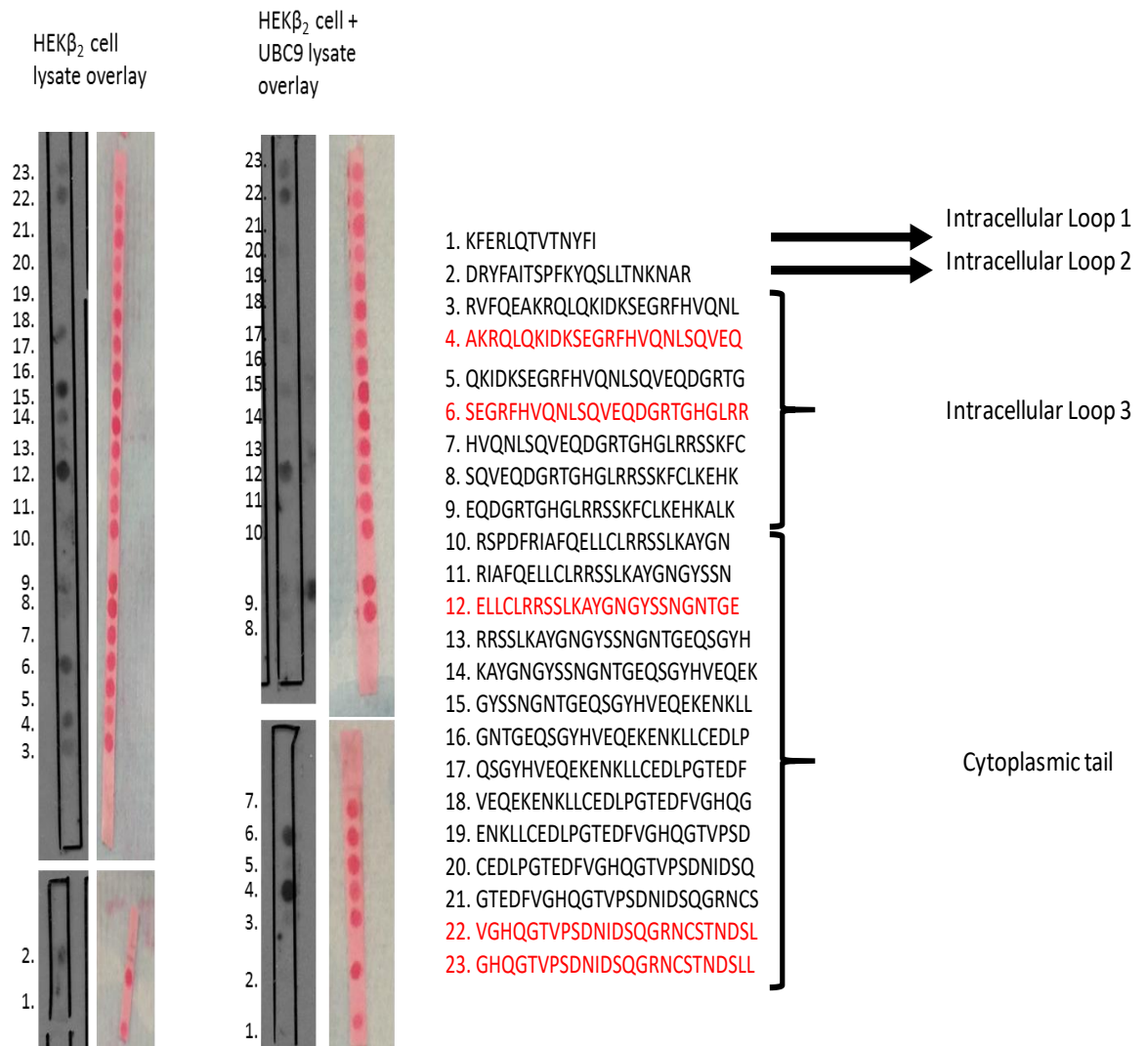


Figure 4.6 β_2 AR-UBC9 interaction assessed by peptide array overlay. β_2 AR peptide array on cellulose incubated overnight with either HEK β_2 lysate or HEK β_2 lysate overexpressed with UBC9. Following overnight incubation with appropriate antibody and ECL detection the following day, the point of interaction was identified with black spots. The text is displayed in red for the positive back spots (N=1). Ponceau identifies all spots within array as control. Primary concentration 1 : 1000, secondary concentration 1 : 1000. Amino acid abbreviations in appendix.

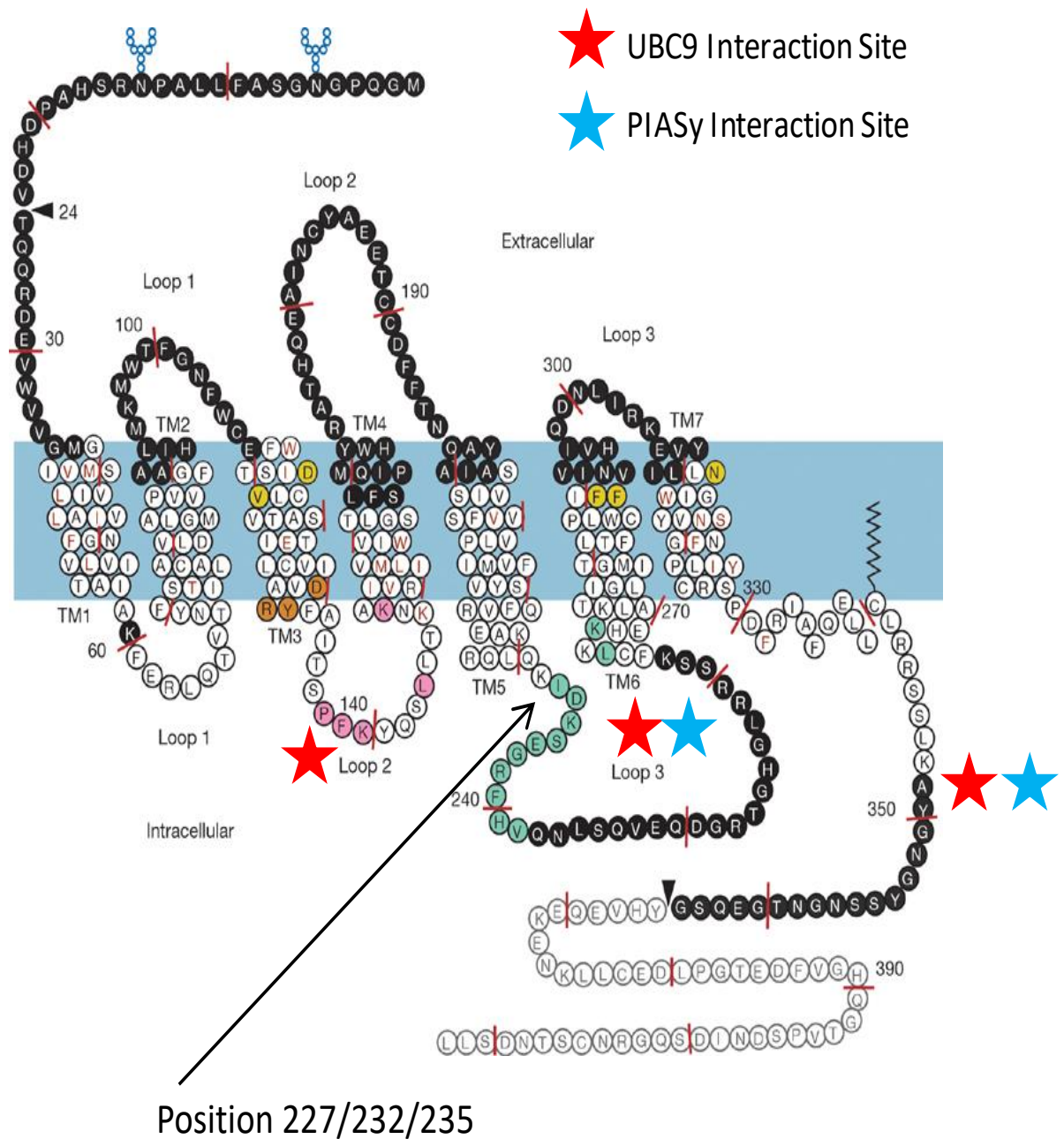


Figure 4.7 B_2AR -PIASy/UBC9 interaction sites identified near SUMOylation sites. The interaction sites for PIASy and UBC9 were found to be near SUMOylation sites 232 and 235 within the third intracellular loop. They were also identified in intracellular loop 2 and the cytoplasmic tail.

4.2.4 Influence of β_2 AR SUMOylation on Receptor Function.

4.2.4.1 β_2 AR SUMOylation Alters Receptor Signalling

The HEK β_2 cell line was used to examine the influence of β_2 AR SUMOylation on receptor signalling. Cells underwent mock transfection with empty transfection reagent or transfection with the E3 ligase PIASy, which promotes SUMOylation of the β_2 AR (Figure 4.4) (described in Chapter 2 - General Materials and Methods). These cells were then stimulated with 10 μ M isoprenaline for both 5 and 10 minutes. Stimulation of HEK β_2 cells by isoprenaline leads to an elevation in 1) phosphorylation of β_2 AR by PKA, 2) ERK activation, and 3) PKA cytosolic activity (Figures 4.1 - 4.3). The next step was to evaluate the effects of β_2 AR SUMOylation on these downstream signals. In comparison to cells that did not have PIASy transfected into them, the SUMOylated β_2 AR exhibited approximately 25% less direct phosphorylation by PKA (Figure 4.8) (N=4) (*p<0.025), approximately 25% reduced PKA activity as measured indirectly by monitoring general PKA substrates (Figure 4.9) (N=4) (*p<0.025) (**p<0.01), as well as an approximate 65% reduction in ERK activation (Figure 4.10) (N=4) (**p<0.001) (**p<0.01). In addition, there is an approximate 25% increase in total β_2 AR at the 10 minute time point in the SUMOylated β_2 AR cell compared to unSUMOylated β_2 AR control (Figure 4.11) (N=4) (*p<0.05). Normally when the β_2 AR is chronically stimulated with agonist it will down regulate to prevent excessive agonist exposure - this down-regulation begins with the receptor becoming internalised and at longer time points degraded by lysosomal degradation (Shenoy, et al., 2001) (Moore, et al., 1999). The data here suggests that there is less internalisation or degradation of the receptor in response to isoprenaline for the SUMOylated β_2 AR compared with wild-type (WT) β_2 AR.

In addition to PKA, the β_2 AR can also be phosphorylated by other kinases, for example G protein-coupled receptor kinases (GRKs). GRKs phosphorylate multiple serine and threonine residues within the C-terminus of the receptor (Ferguson, et al., 1996) (Mak, et al., 2002) (Collins, et al., 1991) (Vaughan, et al., 2006) and in doing so promote β -arrestin1/2 recruitment to the membrane (Violin, et al., 2006) (Vaughan, et al., 2006). This is vital for receptor desensitisation. In light of this, the effect of SUMOylation on β_2 AR phosphorylation by GRK using a site-specific antibody was examined. An approximate 40% reduction in GRK phosphorylation of

the β_2 AR at basal levels was observed following PIASy transfection in comparison to mock transfected cells (Figure 4.12) (N=3) (* p <0.05). No significant difference in GRK phosphorylation existed between unSUMOylated and SUMOylated β_2 AR following 5 and 10 minutes of isoprenaline treatment (Figure 4.12) (N=3). However the detection of total β_2 AR via the GFP-tag antibody is not as clear as prior western blots, and therefore to confirm the influence of receptor SUMOylation on β_2 AR phosphorylation by GRK, this western blot would need to be repeated.

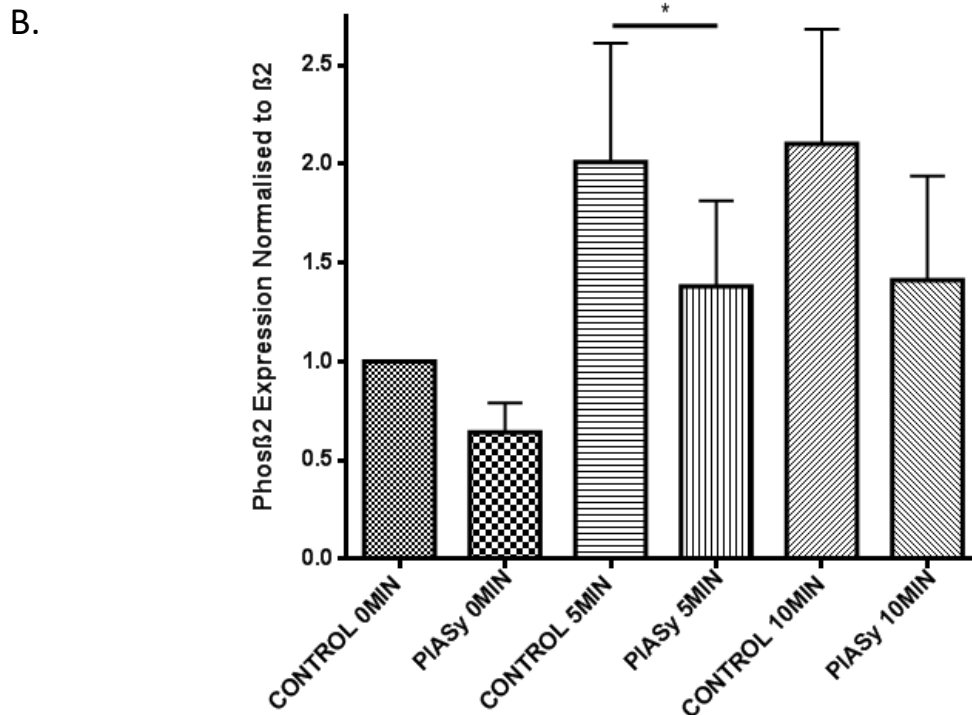
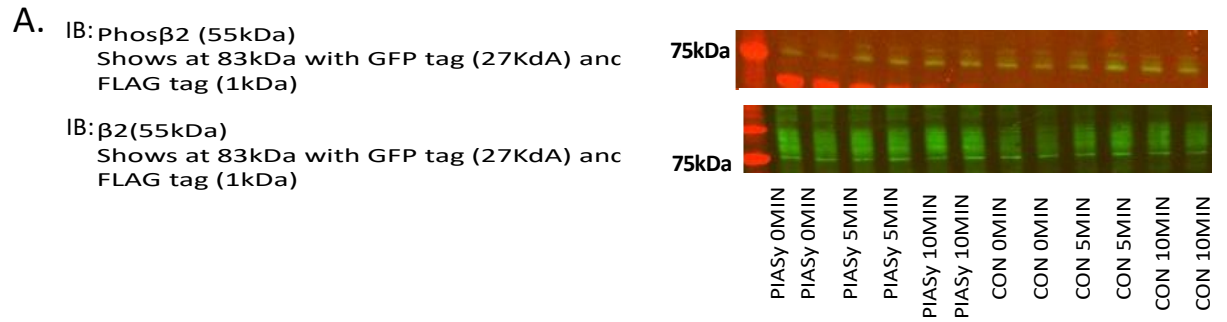
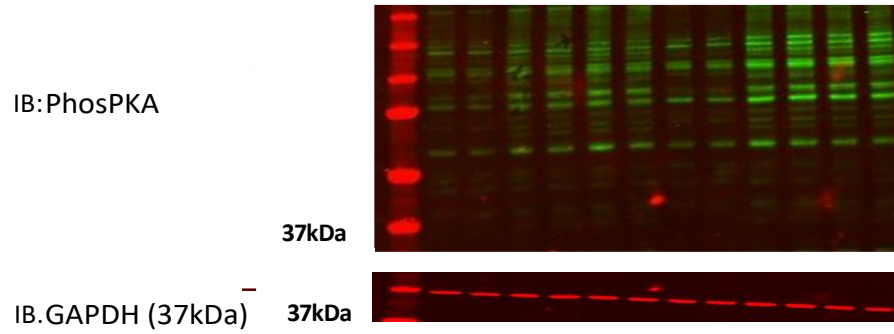


Figure 4.8. β_2 AR SUMOylation reduces isoprenaline-mediated PKA phosphorylation of β_2 AR. (A&B) HEK β_2 cells transfected with PIASy to promote β_2 AR SUMOylation and HEK β_2 mock transfected cells were stimulated with 10 μ M isoprenaline (ISO) for 5 and 10 minutes. SUMOylation of the β_2 AR caused a significant reduction in phos β_2 expression after 5 minutes isoprenaline treatment in comparison to control (N=4) (* p <0.05). Primary concentration 1 : 1000, secondary concentration 1 : 5000. (A) Representative blots shown.

A.



B.

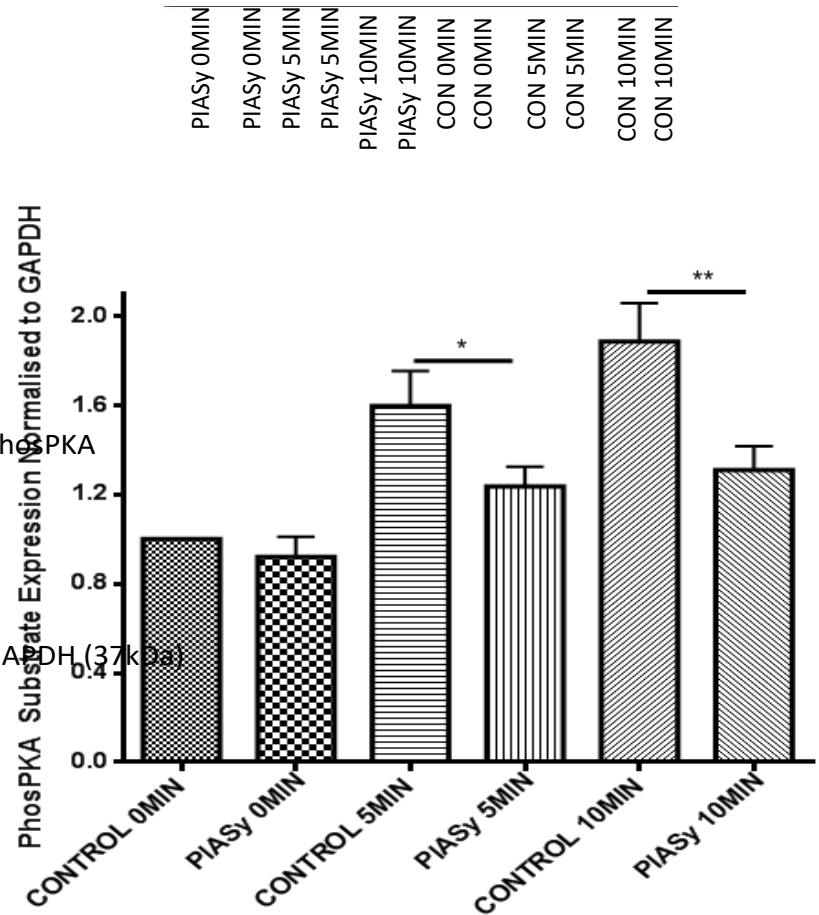


Figure 4.9 β_2 AR SUMOylation reduces isoprenaline-mediated PKA cytosolic activity. (A&B) HEK β_2 cells transfected with PIASy to promote β_2 AR SUMOylation and HEK β_2 mock transfected cells were stimulated with 10 μ M isoprenaline (ISO) for 5 and 10 minutes. SUMOylation of the β_2 AR caused a significant reduction in PKA activity after 5 and 10 minutes 10 μ M isoprenaline treatment in comparison to control (N=4) (* p <0.05) (** p <0.01). Primary concentration 1 : 1000, secondary concentration 1 : 5000. (A) Representative blots shown.

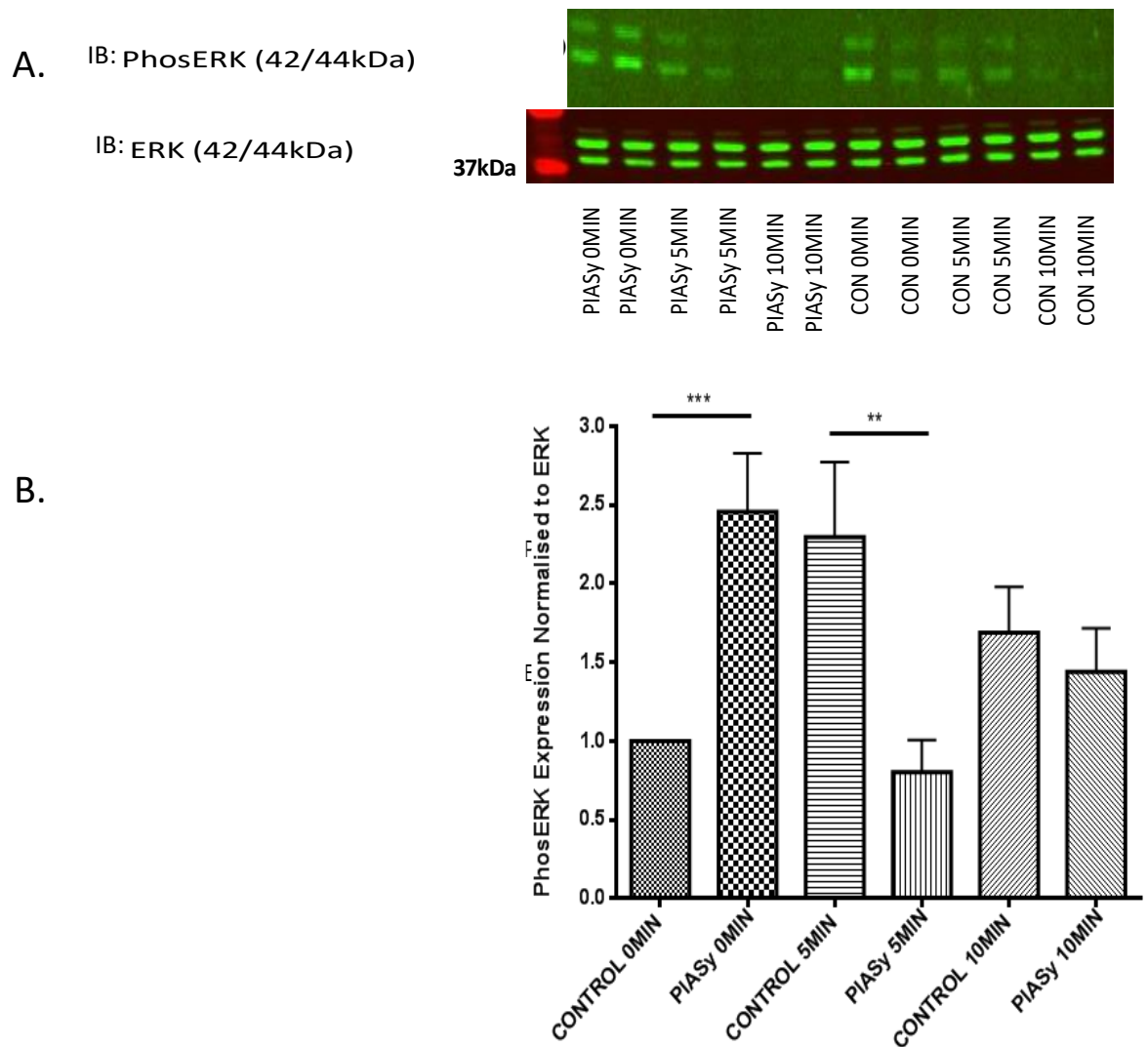


Figure 4.10 β_2 AR SUMOylation reduces isoprenaline-mediated phosphorylation of ERK. (A&B) HEK293 cells transfected with PIASy to promote β_2 AR SUMOylation and HEK293 mock transfected cells were stimulated with 10 μ M isoprenaline (ISO) for 5 and 10 minutes. SUMOylation of the β_2 AR caused a significant difference in phosERK expression at basal levels and after 5 minutes isoprenaline treatment in comparison to control. At basal level PIASy causes an elevation in phosERK expression in comparison to control (N=4) (**p<0.001). At 5 minutes PIASy causes a reduction in phosERK expression in comparison to control (N=4) (**p<0.01). Primary concentration 1 : 1000, secondary concentration 1 : 5000. (A) Representative blots shown.

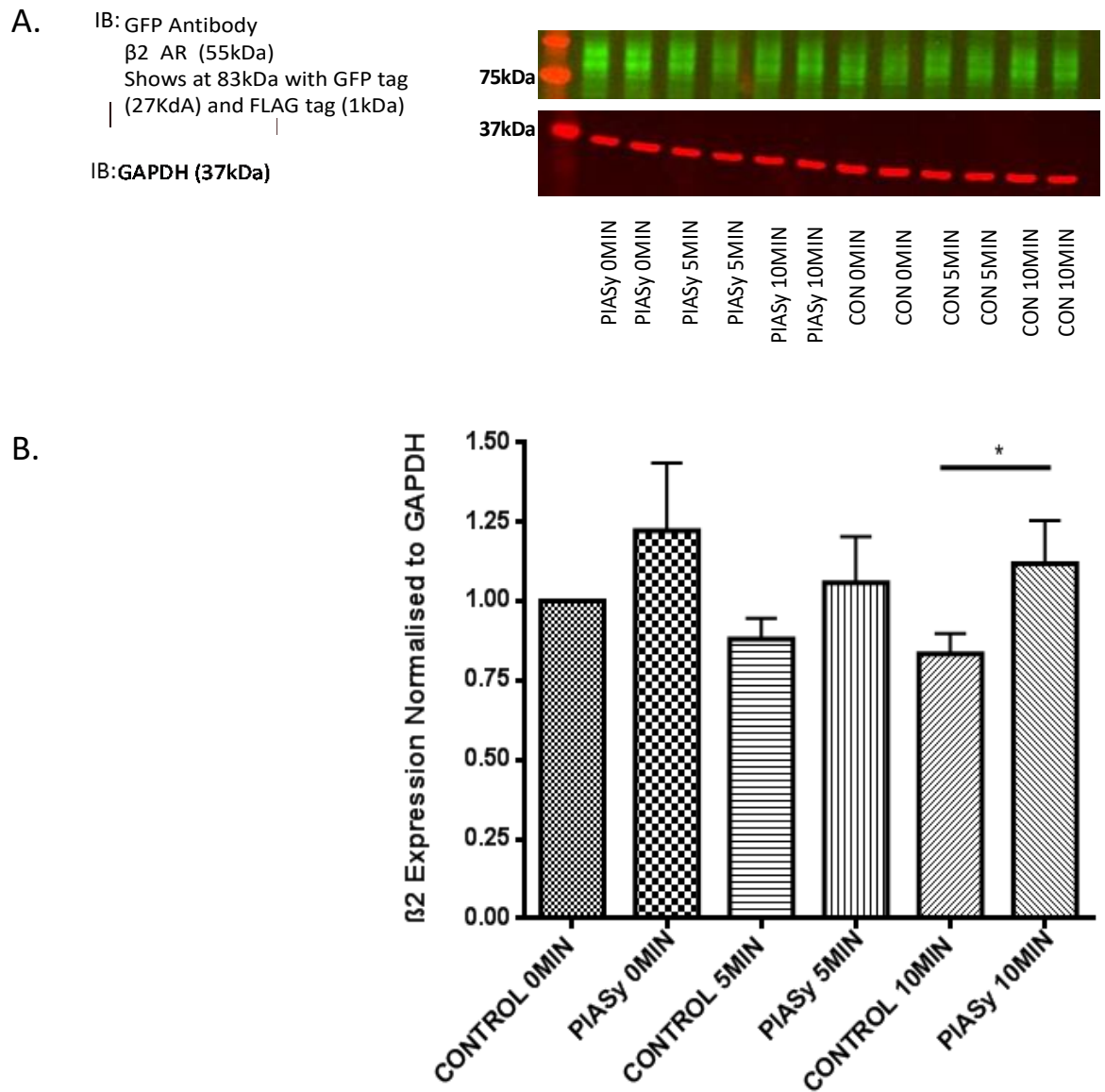


Figure 4.11 β_2 AR SUMOylation reduces isoprenaline-mediated reduction in total β_2 AR. (A&B) HEK β_2 cells transfected with PIASy to promote β_2 AR SUMOylation and HEK β_2 mock transfected cells were stimulated with 10 μ M isoprenaline (ISO) for 5 and 10 minutes. SUMOylation of the β_2 AR caused a significant difference in total β_2 AR expression after 10 minutes isoprenaline treatment in comparison to control cells (N=4) (*p<0.05). Primary concentration 1 : 1000, secondary concentration 1 : 5000. **(A)** Representative blots shown.

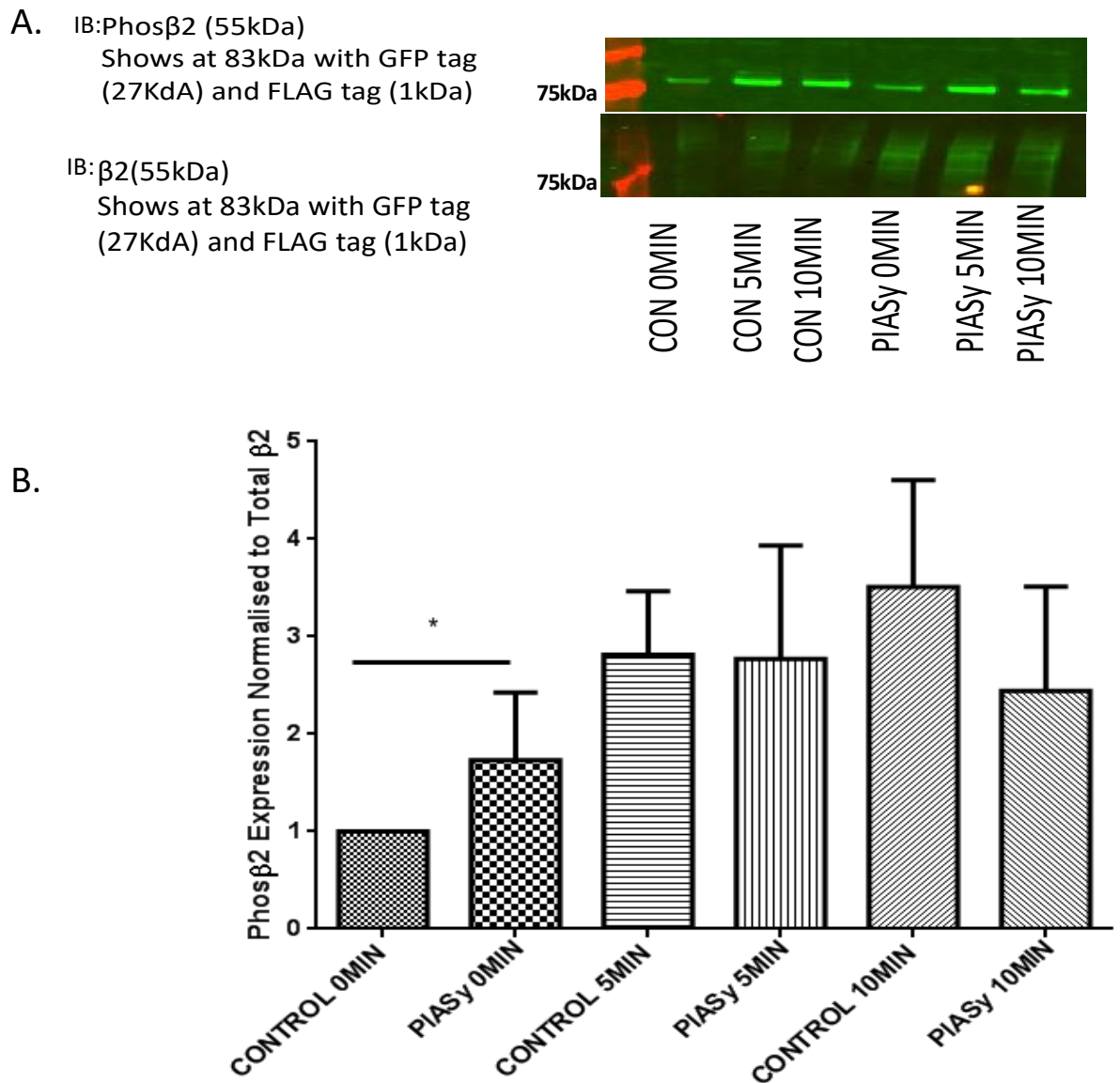


Figure 4.12 β 2AR SUMOylation influence on isoprenaline-mediated GRK phosphorylation of β 2AR is inconclusive. (A&B) HEK β 2 cells transfected with PIAS γ to promote β 2AR SUMOylation and HEK β 2 mock transfected cells were stimulated with 10 μ M isoprenaline (ISO) for 5 and 10 minutes. SUMOylation of the β 2AR caused a significant reduction in phos β 2 expression in basal signalling. There was no difference after isoprenaline treatment in comparison to control (N=3) (*p<0.05). However the detection of total β 2AR via the GFP-tag antibody is not as clear as prior western blots, and therefore to confirm the influence of receptor SUMOylation on β 2AR phosphorylation by GRK, this western blot would need to be repeated. Primary concentration 1 : 1000, secondary concentration 1 : 5000. (A) Representative blots shown.

4.2.4.2 β_2 AR SUMOylation Reduces Receptor Internalisation

Chronic isoprenaline treatment is known to promote β_2 AR internalisation as a medium-term desensitisation mechanism. When the β_2 AR is internalised, it is moved away from the cell surface and isolated within clathrin coated vesicles preventing it from further signalling via the G proteins (Goodman, et al., 1996). There is now evidence for endosomal signalling by the β_2 AR. Irannejad et al (2013) revealed that in HEK293 cells isoprenaline-promoted cAMP production at the plasma membrane via the β_2 AR as expected, but also in the early endosome. Furthermore, inhibition of endocytosis led to a reduction in cAMP production mediated via the β_2 AR (Irannejad, et al., 2013). This group propose that β_2 AR-G_s coupling occurs in the early endosome, promoting a discrete phase of cAMP production (Irannejad & Von Zastrow, 2014).

The Cellomics® ArrayScan® was used to examine the influence of SUMOylation of the β_2 AR on receptor internalisation in response to agonist. HEK β_2 cells underwent mock transfection with empty transfection reagent or transfection with the E3 ligase PIAS γ , which promotes SUMOylation of the β_2 AR (Figure 4.4) (described in Chapter 2 - General Materials and Methods). These cells were then stimulated with 10 μ M isoprenaline for various time points to 90 minutes and internalisation of the β_2 AR was monitored using the Cellomics® ArrayScan®. Analysis of data from procedure above suggested that SUMOylation of the β_2 AR significantly reduces β_2 AR internalisation in response to isoprenaline by approximately 60% in comparison to control (Figure 4.13) (N=3) (*p<0.05) (**p<0.01).

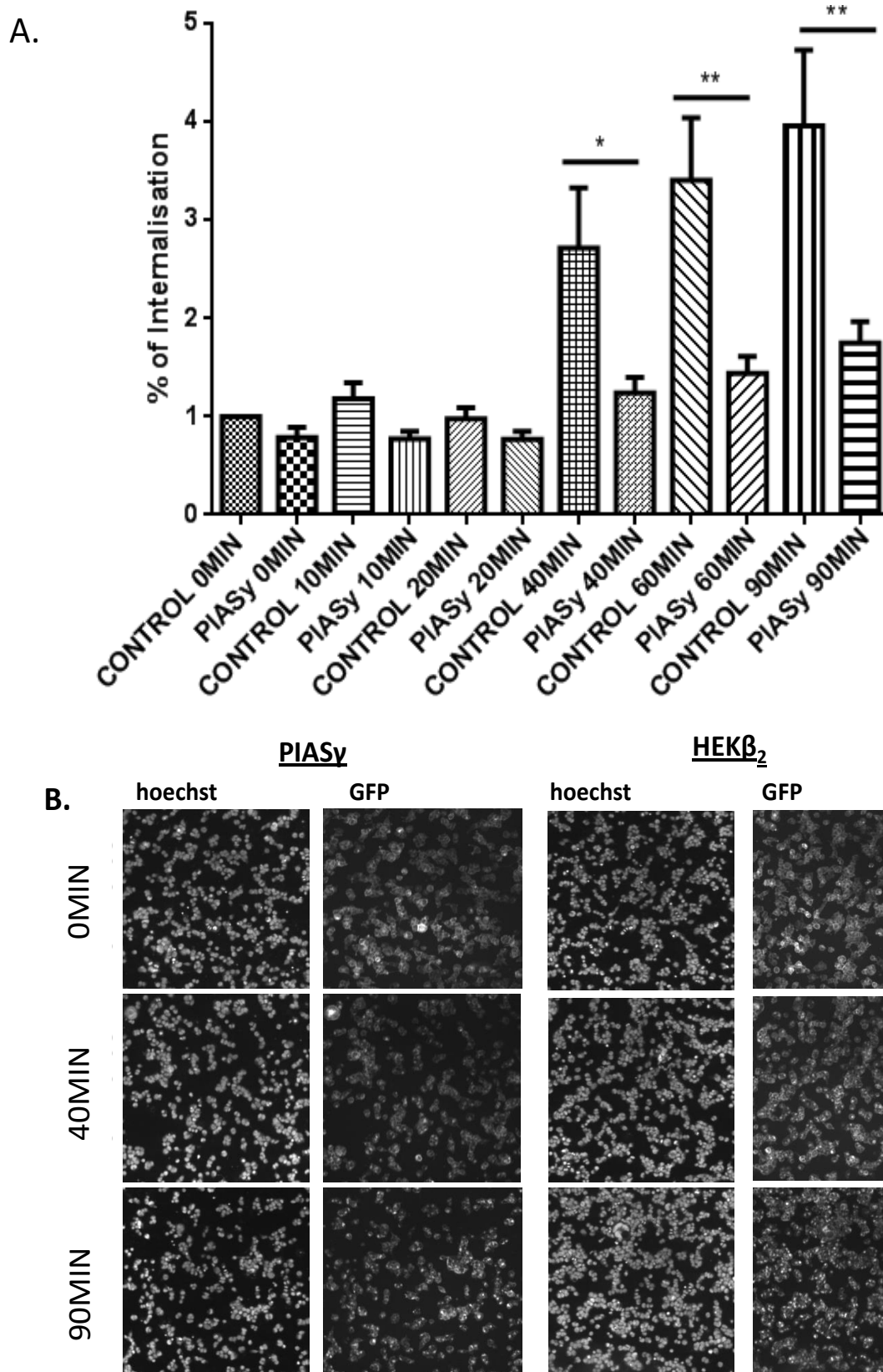


Figure 4.13 β_2 AR SUMOylation delays receptor internalisation. (A&B) HEK β_2 cells overexpressing PIASy via transfection and HEK β_2 mock transfected cells were stimulated with 10 μ M isoprenaline (ISO) for various time points from basal to 90 minutes. SUMOylation of β_2 AR significantly reduces β_2 AR internalisation in response to isoprenaline approximately 60% in comparison to control (N=3) (*p<0.05) (**p<0.01). (B) Representative images from one experiment shown.

4.2.4.3 β_2 AR SUMOylation Influence on Receptor Half-Life is Inconclusive

The β_2 AR has a relatively long half-life with the longest reported being up to 30 hours (Mahan & Insel, 1986) (Fraser & Venter, 1980). HEK β_2 cells underwent mock transfection with empty transfection reagent or transfection with the E3 ligase PIAS γ , which promotes SUMOylation of the β_2 AR (Figure 4.4) (described in Chapter 2 - General Materials and Methods). These cells were then treated with 50 μ g/ml cycloheximide for 3, 5, 8, and 24 hours. This drug acts by preventing protein synthesis therefore allowing us to monitor receptor turnover rate by monitoring the decline of β_2 AR over time. Cycloheximide treatment produced an approximate 50% reduction in β_2 AR expression at the 24 hour time point - in both cells transfected with PIAS γ and those mock transfected - in comparison to the 0 hour time point, indicative that the β_2 AR was being degraded (Figure 4.14) (N=3) (**p<0.001) (****p<0.0001). No significant difference existed between SUMOylated and non SUMOylated β_2 AR in total β_2 AR population at any time point. In conclusion, SUMOylation of β_2 AR does not influence receptor turnover rate under basal conditions. However the detection of total β_2 AR via the GFP-tag antibody is not as clear as prior western blots and therefore to confirm the influence of receptor SUMOylation on β_2 AR half-life this western blot would need to be repeated.

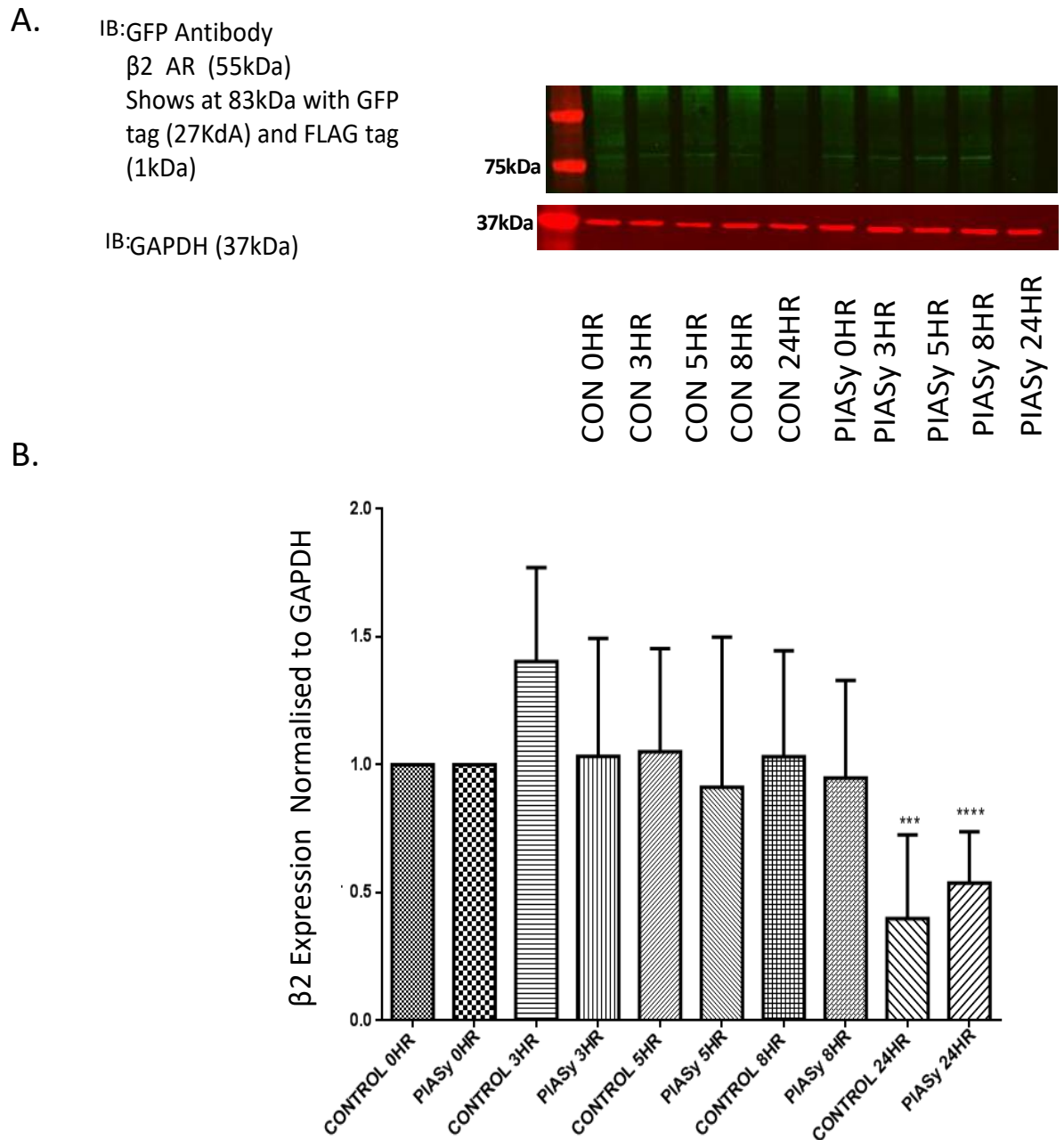


Figure 4.14 β_2 AR SUMOylation influence on receptor half-life is inconclusive. (A&B) HEK β_2 cells overexpressing PIAS γ via transfection and HEK β_2 mock transfected cells were stimulated with 50 μ g/ml cycloheximide for 3, 5, 8 and 24 hours. Cycloheximide treatment produced a significant reduction in β_2 AR at the 24 hour time point - in both cells transfected with PIAS γ and those mock transfected - in comparison to 0 hour time point, indicative that the β_2 AR was being degraded in these cells (N=3) (**p<0.0001) (****p<0.0001). No significant difference existed between SUMOylated and non SUMOylated β_2 AR in total β_2 AR population at any time point (N=3). However the detection of total β_2 AR via the GFP-tag antibody is not as clear as prior western blots and therefore to confirm the influence of receptor SUMOylation on β_2 AR half-life this western blot would need to be repeated. Primary concentration 1 : 1000, secondary concentration 1 : 5000. (A) Representative blots shown.

4.2.4.4 β_2 AR SUMOylation Reduces Ubiquitination

Ubiquitination is a PTM in which a ubiquitin protein is attached to a lysine on the target protein. Ubiquitination is essential for β_2 AR internalisation (Shenoy, et al., 2001). When β_2 AR is internalised, it can either be recycled back to the surface or it can be degraded. The extent of ubiquitination on the internalised β_2 AR determines if its degradation is undertaken by both the 26S proteasome and lysosomal degradation (Gagnon, et al., 1998) (Moore, et al., 1999). HEK β_2 cells underwent mock transfection with empty transfection reagent or transfection with the E3 ligase PIAS γ , which promotes SUMOylation of the β_2 AR (Figure 4.4) (described in Chapter 2 - General Materials and Methods). Cells were then treated with 20 μ M MG132, a proteasome inhibitor, which prevents the degradation of ubiquitinated proteins allowing them to build up within the cell. A 3 hour MG132 timepoint was used to assess ubiquitination at basal levels. Shenoy et al (2001) have previously reported that receptor activation influences ubiquitination, therefore these experiments were also carried out with isoprenaline stimulation in which the protocol was changed to 1 hour 20 μ M MG132 followed by 10 minutes 10 μ M isoprenaline stimulation.

Immunoprecipitation of the β_2 AR was undertaken using FLAG beads to isolate receptor and GST beads used as control. Immunoblotting with antibody to detect ubiquitin chains allowed examination of β_2 AR ubiquitination. As expected, MG132 treatment produced a significant increase in β_2 AR ubiquitination after 3 hours - in both cells transfected with PIAS γ (1.5-fold increase) and those without (2.5-fold increase) - in comparison to the 0 hour time point, indicating that the β_2 AR was being ubiquitinated at basal levels (Figure 4.15) (N=3) (*p<0.05). No significant difference existed between SUMOylated and non SUMOylated β_2 AR in the extent of ubiquitination at basal levels. After treatment of 20 μ M MG132 for 1 hour followed by 10 μ M isoprenaline for 10 minutes SUMOylated β_2 AR was approximately 70% less ubiquitinated in comparison to unSUMOylated β_2 AR (Figure 4.16) (N=3) (*p<0.05). In conclusion, SUMOylation of β_2 AR reduces receptor susceptibility to ubiquitination but only after β_2 AR activation. The outcome of our MG132 studies correlates with work by Shenoy et al (2001) in which proteasomal inhibition mediated a significant increase in ubiquitinated β_2 AR in an agonist-dependent manner. Similarly to other proteins in which the PTMs SUMOylation and

ubiquitination compete (Desterro, et al., 1998) (Meek & Knippschild, 2003) (Kim, et al., 2008) (Mooney, et al., 2010), this may also be the case for the β_2 AR.

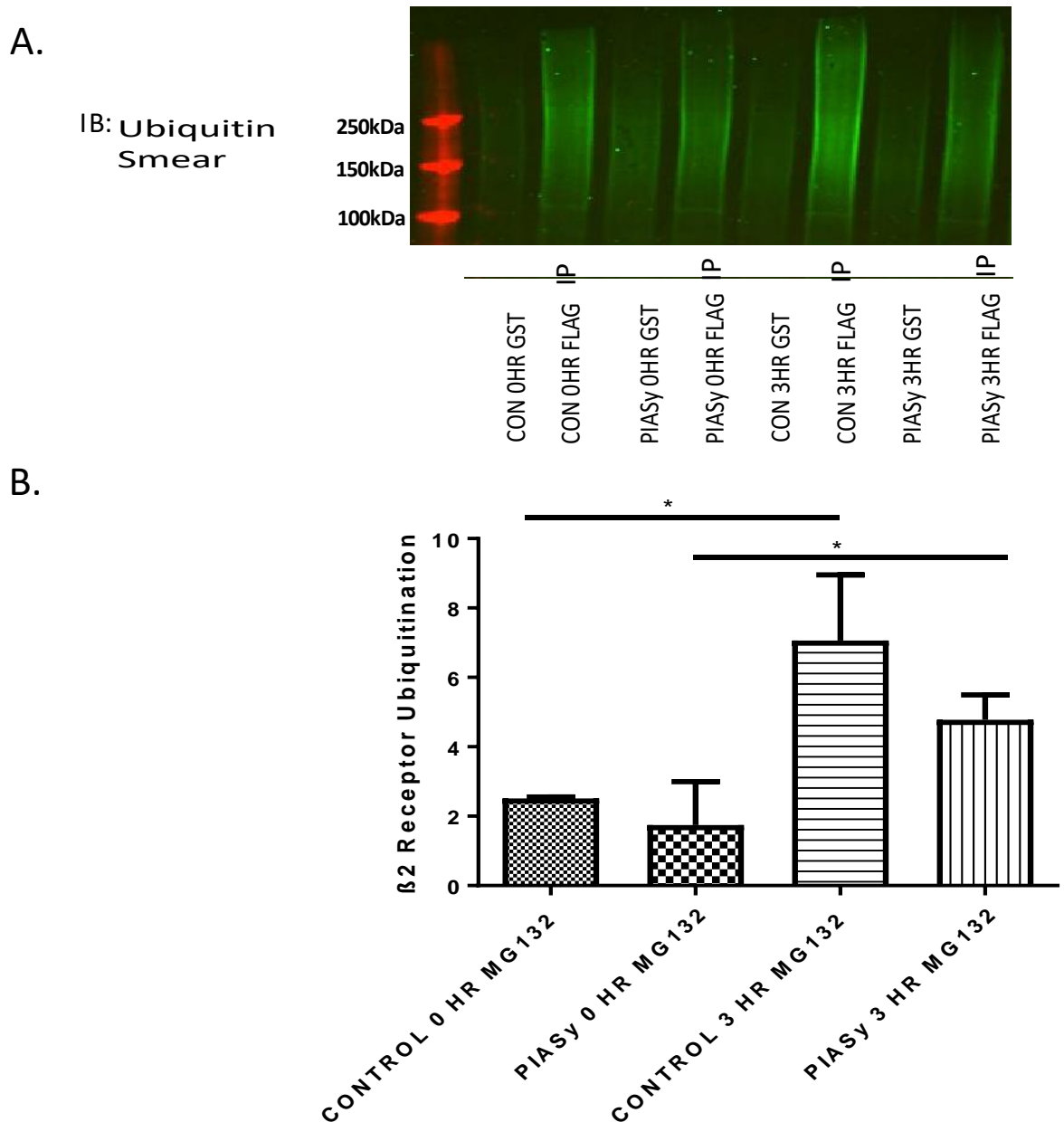


Figure 4.15 β_2 AR SUMOylation does not influence receptor ubiquitination at basal levels. **(A&B)** HEK β_2 cells overexpressing PIASy via transfection and HEK β_2 mock transfected cells were stimulated with 20 μ M MG132 for 3 hours. MG132 treatment caused a significant elevation in β_2 AR ubiquitination in both control and transfected cells at 3 hours in comparison to the 0 time point. No significant difference existed between SUMOylated and non SUMOylated β_2 AR (N=3) (* p <0.05). Primary concentration 1 : 1000, secondary concentration 1 : 5000. **(A)** Representative blots shown.

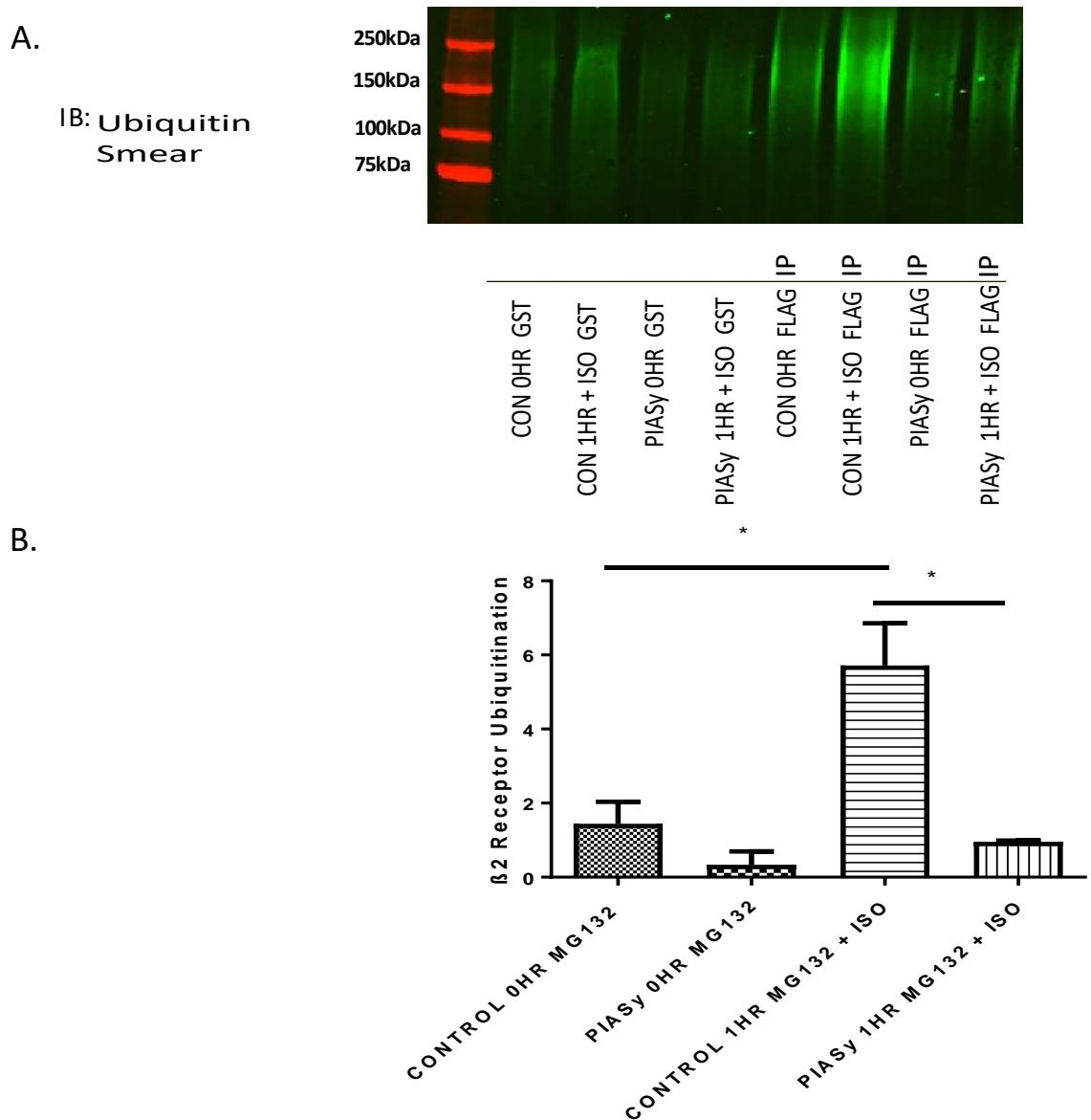


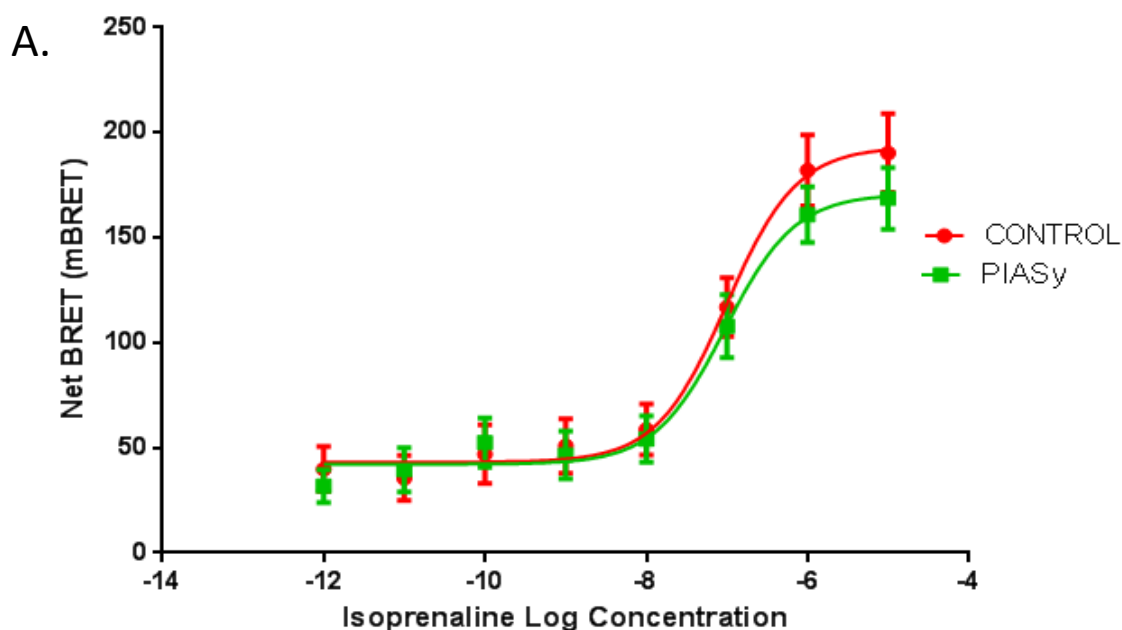
Figure 4.16 β_2 AR SUMOylation reduced isoprenaline-mediated receptor ubiquitination. (A&B) HEK β_2 cells overexpressing PIASy via transfection and HEK β_2 mock transfected cells were stimulated with 20 μ M MG132 for 1 hour followed by either 10 μ M isoprenaline (ISO) for 10 minutes or non-treated. Isoprenaline caused a significant elevation in β_2 AR ubiquitination in control cells in comparison to non-treated cells. SUMOylation of the β_2 AR significantly reduces isoprenaline-mediated ubiquitination in comparison to control unSUMOylated β_2 AR (N=3) (* p <0.05). Primary concentration 1 : 1000, secondary concentration 1 : 5000. (A) Representative blots shown.

4.2.4.5 β_2 AR SUMOylation Does Not Influence β_2 AR- β -arrestin Interaction

β -arrestins play a dual regulatory role in β_2 AR signalling. Firstly, they sterically uncouple the receptor from the $G_{\alpha s}$ subunit therefore preventing further cAMP production. Secondly, they serve as a scaffolding protein, which links the β_2 AR to further trafficking machinery such as the ubiquitin, E3 ligase MDM2 which promotes ubiquitination of the β_2 AR (Ferguson, et al., 1996), and PDE4 to attenuate cAMP signalling (Perry, et al., 2002). Additionally, they also allow G protein independent signalling (McDonald, et al., 2000).

β_2 AR interaction with β -arrestin is vital for internalisation. Stimulation with isoprenaline mediates an interaction between β_2 AR and β -arrestin following GRK phosphorylation of the receptor. Using the BRET assay, HEK293 cells were transfected with β_2 AR tagged with YFP and β -arrestin2 tagged with RLuc 6 (Lorenz, et al., 1991) (ratio 4:1), in addition to mock transfection with empty transfection reagent or transfection with the E3 ligase PIASy, which promotes SUMOylation of the β_2 AR (Figure 4.4) (described in Chapter 2 - General Materials and Methods). These cells were then stimulated with isoprenaline and subjected to the BRET assay. This assay is designed to assess the interaction between the β_2 AR and β -arrestin using the fluorescent tags YFP and RLuc 6. To assess the receptor's interaction with β -arrestin the EC_{50} was quantified from these experiments. This is the concentration of isoprenaline that was required to cause 50% of the maximal BRET response - a response that is indicative of the β_2 AR- β -arrestin interaction.

This technique revealed that there was no significant difference in EC_{50} between SUMOylated β_2 AR and control indicating SUMOylation does not influence how the β_2 AR interacts with β -arrestin (Figure 4.17) (N=3). In conclusion, SUMOylation of the β_2 AR does not influence the capability of the receptor to interact with β -arrestin. This was as expected based upon two reasons; firstly, GRK-mediated phosphorylation - the initiating step for β -arrestin translocation - does not appear to be influenced by receptor SUMOylation, and secondly, the suspected SUMOylation sites on the β_2 AR are within the third intracellular loop, not the cytoplasmic tail where the β -arrestin interaction occurs (Krasel, et al., 2005). Therefore β -arrestin agonist-dependent translocation would not be expected to change following receptor modification by SUMO.



B.

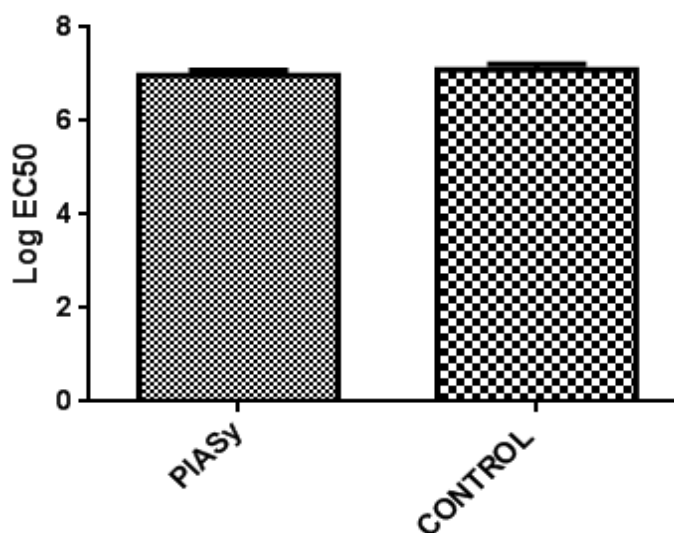


Figure 4.17 β_2 AR SUMOylation does not influence β_2 AR- β -arrestin interaction. (A&B) BRET assay was used to ascertain the relationship between β_2 AR and β -arrestin by tagging proteins with YFP and RLuc 6, respectively. In HEK293 cells these proteins were expressed either with or without PIASy to promote SUMOylation of the β_2 AR. Cells were stimulated with isoprenaline to mediate β_2 AR- β -arrestin binding and BRET was measured to quantify interaction. No significant difference existed in EC_{50} between unSUMOylated and SUMOylated β_2 AR therefore SUMOylation of the receptor does not influence the interaction between β_2 AR- β -arrestin (N=3). **(A)** Representative graph from one experiment shown.

4.2.4.6 β_2 AR SUMOylation Prolongs Cellular Response to cAMP

The β_2 AR signals via stimulatory G protein (G_s) and as mentioned previously G_s activates AC. When $G_{\alpha s}$ stimulates the catalytic domain, AC catalyses the conversion of ATP to cAMP. cAMP FRET was used to determine how long after β_2 AR isoprenaline-mediated stimulation, the cAMP levels within the cell interior remain elevated, and whether SUMOylation of the β_2 AR influences this timeframe. HEK β_2 cells were transfected with the EPAC cAMPs-1 FRET sensor, in addition to mock transfection with empty transfection reagent or transfection with the E3 ligase PIAS γ , which promotes SUMOylation of the β_2 AR (Figure 4.4) (described in Chapter 2 - General Materials and Methods). These cells were stimulated with 10 μ M isoprenaline and subjected to cAMP FRET. The representative examples demonstrate the time taken for isoprenaline to induce stimulation of cAMP and the subsequent switching off of AC / hydrolysis of cAMP by PDEs during desensitisation. The data generated by the cAMP FRET probes suggest that cAMP degradation/desensitisation is significantly different in cells overexpressing PIAS γ in comparison to mock transfected. Following stimulation with isoprenaline both cells over expressing PIAS γ and mock transfected show an increase in FRET ratio, which is indicative of a rise in cAMP. In mock transfected control cells the FRET ratio falls at approximately 12 minutes after isoprenaline stimulation indicating that less cAMP is produced due to desensitisation mechanisms. In contrast, cAMP degradation does not occur until approximately 17 minutes following isoprenaline stimulation in cells transfected with PIAS γ (Figure 4.18) (Control N=19, PIAS γ N=28) (**p<0.001). In conclusion, SUMOylation of the receptor significantly prolongs the time for which cAMP is elevated within the cytosol. This may be due to the delayed desensitisation of the receptor in the SUMO modified form, exemplified by less agonist-mediated PKA phosphorylation of the β_2 AR (Figure 4.8), and delayed receptor internalisation (Figure 4.13). In conclusion, the SUMOylated form of the β_2 AR mediates prolonged cAMP signalling due to lessened desensitisation and internalisation. However, as the probe utilised within these experiments was cytosolic, it would be important to repeat these experiments using a membrane tethered probe in the vicinity of the β_2 AR.

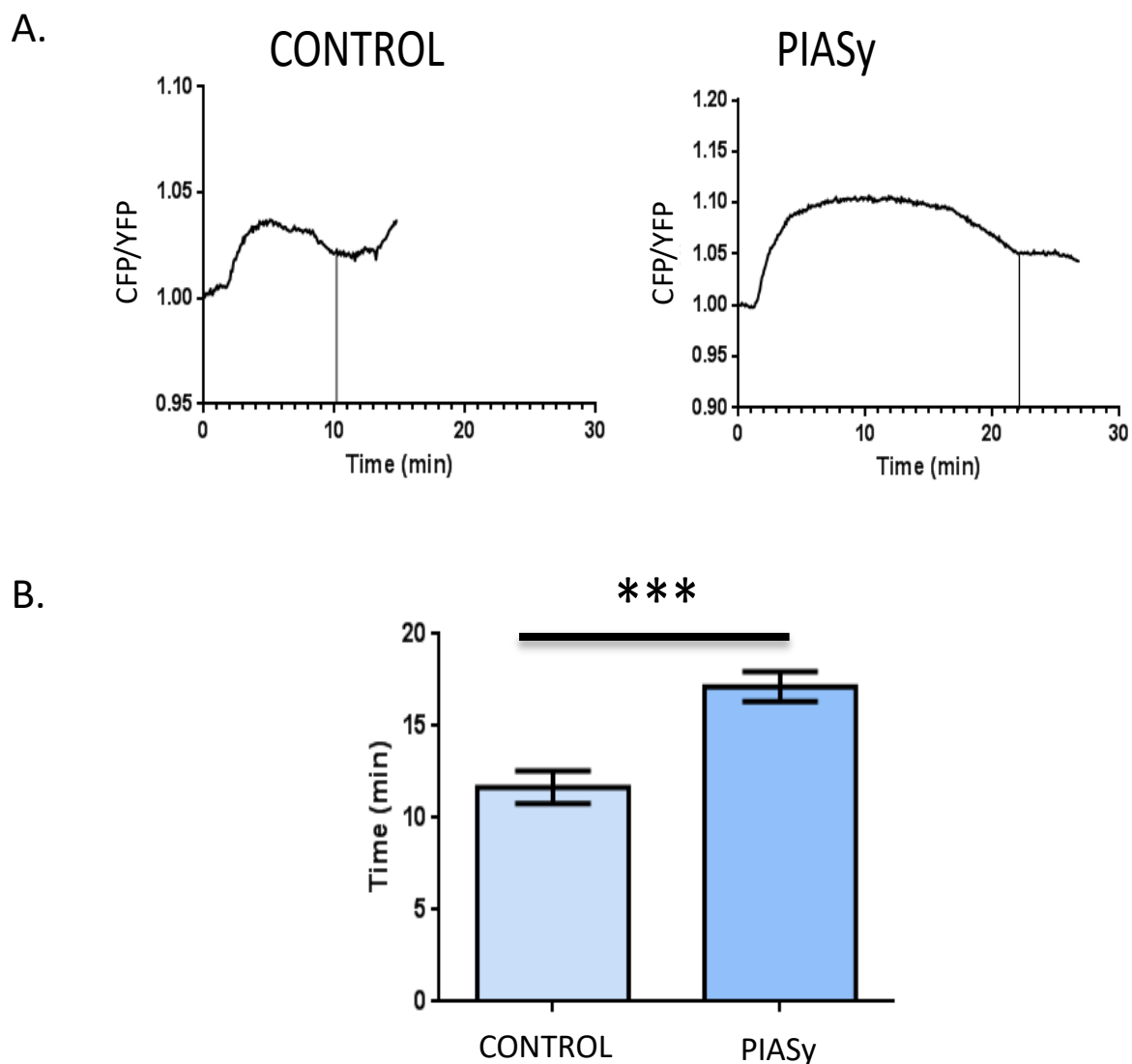


Figure 4.18 β_2 AR SUMOylation prolongs isoprenaline-mediated cellular levels of cAMP. (A&B) Isoprenaline mediates β_2 AR signalling which results in cAMP formation. HEK β_2 either mock transfected or transfected with PIASy to promote SUMOylation of the β_2 AR were stimulated with isoprenaline and subject to FRET. SUMOylation of the receptor significantly prolongs the time to cAMP degradation within the cell in response to isoprenaline (Control N=19, PIASy N=28) (** $p < 0.001$). (A) Representative traces from one experiment shown above bar graph.

4.2.4.7 β_2 AR SUMOylation Does Not Influence β_2 AR-Ligand Interaction

As the results suggest a desensitisation phenotype is induced following PIASy transfection, radioligand binding studies were used to ascertain if β_2 AR SUMOylation influences the ligand-receptor interaction. Once again, HEK β_2 cells were transfected with PIASy to promote SUMOylation of the β_2 AR (described in Chapter 2 - General Materials and Methods) or mock transfected, and membrane preparations made for radioligand binding studies. Saturation radioligand binding studies were performed to reveal how the receptor interacts with the radioligand, namely 3 H-DHA. This was assessed from two parameters; K_d and B_{max} . K_d is the dissociation constant indicative of the β_2 AR affinity for 3 H-DHA and B_{max} is the number of binding sites available for 3 H-DHA. There was no significant difference in K_d and B_{max} between SUMOylated β_2 AR and control indicating SUMOylation does not influence how the β_2 AR interacts with 3 H-DHA (Figure 4.19) (N=3). This was expected as the areas which are important for β_2 AR-ligand interaction - asparagines 113 and 293, serines 203 and 207 - are found within the transmembrane domains, distinct from the suspected SUMOylation sites in the third intracellular loop (Liggett, 2002) (Strader, et al., 1988) (Strader, et al., 1989) (Wieland, et al., 1996).

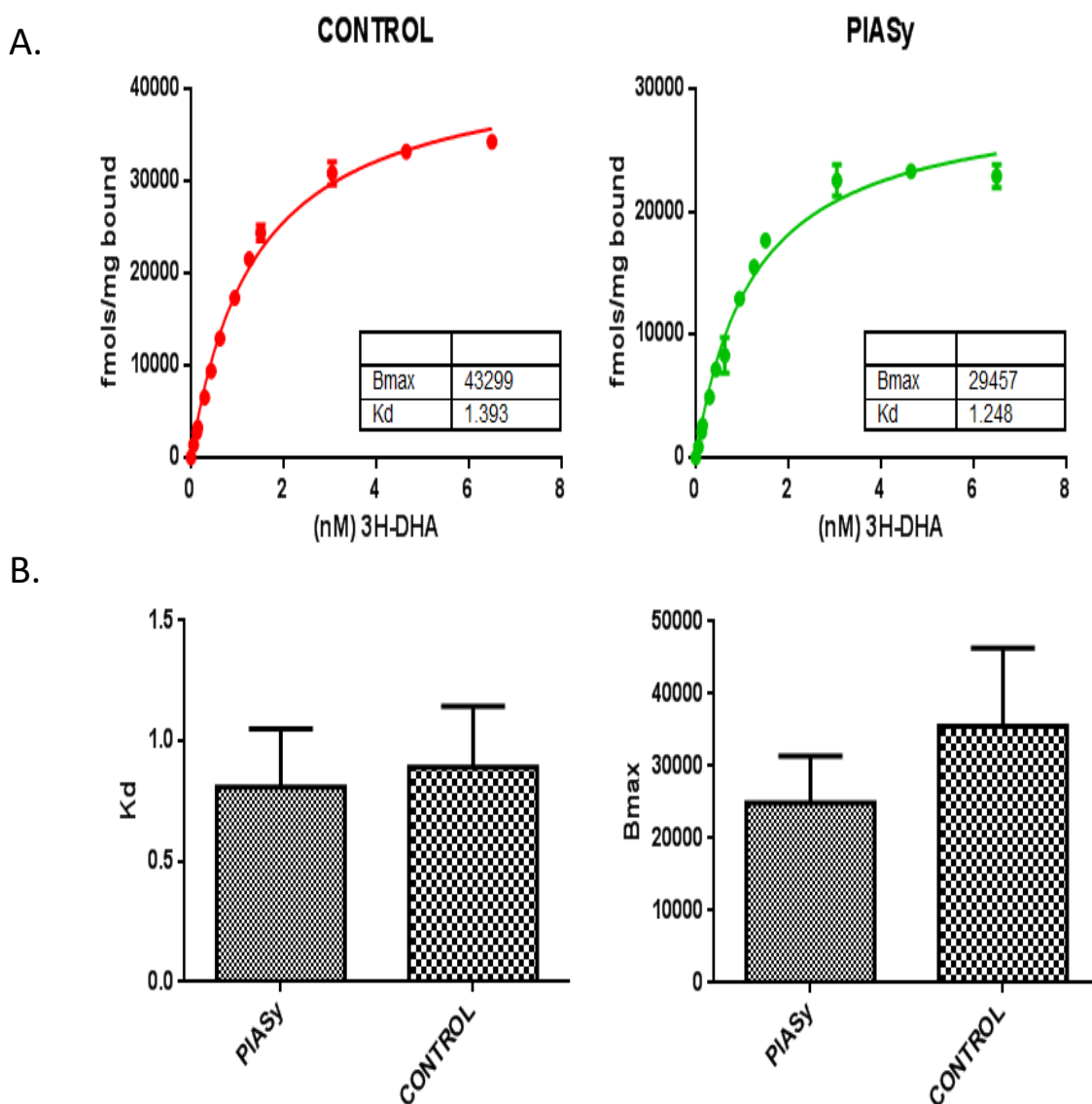


Figure 4.19 β_2 AR SUMOylation does not influence K_d or B_{max} . (A&B)HEK β_2 transfected either with PIASy to promote SUMOylation of the β_2 AR or mock transfected were used to make membrane preparations for saturation binding studies. SUMOylation of the receptor does not influence K_d or B_{max} therefore SUMOylation of the receptor does not influence how the receptor binds to radioligand (N=3). **(A)** Representative traces from one experiment shown above bar graphs.

Competition binding studies, also known as displacement studies, were used to assess if β_2 AR SUMOylation influences the isoprenaline binding pocket. Here a single concentration of radioligand ^3H -DHA was competed for by multiple concentrations of non-radioactively labelled isoprenaline. To assess the receptor's interaction with isoprenaline, the IC_{50} was quantified from these competition experiments. This is the concentration of isoprenaline that was required to cause 50% inhibition in ^3H -DHA binding. These experiments revealed that there was no significant difference in IC_{50} between SUMOylated β_2 AR and control indicating SUMOylation does not influence how the β_2 AR interacts with isoprenaline (Figure 4.20) (N=3). This was expected due to distinct locations of ligand interaction sites and SUMO susceptible lysines.

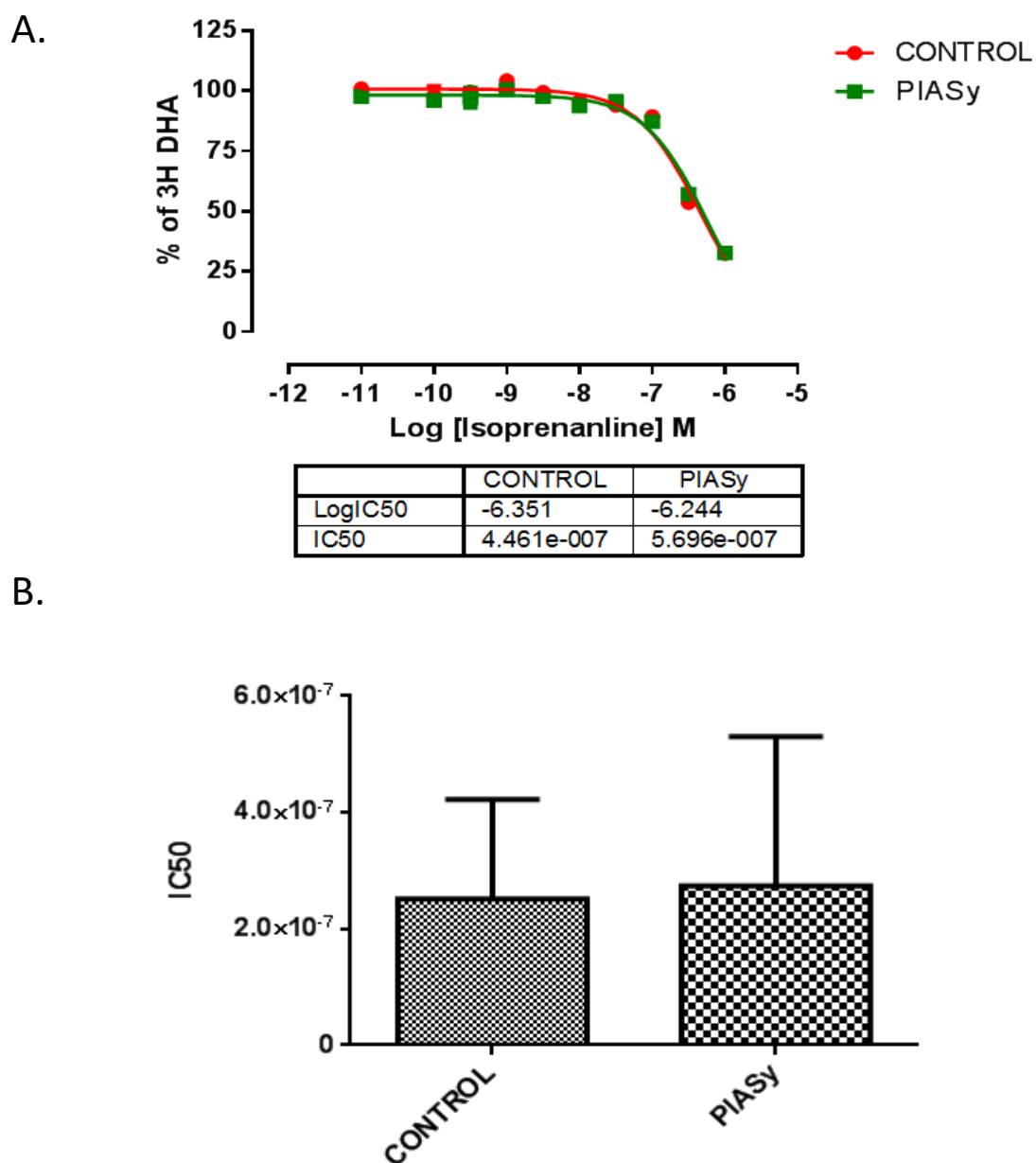


Figure 4.20 β_2 AR SUMOylation does not influence IC_{50} . (A&B) HEK β_2 transfected either with PIASy to promote SUMOylation of the β_2 AR or mock transfected were used to make membrane preparations for saturation binding studies. SUMOylation of the receptor does not influence IC_{50} therefore SUMOylation of the receptor does not influence how the receptor binds to isoprenaline (N=3). (A) Representative trace from one experiment shown above bar graph.

4.2.4.8 β_2 AR SUMOylation Does Not Influence β_2 AR-G Protein Interaction

The β_2 AR signals via stimulatory G protein (G_s), which activates AC to produce cAMP. Although this is the classical mechanism by which the β_2 AR signals, the β_2 AR can also mediate negative effects through G_i proteins (Daaka, et al., 1997). The switch between stimulatory G_s signalling and inhibitory G_i signalling occurs following direct PKA phosphorylation of the receptor (Hausdorff, et al., 1989) (Strulovici, et al., 1984). To determine if SUMOylation of the β_2 AR influences G protein interaction, SPASM sensor experiments were used. SPASM sensors are BRET sensors, which are based on a recently developed technique termed systemic protein affinity strength modulation (SPASM) and involve the fusion of a native peptide from the C-terminus of a G_α subunit to the C-terminus of the intact GPCR (Sivaramakrishnan & Spudich, 2011). Upon activation of the GPCR, the C-terminus of the G_α subunit slots itself into a cytosolic groove on the GPCR (Choe, et al., 2011) (Rasmussen, et al., 2011) (Chung, et al., 2011). Therefore, a mimic of this peptide will slot into this same area on the GPCR as the native C-terminus of the G_α subunit. Hence the β_2 AR SPASM sensors responded to stimulation with isoprenaline causing BRET to occur when the receptor is activated. SPASM sensors were designed to assess the interaction between the β_2 AR- G_s and β_2 AR- G_i .

Two types of experiment were completed with the SPASM sensors; dose response experiments and kinetics experiments. Dose response experiments examined the interaction between the β_2 AR and the G protein in response to increasing isoprenaline concentrations, whereas the kinetics experiments assessed the interaction produced from one concentration of isoprenaline over time. The SPASM sensors were stably expressed in HEK293 cells using the Flp-In T-Rex[®] system with mock transfection with empty transfection reagent or transfection with the E3 ligase PIAS γ , which promotes SUMOylation of the β_2 AR (Figure 4.4) (described in Chapter 2 - General Materials and Methods). For dose response experiments to assess the interaction between β_2 AR and the G protein the EC_{50} was quantified. This is the concentration of isoprenaline that was required to cause 50% of the maximal BRET, indicative of β_2 AR-G protein interaction. Following stimulation by isoprenaline the G protein mimic peptide interacts with the receptor initiating an increase in BRET dependent upon isoprenaline concentration. Using the dose response approach, I observed no significant difference in EC_{50} between SUMOylated β_2 AR and control indicating that

SUMOylation does not influence interaction between β_2 AR and either of the G proteins, G_i or G_s (Figure 4.21) (N=3). This was unexpected as the third intracellular loop which is known to contain the SUMO sites, is also known to be important for G protein coupling, and therefore we would expect a change to be observed (O'Dowd, et al., 1988).

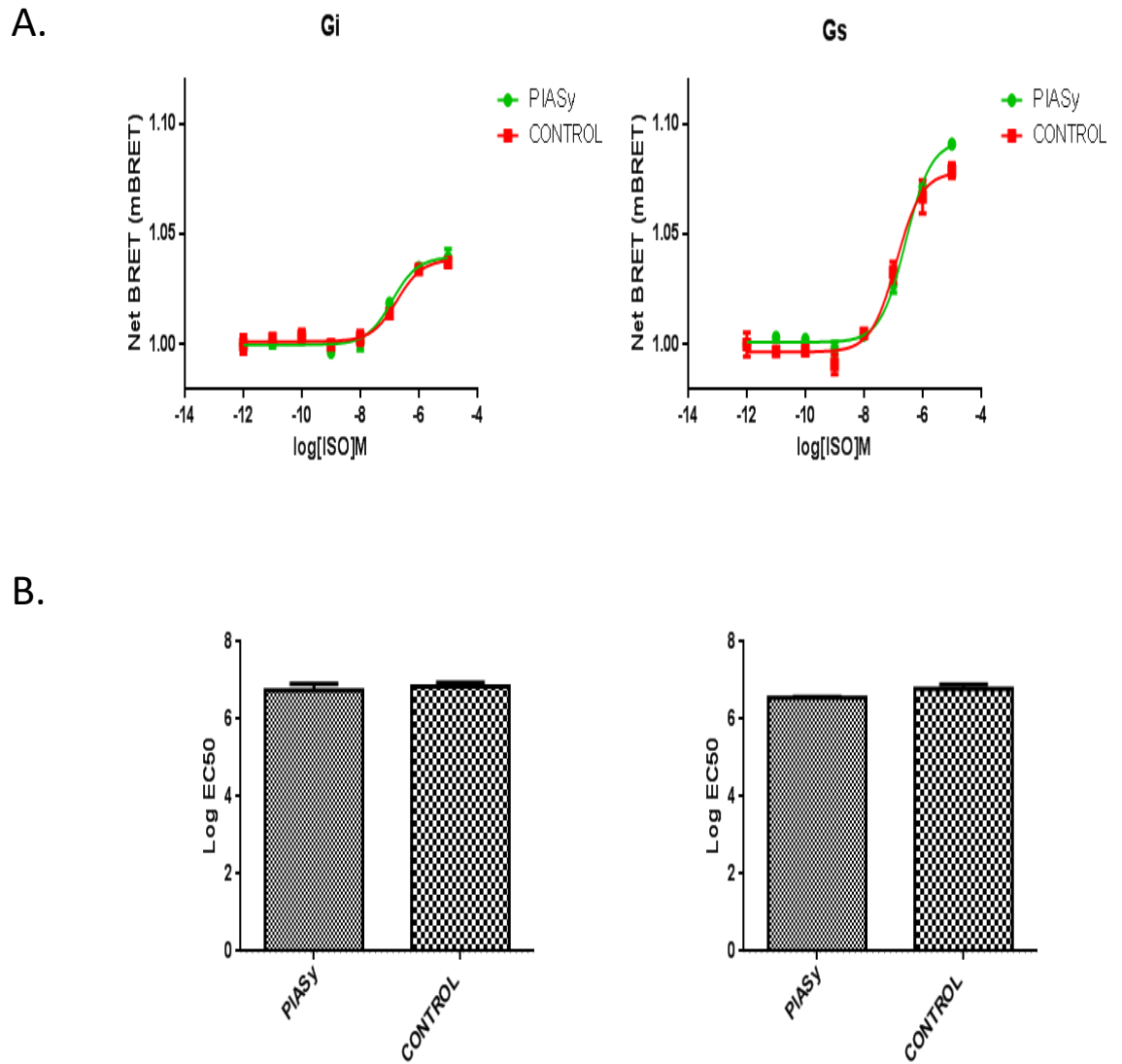


Figure 4.21 Dose response SPASM sensor experiment - β_2 AR SUMOylation does not influence β_2 AR- G_s/G_i interaction. (A&B) Flp-In T-Rex $\text{\textcircled{R}}$ HEK293 cells expressing SPASM sensors were either mock transfected or transfected with PIASy to promote SUMOylation of the β_2 AR. SUMOylation of the receptor does not influence EC_{50} therefore SUMOylation of the receptor does not influence how the receptor interacts with G proteins (N=3). **(A)** Representative traces from one experiment shown above bar graphs.

For kinetics experiments to assess the interaction between β_2 AR and the G proteins, a comparison was made at various time points following isoprenaline stimulation. Following stimulation with isoprenaline, no significant difference between transfected and mock transfected cells was observed for interactions with G_i . In fact, the interaction with G_i following isoprenaline was slight, just above the detection sensitivity of the assay. In contrast, the interaction between β_2 AR and G_s showed a marked increase but again no significant difference between cells with and without PIASy. There was no significant difference in the BRET mediated by isoprenaline at any time point for either G protein, therefore SUMOylation does not influence interaction between β_2 AR and either G protein, G_i or G_s (Figure 4.22) (N=3). As mentioned above, this was unexpected as the third intracellular loop is known to be the site for both SUMOylation and G protein coupling (O'Dowd, et al., 1988). However, these experiments are the first to use the SPASM sensor probes donated by the Milligan group of University of Glasgow, and further probe optimisation, specifically for the β_2 AR- G_i probe which lacked response in kinetics experiments, is required.

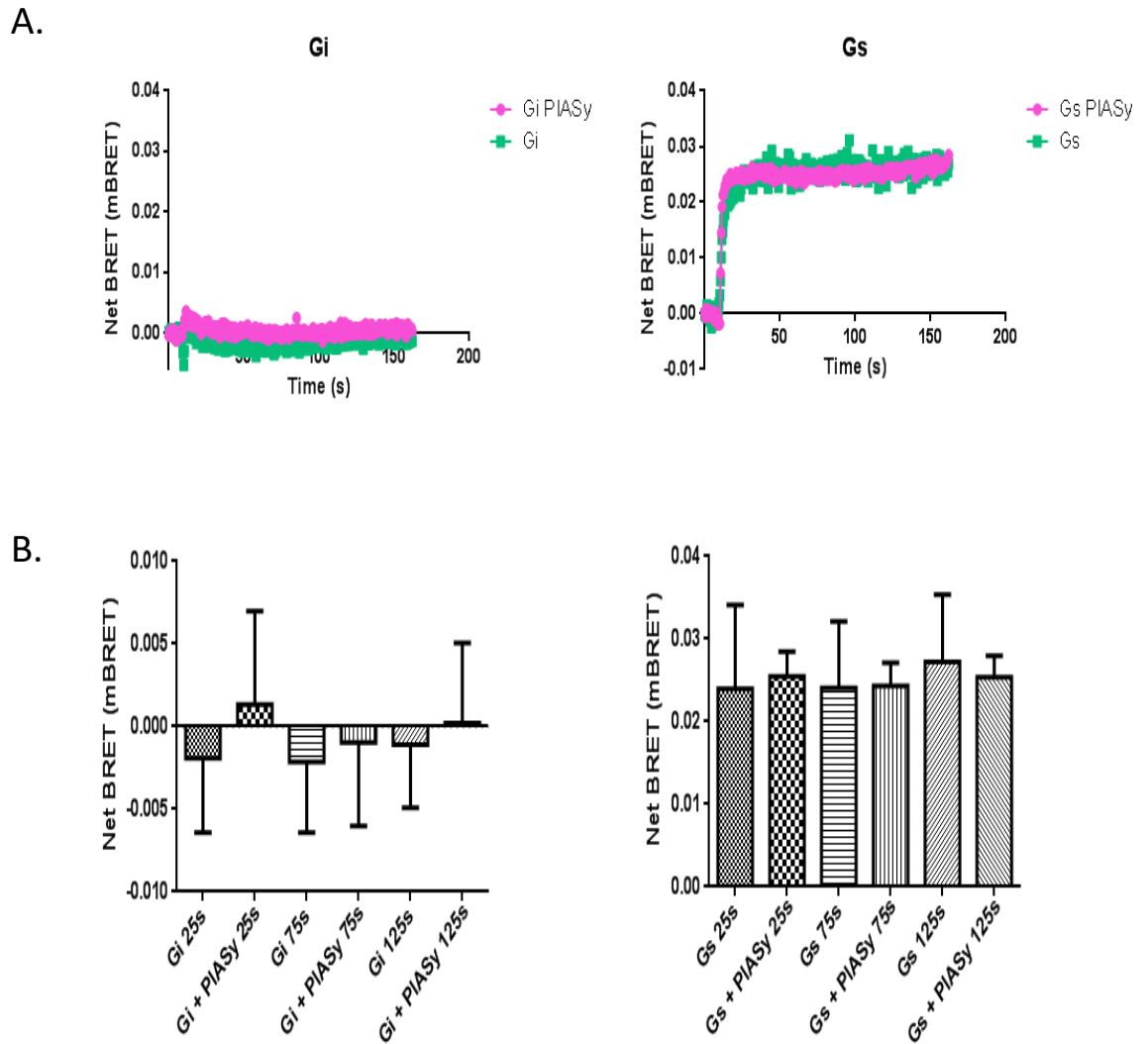


Figure 4.22 Kinetics SPASM sensor experiment - β_2 AR SUMOylation does not influence β_2 AR-G_s/G_i interaction. (A&B) Flp-In T-Rex[®] HEK293 cells expressing SPASM sensors were either mock transfected or transfected with PIASy to promote SUMOylation of the β_2 AR. SUMOylation of the receptor does not influence how the receptor interacts with G proteins at any time point following isoprenaline stimulation (N=3). **(A)** Representative traces from one experiment shown above bar graphs.

4.3 Discussion

The β_2 AR is susceptible to multiple post-translational modifications (PTMs) which are implicated in receptor signalling: phosphorylation by both PKA and GRK, which is vital in the desensitisation process (Bouvier, et al., 1989) (Vaughan, et al., 2006) (Nobles, et al., 2011); ubiquitination mediated by NEDD4, which is essential for receptor degradation (Shenoy, et al., 2008); glycosylation which has been implicated in β -arrestin recruitment, receptor internalisation, receptor dimer formation and membrane insertion, however the exact function remains unclear (Rands, et al., 1990) (Li, et al., 2017) (Mialet-Perez, et al., 2004); and palmitoylation which has been shown to influence phosphorylation of the receptor, in addition to adequate G_s coupling (Ovchinnikov, et al., 1988) (Moffett, et al., 2001) (De Lean, et al., 1980) (O'Dowd, et al., 1988). The data within this chapter describes a novel and never before reported PTM of the β_2 AR, namely SUMOylation. In a similar manner to the other PTMs, SUMOylation influences the signalling of the β_2 AR including desensitisation, internalisation and downstream signalling.

To promote β_2 AR SUMOylation in order to characterise the modification biochemically, the E3 ligase PIAS γ was overexpressed using transient liposomal transfection. A similar approach of enhancing the components of the SUMOylation cascade has been used for other proteins (Sachdev, et al., 2001) (Leight, et al., 2005) (Kho, et al., 2011). In all cases, this was shown to promote SUMOylation of the respective protein, evident by the presence of the “ghost band” at approximately 12-22kDa higher than the original protein band assessed via immunoblotting (Park-Sarge & Sarge, 2005).

The SUMOylation of SERCA2a (Kho, et al., 2011) was the basis for our hypothesis that other cardiac signalling proteins, namely the β_2 AR, could also be SUMOylated. The susceptibility of SERCA2a to SUMOylation was discovered via a proteomics screen which identified an interaction between SUMO-1 and SERCA2a. Additional evidence was provided by *in vivo* interactions discovered between SERCA2a-UBC9 and SERCA2a-SUMO-1. SUMOylated lysines within SERCA2a - K480 and K585 - were conserved between four different species. These sites are located within the ATP binding domain of SERCA2a, and therefore SUMOylation was speculated to influence the intrinsic ATPase activity of SERCA2a. Kho et al (2011) reported that

SERCA2a SUMOylation acts to increase ATPase activity of the protein, and therefore would promote Ca^{2+} uptake into the SR. SUMOylation of SERCA2a also influences the stability of the protein as the lysines susceptible to SUMOylation are also susceptible to ubiquitination. This has been observed for other proteins also. For example, I κ B α can be modified by ubiquitin and SUMO on the same lysine residue (Desterro, et al., 1998). Degradation of proteins is normally mediated by ubiquitination, which has been implicated in both proteasomal and lysosomal degradation (Naujokat & Hoffman, 2002) (Moore, et al., 1999). Therefore, SUMOylation of SERCA2a inhibits ubiquitin-mediated degradation of this important cardiac protein.

Unlike SERCA2a SUMOylation, SUMOylation of the β_2 AR was not associated with any specific SUMO isoform - paralogue 1 or 2/3. Initial peptide array data, indicative of β_2 AR SUMOylation, was generated using an ENZO *in vitro* SUMOylation kit. The paralogues within this kit are His tagged and therefore a His antibody detects all SUMO paralogues without deciphering between them. To assess paralogue specificity two methods could be used; paralogue specificity SUMOylation arrays or SUMO-specific antibody immunoprecipitation. *In vitro* SUMOylation of the β_2 AR peptide array could be mediated using individual His tagged SUMO paralogues to determine which isoform is responsible for β_2 AR SUMOylation. SUMO specific agarose beads linked to either SUMO-1 or SUMO-2/3 antibodies could be incubated with HEK β_2 lysate overexpressing PIAS γ to mediate β_2 AR SUMOylation, with subsequent probing of the immunoprecipitate for the receptor to determine if an interaction occurred between β_2 AR-SUMO-1, β_2 AR-SUMO-2/3 or both.

In a similar fashion to SERCA2a, the stability of β_2 AR was influenced by SUMOylation. Following prolonged ligand activation, the receptor is down regulated to prevent excessive agonist exposure - this was observed at 10 minutes of isoprenaline stimulation (10 μ M). However, SUMOylation of the β_2 AR, mediated by the overexpression of PIAS γ , delayed receptor down-regulation. Unlike SERCA2a SUMOylation, SUMOylation of the β_2 AR did not influence receptor half-life, however it did impact on receptor ubiquitination following isoprenaline treatment. Ubiquitination of the β_2 AR occurs within two areas; the third intracellular loop (K263 and K270) and the cytoplasmic tail (K348, K372 and K375)

(Shenoy, et al., 2008). The third intracellular loop is also the location of the confirmed SUMOylation sites K232 and K235. Although SUMOylation does not occur on the ubiquitin lysines, the presence of the bulky SUMO modification within the same intracellular loop at a 30 amino acid proximity to the ubiquitination sites could act to sterically hinder the process. For example, Syntaxin-1A (Stx1A) SUMOylation at lysines 252, 253 and 256 acts to influence interactions within the SNARE domain (amino acids 191-235) of the protein (Craig, et al., 2015). Furthermore, steric hindrance via SUMOylation has been reported before for DNA binding to both hepatoma-derived growth factor (HDGF) and Rad1 (a cell cycle checkpoint protein) (Thakar, et al., 2008) (Sarangi & Zhao, 2015). Based upon these observations it is possible to speculate that SUMO modification could sterically hinder ubiquitination by preventing the ubiquitin machinery such as NEDD4 (Shenoy, et al., 2008) from accessing the lysines within the third intracellular loop. Additionally, the ubiquitin susceptible lysines within the cytoplasmic tail may also be subject to SUMOylation. The initial identification of the SUMO sites via sequence analysis software has been reported to miss certain SUMO specific sites. This was the case for caveolin-3 SUMOylation. The preferential solo SUMO site identified via sequence software analysis was K38, however if K38 was mutated then SUMOylation was possible at sites 15, 20, 30, 69, 108 and 144 (Fuhs & Insel, 2011). Furthermore, the initial identification of the β_2 AR sites by software sequence analysis and subsequent peptide array was completed in the Baillie group in 2010. Since then, advancement in the SUMOylation consensus motifs to reveal both HCSMs and inverted motifs (Matic, et al., 2010) (Impens, et al., 2014) means that SUMO susceptible lysines could have remained unidentified in these screens.

SUMOylation of the β_2 AR also influences trafficking of the receptor. SUMOylation has been reported in the trafficking of other proteins: DISC1 SUMOylation promotes nuclear translocation (Tankou, et al., 2016); LEF-1 SUMOylation targets the protein to nuclear bodies (Sachdev, et al., 2001); SUMOylation of the GluK2 subunit at K886 promotes internalisation dependent upon PKC phosphorylation at site 868 (Chamberlain, et al., 2012). The β_2 AR is internalised in response to isoprenaline stimulation and data presented within this chapter demonstrates that SUMOylation of the β_2 AR causes a reduction in receptor internalisation in response to isoprenaline stimulation. Therefore, in line with the novel concept of β_2 AR

endosomal signalling (Irannejad, et al., 2013) (Irannejad & Von Zastrow, 2014), we would expect SUMOylation of the receptor to inhibit β_2 AR- G_s mediated cAMP production within the endosome. This hypothesis could be assessed by utilising FRET probes which detect endosomal cAMP levels. To internalise the β_2 AR there are various steps which are essential: GRK phosphorylation at sites 355/356 in the cytoplasmic tail (Vaughan, et al., 2006); β_2 AR- β -arrestin2 interaction (Krasel, et al., 2005); β_2 AR- β -arrestin2 complex interaction with AP-2 of clathrin to initiate the formation of the endosome (Laporte, et al., 2000); β -arrestin2 ubiquitination (Shenoy, et al., 2001). The data presented within this chapter suggests that receptor SUMOylation mediates no significant change to isoprenaline-dependent GRK phosphorylation of the receptor. However the detection of total β_2 AR via the GFP-tag antibody is not as clear as prior western blots, and therefore to confirm the influence of receptor SUMOylation on β_2 AR phosphorylation by GRK, this western blot would need to be repeated. SUMOylation has previously been shown to alter the outcome of phosphorylation, not phosphorylation susceptibility. In this case PDE4D5 - an enzyme which degrades cAMP - is susceptible to SUMOylation and phosphorylation. Although SUMOylation does not prevent the enzyme from becoming phosphorylated, it does change the conformation of PDE4D5 therefore changing the output of phosphorylation (Li, et al., 2010). However, the outcome of GRK-mediated phosphorylation of the receptor is promoting the interaction between β_2 AR- β -arrestin and the data within this chapter utilising the BRET technique implies there is no significant change in this interaction following receptor SUMOylation.

β -arrestin is one of many proteins that has been reported to be a SUMO substrate following overexpression of SUMO-1 (Xiao, et al., 2015). SUMOylation prevents β -arrestin from binding to TRAF6 gene, a gene which encodes for the TNF receptor associated family. This leads to TRAF6 oligomerisation and auto ubiquitination, and consequently leads to TRAF6-mediated activation of NF- κ B/AP-1. It is unknown if β -arrestin SUMOylation can also be mediated by PIASy and therefore this could be a contributing factor in β_2 AR internalisation. If the SUMOylation and ubiquitination compete for lysines within the same area of β -arrestin as has been reported for other proteins including SERCA2a (Kho, et al., 2011), I κ B α (Desterro, et al., 1998) MDM2, (Meek & Knippschild, 2003) NEMO (Huang, et al., 2003), axin (Kim, et al., 2008), and RNA helicases p68 and p72 (Mooney, et al., 2010), then

SUMOylation of β -arrestin may alter the stoichiometry of the scaffold. Additionally if the arrestin were SUMOylated it would raise questions in the following areas; firstly would the SUMOylated arrestin sterically hinder internalisation as has been seen for other proteins (Thakar, et al., 2008) (Sarangi & Zhao, 2015), or secondly, could SUMOylation of the arrestin mediate a conformational change of the protein causing a change in arrestin function, similar to PDE4D5 (Li, et al., 2010).

The β_2 AR traditionally signals via the G_s protein mediating PKA activation with the kinase capable of phosphorylating multiple substrates, one of which is the receptor itself (Daaka, et al., 1997). The consensus sequences for PKA-mediated phosphorylation are within the C-terminus of intracellular loop 3 (serines 261 and 262) and in proximal cytoplasmic tail (serines 345 and 346) (Bouvier, et al., 1989). Phosphorylation results in reduced coupling between the β_2 AR and G_s , switching it to G_i , with a mutant β_2 AR lacking these phospho-sites incapable of signalling via G_i (Hausdorff, et al., 1989) (Strulovici, et al., 1984) (Daaka, et al., 1997). SUMOylation of the β_2 AR mediates a reduction in isoprenaline-dependent PKA-mediated phosphorylation of the β_2 AR at serines 345/346. As mentioned above it is possible that all SUMOylation sites on the β_2 AR have not been identified and therefore sites within the cytoplasmic tail could be SUMOylated. An interaction between the PTMs phosphorylation and SUMOylation has been reported before. This was first identified in heat shock factors, in which stress-induced phosphorylation, resulted in increased levels of SUMO modification (Hietakangas, et al., 2003). By contrast, phosphorylation can also negatively regulate SUMO modification. For example, phosphorylation of ELK1 (transcription factor which regulates early gene expression) results in a reduction in ELK1 SUMO modification (Yang, et al., 2003). Additionally, if additional SUMOylation sites were to exist in the cytoplasmic tail, this could act to sterically hinder phosphorylation.

The SUMO susceptible lysines 232 and 235 could influence the dynamics of the third intracellular loop. The traditional signalling pathway via G_s begins with receptor agonist binding initiating PKA activation via production of cAMP. The receptor undergoes a conformational change to allow activation of the signal transduction pathway. Glutamine 268 within the intracellular loop interacts with arginine 131 from the third transmembrane helix to constitute an ionic lock in the

resting β_2 AR - which must be disrupted upon receptor activation (Ballesteros, et al., 2001) (Yao, et al., 2006). It is possible the bulky SUMO modification within this region could hinder lock disruption resulting in dampened, downstream signalling. The data within this chapter suggests that the SUMOylated receptor mediates no change in β_2 AR-G protein interaction and no change in β_2 AR-ligand interaction therefore it is probable that SUMO modification may interfere with the helical movements of the receptor. However, the experiments assessing the β_2 AR-G protein interaction are the first to use the SPASM sensor probes and further probe optimisation, specifically for the β_2 AR-G_i probe which lacked response in kinetics experiments, is required.

The final aspect of β_2 AR signalling that SUMOylation was shown to influence was cAMP dynamics. SUMOylation of the receptor causes an increase in the time taken for cytosolic cAMP levels to fall following receptor activation. Traditionally, PDE4D5 is recruited to the receptor following activation via its interaction with β -arrestin (Perry, et al., 2002) This enzyme mediates downregulation of cAMP and therefore a reduction in PKA activity, which leads to less phosphorylation of the β_2 AR. It has been shown that PDE4D5 is susceptible to SUMOylation via PIAS γ at lysine 232. Normally PDE4D5 activity would be enhanced by PKA phosphorylation and reduced by ERK phosphorylation, however when the PDE is SUMOylated it becomes more susceptible to PKA activation and less susceptible to ERK inhibition - leading to a more active PDE4D5. In our set up, it is probable that overexpression of PIAS γ in addition to SUMOylating the receptor would also be promoting SUMOylation of the PDE (Li, et al., 2010). With cAMP levels being maintained at a low level by the enhanced activity of PDE4D5, there will be less activation of PKA, and therefore less PKA phosphorylation of the receptor and other substrates. Therefore, it is possible that PIAS γ overexpression has both promoted SUMOylation of the β_2 AR and PDE4D5. Further experiments will need to be conducted to determine the functional outcomes of each individual SUMOylation event. In contrast to what is observed with reduced PKA activity, cAMP levels are elevated following SUMOylation of the β_2 AR. Further cAMP assays will need to be completed to determine the outcome of cAMP dynamics mediated by receptor SUMOylation. Indeed, the answer to this contradiction may lie in the compartmentalisation of signalling components. As the cAMP reporter constructs are cytosolic they only pick up "global" bulk changes in the cyclic-nucleotide. Spatially targeted cAMP probes

that locate to the plasma membrane are more likely to report on cAMP changes in the vicinity of the β_2 AR.

For future work, the SUMOylation of the β_2 AR should be assessed in a physiologically relevant model. A more appropriate cell type would be the cardiomyocyte which expresses both β_1 AR and β_2 AR, at 75-80% and 20-25% respectively (Madamanchi, 2007). Liposomal transfection utilised in this chapter to promote β_2 AR SUMOylation is not the optimum method to enhance PIASy in cardiomyocyte. Neonatal cardiomyocytes transfection rates of only up to 15% are reported, with adult cardiomyocytes proving even more difficult to transfect than neonatal cardiomyocytes (Djurovic, et al., 2004). In comparison with transfection, viral based techniques enable much more efficient and stable gene transfer for cardiac cells (Louch, et al., 2011). Therefore, future experiments will utilize a PIASy adenovirus.

In conclusion, I have validated the SUMOylation sites 232 and 235 on the β_2 AR and successfully promoted SUMOylation of the β_2 AR *in vitro* via the use of the E3 ligase PIASy. SUMOylation of the β_2 AR has been shown to influence downstream signalling, internalisation and down-regulation of the receptor. These changes could be associated to steric hindrance of the bulky SUMO modification, speculative unidentified SUMOylation sites, and ubiquitin-SUMOylation competitions.

Chapter 5 Analysis of β_2 AR SUMOylation in Animal Models of Heart Failure (HF)

5.1 Introduction

5.1.1 The Need for Animal Models of HF

Heart failure (HF) is often regarded as the inadequacy of cardiac output resulting in the metabolic needs of organs and tissues being unmet. The primary symptoms, which present clinically, include dyspnea, fatigue, exercise intolerance, and retention of fluid in the lungs and peripheral tissues (Houser, et al., 2012). HF can be managed by multiple approaches ranging from lifestyle changes and pharmacological therapies, to more extreme approaches, such as implantable devices and cardiac surgery. However, the prognosis is poor with average life expectancy around three years post diagnosis (Dickstein, et al., 2008). Although the current standard of care improves outcomes, the syndrome continues to progress and there is a need for novel therapies that can prevent, inhibit progression, and/or reverse the structural and functional defects of the failing heart. Research to identify novel targets for HF therapy usually requires preclinical testing in appropriate animal models. The two models presented in this thesis are the transverse aortic constriction (TAC) pressure overload HF model in mice and the left anterior descending (LAD) artery balloon occlusion ischemic HF model in pigs.

5.1.2 Minimally Invasive TAC Pressure Overload HF Model in Mice

The TAC model is based on HF mediated by aortic stenosis (AS). Common causes of AS include atherosclerotic disease, calcification and aortic valve malformations. All of these result in a stiffness of the aortic valve and reduce the orifice area. The increased resistance to LV (left ventricular) ejection results in an increased LV afterload, which is the pressure which the LV must develop to propel blood across the reduced aortic orifice (Houser, et al., 2012). The TAC model mimics LV pressure overload, which allows the study of compensated hypertrophy of the heart with progression to HF (Lompre, et al., 1979) (Mercadier, et al., 1981) (Izumo, et al., 1987). A silk suture around the aortic arch acts to create a greater LV afterload (Figure 5.1). Mice undergoing SHAM surgery are treated in the exact same surgical manner - only no suture is used to tie off the aorta.

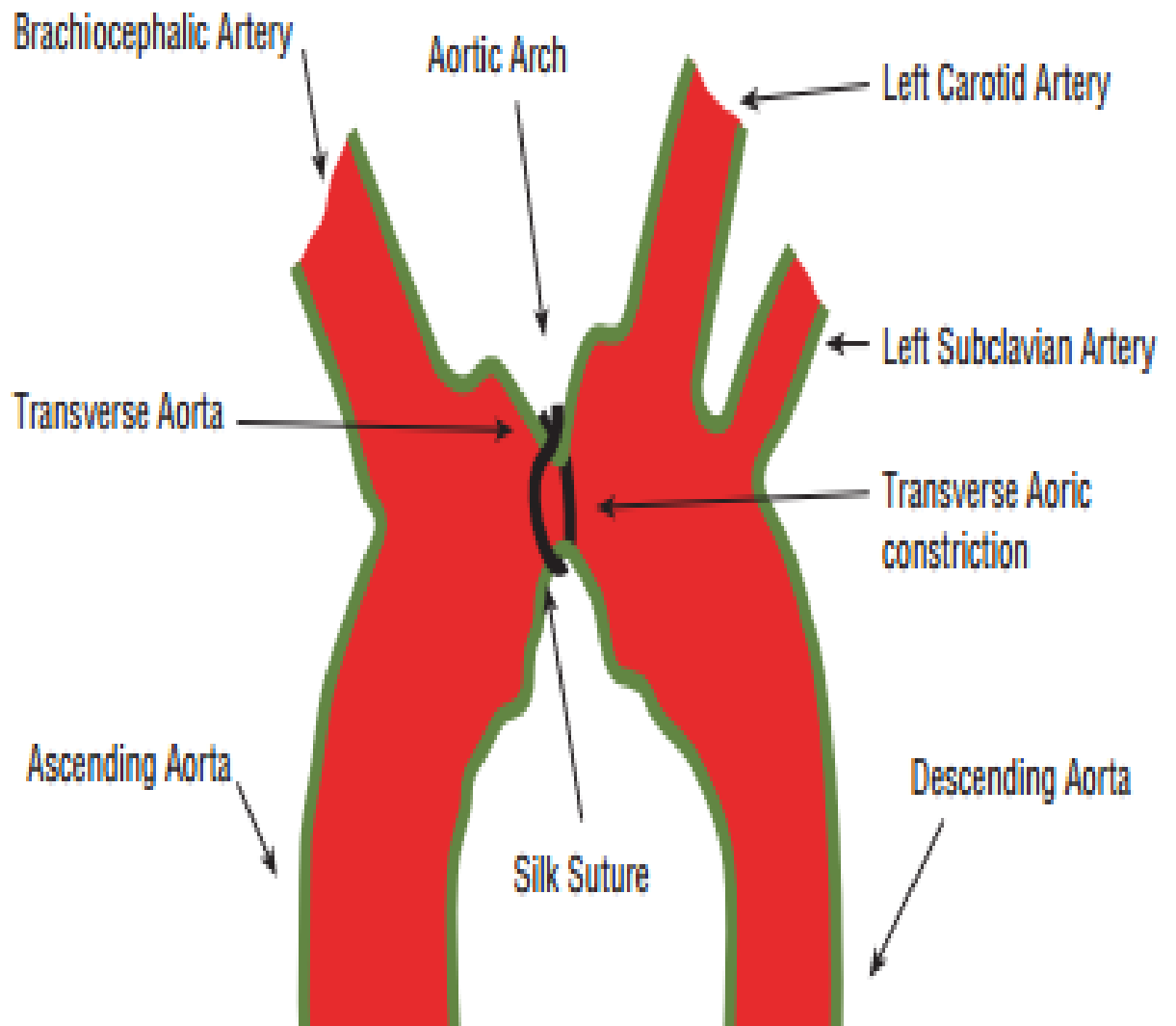


Figure 5.1 Location of aortic ligation during TAC surgery. The constriction is made at the aortic arch with 5-0 silk suture under the guidance of a 27G needle to provide a 0.4mm diameter passage (Ardehali, et al., 2013).

In the model, there is an initial compensatory phase, in which the elevated wall stress mediates myocardial growth creating a thicker and “stronger” LV that is capable of maintaining ejection fraction into the aorta. However, this phase becomes maladaptive with increased fibrosis occurring due to elevated cardiac fibroblast proliferation and collagen synthesis in response to the growing myocardium (Diez, et al., 2007). The stiffening of the LV leads to diastolic dysfunction - a structural milestone in the transition from the compensated state to HF (Krayenbuehl, et al., 1989) (Heyman, et al., 2005) (Monrad, et al., 1988). This leads to the manifestation of HF symptoms, where the heart is in a state of both LV systolic and diastolic dysfunction (Houser, et al., 2012) (Peske, 2004).

Kho et al (2011) used the TAC model in mice to study the influence of SERCA2a SUMOylation on HF and reported that around 2 months post TAC surgery mice were in a state of HF. These mice had a fractional shortening of below 50%, in which fractional shortening is a reduction in the diastolic dimensions of the heart that occurs by the end of systole. For example, when the healthy heart contracts to a state of systole, the diastolic dimensions should become smaller therefore forcing blood out, but in a stiffened state the heart will be limited in its contractility and the diastolic dimensions will remain constant leading to a lower fractional shortening percentage. This means less blood will be expelled with each beat. In addition to changes in fractional shortening these mice had a reduced LV ejection fraction, elevated LV pressure and an increased LV end diastolic diameter, indicative of LV dilation. This provides further evidence these mice are in HF, as both LV end systolic and diastolic diameter become increased in this condition (Peske, 2004). Further evidence of cardiac remodelling came from an increase in heart-to-body weight ratio in comparison to the appropriate SHAM control. The HF mice displayed reduced SUMOylated SERCA2a levels, but restoration of SUMOylated SERCA2a by SUMO-1 gene transfer led to improved LV function, as well as stabilising the heart-to-body weight ratios (Kho, et al., 2011).

The traditional TAC model requires thoracotomy to gain access to the aortic arch along with mechanical ventilation, but this can be time consuming and technically complex. Mechanical ventilation is essential due to the partial thoracotomy and sternum retraction required for the surgery. This process increases the time the animal is under anaesthesia, as intubation is required both prior to and following

surgery, but only when the animal begins to breathe spontaneously during recovery (deAlmeida, et al., 2010). Martin et al (2012) reported findings on a minimally invasive model of the TAC procedure, which circumvents these requirements, making the surgery both quicker and easier. In the minimally invasive procedure a small horizontal skin incision of about 1cm at the level of the suprasternal notch allows trachea location, and using the trachea for anatomical placement the aortic arch is located. Access to the arch is then optimised using a 5mm cut in the sternum. As the thoracotomy is no longer required, the animal can breathe without support of mechanical ventilation throughout the entire procedure. This procedure is therefore less invasive than traditional TAC surgery, making both pre-surgical preparation and recovery quicker. The minimally invasive TAC model displayed similar results to traditional TAC surgery, with cardiac hypertrophy being indicated by increased LV wall thickness, elevated systolic pressure, increased individual cardiomyocyte size and increased heart-to-body weight ratio, in comparison to SHAM control. In addition, sacrifice data identified that TAC animals had elevated cardiac fibroblast proliferation and collagen production, as well as elevated activity in inflammatory signalling pathways in comparison to SHAM animals.

5.1.3 LAD Artery Balloon Occlusion Ischemic HF Model in Pigs

The LAD artery balloon occlusion model is an ischemia/reperfusion model that acts to mimic an acute myocardial infarction (MI) (Koudstaal, et al., 2014). The LAD artery provides the blood supply for over half the myocardium, and is often the largest coronary artery, therefore a major blockage in this artery can be detrimental to the heart (Ahmed, 2015) (Figure 5.2). This model is based on occluding the LAD for ninety minutes to initiate a period of myocardial ischaemia. During this period, an “ischemic cascade” is triggered, in which the heart cells which are supplied by the LAD become necrotic and die with a collagen scar forming in their place. After ninety minutes, the myocardium is re-perfused by removing the blockage in the LAD artery, but this in itself can promote problems as although re-perfusion saves viable myocytes, it also accelerates the degradation of injured myocytes and permits infarct scar growth. After an MI, the scar tissue deleteriously affects the function of the heart by making it stiffer and disrupting communication between cardiomyocytes (Simonis, et al., 2012). The

LAD artery balloon occlusion model promotes an infarct size of approximately 10-15% of the LV, increases LV end diastolic diameter and reduces LV ejection fraction by approximately 35-45% 4 weeks post-surgery (Koudstaal, et al., 2014).

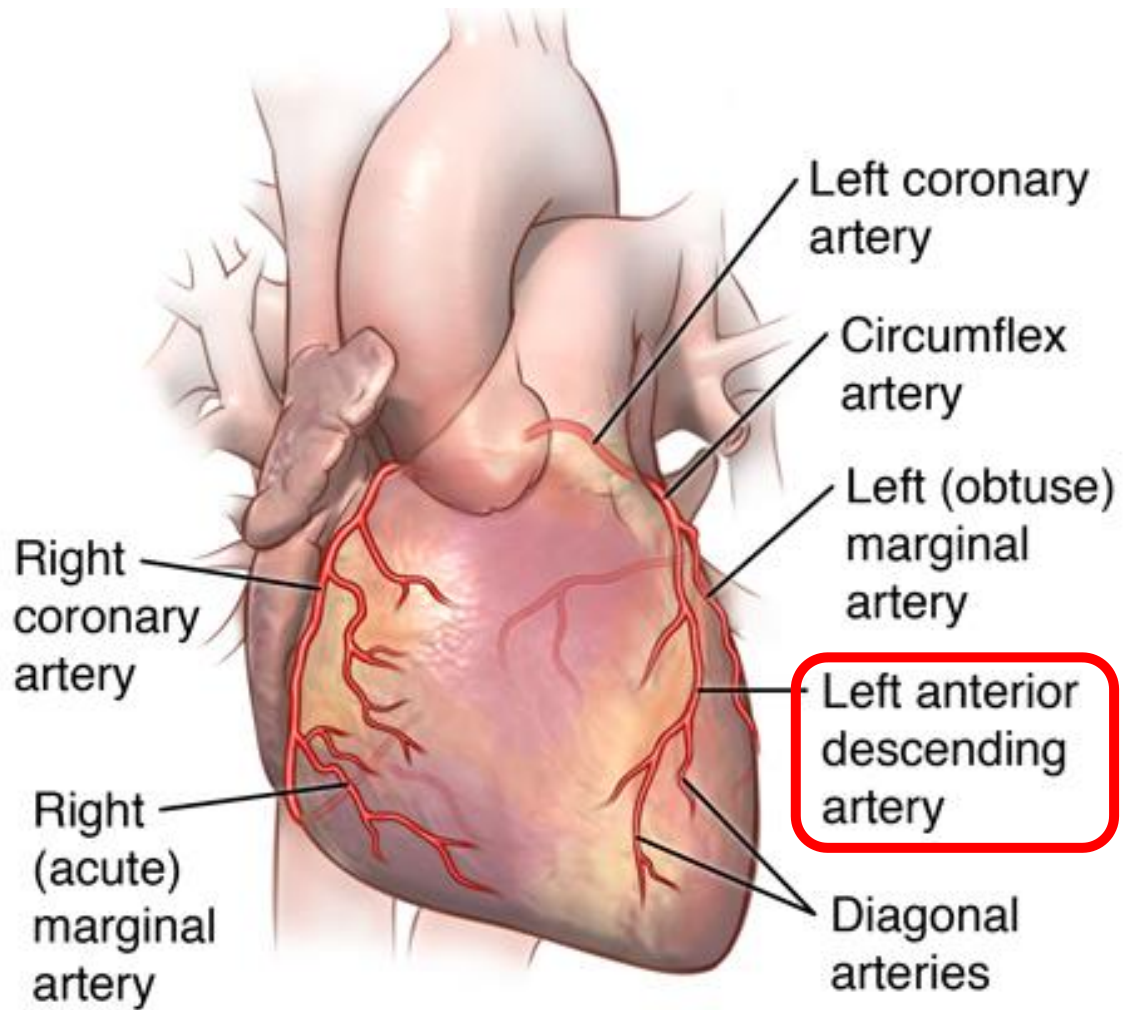


Figure 5.2 Location of the LAD artery for balloon occlusion. This model is based on occluding the LAD for 90 minutes to initiate a period of myocardial ischaemia (www.hopkinsmedicine.org, 2017). LAD (left anterior descending).

The Hajjar group also examined the SUMOylation of SERCA2a in the LAD artery balloon occlusion ischemic HF model in pigs (Tilemann, et al., 2013). This was the next step following their study in rodents (Kho, et al., 2011), as pigs are increasingly being used in cardiovascular research due to their similarity in cardiac function and anatomy with the human heart (Crick, et al., 1998) (Stubhan, et al., 2008). For instance, pig heart-to-body weight ratio, cardiac size and coronary artery anatomy distribution have all shown to have a high degree of similarity to man (Crick, et al., 1998). Moreover, cardiomyocyte metabolism, electrophysiological properties and response to an ischemic insult, such as MI, have been reported to match the human situation (Heusch, et al., 2011) (Skychally, et al., 2009). In the pig LAD artery balloon occlusion ischemic HF model, the Hajjar group found that HF mediates a reduction in SUMOylated SERCA2a, but when this modified protein was restored via SUMO-1 gene transfer there was an increase in cardiac contractility, improved LV ejection fraction and an alleviation of deteriorating LV volumes (Tilemann, et al., 2013). With regards to the HF phenotype Tilemann et al (2013) reported similar findings to Koudstaal et al (2014), with a reduction in LV ejection fraction and cardiac output, in conjunction with LV end systolic and diastolic diameter becoming increased, all indicative of the animal being in a state of HF.

5.2 Aims

As HF has been shown to result in a decreased expression of SUMO protein, I hypothesise that SUMOylation of the β_2 AR is reduced in HF in a similar fashion to SERCA2a.

The aims of this chapter are to: -

1. Establish and characterise the minimally invasive TAC pressure overload model of HF in mice
2. Evaluate SUMOylation of the β_2 AR in the minimally invasive TAC pressure overload model of HF in mice and the LAD artery balloon occlusion ischemic HF model in pigs

5.3 Results

5.3.1 Minimally Invasive TAC Pressure Overload Model in Mice

I aimed to establish a minimally invasive TAC model of HF in C57BL/6 mice with the intention of creating a model in which we could investigate the role of β_2 AR SUMOylation in the HF phenotype. The following results relate to this model.

5.3.1.1 The Influence of TAC Surgery on Echocardiographic Parameters

Echocardiographic assessment of left ventricular (LV) function was performed before and after TAC surgery (Figure 2.7). Through this method we were able to determine the following parameters; cardiac output, stroke volume, fractional shortening, ejection fraction and relative wall thickness by assessing the echocardiographic parameters discussed in section 2.15.4 - Transthoracic Echocardiography (Figure 2.8 & 5.3A). These parameters were assessed in relation to body weight and tibia length over the 8-week time period. Both tibia length and body weight were assessed throughout the study as at the beginning of the study it was not known if TAC surgical intervention would influence the body weight of the animal, and therefore taking both measurements was appropriate to ensure reliable comparisons between groups.

Throughout the study there was no significant difference observed in body weight and tibia length between TAC and SHAM groups (Figure 5.3B) (TAC N=17, SHAM N=9). At both 3 and 8 weeks post TAC, there was an approximate 40-50% reduction in cardiac output and an approximate 35-40% reduction in stroke volume in TAC mice in comparison to SHAM mice, but a significant increase in relative wall thickness by approximately 60% in TAC mice in comparison to SHAM mice (Figure 5.4) (TAC N=17, SHAM N=9) (** $p < 0.01$) (** $p < 0.001$) (**** $p < 0.0001$). There was no significant difference observed in fractional shortening or ejection fraction in TAC mice in comparison to SHAM mice (Figure 5.4) (TAC N=17, SHAM N=9).

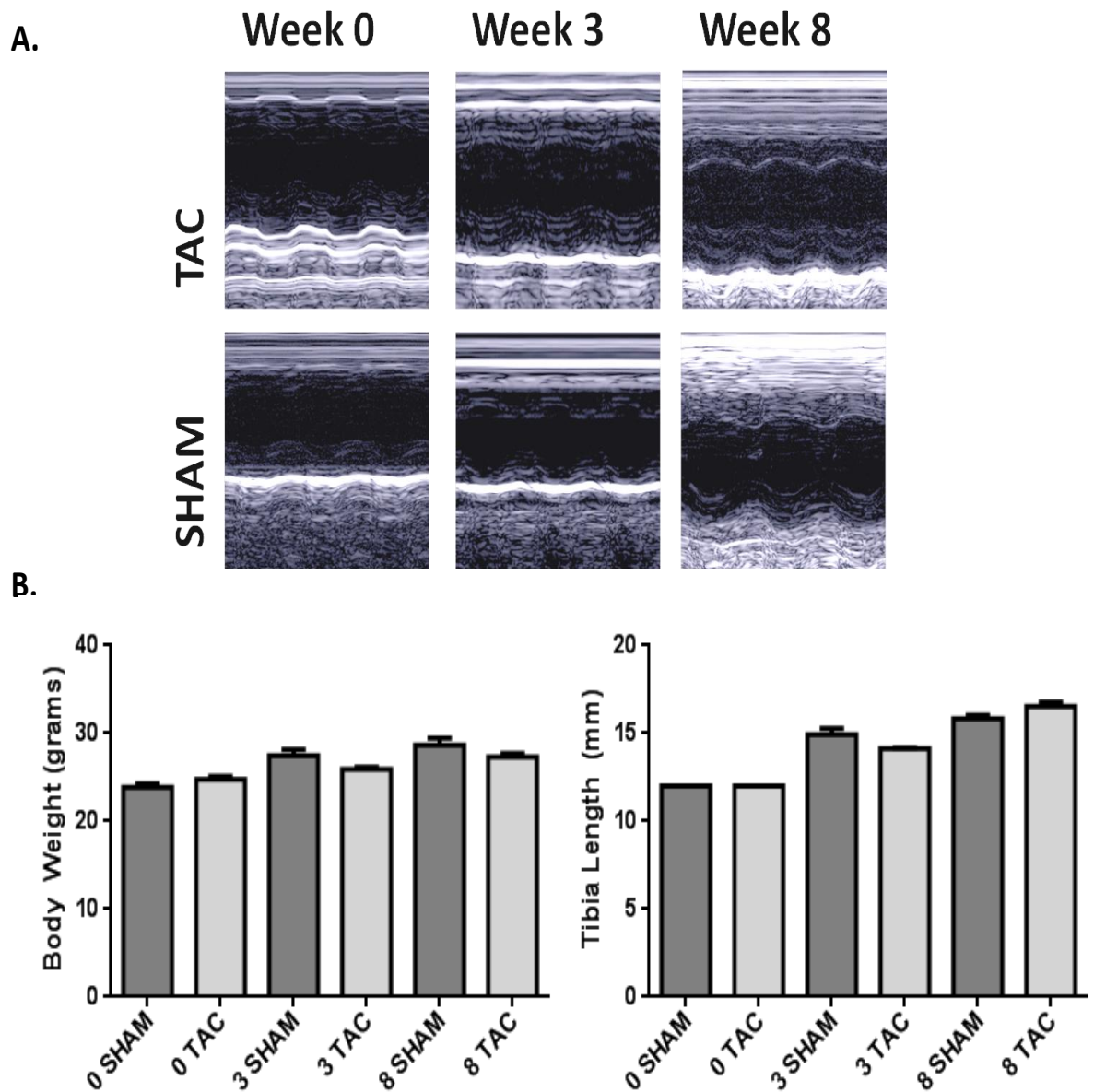


Figure 5.3 Echocardiographic representative images and physical body measurements used to determine cardiac remodelling and function. (A) Echocardiographic assessment of left ventricular (LV) function was performed both 3 and 8 weeks after surgery, as well as before surgery. The measurements taken include LVEDD, LVEDD, PWTs, PWTd, AWTs, AWTd. Representative traces from one echocardiogram shown above bar graphs. **(A&B)** Cardiac parameters were assessed in relation to BW and TL. Throughout the study no significant difference in BW or TL was observed between the TAC and SHAM groups. (TAC N=17, SHAM N=9). LVEDD (LV end diastolic diameter), LVEDS (LV end systolic diameter), PWTs (posterior wall thickness during systole), PWTd (posterior wall thickness during diastole), AWTs (anterior wall thickness during systole), AWTd (anterior wall thickness during diastole), BW (body weight), TL (tibia length), TAC (transverse aortic constriction).

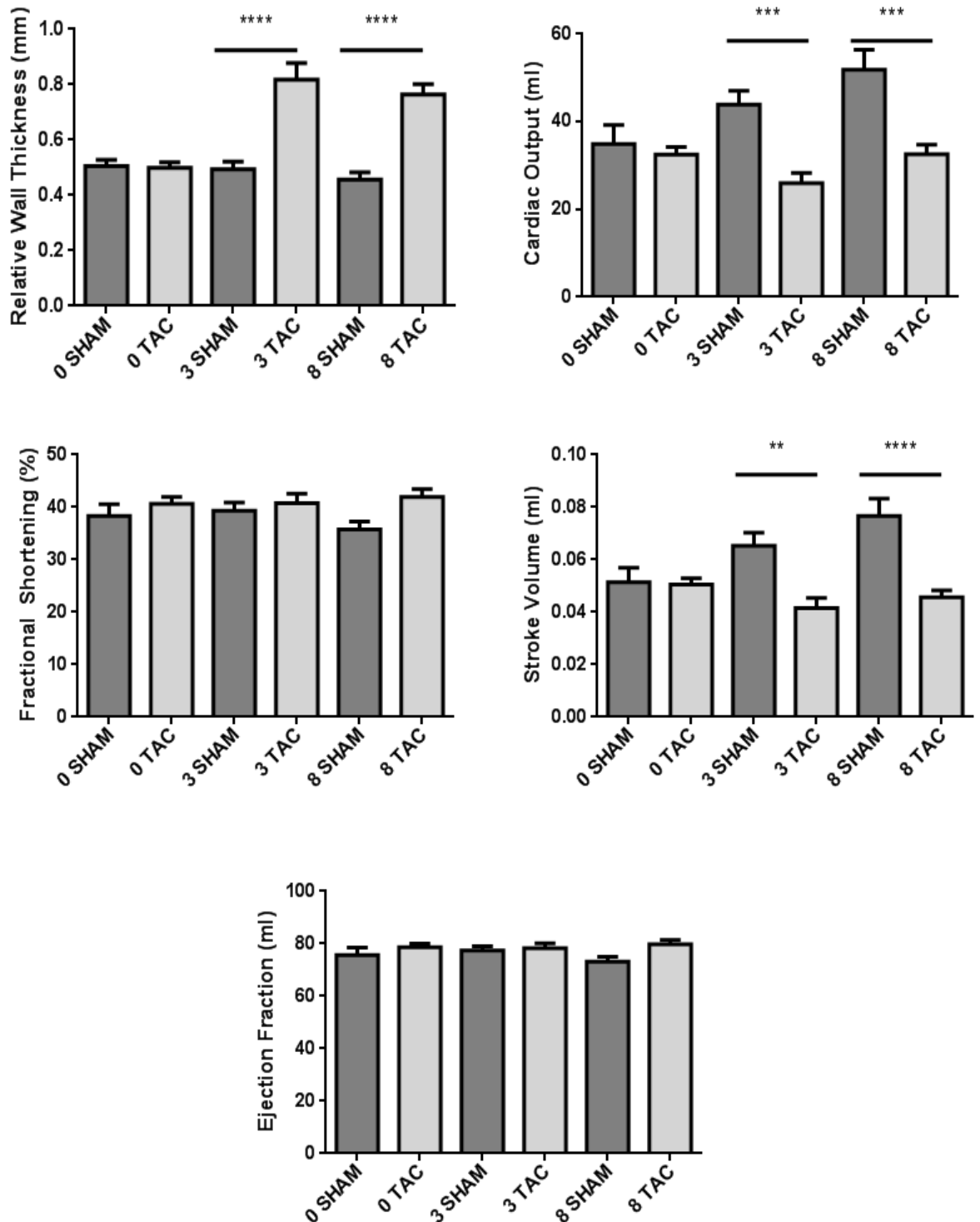


Figure 5.4 Cardiac function and remodelling assessed following TAC surgery. At both 3 and 8 weeks post TAC, there was a significant reduction in cardiac output and stroke volume in TAC mice in comparison to SHAM mice, but an increase in relative wall thickness (TAC N=17, SHAM N=9) (**p<0.01) (**p<0.001) (****p<0.0001). There was no difference observed in fractional shortening or ejection fraction in TAC mice in comparison to SHAM mice (TAC N=17, SHAM N=9). TAC (transverse aortic constriction).

5.3.1.2 The Influence of TAC Surgery on Left Ventricular Mass

Echocardiographic assessment of the measurements discussed in section 2.15.4 - Transthoracic Echocardiography (Figure 2.8) and comparing them to physical body measurements of weight and tibia length allowed assessment of the following ratios: LV mass-to-body weight and LV mass-to-tibia length. These measurements allowed the assessment of heart size in comparison to the size of the animal throughout the time course of the study. An increase in LV mass-to-body weight and LV mass-to-tibia length ratios would be expected in TAC animals in comparison to SHAM animals as this surgical intervention initiates a hypertrophic response (Kho, et al., 2011) (Martin, et al., 2012).

The data showed that there was a trend for an increased LV mass-to-body weight and LV mass-to-tibia length ratio in TAC mice in comparison to SHAM mice at the 3 and 8 week time point, however significant changes were only observed at the three week time point, 35% increase in LV mass : body weight and 50% increase in LV mass : tibia length from SHAM to TAC (Figure 5.5) (TAC N=17, SHAM N=9). This indicates that the TAC surgical intervention has initiated a hypertrophic response.

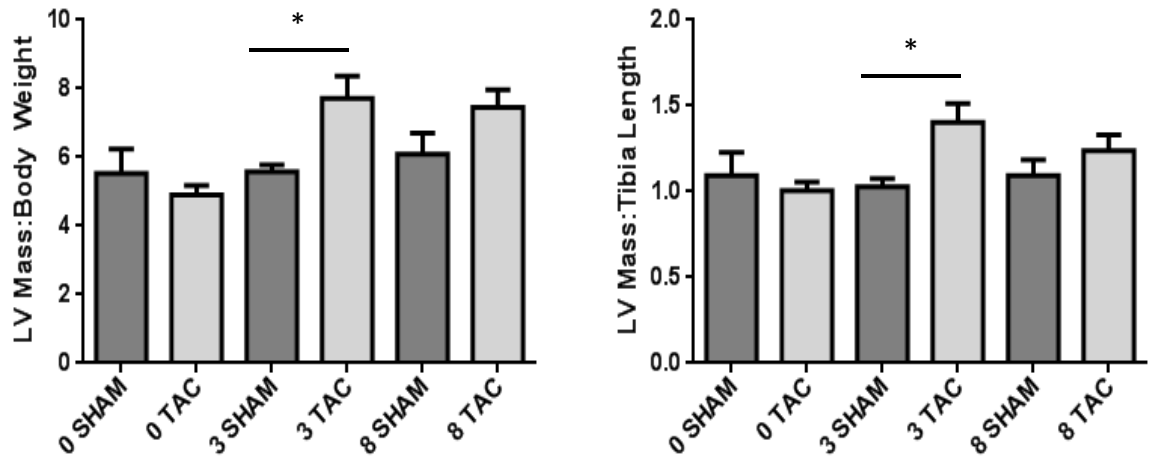


Figure 5.5 Left ventricular mass indices assessed following TAC surgery. There was an increased LV mass-to-body weight and LV mass-to-tibia length ratio in TAC mice in comparison to SHAM mice at the 3 and 8 week time point, however this was only significant at the 3 week time point (* $p < 0.05$) (TAC N=17, SHAM N=9). TAC (transverse aortic constriction), LV (left ventricle).

5.3.1.3 The Influence of TAC Surgery on Whole Heart Mass

In addition to echocardiographic assessment of heart size, physical assessment of whole heart mass was assessed following TAC surgery. Animals were sacrificed at 8 weeks post TAC surgery and organs were harvested. Organ weight was compared to both body weight and tibia length. An increase in whole heart mass would be expected in TAC animals in comparison to SHAM animals as this surgical intervention initiates a hypertrophic response (Kho, et al., 2011) (Martin, et al., 2012).

There was a significant increase of approximately 20% in TAC mice in comparison to SHAM mice in the following ratios; heart-to-body weight, LV-to-body weight and heart weight-to-tibia length (Figure 5.6) (TAC N=17, SHAM N=9) (* $p < 0.05$) (** $p < 0.001$). There was a trend for LV weight-to-tibia length to increase in TAC mice, in comparison to SHAM mice, however no significant changes were observed (Figure 5.6) (TAC N=17, SHAM N=9). Similarly, to the echocardiographic data, physical assessment of the heart revealed that the TAC surgical intervention has initiated a hypertrophic response.

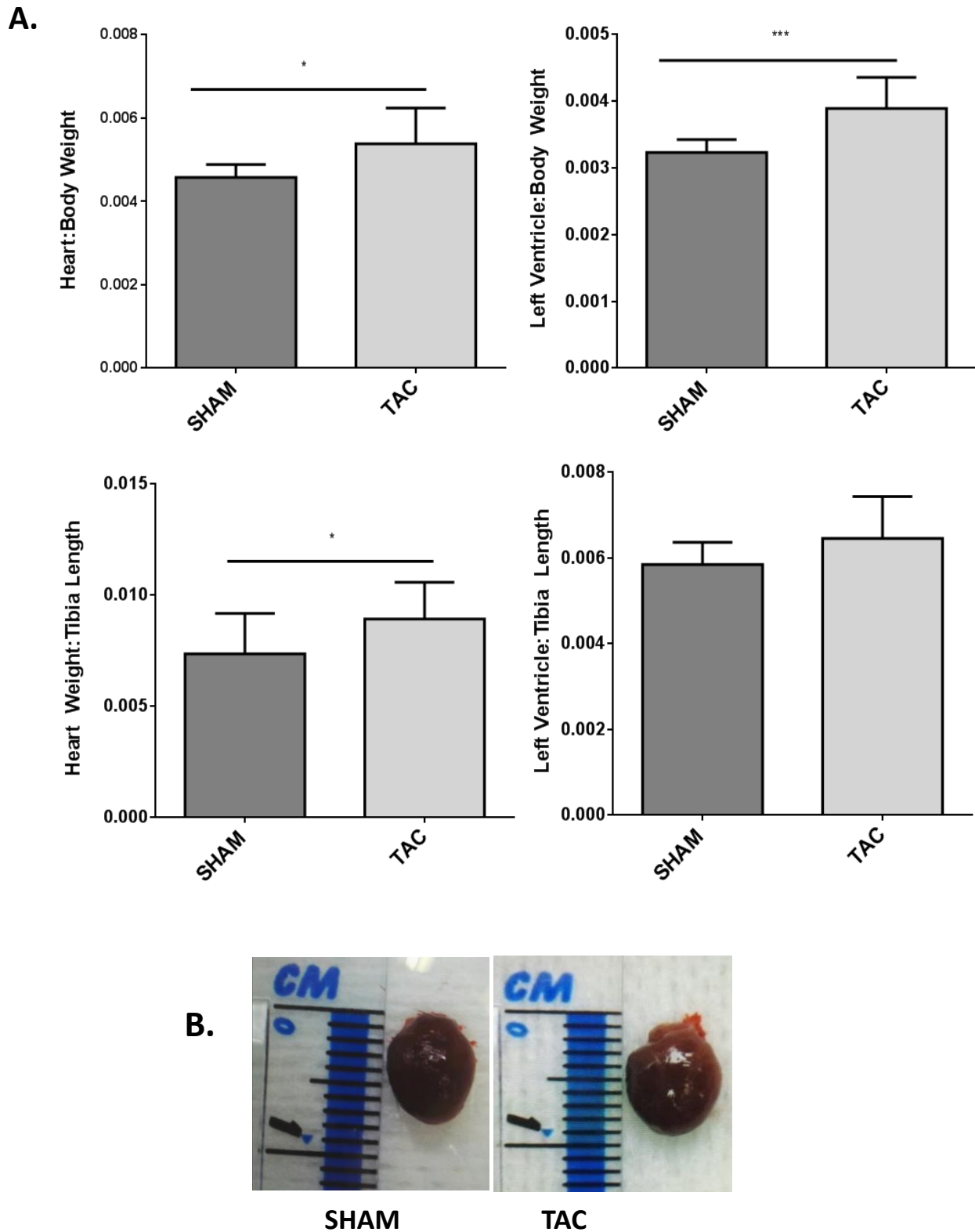


Figure 5.6 Heart weight is increased by TAC surgery. (A) There was a significant increase in TAC mice in comparison to SHAM mice in the following ratios; heart-to-body weight, LV-to-body weight and heart weight-to-tibia length. There was a trend for LV weight-to-tibia length to increase in TAC mice in comparison to SHAM mice (TAC N=17, SHAM N=9) (* $p < 0.05$) (** $p < 0.01$). **(B)** Representative hearts from TAC and SHAM animals shown. TAC (transverse aortic constriction), LV (left ventricle).

5.3.1.4 The Influence of TAC Surgery on Other Organs

To determine that the TAC surgical intervention only initiated a cardiac response, the other organs of the body were physically examined. The weights of other organs were normalised against both body weight and tibia length. No differences would be expected to be observed in the kidney and liver, however some groups report an increase in lung mass following TAC surgery (Lu, et al., 2010) (Xu, et al., 2011) (Lu, et al., 2010) (Takimoto, et al., 2005).

No significant differences were observed in body weight or tibia length (Figure 5.7) (TAC N=17, SHAM N=9) or in the ratios lung-to-body weight, liver-to-body weight, kidney-to-body weight, lung-to-tibia length, liver-to-tibia length, kidney-to-tibia length between TAC and SHAM groups at point of sacrifice (Figure 5.8) (TAC N=17, SHAM N=9). This indicates that the TAC surgical intervention only mediated effects on the heart.

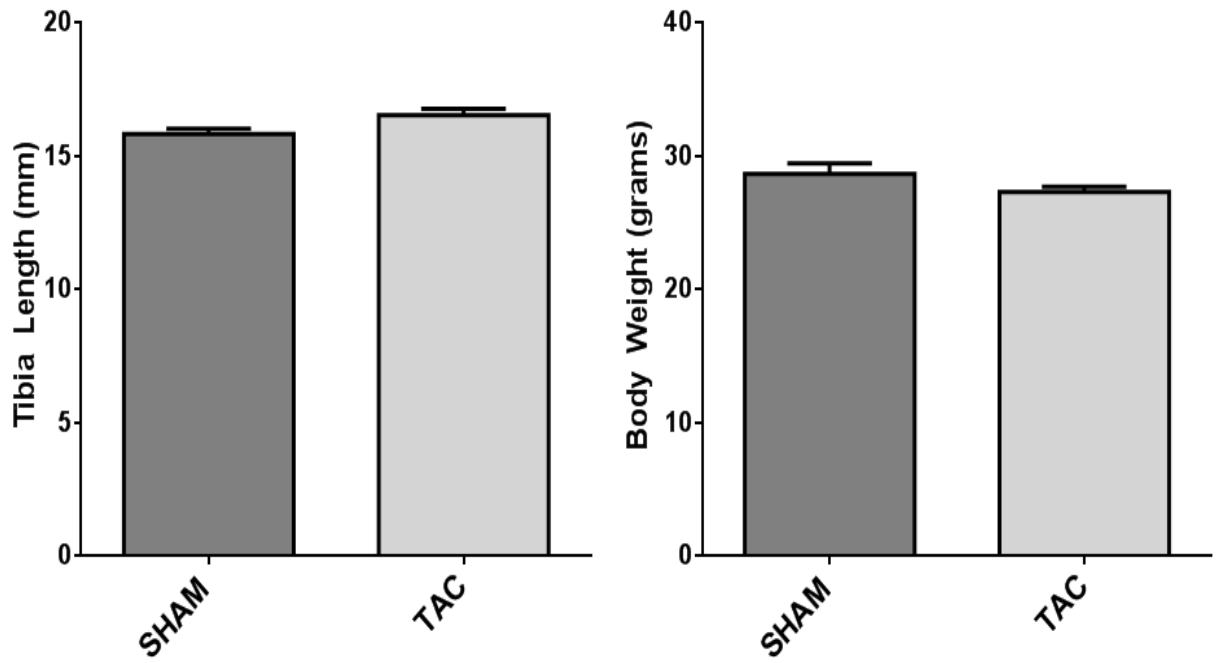


Figure 5.7 TAC surgery does not influence body weight or tibia length. No significant differences were observed in body weight or tibia length between TAC and SHAM groups at point of sacrifice (TAC N=17, SHAM N=9). TAC (transverse aortic constriction).

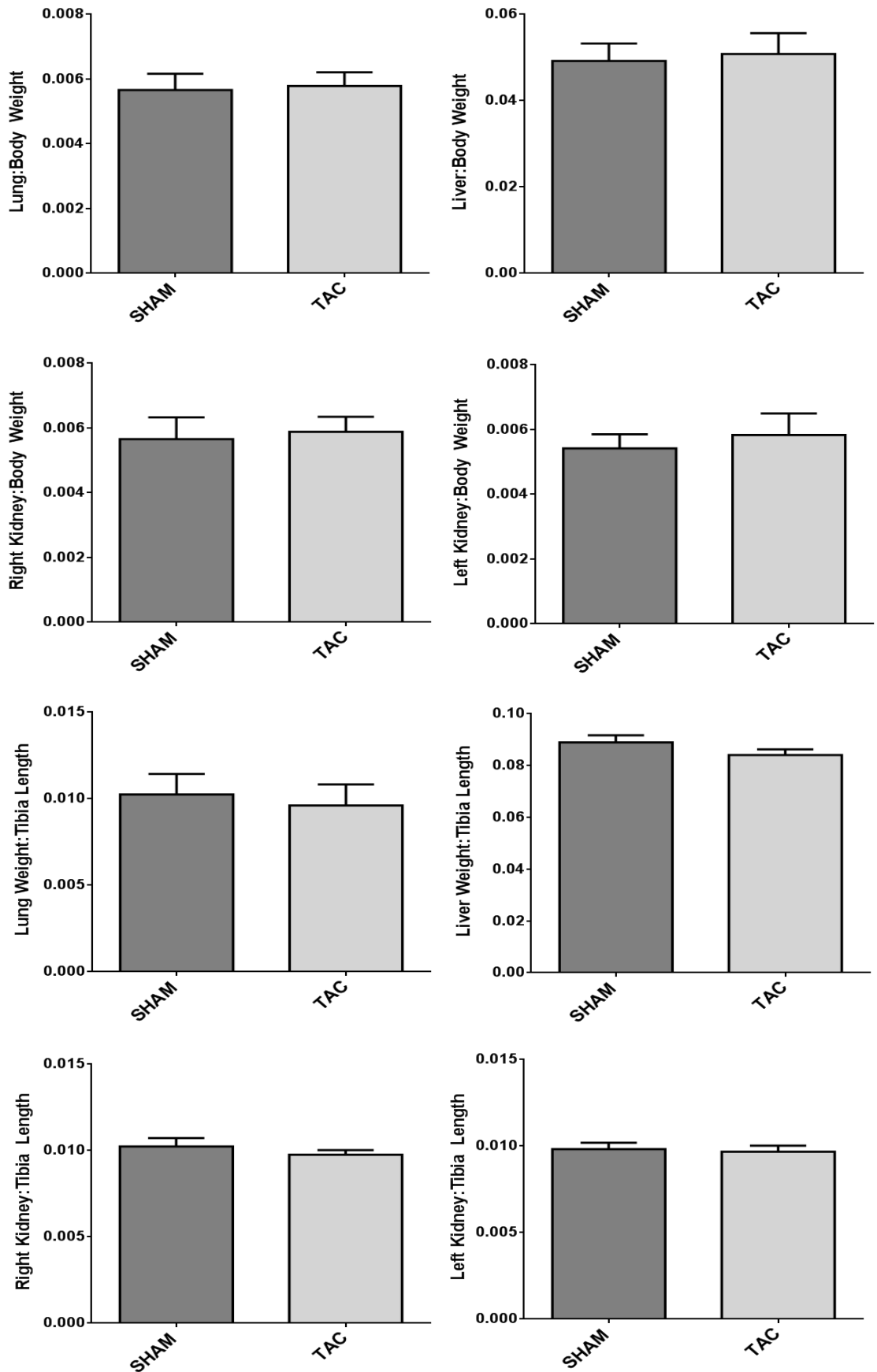


Figure 5.8 TAC surgery does not influence other organs. No significant differences were observed between TAC and SHAM groups at point of sacrifice in the following ratios; lung-to-body weight, liver-to-body weight, kidney-to-body weight, lung-to-tibia length, liver-to-tibia length, kidney-to-tibia length (TAC N=17, SHAM N=9). TAC (transverse aortic constriction).

5.3.1.5 Identification of TAC Mice with the Strongest Hypertrophic Response

The TAC surgery can mediate variable response between animals. The success of this model can be dependent on the tightness of the suture around the aortic arch, as this will determine the degree of hypertrophic development, and therefore the time frame in which HF and cardiac dilatation develops (deAlmeida, et al., 2010). Although the aortic constriction is standardised by a needle aligned against the vessel when tying off the suture, constriction does vary between mice with some animals having tighter banding than others. This variability is even more pronounced in the minimally invasive TAC model due to the lack of thoracotomy, and therefore there is a limited view of the aortic arch when the suture is being tied. This can result in different anatomical placement in every animal, since the aortic arch may be more easily accessed in some mice. Regardless of the thoracotomy giving better access in the standard TAC model, Kho et al. (2011) still used isolation criteria to identify animals which displayed a stronger HF phenotype for further study. Parameters used were pressure gradient greater than 30mmHg, in addition to fractional shortening of less than 50%. In the TAC establishment study the animals that displayed the greatest changes in relative wall thickness were identified to have the strongest hypertrophic phenotype.

Using this isolation criteria, the echocardiographic parameters (fractional shortening and ejection fraction) were re-examined (Table 5.1). Despite the significant hypertrophic changes observed, fractional shortening and ejection fraction, which are normally reduced by aortic banding models (Martin, et al., 2012), were unchanged in the TAC establishment study (TAC N=6, SHAM N=6). This strongly suggested that the mice have not yet progressed to HF and are still in a state of compensatory hypertrophy.

Table 5.1 Echocardiographic data from RWT criterion animals

		0 Weeks		3 Weeks		8 Weeks	
Parameter		TAC	SHAM	TAC	SHAM	TAC	SHAM
Fractional Shortening (%)	Mean±SEM	39.73 ±1.92	39.64 ±1.51	41.12 ±2.90	40.90 ±1.93	42.41 ±3.14	35.50 ±2.10
	P Value	0.9725		0.9693		0.0972	
Ejection Fraction (ml)	Mean±SEM	77.78 ±2.11	77.8 ±1.74	78.87 ±2.79	79.12 ±2.09	80.06 ±3.21	72.74 ±2.59
	P Value	0.992		0.9449		0.1016	

5.3.1.6 The Influence of TAC Surgery on Cardiomyocyte Cross Sectional Area

Considering the variability observed in response to the TAC surgery in the study animals, the decision was made to examine cardiomyocyte hypertrophy and fibrosis only in those animals displaying the greatest response to surgical intervention based on criterion described in section 5.3.1.5 - Identification of TAC Mice with the Strongest Hypertrophic Response. Using wheat germ agglutinin (WGA) staining - a membrane stain to ascertain cell size - the cardiomyocyte cross sectional area was measured. Using this method, I observed a significant increase of approximately 35% in cardiomyocyte cross sectional area in the TAC animals in comparison to SHAM animals (Figure 5.9) (TAC N=6, SHAM N=6) (* $p < 0.05$). This is indicative of increased hypertrophy in these animals, as would be expected following TAC surgical intervention (Kho, et al., 2011) (Martin, et al., 2012).

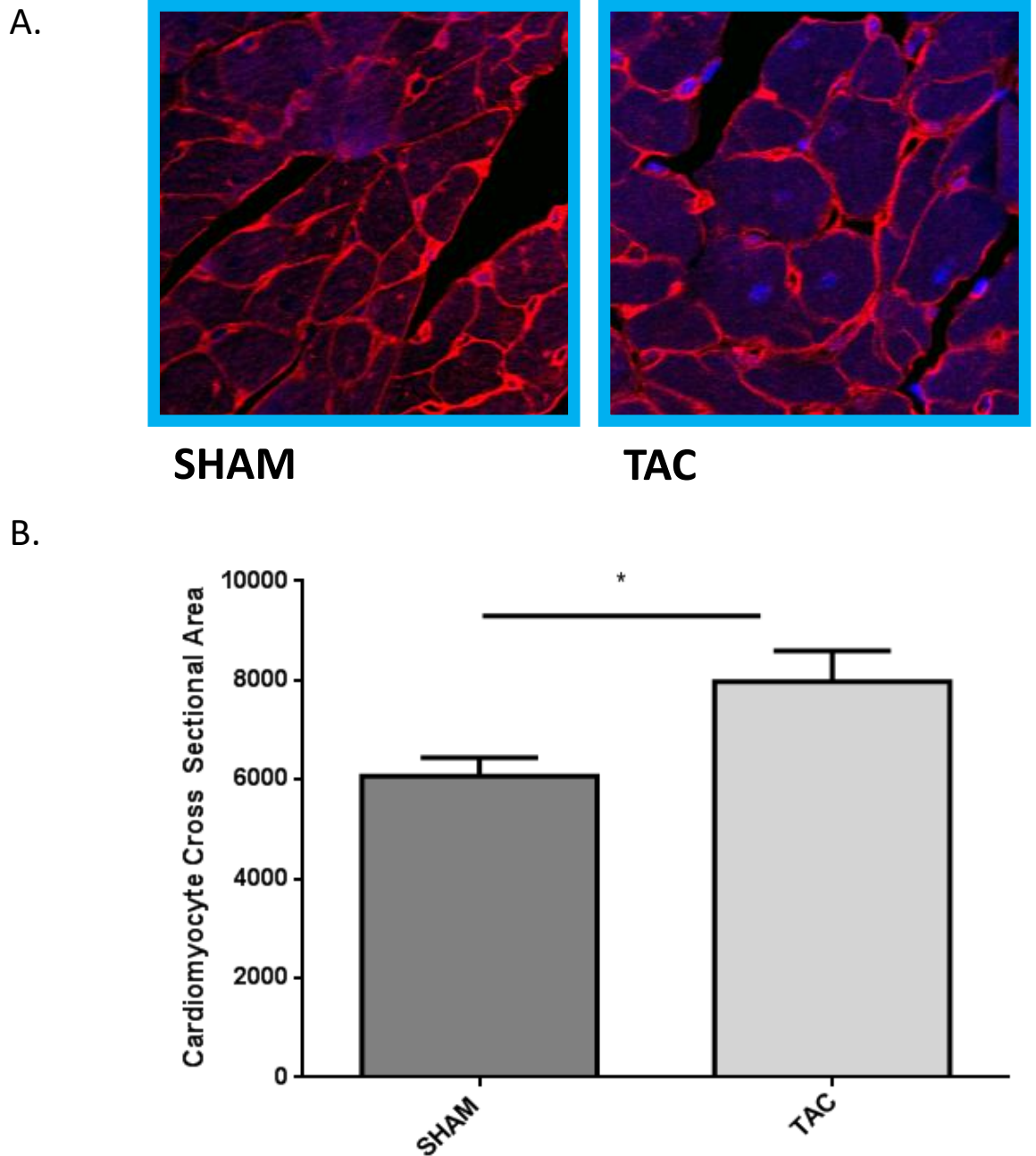


Figure 5.9 TAC surgery increases cardiomyocyte size. (A&B) There was a significant increase in cardiomyocyte cross sectional area in the TAC animals in comparison to the SHAM animals (TAC N=6, SHAM N=6) (* $p < 0.05$). TAC (transverse aortic constriction). (A) Representative images of WGA staining are shown above bar graph.

5.3.1.7 The Influence of TAC Surgery on Cardiac Fibrosis

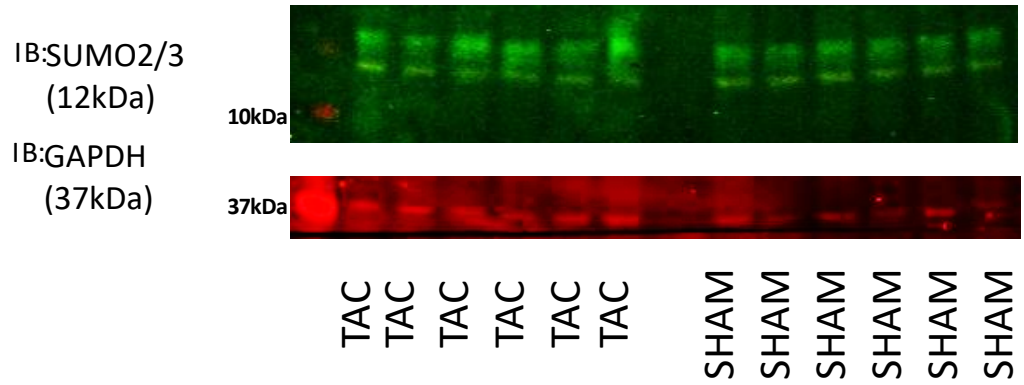
Using picosirius red staining - a stain which recognises collagen deposition - the volume of fibrotic tissue within cross sections of the hearts was assessed. Fibrosis was assessed both perivascularly and interstitially. The measurements from these individual areas were combined to give total fibrosis. There was a 1-fold significant increase in fibrotic tissue area in the TAC mice in comparison to the SHAM (Figure 5.10) (TAC N=6, SHAM N=6) (** $p < 0.01$) (** $p < 0.001$). This increase in fibrosis is associated with cardiac remodelling and hypertrophy, as would be expected following TAC surgery (Kho, et al., 2011) (Martin, et al., 2012).

5.3.1.8 TAC Model Influences SUMOylation Pathway Machinery

Intermediates within the SUMOylation pathway were examined in TAC in comparison to SHAM via immunoblot analysis. The SUMOylation pathway consists of the following components; the SUMO paralogues 1, 2 and 3 and the SUMOylation enzymes consisting of E1 activating enzyme, UBC9 E2 conjugating enzyme, and E3 ligases, such as PIASy. SUMO-1, SUMO-2/3, UBC9, and the E3 ligase PIASy which we have shown promotes β_2 AR SUMOylation were examined in both TAC and SHAM mice tissue, in addition to examination of SUMOylated β_2 AR levels using the Badrilla ® custom designed antibody.

There was no significant difference in SUMO-2/3 and expression between TAC and SHAM mice (Figure 5.11) (TAC N=6, SHAM N=6). PIASy expression between TAC and SHAM animals was inconclusive due to poor quality of western blot (Figure 5.12) (TAC N=6, SHAM N=6). TAC animals display a significant reduction of approximately 30% in UBC9 expression in comparison to SHAM animals (Figure 5.13) (TAC N=6, SHAM N=6) (** $p < 0.01$). The impact of TAC surgery on SUMO-1 expression was unable to be assessed in this study. No bands for SUMO-1 were detected in the mouse cardiac lysate (Figure 5.14A), although the SUMO-1 antibody I used has been shown to be functional as SUMO-1 expression was identified at the correct molecular weight in both pig cardiac tissue and HEK β_2 cell lysate (Figure 5.14B). No significant difference was observed in SUMO- β_2 AR expression between TAC and SHAM mice (Figure 5.15A) (TAC N=6, SHAM N=6). However, the appropriate quantification would involve normalising the SUMO- β_2 AR band to the total β_2 AR band, and a signal could not be detected using two total β_2 AR antibodies in the mouse lysate as the band was below the threshold of detection (Figure 5.15B). The capability of these antibodies was tested via the detection of β_2 AR present in the stable HEK β_2 cell line, in comparison to standard HEK cells. Both antibodies successfully detected β_2 AR (Figure 5.16). In this instance SUMO- β_2 AR was therefore quantified to GAPDH loading control (Figure 5.15A).

A.



B.

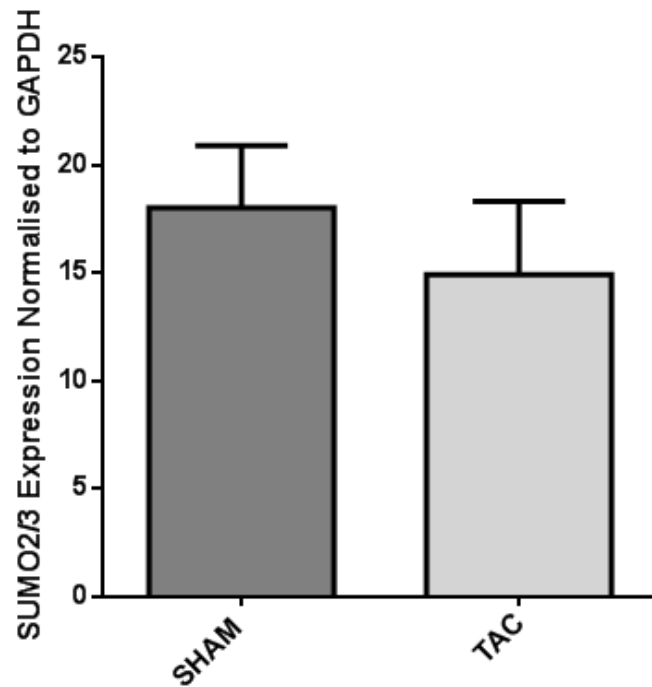


Figure 5.11 TAC surgery does not influence SUMO-2/3 expression. (A&B) There is no significant change in SUMO-2/3 expression in the HF model in comparison to SHAM (TAC N=6, SHAM N=6). TAC (transverse aortic constriction). Primary concentration 1 : 1000, secondary concentration 1 : 5000. (A) Representative blots shown.

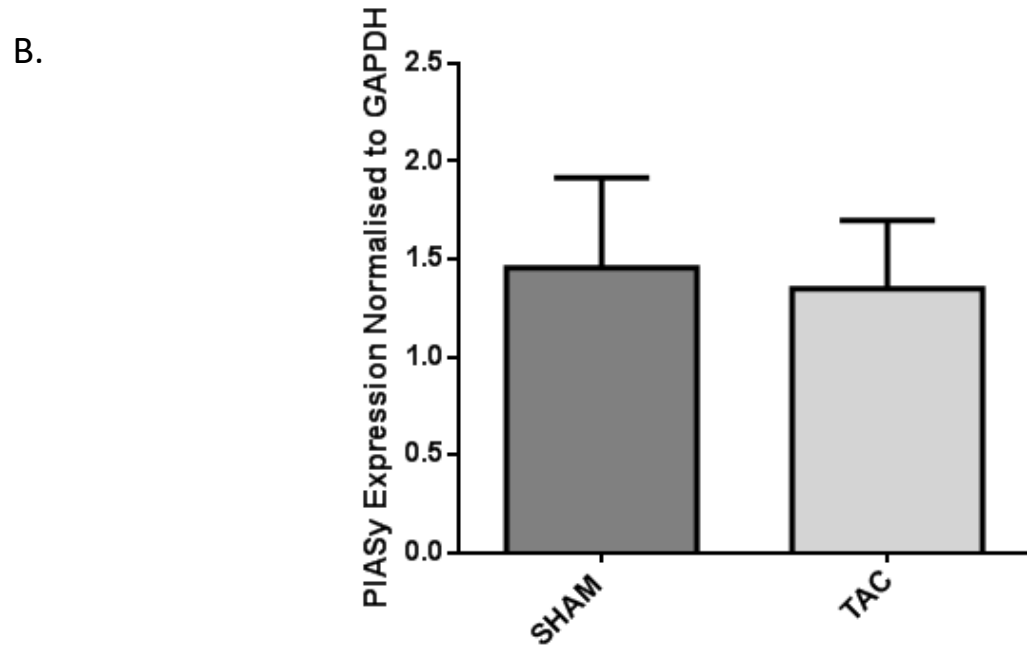
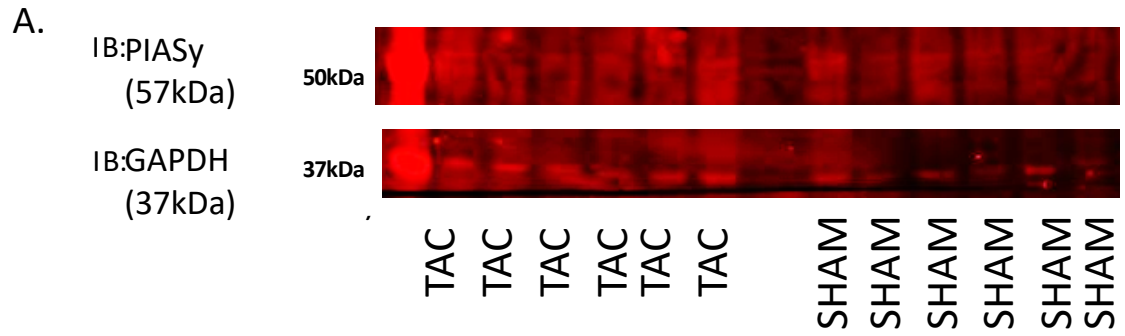
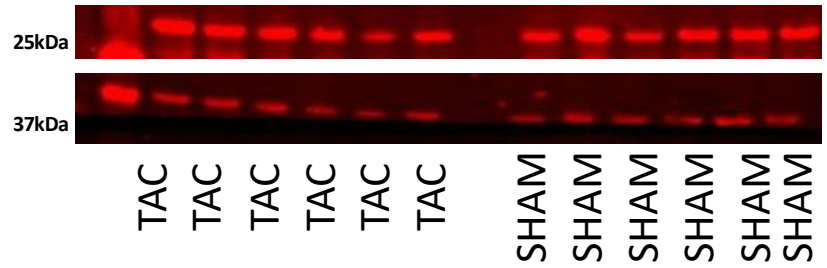


Figure 5.12 TAC surgery influence on PIASy expression is inconclusive. (A&B) PIASy expression in the HF model in comparison to SHAM animals is inconclusive due to poor quality of western blot (TAC N=6, SHAM N=6). TAC (transverse aortic constriction). Primary concentration 1 : 1000, secondary concentration 1 : 5000. (A) Representative blots shown.

A.

IB:UBC9
(20kDa)
IB:GAPDH
(37kDa)



B.

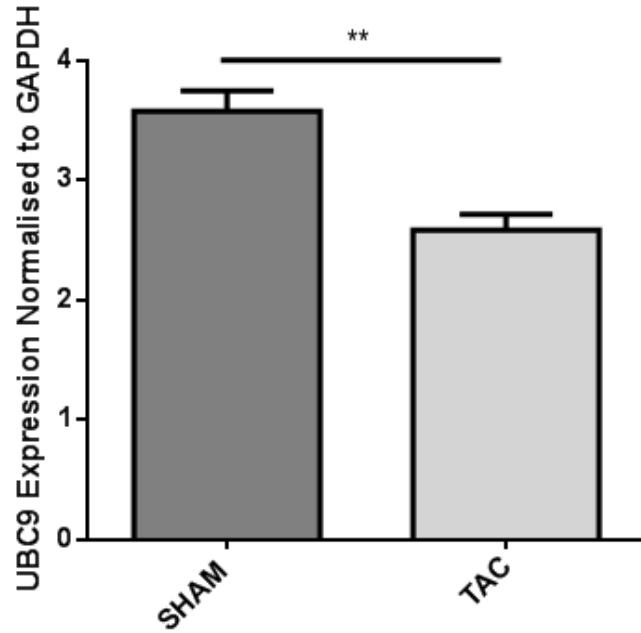


Figure 5.13 TAC surgery reduces UBC9 expression. (A&B) There is a significant reduction in UBC9 expression in the HF model in comparison to SHAM (TAC N=6, SHAM N=6) (** $p < 0.01$). TAC (transverse aortic constriction). Primary concentration 1 : 1000, secondary concentration 1 : 5000. (A) Representative blots shown.

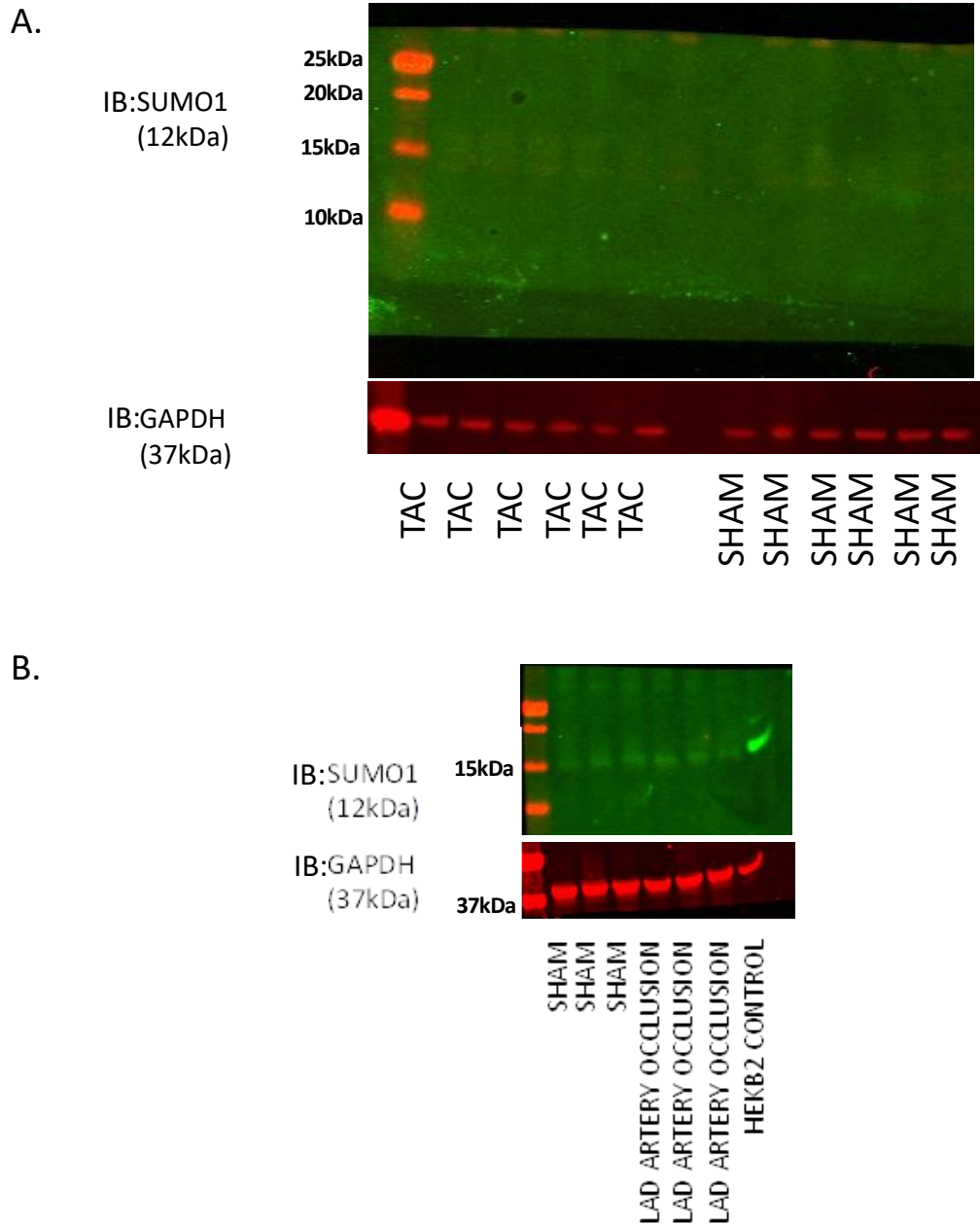


Figure 5.14 TAC surgery influence on SUMO-1 expression is inconclusive. (A) Assessment of SUMO-1 expression in TAC model of HF is inconclusive due to lack of antibody detection. **(B)** SUMO-1 antibody is functional proven by detecting cell lysate and pig cardiac tissue (TAC N=6, SHAM N=6). TAC (transverse aortic constriction). Primary concentration 1 : 1000, secondary concentration 1 : 5000. **(A&B)** Representative blots shown.

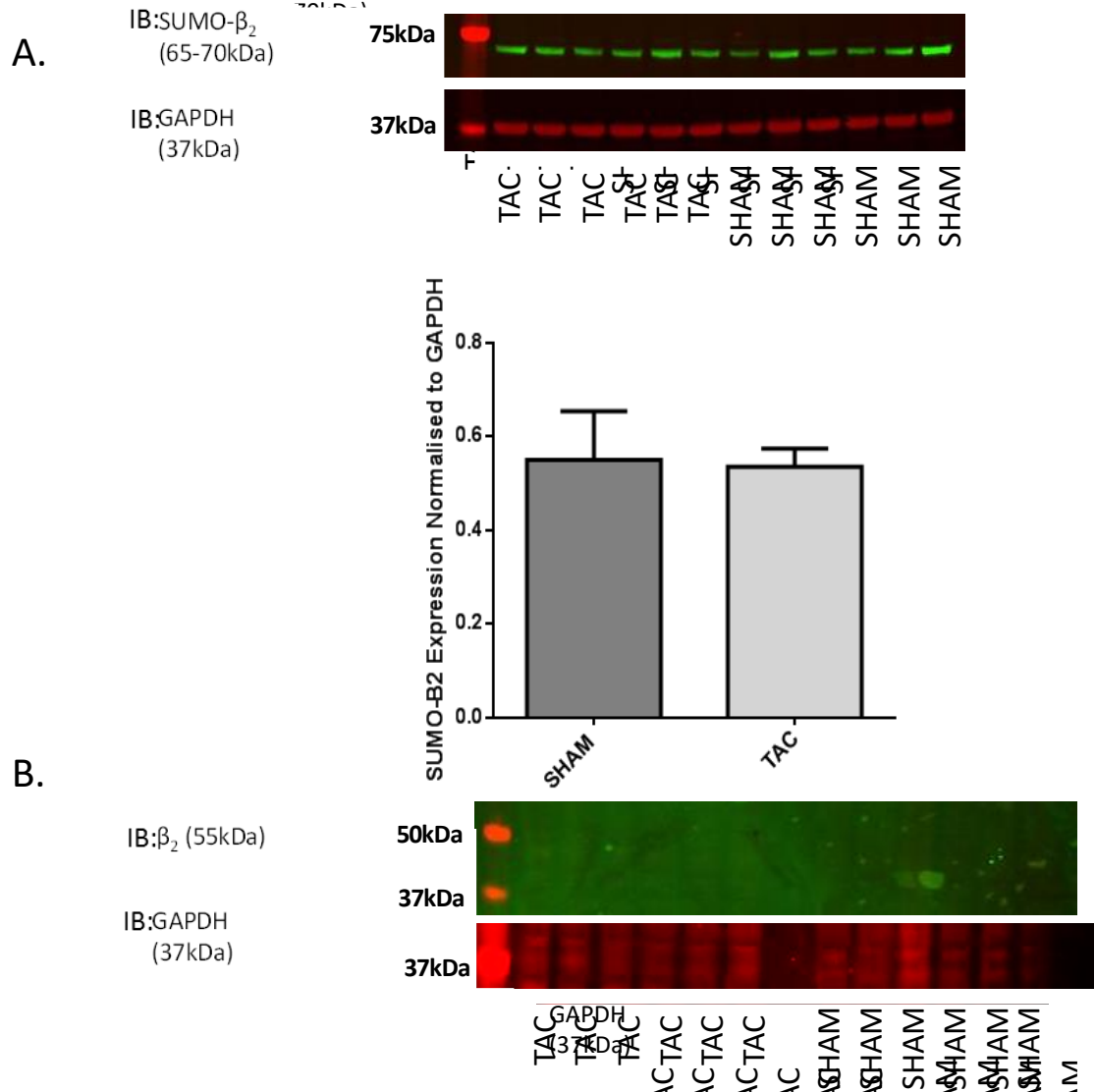


Figure 5.15 TAC surgery does not influence SUMO- β_2 AR expression. (A) There is no significant change in SUMO- β_2 AR expression in the HF model in comparison to SHAM (TAC N=6, SHAM N=6). (B) β_2 AR antibody displays no signal with cardiac lysate. TAC (transverse aortic constriction) β_2 AR (beta 2 adrenoceptor). Primary concentration 1 : 500, secondary concentration 1 : 5000. (A&B) Representative blots shown.

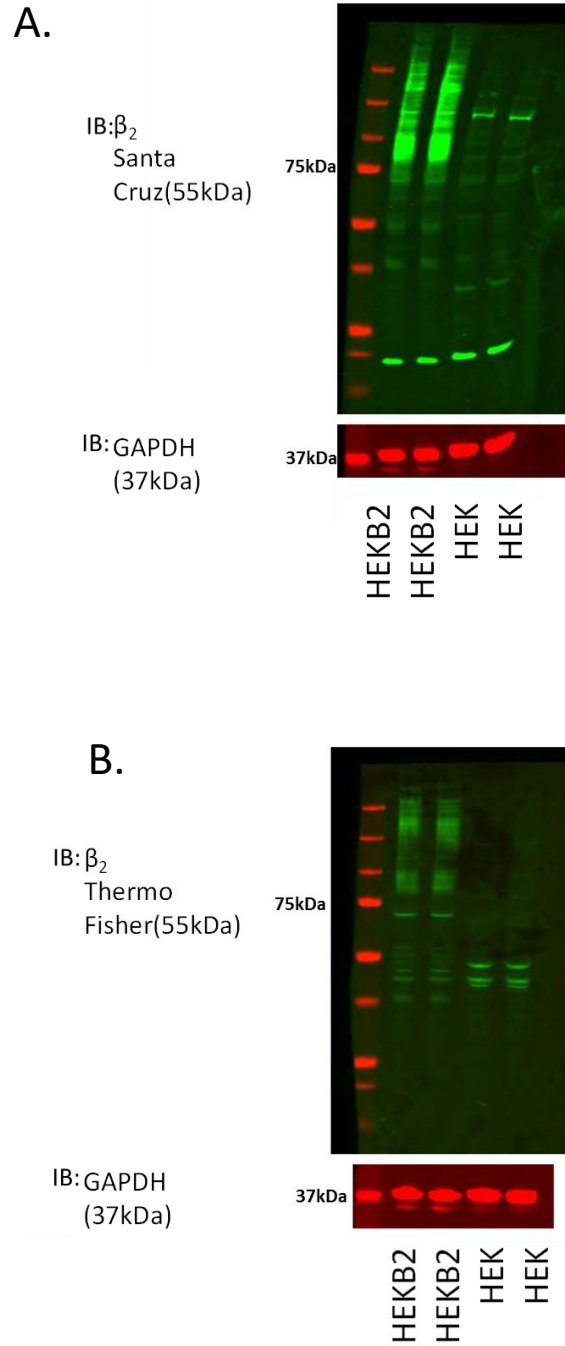


Figure 5.16 Testing of β_2 AR antibodies with cell lysate. The capability of the β_2 AR antibodies, Santa Cruz antibody (A) and ThermoFisher antibody (B), was tested via the detection of β_2 AR present in the stable HEKB β_2 cell line, in comparison to standard HEK cells. Both antibodies successfully detected β_2 AR. β_2 AR (beta 2 adrenoceptor). Primary concentration 1 : 1000, secondary concentration 1 : 5000. (A&B) Representative blots shown.

5.3.2 LAD Artery Balloon Occlusion Ischemic HF Model in Pigs

A student placement within the Hajjar group (New York) allowed me to access pig cardiac tissue from the LAD artery balloon occlusion model of HF. This allowed the investigation of the β_2 AR SUMOylation in an animal model which is considered to be more relevant to the human cardiac system than rodents. The following results relate to the LAD artery balloon occlusion model.

5.3.2.1 LAD Artery Balloon Occlusion Ischemic HF Model Influences SUMOylation Pathway Machinery

Similarly to the TAC study, the SUMOylation pathway and SUMOylated- β_2 AR were examined in LAD artery balloon occlusion in comparison to SHAM via immunoblot analysis.

On visualising SUMO-2/3 using western blotting, a band would be expected at approximately 12kDa, which is the case for the HEK β_2 control lysate (Figure 5.17). The only band present within the pig samples appears below 37kDa (Figure 5.17) but there is no information regarding this antibody having unspecific binding. It is probable that this band could indicate chains of SUMO-2/3 within the pig samples, or possibly a protein which SUMO-2/3 has modified. When the present band was quantified there was a significant reduction of approximately 30% in the LAD artery occlusion model in comparison to SHAM (Figure 5.17) (LAD artery occlusion N=3, SHAM N=3) (**p<0.01). There was no significant difference in SUMO-1 and PIAS γ expression in the LAD artery occlusion model in comparison to SHAM (Figure 5.18 & 5.19) (LAD artery occlusion N=3, SHAM N=3). There is a significant 1.5-fold increase in SUMOylated β_2 AR expression in the LAD artery occlusion model in comparison to SHAM (Figure 5.20) (LAD artery occlusion N=3, SHAM N=3) (*p<0.05). UBC9 expression shows a trend to be reduced by approximately 60% in the LAD artery occlusion model in comparison to SHAM (Figure 5.21) (LAD artery occlusion N=3, SHAM N=3). However, this blot shows high variability and to determine differences in UBC9 between healthy and diseased phenotypes more n numbers would be required.

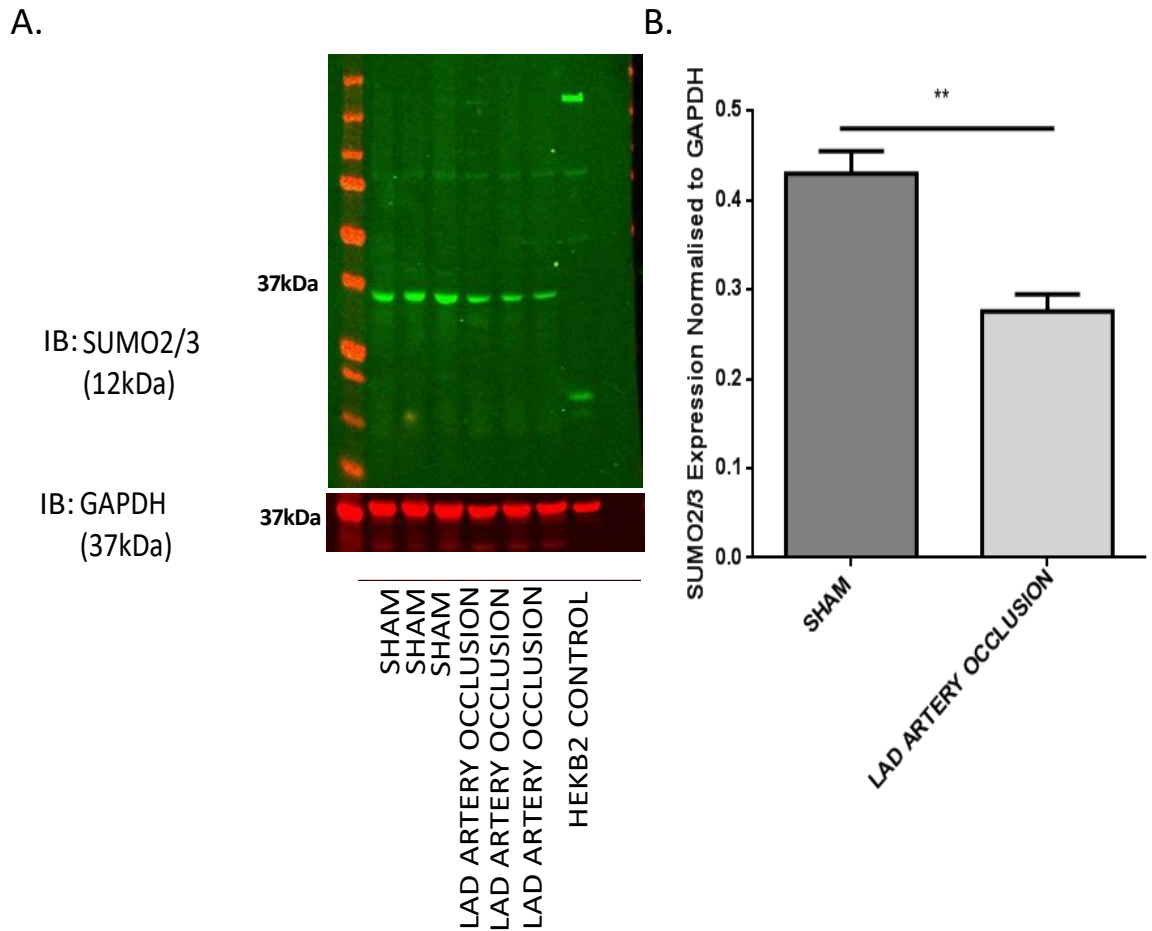
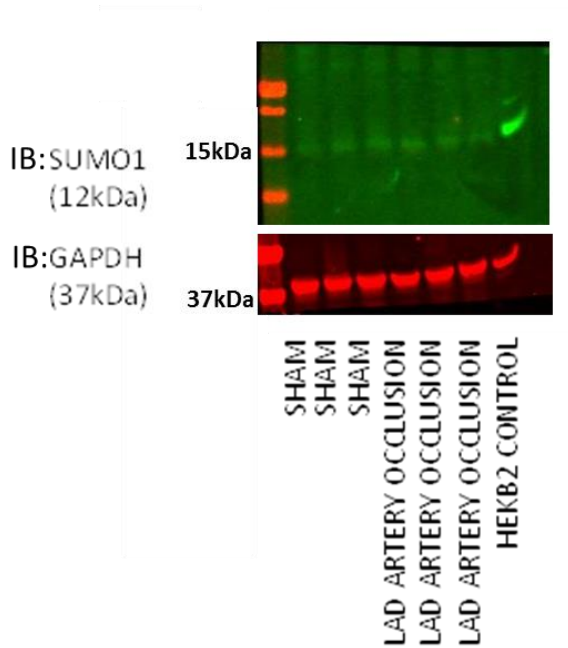


Figure 5.17 LAD artery balloon occlusion reduces SUMO-2/3 expression. (A&B) There is a significant reduction in SUMO-2/3 expression in the HF model in comparison to SHAM (LAD artery occlusion N=3, SHAM N=3) (** $p < 0.01$). HF (heart failure), LAD (left anterior descending). Primary concentration 1 : 1000, secondary concentration 1 : 5000. **(A)** Representative blots shown.

A.



B.

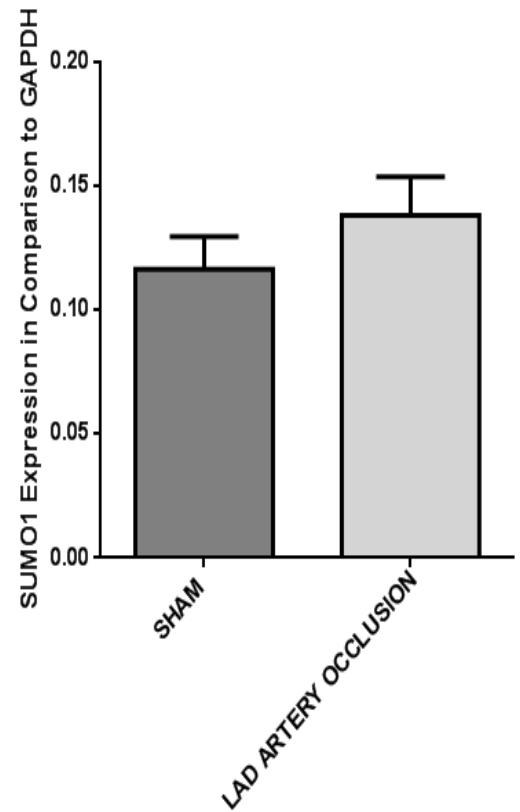
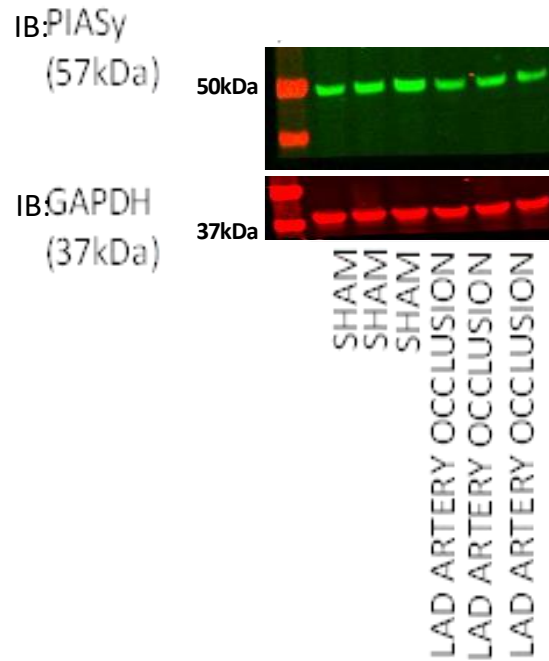


Figure 5.18 LAD artery balloon occlusion does not influence SUMO-1 expression. (A&B) There is no significant difference in SUMO-1 expression in the HF model in comparison to SHAM (LAD artery occlusion N=3, SHAM N=3). HF (heart failure), LAD (left anterior descending). Primary concentration 1 : 1000, secondary concentration 1 : 5000. **(A)** Representative blots shown.

A.



B.

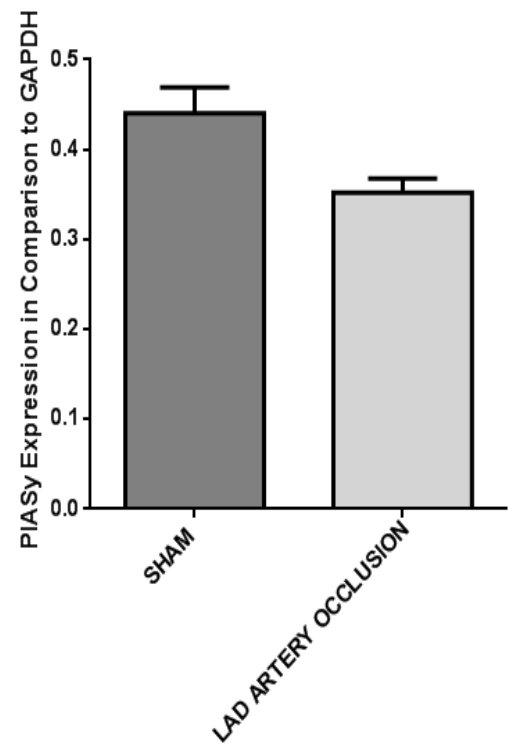


Figure 5.19 LAD artery balloon occlusion reduces PIASy expression. (A&B) There is a trend for PIASy expression to be reduced in the HF model compared to SHAM, however no significant differences are observed (LAD artery occlusion N=3, SHAM N=3). HF (heart failure), LAD (left anterior descending). Primary concentration 1 : 1000, secondary concentration 1 : 5000. **(A)** Representative blots shown.

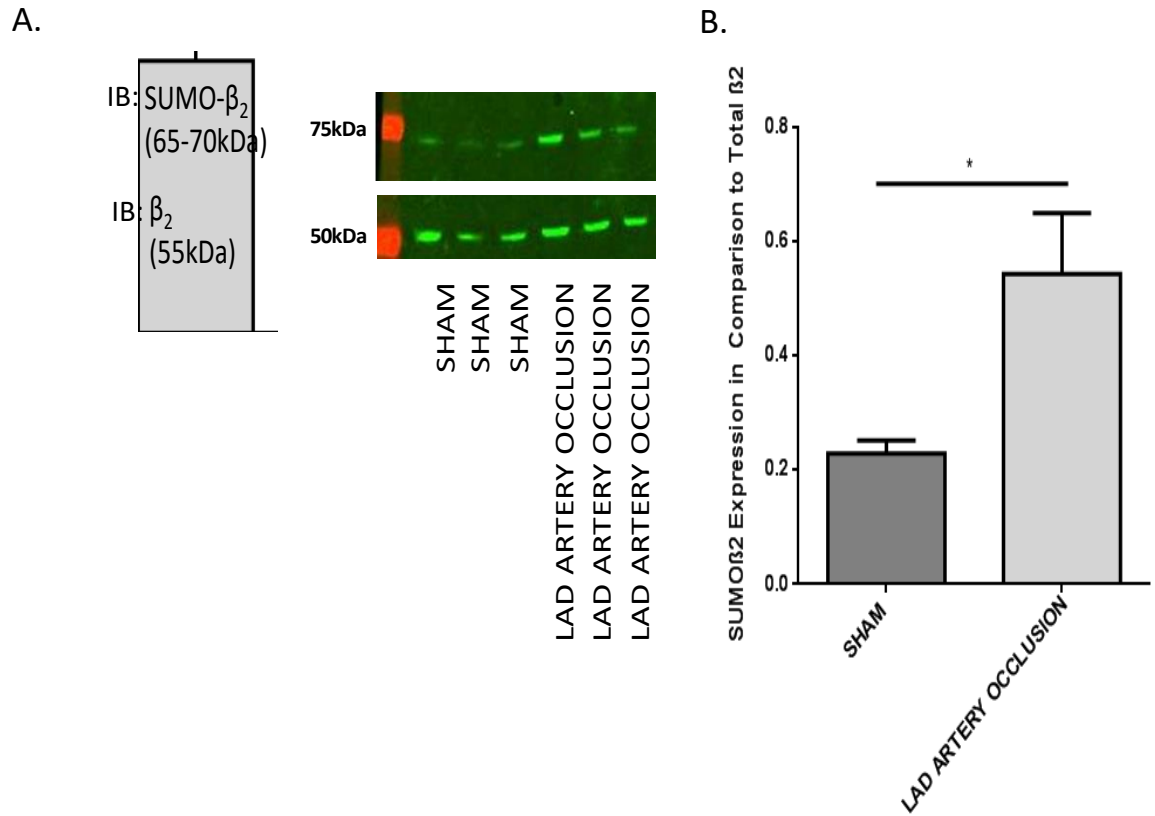


Figure 5.20 LAD artery balloon occlusion increases SUMO- β_2 AR expression. (A&B) There is a significant reduction in SUMO- β_2 AR expression in the HF model in comparison to SHAM (LAD artery occlusion N=3, SHAM N=3) (* p <0.05). HF (heart failure), LAD (left anterior descending). Primary concentration 1 : 500, secondary concentration 1 : 5000. (A) Representative blots shown.

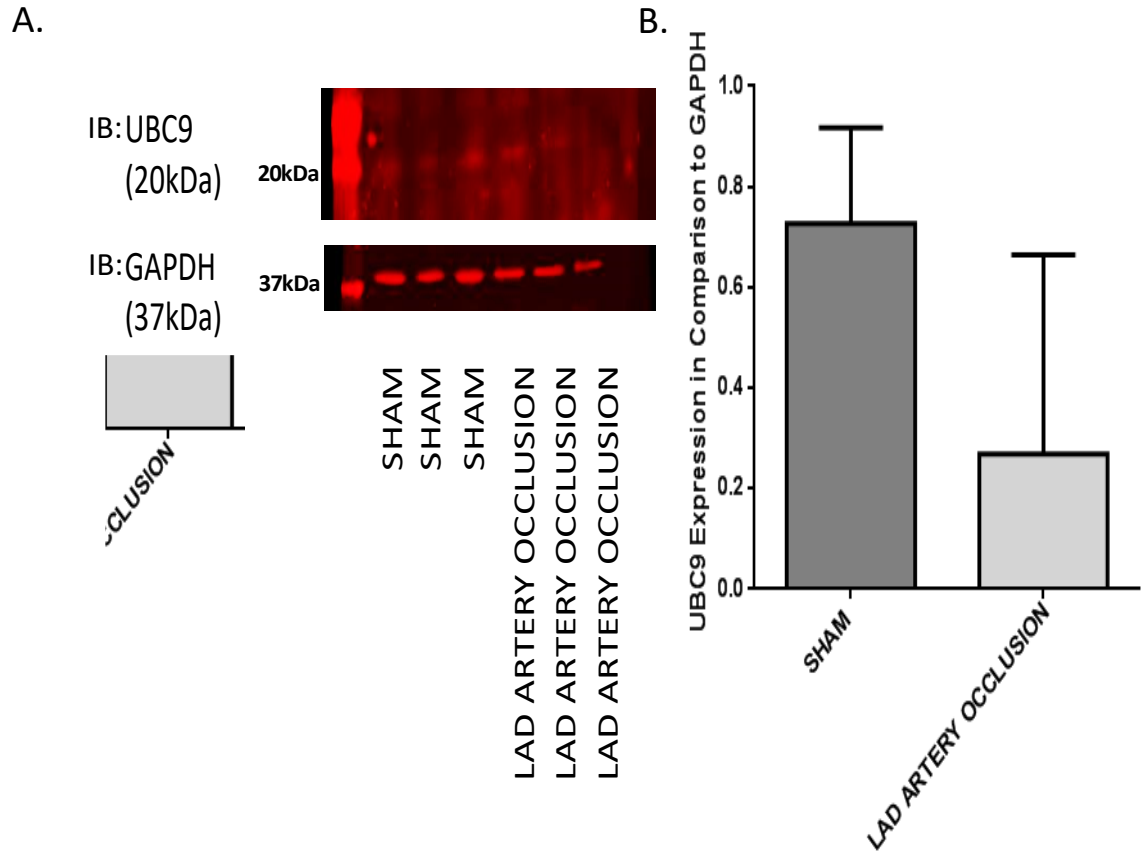


Figure 5.21 LAD artery balloon occlusion reduces UBC9 expression. (A&B) There is a trend for UBC9 expression to be reduced in the HF model compared to SHAM, however no significant differences are observed. More n numbers would be required to account for variability (LAD artery occlusion N=3, SHAM N=3). HF (heart failure), LAD (left anterior descending). Primary concentration 1 : 1000, secondary concentration 1 : 5000. **(A)** Representative blots shown.

5.4 Discussion

I aimed to establish the minimally invasive TAC model of pressure overload HF within our animal unit at University of Glasgow, as this model had not been used within our institute. I intended to use this model to assess the SUMOylation of the B_2AR , in a similar manner to which the Hajjar group assessed the SUMOylation of SERCA2a (Kho, et al., 2011). This surgical intervention initially leads to compensated hypertrophy of the heart, but over time this response to the chronic hemodynamic load becomes maladaptive resulting in cardiac dilatation and HF (Heineke & Molkentin, 2006). Three weeks post TAC surgery the animals from my study experienced reduced cardiac output and stroke volume, indicative of reduced cardiac function. This was in conjunction with increased relative wall thickness in comparison to SHAM mice. This provides evidence cardiac remodelling had been initiated in these mice. However, despite the significant hypertrophic changes observed, echocardiographic data failed to demonstrate anticipated changes in two important cardiac function parameters; fractional shortening and ejection fraction. This provides evidence that the mice have not yet progressed to HF, and are still in a state of compensatory hypertrophy.

Additional data to support the echocardiography data indicating hypertrophic response is illustrated at organ harvest. Both heart and LV-to body weight/tibia length were increased in the animals that underwent TAC surgery in comparison to SHAM. The heart was the only organ influenced by the TAC model, with no other organs showing differences between TAC and SHAM groups. Multiple TAC studies have reported elevated lung weight in relation to LV hypertrophy and dysfunction (Lu, et al., 2010) (Xu, et al., 2011) (Lu, et al., 2010) (Takimoto, et al., 2005), but this was not observed in the current TAC establishment study. The increase in lung weight is often believed to be associated with pulmonary oedema but Chen et al (2012) identified it was associated with massive lung fibrosis, leukocyte infiltration and vascular remodelling. The same group reported that the increase in lung weight and the lung-to-body weight ratio after TAC are significantly related to the increase of LV weight and the reduction in LV ejection fraction. In addition, when this group examined a group of mice regarded as severe HF phenotype, in comparison to moderate HF phenotype, the lung-to-body weight ratio was significantly greater in the severe group (Chen, et al., 2012). Neither Martin et al (2012) or Kho et al (2011) reported any changes to lung weight in their TAC studies.

The fact that this TAC establishment study did not identify changes in lung-to-body weight ratio between TAC and SHAM animals supports the fact that the mouse model has not begun to develop HF in the time frame of this study, and the animals are in a state of cardiac hypertrophy.

Although HF was not initiated in this study, the time frame of the surgical protocol - 8 weeks for HF development - was appropriate as this was based upon the TAC protocol utilised by both Martin et al (2012) and Kho et al (2011). Therefore, future studies should be extended to allow time for HF development. This outcome is further supported by the fact that the animals in this study did not appear to experience as severe a hypertrophic response as was observed in the similar minimally invasive TAC study (Martin, et al., 2012), in which the heart-to-body weight ratio was twice the value in the TAC animals as it was in SHAM.

Further evidence to show that the current study model was successful in promoting cardiac remodelling, which could eventually progress to HF was histological analysis. TAC animals had significantly greater fibrotic tissue in their hearts in comparison to SHAM animals, as well as having larger individual cardiomyocytes - indicative of hypertrophy. There are drawbacks with assessing cardiomyocyte cross sectional area to consider; the cross-sectional area gives only a 2D picture of a 3D cell and ignores the length of the cardiomyocyte, which can vary considerably within the same heart (Bensley, et al., 2016). Alternate methods can be used to account for this, one such option includes using multiple thin serial sections to identify cell boundaries and then reconstruct the images to measure cell volume, but this is technically challenging to achieve (Bruel & Nyengaard, 2005). Another approach is to use much thicker sections -approximately 40µm - and take multiple images at different focal planes, and then the entire sample volume can be reconstructed (Bensley, et al., 2016).

A parameter that was not assessed in the TAC establishment study was blood pressure. Both Kho et al (2011) and Martin et al (2012) identified elevated systolic blood pressure in TAC animals in comparison to SHAM. I anticipate our animals would have displayed similar results, but this was not assessed for the reason that prior to the study I could not be certain how the C57BL/6 mice would respond to TAC surgical intervention. The decision was therefore made to minimise handling of the animals following TAC surgery, and unlike echocardiography, blood

pressure would have been measured via the tail-cuff system with the animals conscious therefore initiating unnecessary stress. For future studies, blood pressure is an imperative parameter to assess.

Although the mice failed to develop HF, the expression of the proteins of the SUMOylation pathway, as well as β_2 AR SUMOylation were examined, since ongoing changes mediated during cardiac remodelling could be important in the development of HF. Similarly to SERCA2a SUMOylation (Kho, et al., 2011), I hypothesised that SUMOylation of the β_2 AR would be diminished by HF and therefore could be changed during the cardiac remodelling process. However, in the TAC establishment study no significant changes in the expression of SUMOylated β_2 AR were observed between TAC and SHAM animals. Other components of the SUMOylation pathway were also assessed; namely SUMO, UBC9 and PIAS γ . The only SUMOylation pathway component that showed significant changes in a state of cardiac remodelling was the E2 conjugating enzyme UBC9. UBC9 was significantly reduced in TAC mice in comparison to SHAM mice. This is in contrast to what is reported by Kho et al (2011), in which no changes were observed in UBC9. However, the changes reported by Kho et al (2011) were in a state of HF and the changes within the TAC establishment study relate to cardiac hypertrophy. Changes in UBC9 have been reported before in disease. Increased UBC9 expression has been reported in both primary lung cancer tissue in comparison to premalignant and/or normal tissue (Li, et al., 2013), and in a mouse model of Alzheimer's disease (Nistico, et al., 2014). Furthermore, elevating UBC9 in mice suffering from cardiomyopathy resulted in decreased fibrosis, reduced hypertrophy and improved cardiac function and survival (Gupta, et al., 2016). Therefore the role of UBC9 in the development of HF still remains to be elucidated, with studies examining UBC9 expression at various time points following TAC surgery being an avenue to explore.

To examine the SUMOylation pathway and SUMOylation of the β_2 AR within a HF model, tissue from the LAD artery balloon occlusion in the pig was provided by the Hajjar group (Tilemann, et al., 2013).

Both paralogues SUMO-1 and SUMO-2/3 were difficult to assess, as although positive controls confirmed the antibody was functional, the signal was weak, regardless of the same amount of protein being loaded for pig tissue lysate

samples and the positive control HEK293T cell lysate sample. This is similar to what I observed in the mouse tissue lysate samples, where no SUMO-1 expression was observed. This would imply that there is a greater concentration of the SUMO paralogues within the cell lysate. The difference between these two lysate preparations is the lysis buffer. HEK293T cells were lysed via manual scraping of cells in 3T3 lysis buffer, whereas the pig and mouse tissue undergo lysis via homogenisation in RIPA buffer. RIPA buffer contains harsh denaturing ionic detergents whereas 3T3 lysis buffer only has milder, non-ionic detergents. These variations in lysis buffer could be responsible for the proteins showing different expression in the different tissue types (Advansta, 2014).

Another contrast between cell lysate and animal tissue lysate existed with the SUMO-2/3 paralogue band presenting at a greater molecular weight in the pig tissue as what was seen in the HEK293T cells. One such reason for this could be the formation of SUMO paralogue chains, which is only feasible for the SUMO-2/3 paralogue (Bylebyl, et al., 2003) (Tatham, et al., 2001)(Ulrich, 2008). In the pig tissues, the antibody could be identifying a series of SUMO-2/3 paralogues within a chain, which would therefore increase the molecular weight. This SUMO-2/3 band indicates that SUMO-2/3 is significantly reduced in the HF animals in comparison to SHAM, but due to the unexpected band shift, further work is needed to confirm this. In support of this notion, SUMO-1 has been shown to be reduced in HF therefore SUMO-2/3 could also be reduced (Kho, et al., 2011) (Tilemann, et al., 2013). Although the SUMO-1 paralogue has a weak signal it does display at the correct molecular weight. No significant difference was identified between TAC and SHAM groups for this protein. This is in contrast to what is reported by Kho et al (2011) who have shown that SUMO-1 expression is reduced in HF. However with the low n numbers of this study (n=3) further assessment of the SUMO paralogues is necessary.

Expression of the E2 conjugating enzyme UBC9 showed a trend to be reduced in HF in comparison to SHAM. This is in agreement to what was observed in the TAC establishment study, with UBC9 expression being significantly reduced in cardiac remodelling, however the immunoblots from the pig cardiac lysate showed a high degree of variability and further n numbers would be required to confirm this finding. Although Kho et al (2011) reported no changes in UBC9, the evidence from

both the TAC mouse study and LAD artery balloon occlusion pig study suggest UBC9 levels could be altered in the development of HF. There was no significant difference observed between HF and SHAM groups for the E3 ligase PIAS γ .

In contrast to what is observed for SUMOylated-SERCA2a - HF reduces SUMOylated SERCA2a expression - the SUMOylated form of the β_2 AR shows a significant increase in HF animals in comparison to SHAM. Although unexpected - as our hypothesis expected β_2 AR SUMOylation to be compromised during HF - this finding does confirm that SUMOylation of other cardiac signalling proteins can be influenced by cardiac disease. It may also be the case that important cardiac proteins may be SUMOylated as a preventative response before HF is reached.

SUMOylation can be positive or negative, dependent upon the protein being modulated. SUMO modification of transcription factors involved in cancer has been shown to have conflicting outcomes; for example, SUMOylation of Myc promotes oncogenesis whereas SUMOylation of MITF prevents it (Yang & Chiang, 2013). SUMOylation is also not limited to influencing one disease state. SERCA2a SUMOylation has been proven to be beneficial in restoring cardiac function during heart failure (Kho, et al., 2011) (Tilemann, et al., 2013), and in contrast SUMOylation of the nuclear receptor PPAR γ promotes diabetes development (Yang & Chiang, 2013). The varying outcomes of protein SUMOylation can be attributed to the complexity of the signalling pathway: substrates can show SUMO paralogue preference (Vertegaal, et al., 2006); PIAS enzymes can show substrate and isoform preference (Sachdev, et al., 2001) (Chun, et al., 2003) (Gocke, et al., 2005); the capacity of SUMO chain formation may mean that similarly to ubiquitination, chains of SUMO molecules may influence protein fate (Wang & Dasso, 2009). It is therefore important to understand the components of the SUMO pathway which are involved in the SUMOylation of individual proteins. With regards to the β_2 AR, the work within this thesis suggests that E3 ligase PIAS γ is vital to mediate receptor SUMOylation.

In conclusion I have identified a significant increase in β_2 AR SUMOylation in the pig LAD artery balloon occlusion model of HF. Additionally the data presented within this chapter is evidence of a reduction in UBC9 expression during the development of HF. The long term aim is to lengthen the time of the TAC study

to promote HF development and thereby allow manipulation of β_2 AR SUMOylation using PIASy adenovirus and determine the phenotypic outcome.

Chapter 6 General Discussion

Based on the work by Kho et al (2011) which identified the SUMOylation of SERCA2a and the subsequent protective role in heart failure (HF), the aims of this thesis were as follows:

- 1) Determine the susceptibility of the β_2 AR to SUMOylation
- 2) Develop a polyclonal antibody capable of detecting SUMOylated- β_2 AR
- 3) Assess the outcome of β_2 AR SUMOylation on receptor signalling
- 4) Examine the changes to β_2 AR SUMOylation in heart failure (HF)

6.1 The Susceptibility of the β_2 AR to SUMOylation

The β_2 AR is a well characterised receptor in terms of post-translational modifications (PTM). As discussed in Chapter 1 - Introduction, it has been shown to be susceptible to phosphorylation, ubiquitination, glycosylation and palmitoylation (Bouvier, et al., 1989) (Vaughan, et al., 2006) (Nobles, et al., 2011) (Shenoy, et al., 2008) (Rands, et al., 1990) (Li, et al., 2017) (Mialet-Perez, et al., 2004) (Ovchinnikov, et al., 1988) (Moffett, et al., 2001) (De Lean, et al., 1980) (O'Dowd, et al., 1988) (Figure 6.1). The identification of SUMOylation of the cardiac signalling protein SERCA2a (Kho, et al., 2011), in addition to SUMOylation of 5 different GPCRs (Tang, et al., 2005) (Dutting, et al., 2011) (Gowran, et al., 2009) (Li & Muma, 2013) (Zhang, et al., 2017) led us to believe that the β_2 AR, which is both a cardiac signalling protein and GPCR, may be a substrate for SUMOylation.

We have confirmed the susceptibility of the β_2 AR to SUMOylation in three ways; firstly, by identifying the SUMO accepting lysines 232 and 235 via peptide array (Figure 3.6 & 6.1), secondly, following overexpression of the SUMO E3 ligase PIASy we observed the ghost band shift (Figure 4.4) which is characteristic of SUMOylation (Park-Sarge & Sarge, 2005), and thirdly, we have confirmed an interaction exists between the β_2 AR and the enzymes of the SUMOylation cascade UBC9 and PIASy via peptide array (Figure 4.5, 4.6 & 6.1). However, the SUMO accepting lysines 232 and 235 may not be the only lysines within the β_2 AR which are capable of covalently binding to SUMO. As mentioned previously, the initial software sequence analysis of the β_2 AR was completed in 2010, and at this time

point the software accounted for amino acids which formed the traditional consensus motif γ KxE/D, (Hay, 2005) (Rodriguez, et al., 2001) (Bernier-Villamor, et al., 2002), phosphorylation-dependent SUMO motifs (PDSMs) (Hietakangas, et al., 2003) (Yang, et al., 2003), and negatively charged amino acid-dependent SUMO motifs (NDSMs) (Yang, et al., 2006). Further amino acid sequences, such as hydrophobic cluster-dependent SUMO motifs (HCSMs) and inverted SUMO motifs (Matic, et al., 2010) (Impens, et al., 2014), are now known to influence substrate susceptibility to SUMOylation, therefore the software sequence analysis for the β_2 AR should be repeated using software which accounts for the novel motifs, possibly leading to identification of further SUMOylation susceptible lysines.

Further research into the role of individual SUMO sites is important. For example, it is known when PKA phosphorylates the β_2 AR this mediates a switch in signalling from G_s to G_i (Daaka, et al., 1997), therefore, in a similar manner, it would be important to identify if SUMOylation of specific lysines initiated tailored signalling changes. Kho et al (2011) determined the role of SUMOylation at lysines 480 and 585 of SERCA2a by generating mutants in which the lysines were mutated to arginines. This exposed SUMOylation at these specific lysines to be responsible for decreasing the ATPase activity of SERCA2a and preventing ubiquitination of the protein. A similar approach should be utilised for the β_2 AR to determine if the signalling changes observed with the SUMOylated receptor are lost when the SUMO-lysines are mutated.

This thesis did not assess what drives the SUMOylation of the β_2 AR. In Chapter 5 - Analysis of β_2 AR SUMOylation in Animal Models of Heart Failure, we identified that in the LAD artery occlusion model of HF, SUMOylation of the receptor was increased in HF pigs in comparison to SHAM pigs. In the HF phenotype levels of circulating catecholamines are increased (Kaumann, et al., 1999), leading to β_2 AR agonist occupation, suggesting that agonist occupation could promote SUMOylation of the β_2 AR. This is a likely scenario, as other post-translational modifications such as phosphorylation and ubiquitination, are also driven by agonist occupation of the receptor (Bouvier, et al., 1989) (Vaughan, et al., 2006) (Nobles, et al., 2011) (Shenoy, et al., 2008). This assumption will be assessed in future cardiomyocyte studies utilising the SUMO- β_2 AR antibody following isoprenaline stimulation. Another avenue to explore is the possibility that

increased levels of oxidative stress associated with the HF phenotype (Keith, et al., 1998) have promoted SUMOylation of the β_2 AR in the HF mice in comparison to SHAM mice. Prior studies have reported that an increase in cellular oxidative stress leads to a global increase in protein SUMOylation identified by mass spectrometry (Zhou, et al., 2004). This hypothesis could be assessed in the cardiomyocytes by enhancing oxidative stress in the cells via the addition of hydrogen peroxide (Ali, et al., 2013) and assessing SUMOylation of the β_2 AR using the SUMO- β_2 AR specific antibody.

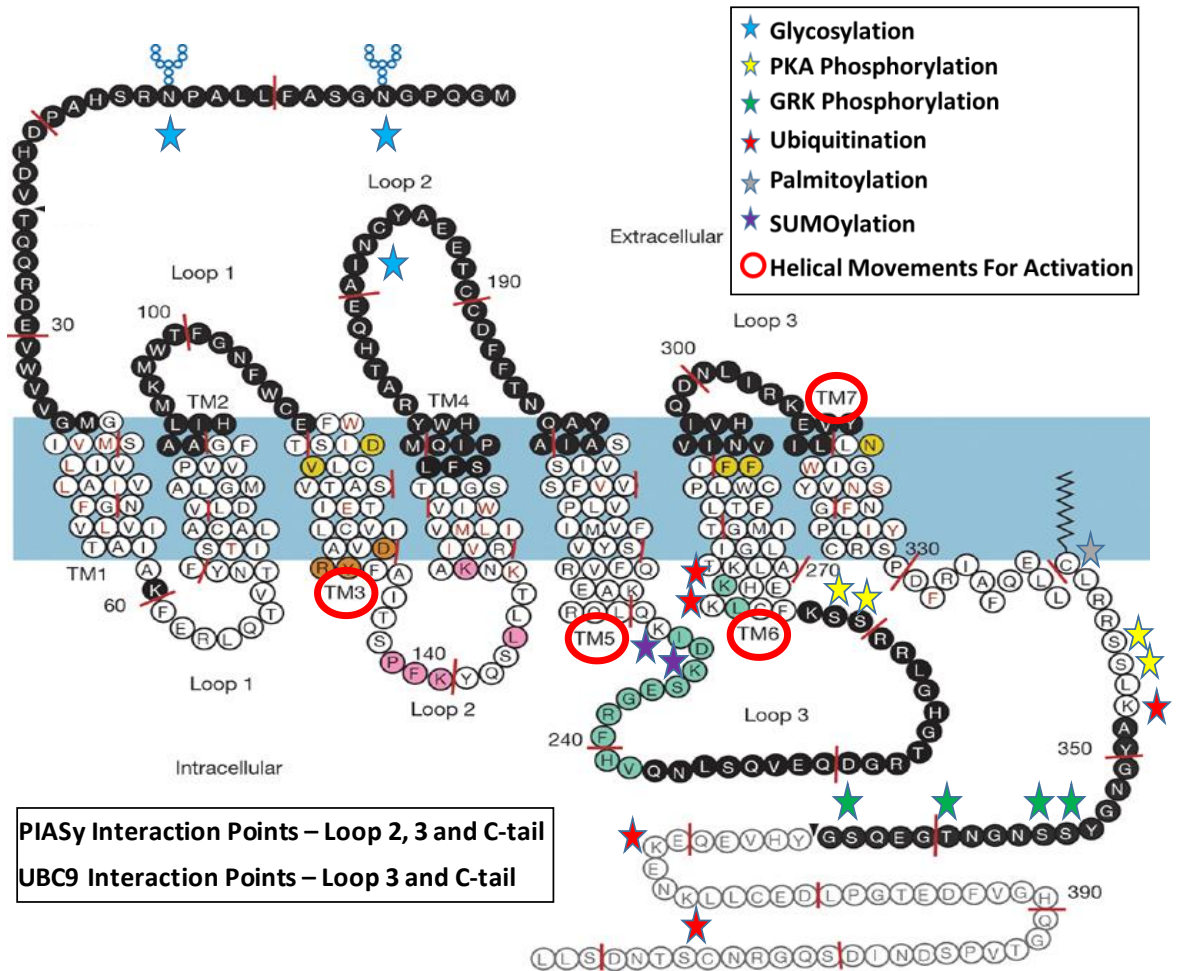


Figure 6.1 Post Translational Modifications and SUMO-Enzyme Interactions of the β_2 AR. The β_2 AR is susceptible to phosphorylation, ubiquitination, glycosylation and palmitoylation. In this thesis, we have identified the susceptibility of the receptor to SUMOylation at lysines 232 and 235. Interaction sites have been identified between the receptor and enzymes of the SUMOylation cascade, PIASy and UBC9. We hypothesise SUMOylation to be mediating β_2 AR signalling changes via sterically hindering the movements of TM5 and TM6, and inhibiting ubiquitination within intracellular loop 3. TM (transmembrane domain). Amino acid abbreviations in appendix.

6.2 SUMO- β_2 AR Polyclonal Antibody Development

Following identification of receptor susceptibility, we aimed to produce a first-in-class SUMO specific antibody against the SUMO-modified form of the β_2 AR. As discussed in Chapter 3 - Production of a SUMO- β_2 AR Specific Polyclonal Antibody, antibodies which have identified the phosphorylated forms of the receptor - phospho- β_2 AR at serines 345/346 (PKA-mediated phosphorylation) and phospho- β_2 AR at serines 355/356 (GRK-mediated phosphorylation) - were vital in exposing β_2 AR signalling pathways (Shenoy, et al., 2006). We wished to produce such an antibody for the SUMOylated form of the receptor.

The SUMO- β_2 AR antibody we have produced in conjunction with Badrilla® is capable of detecting the epitope against which it was raised via peptide array (Figure 3.11), and also detecting the SUMOylated β_2 AR within HEK293 cells following transient transfection of the E3 ligase PIASy (Figure 3.12), and in cardiac tissue lysate (Figure 5.15 & 5.20). This is the first antibody to be reported that is capable of detecting the SUMOylated form of a protein and therefore the antigen design, custom affinity chromatography and testing procedures could be used to allow the generation of a panel of SUMO-substrate specific antibodies. Future steps would involve further validation to assess the precise molecular weight at which SUMO- β_2 AR presents, in addition to modifying the testing procedure to determine whether the custom antibody is capable of deciphering between different SUMO paralogues which modify the β_2 AR.

In addition to paving the way for the production of a panel of SUMO-substrate antibodies, this work also provides the first evidence that an antibody could be raised to recognise an interaction between two proteins. Although SUMOylation is a post-translational modification, the SUMO protein itself has an approximate weight of 11kDa, in contrast to modifications such as phosphorylation, which increase the molecular weight of the substrate by as little as 1kDa (Park-Sarge & Sarge, 2005). This means that the SUMO- β_2 AR antibody production protocol could be utilised to assess protein-protein interactions or dimer formations which are suspected to play a role in disease states.

In HF, there is an increased volume of circulating cTNI, and it has been shown that elevation of troponin within serum correlates with adverse outcomes in HF (Kociol,

et al., 2010) (Wettersten & Maisel, 2015) (Francis, et al., 1995) (Januzzi, et al., 2012). With regards to a diagnostic approach using the SUMO- β_2 AR antibody, there is no evidence in the literature of the receptor being assessed in blood samples, therefore I do not believe the antibody could be used in this manner to assess SUMO- β_2 AR as a biomarker of HF. Based on the work within our study a more invasive approach would be required to assess modification of the receptor by SUMO, such as a myocardial biopsy.

6.3 The Influence of β_2 AR SUMOylation on Receptor Signalling

For many proteins SUMOylation has been shown to influence receptor signalling, and many of these similar changes were observed for the β_2 AR. In Chapter 4 - *In Vitro* SUMOylation of the β_2 AR, we report that SUMOylation of the receptor mediated via overexpression of the E3 ligase PIAS γ was shown to reduce β_2 AR-mediated activation of PKA and subsequent downstream signalling (Figure 4.8, 4.9 & 4.10), inhibit β_2 AR ubiquitination and degradation (Figure 4.11 & 4.16), and delay β_2 AR internalisation (Figure 4.13).

We predict the reduction in β_2 AR-mediated activation of PKA and subsequent downstream signalling (Figure 4.8, 4.9 & 4.10) to be mediated by SUMO covalently binding to lysines 232 and 235 within the third intracellular loop, therefore sterically hindering helical movements in this area that are vital for receptor activation (Ballesteros, et al., 2001) (Yao, et al., 2006) (Figure 6.1). To confirm this hypothesis the crystal structure of the SUMO modified β_2 AR would be essential.

The PTMs ubiquitination and SUMOylation have been reported to compete for lysine residues for many proteins, two examples including SERCA2a (Kho, et al., 2011), and I κ B α (Desterro, et al., 1998), which in both cases SUMOylation causes a reduction in ubiquitination and protein degradation. This pattern was also observed for the β_2 AR (Figure 4.11 & 4.16). However, ubiquitination of the β_2 AR occurs at distinct lysines - K263, K270, K348, K372, K375 (Shenoy, et al., 2008) - from those identified as the SUMO susceptible lysines in this thesis - K232 and K235. However, we predict that the presence of the bulky SUMO modification within the same intracellular loop at a 30 amino acid proximity to the

ubiquitination sites could act to sterically hinder the process by preventing ubiquitin machinery such as NEDD4 (Shenoy, et al., 2008) from accessing the lysines (Figure 6.1). Furthermore, the cytoplasmic tail may contain lysines which are susceptible to both SUMO and ubiquitin modification, that were not identified in the initial software sequence analysis. Future work would assess the susceptibility of the β_2 AR to SUMOylation at lysines out with 232 and 235.

SUMOylation of the β_2 AR was also shown to delay internalisation of the receptor (Figure 4.13), a pattern which was also reported for other proteins namely DISC1 (Tankou, et al., 2016), LEF-1 (Sachdev, et al., 2001), and the GluK2 subunit (Chamberlain, et al., 2012). Although the interaction between β_2 AR and β -arrestin which is vital for internalisation was not influenced by SUMOylation of the β_2 AR (Figure 4.24), the β -arrestin itself has been shown to be susceptible to SUMOylation (Xiao, et al., 2015). It is therefore possible that in the internalisation experiments, transient transfection of the E3 ligase PIASy may be leading to the modification of both the β_2 AR and β -arrestin, with the latter influencing the internalisation process. It will be imperative to assess the SUMOylation status of β -arrestin in the presence of PIASy.

Although the work within this thesis focuses on cardiovascular disease the changes outlined above could be important for other disease states that are out with the scope of this thesis. In arthritis, β_2 AR signalling has conflicting outcomes, either promoting or inhibiting inflammation in autoimmunity. It has been discovered that time-dependent phosphorylation patterns of the β_2 AR after induction of arthritis in an animal model influenced the disease outcomes (Lorton, et al., 2017). As we have identified that SUMOylation of the receptor leads to a reduction in PKA-mediated phosphorylation, and dampens downstream signalling, this could shed new light on arthritis research. Another area of research which could be impacted by our findings is work focussing on Alzheimer's disease. Amyloid plaque is primary cause of Alzheimer's disease and activation of the β_2 AR has been shown to lead to the production of amyloid plaque. This is dependent upon agonist-induced endocytosis of the β_2 AR, and as we have shown SUMOylation can influence the trafficking of the receptor, these finding could impact upon the ability of the β_2 AR to promote plaque formation (Ni, et al., 2006).

6.4 SUMOylation of the β_2 AR in HF

Kho et al (2011) identified that cardiac signalling protein SERCA2a is modified by SUMO-1, and that this modification is reduced in the pathogenesis of HF. The group proved that restoring SUMO-1 expression via adenoviral gene transfer is beneficial as it improves cardiac function and also stabilizes heart weight to body weight ratio - indicative of reduced hypertrophic response. This work was pivotal in our belief that the β_2 AR SUMOylation may also be diminished in the HF phenotype and therefore could be changed during the cardiac remodelling process.

In Chapter 5 - Analysis of β_2 AR SUMOylation in Animal Models of Heart Failure, we assessed SUMOylation of the β_2 AR and SUMOylation pathway components in two animal models of HF; transverse aortic constriction (TAC) pressure overload HF model in mice and the left anterior descending (LAD) artery balloon occlusion ischemic HF model in pigs. In the TAC pressure overload establishment study no significant changes in the expression of SUMOylated β_2 AR were observed between TAC and SHAM animals (Figure 5.15), however in the LAD artery balloon occlusion ischemic study the SUMOylated form of the β_2 AR shows a significant increase in HF animals in comparison to SHAM (Figure 5.20). Although unexpected - as our hypothesis expected β_2 AR SUMOylation to be compromised during HF - this finding does confirm that SUMOylation of other cardiac signalling proteins can be influenced by cardiac disease.

It is important to consider why the β_2 AR may be SUMOylated in HF. In failing human hearts although the β_1 AR is downregulated, the abundance of β_2 AR remains unchanged (Bristow, et al., 1986) (Jensen, et al., 2009). In Chapter 1 - Introduction, the cardio-protective role for β_2 AR is discussed: in isolated myocytes β_2 AR stimulation protects against stress-induced apoptosis (Chelsey, et al., 2000); in a rat model of myocardial infarction-induced HF, selective activation of the β_2 AR improves cardiac function and reduces apoptosis (Ahmet, et al., 2004); and in HF there is enhanced signalling of β_2 AR via the G_i pathway, which reduces the positive inotropic effects of β_1 AR stimulation and activates cardio-protective signalling pathways (Bohm, et al., 1994) (Chelsey, et al., 2000) (Feldman, et al., 1988) (Zhu, et al., 2001). With regards to the results presented within Chapter 4 - *In Vitro* SUMOylation of the β_2 AR, SUMOylation of the receptor leads to a reduction in degradation of the receptor (Figure 4.11). This would therefore

promote cardio-protective effects of the receptor by maintaining receptor levels. However, in HF there is enhanced signalling of β_2 AR via the inhibitory G_i protein which is cardio-protective. In contrast to this notion, the data presented in Chapter 4 - *In Vitro* SUMOylation of the β_2 AR, reveals that SUMOylation of the receptor causes a reduction in the switch from G_s to G_i signalling, and therefore SUMOylation of the β_2 AR would inhibit this cardio-protective effect.

In addition to the traditional opposing roles of the BARs - β_2 AR cardio-protective and β_1 AR cardio-toxic - the receptors also exist in distinct locations, described in detail in Chapter 1 - Introduction. The β_2 AR is exclusively localised to T-tubules whereas β_1 AR are present in both the domes and T-tubules of the cardiomyocyte (Nikolaev, et al., 2010). Furthermore, spatial compartmentation of the cAMP signal can influence the outcome of receptor stimulation, with β_1 AR stimulation promoting cAMP production which propagates throughout the entire cell, and β_2 AR stimulation leading to locally confined cAMP at the T-tubules (Nikolaev, et al., 2006). However, this organisation is disrupted during HF leading to the β_2 AR signals now manifesting in a similar manner to that of the β_1 AR, contributing to the cardio-toxic effects (Xiao, 2001) (Engelhardt, et al., 1999) (Communal, et al., 1999)(del Monte, et al., 1993) (Dorn, et al., 1999). However, as we have identified that the SUMOylated form of the β_2 AR displays depressed signalling, this modification which is increased in HF could be protective, to inhibit the deleterious switch to β_1 AR-like signalling.

The role of β_2 AR SUMOylation in HF remains speculative. Idealistically the best way to examine the influence of β_2 AR SUMOylation would be to assess the impact of PIASy adeno-associated viral gene transfer on animals which have undergone either the TAC surgery or LAD artery balloon occlusion, to determine if enhanced SUMOylation of the receptor worsens the HF phenotype or prevents its development. Following confirmation of the role of β_2 AR SUMOylation it would be possible to follow the route of the SERCA2a SUMOylation research. Kho et al (2015) identified a small molecule, N106, which promotes SUMOylation of SERCA2a by directly activating the SUMO E1 activating enzyme. In a mouse model of HF, this molecule improves ventricular function. Once the outcome of β_2 AR SUMOylation in HF is confirmed we could manipulate SUMOylation of the receptor in a similar

manner to this, possibly leading to a potential therapeutic strategy for HF treatment.

6.5 Final Conclusion

To conclude we present the first evidence that the β_2 AR is susceptible to SUMOylation and mediate this change in *in vitro* studies. We have uncovered that this novel post-translational modification acts to influence the receptors downstream signalling, desensitisation and degradation which could be important for a range of disease states. We have designed a first-in-class SUMO- β_2 AR antibody - which paves the way for a panel of SUMO specific antibodies and antibodies which can identify protein-protein interactions - and utilised it to assess SUMOylation of the β_2 AR in animal models of HF. In line with our hypothesis, SUMOylation does influence the β_2 AR in the HF phenotype, although not a decrease in SUMOylation as was expected, but an increase. Future work in animal models promoting SUMOylation of the receptor is vital to assess the role of this important post-translational modification of the β_2 AR, allowing us to harness this change as a therapeutic treatment for HF.

Chapter 7 Appendix

Amino Acid	1 Letter Abbreviation
Alanine	A
Arginine	R
Asparagine	N
Aspartic acid	D
Cysteine	C
Glutamic acid	E
Glutamine	Q
Glycine	G
Histidine	H
Isoleucine	I
Leucine	L
Lysine	K
Methionine	M
Phenylalanine	F
Proline	P
Serine	S
Threonine	T
Tryptophan	W
Tyrosine	Y
Valine	V

(i-base.info, 2017)

Chapter 8 References

- Abcam. (2017). *www.abcam.com*. Retrieved March 31, 2017, from <http://www.abcam.com/protocols/ihc-antigen-retrieval-protocol>
- Advansta. (2014). *https://advansta.com*. Retrieved April 12, 2017, from <https://advansta.com/detergent-lysis-buffer/>
- AHA. (2016, March 25). *Recognizing Advanced Heart Failure and Knowing Your Options*. Retrieved April 14, 2017, from http://www.heart.org/HEARTORG/Conditions/HeartFailure/Recognizing-Advanced-Heart-Failure-and-Knowing-Your-Options_UCM_441926_Article.jsp#.WPC2J2nyvcs
- Ahmed, M. (2015). *http://myheart.net*. Retrieved March 30, 2017, from <http://myheart.net/articles/the-lad-artery/>
- Ahmet, I., Krawczyk, M., Heller, P., Moon, C., Lakatta, E., & Talan, M. (2004). Beneficial effects of chronic pharmacological manipulation of beta-adrenoreceptor subtype signaling in rodent dilated ischemic cardiomyopathy. *Circulation*, 1083-1090.
- Alberts, B., Johnson, A., Lewis, J., Walter, P., Raff, M., & Roberts, K. (2002). Chapter 24. In *Molecular Biology of the Cell (4th ed.)*. . Routledge: ISBN.
- Ali, M., Kandasamy, A., Fan, X., & Schulz, R. (2013). Hydrogen peroxide-induced necrotic cell death in cardiomyocytes is independent of matrix metalloproteinase-2. *Toxicol In Vitro*, 1686-1692.
- Alousi, A., Jasper, J., Insel, P., & Motuski, H. (1991). Stoichiometry of receptor-Gs-adenylate cyclase interactions. *FASEB J*(5), 2300-2303.
- Ambrosy, A., Fonarow, G., Butler, J., Chioncel, O., Greene, S., Vaduganathan, M., . . . Gheorghiade, M. (2014). The global health and economic burden of hospitalizations for heart failure: lessons learned from hospitalized heart failure registries. *Journal of the American College of Cardiology* (63), 1123-1133.
- Anderson, H., Galyean, R., McClintock, R., & Rivier, J. (1984). Reversed-phase high-performance liquid chromatography: preparative purification of synthetic peptides. *J Chromatogr*(288), 303-328.
- Angers, S., Salahpour, A., Joly, E., Hilaiet, S., Chelsky, D., Dennis, M., & Bouvier, M. (2000). Detection of beta 2-adrenergic receptor dimerization in living cells using bioluminescence resonance energy transfer (BRET). *Proc Natl Acad Sci U S A*(97), 3684-3689.
- Angres, S., Salahpour, A., Joly, E., Hilaiet, S., Chelsky, D., Dennis, M., & Bouvier, M. (2000). Detection of beta 2 adrenergic receptor dimerisation in living cells using bioluminescence resonance energy transfer (BRET). *Proc Natl Acad Sci*(97), 3684-3689.
- Annderson, R., Yanni, J., Boyett, M., Chandler, N., & Dobrzynski, H. (2009). The anatomy of the cardiac conduction system. *Clinical Anatomy*(22), 93-113.

- Apionishev, S., Malhotra, D., Raghavachari, S., Tanda, S., & Rasooly, R. (2001). The Drosophila UBC9 homologue lesswright mediates the disjunction of homologues in meiosis I. *Genes Cells*(6), 215-224.
- Ardehali, H., Bolli, R., & Losordo, D. (2013). Transverse Aortic Constriction: a Model to Study Heart Failure in Small Animals. In S. Verma, P. Krishnamurthy, & R. Kishore (Eds.), *Manual of Research Techniques in Cardiovascular Medicine* (pp. 164-169). John Wiley & Sons, Ltd.
- Arur, S., & Schedl, T. (2014). Generation and purification of highly specific antibodies for detecting post-translationally modified proteins in vivo. *Nature Protocols*(9), 375-395.
- Asahi, M., Nakayama, H., Tada, M., & Otsu, K. (2003). Regulation of sarco(endo)plasmic reticulum Ca²⁺ adenosine triphosphatase by phospholamban and sarcolipin: implication for cardiac hypertrophy and failure. *Trends in cardiovascular medicine*(13), 152-157.
- Ayaydin, F., & Dasso, M. (2004). Distinct in vivo dynamics of vertebrate SUMO paralogues. *Mol. Biol. Cell*(15), 5208-5218.
- Bachant, J., Alacasabas, A., Blat, Y., Kleckner, N., & Elledge, S. (2002). The SUMO-1 isopeptidase Smt4 is linked to centromeric cohesion through SUMO-1 modification of DNA topoisomerase II. *Mol Cell*(9), 1169-1182.
- Baillie, G., Sood, A., McPhee, I., Gall, I., Perry, S., Lefkowitz, R., & Houslay, M. (2003). beta-Arrestin-mediated PDE4 cAMP phosphodiesterase recruitment regulates beta-adrenoceptor switching from G_s to G_i. *Proc Natl Acad Sci USA*(100), 940-945.
- Ballesteros, J., Jensen, A., Liapakis, G., Rasmussen, S., Shi, L., Gether, U., & Javtich, A. (2001). Activation of the B₂-Adrenergic Receptor Involves Disruption of an Ionic Lock between the Cytoplasmic Ends of Transmembrane Segments 3 and 6. *Journal of Biological Chemistry*(276), 29171-29177.
- Bang, I., & Choi, H. (2015). Structural Features of B₂ Adrenergic Receptor: Crystal Structures and Beyond. *Mol Cells*, 105-111.
- Bang, I., & Choi, H. (2015). Structural Features of β₂ Adrenergic Receptor:Crystal Structures and Beyond. *Mol. Cells*(38), 105-111.
- Barak, L., Ferguson, S., Zhang, J., Martenson, C., Meyer, T., & Caron, M. (1997). Internal trafficking and surface mobility of a functionally intact beta 2 adrenergic receptor green fluorescent protein conjugate . *Mol Pharmacol*(51), 177-184.
- Bawa-Khalfe, T., & Yeh, E. (2010). SUMO losing balance: SUMO proteases disrupt SUMO homeostasis to facilitate cancer development and progression. *Genes Cancer*(1), 748-752.
- BCBST. (2016). *BlueCross BlueShield of Tennessee Medical Policy Manual*. Retrieved April 14, 2017, from http://www.bcbst.com/mpmanual/Surgical_Ventricular_Restoration.htm

- Beckerman, J. (2016, October 6). *Heart Disease and Diuretics*. Retrieved April 14, 2017, from <http://www.webmd.com/heart-disease/guide/medicine-diuretics#1>
- Benovic, J., Kuhn, H., Weyand, I., Codina, J., Caron, M., & Lefkowitz, R. (1987). Functional desensitisation of the isolated beta adrenergic receptor by the beta adrenergic receptor kinase: potential role of an analog of the retinal protein arrestin (48kDa protein). *PNAS*(84), 8879-8882.
- Benovic, J., Mayor, F., Staniszewski, C., Lefkowitz, R., & Caron, M. (1987). Purification and characterisation of the beta adrenergic receptor kinase. *J Biol Chem*(262), 9026-9032.
- Bensley, J., Matteo, R., Harding, R., & Black, M. (2016). Three-dimensional direct measurement of cardiomyocyte volume, nuclearity, and ploidy in thick histological sections. *Scientific Reports* (6), 23756-23766.
- Benya, R., Kusui, T., Katsuno, T., Tsuda, T., Mantey, S., Battey, J., & Jensen, R. (2000). Glycosylation of the gastrin releasing peptide receptor and its effect on expression, G protein coupling, and receptor modulatory processes. *Mol Pharmacol*(58), 1490-1501.
- Bergelson, J., Cunningham, J., Droguett, G., Kurt-Jones, E., Krivthivas, A., Hong, J., . . . Finberg, R. (1997). Isolation of a common receptor for coxsackie B viruses and adenoviruses 2 and 5. *Science*(275), 1320-1323.
- Bernier-Villamor, V., Sampson, D., Matunis, M., & Lima, C. (2002). Structural basis for E2-mediated SUMO conjugation revealed by a complex between ubiquitin conjugating enzyme UBC9 and RanGAP1. *Cell*(108), 345-356.
- Bernstein, D., Fajardo, G., Zhao, M., Urashima, T., Powers, J., Berry, G., & Kobilka, B. (2005). Differential cardioprotective/cardiotoxic effects mediated by beta-adrenergic receptor subtypes. *Am J Physiol Heart Circ Physiol*, 2441-2449.
- Bers, D. (2002). Cardiac excitation-contraction coupling. *Nature*(415), 198-205.
- Bers, D. (2002). Cardiac Na/Ca exchange function in rabbit, mouse and man: what's the difference? *J Mol Cell Cardiol*(34), 369-373.
- Bettermann, K., Benesch, M., Weis, S., & Haybaeck, J. (2012). SUMOylation in carcinogenesis. *Cancer Letters*(316), 113-125.
- Beuckelmann, D., Nabauer, M., Kruger, C., & Erdmann, E. (1995). Altered diastolic [Ca²⁺]_i handling in human ventricular myocytes from patients with terminal heart failure. *American Heart Journal*(129), 684-689.
- BHF. (2015). *Heart Statistics*. Retrieved April 14, 2017, from <https://www.bhf.org.uk/research/heart-statistics>
- Billington, C., & Penn, R. (2003). Signaling and regulation of G protein coupled receptors in airway smooth muscle. *Resp Res*(4), 2.
- Black, J., Crowther, A., Shanks, R., Smith, L., & Dornhorst, A. (1964). A new adrenergic betareceptor antagonist. *The Lancet*, 1080-1081.

- Bodi, I., Mikala, G., Koch, S., Akhter, S., & Schwartz, A. (2005). The L-type calcium channel in the heart: the beat goes on. *J Clin Invest*(115), 3306-3317.
- Bodor, G., Oakeley, A., Allen, P., Crimmins, D., Ladensons, J., & Anderson, P. (2001). Troponin I phosphorylation in the normal and failing adult human heart. *Circulation Research*(104), 1424-1429.
- Bohm, M., Eschenhagen, T., Gierschlik, P., Larisch, K., Lensche, H., Mende, U., . . . Steinfath, M. (1994). Radioimmunochemical quantification of Gi alpha in right and left ventricles from patients with ischaemic and dilated cardiomyopathy and predominant left ventricular failure. *J Mol Cell Cardiol*, 133-149.
- Bohren, K., Nadkarni, V., Song, J., Gabbay, K., & Owerbach, D. (2004). A M55V polymorphism in a novel SUMO gene (SUMO-4) differentially activates heat shock transcription factors and is associated with susceptibility to type 1 diabetes mellitus. *J Biol Chem*(279), 27233-27238.
- Bolger, G., Baillie, G., Li, X., Lynch, M., Herzyk, P., Mohamaed, A., . . . Houslay, M. (2006). Scanning peptide array analyses identify overlapping binding sites for the signalling scaffold proteins, B-arrestin and RACK1, in cAMP specific phosphodiesterase PDE4D5. *Biochemical Journal*(398), 23-36.
- Bouvier, M., Collins, S. O., Campbell, P., de Blasi, A., Kobilka, B., MacGregor, C., . . . Lefkowitz, R. (1989). Two distinct pathways for cAMP mediated down regulation of the B2 adrenergic receptor. Phosphorylation of the receptor and regulation of its mRNA level. *J Biol Chem*(264), 16786-16792.
- Bradford, M. (1976). A rapid and sensitive method for the quantification of microgram quantities of protein utilizing the principle of protein-dye binding. *Anal Biochem*(72), 248-254.
- Bristow, M., Ginsburg, R., Umans, V., Fowler, M., Minobe, W., Rasmussen, R., . . . Shah, P. (1986). Beta 1- and beta 2-adrenergic-receptor subpopulations in nonfailing and failing human ventricular myocardium: coupling of both receptor subtypes to muscle contraction and selective beta 1-receptor down-regulation in heart failure. *Circ Res*, 297-309.
- Bristow, M., Minobe, W., Reynolds, M., Port, J., Rasmussen, R., Ray, P., & Feldman, A. (1993). Reduced beta 1 receptor messenger RNA abundance in the failing human heart. *J Clin Invest*(92), 2737-2745.
- Bruce, D. (2014). *Abcam p65 and the NF-κB inflammatory pathway*. Retrieved July 4, 2017, from <http://www.abcam.com/cancer/p65-and-the-nf-b-inflammatory-pathway>
- Bruel, A., & Nyengaard, J. (2005). Design-based stereological estimation of the total number of cardiac myocytes in histological sections. *Basic Res Cardiol*(4), 311-319.

- Bueno, O., De Windt, L., Tymitz, K., Witt, S., Kimball, T., Klevitsky, R., . . . Molkentin, J. (2000). The MEK1-ERK1/2 signaling pathway promotes compensated cardiac hypertrophy in transgenic mice. *EMBO J*(19), 6341-6350.
- Bylebyl, G. R., Belichenko, I., & Johnson, E. (2003). The SUMO isopeptidase Ulp2 prevents accumulation of SUMO chains in yeast. *J. Biol. Chem*(278), 44113-44120.
- Calebiro, D., Nikolaev, V., Gagliani, M., Fillippis, T., Dees, C., Tacchetti, C., . . . Lohse, M. (2009). Persistent cAMP-Signals Triggered by Internalized G-Protein-Coupled Receptors. *PLOS Biology*, 1371-1381.
- Calebiro, D., Rieken, F., Wagner, J., Sungakaworn, T., Zabel, U., Borzi, A., . . . Lohse, M. (2013). Single-molecule analysis of fluorescently labeled G-protein-coupled receptors reveals complexes with distinct dynamics and organization. *Proc Natl Acad Sci U S A*(110), 743-748.
- Campbell, N., Reece, J., Urry, L., Cain, M., Wasserman, S., Minorsky, P., & Jackson, R. (2008). Circulation and Gas Exchange. In B. Wilbur (Ed.), *Biology Eighth Edition* (pp. 898-906). San Francisco: Pearson.
- Campbell, T., & MacDonald, P. (2003). Digoxin in heart failure and cardiac arrhythmias. *Med J Aust*(179), 98-102.
- Castelvecchio, S., Menincanti, L., & Donato, M. (2010). Surgical Ventricular Restoration to Reverse Left Ventricular Remodeling. *Curr Cardiol Reviews*(6), 15-23.
- Chamberlain, S., Gonzalez-Gonzalez, I., Wilkinson, K., Konopacki, F., Kantamneni, S., Henley, J., & Mellor, J. (2012). SUMOylation and phosphorylation of GluK2 regulate kainate receptor trafficking and synaptic plasticity. *Nat Neurosci*(15), 845-852.
- Chang, P., Fitzgerald, L., Geelen, A., Izumiya, Y., Ellison, T., Wang, D., . . . Kung, H. (2009). KRAB domain-associated protein-1 as a latency regulator for Kaposi's sarcoma-associated herpesvirus and its modulation by the viral protein kinase. *Cancer Research*(69), 5681-5689.
- Chelsey, A., Lundberg, M., Asai, T., Xiao, R., Ohtani, S., Lakatta, E., & Crow, M. (2000). The beta(2)-adrenergic receptor delivers an antiapoptotic signal to cardiac myocytes through G(i)-dependent coupling to phosphatidylinositol 3'-kinase. *Circ Res*, 1172-1179.
- Chen, M., & Malbon, C. (2009). G protein coupled receptor associated A-kinase anchoring proteins AKAP5 and AKAP12: differential trafficking and distribution. *Cell signal*(21), 136-142.
- Chen, Y., Guo, H., Xu, D., Xu, X., Wang, H., Hu, X., . . . Weir, K. (2012). Left ventricular failure produces profound lung remodeling and pulmonary hypertension in mice: heart failure causes severe lung disease. *Hypertension*(59), 1170-1178.

- Chen, Y., Li, Z., Zhu, M., & Cao, Y. (2012). Effects of exercise training on left ventricular remodelling in heart failure patients: an updated meta-analysis of randomised controlled trials. *Int J Clin Pract*(66), 782-791.
- Chen, Z., Stokes, D., & Jones, L. (2005). Role of Leucine 31 of Phospholamban in Structural and Functional Interactions with the Ca²⁺ Pump of Cardiac Sarcoplasmic Reticulum. *The Journal of Biological Chemistry*(280), 10530-10539.
- Cherevoz, V., Rosenbaum, D., Hanson, M., Rasmussen, S., Thian, F., Kobilka, T., . . . Stevens, R. (2007). High resolution crystal structure of an engineered human β_2 adrenergic G protein coupled receptor. *Science*(318), 1258-1265.
- Chistiakov, D., Ashwell, K., Orekhov, A., & Bobryshev, Y. (2015). Innervation of the arterial wall and its modification in atherosclerosis. *Autonomic Neuroscience*, 7-11.
- Choe, H. W., Kim, Y., Park, J., Morizumi, T., Pai, E., Krauss, N., . . . Ernst, O. (2011). Crystal structure of metarhodopsin II. *Nature*(471), 651-655.
- Choi, J., Park, J., Park, S., Lee, H., Han, S., Park, K., & Suh, Y. (2015). Regulation of mGluR7 Trafficking by SUMOylation in Neurons. *Neuropharmacology*(102), 229-235.
- Chun, T., Itoh, H., Subramanian, L., Iniquez-Lluhi, J., & Nakao, K. (2003). Modification of GATA-2 transcriptional activity in endothelial cells by the SUMO E3 ligase PIASy. *Circ Res*(92), 1201-1208.
- Chung, K., Rasmussen, S., Liu, T., Li, S., Devree, B., Chae, P., . . . Sunahara, R. (2011). Conformational changes in the G protein Gs induced by the β_2 adrenergic receptor. *Nature*(477), 611-615.
- Cleland, J., Swedberg, K., Follath, F., Komajda, M., Cohen-Solal, A., Aguilar, J., . . . Mason, J. (2003). The EuroHeart Failure survey programme—a survey on the quality of care among patients with heart failure in Europe. *European Heart Journal*(24), 442-463.
- Cleveland, J., Gemmell, I., Khand, A., & Boddy, A. (1999). Is the prognosis of heart failure improving? *European Journal of Heart Failure*(1), 229-241.
- Collins, S., Lohse, M., O'Dowd, B., Caron, M., & Lefkowitz, R. (1991). Structure and regulation of G protein coupled receptors: the beta 2 adrenergic receptor as a model. *Vitam Horm*(46), 1-39.
- Colucci, W. (2016, July 12). *Hydralazine plus nitrate therapy in patients with heart failure with reduced ejection fraction*. Retrieved April 14, 2017, from <http://www.uptodate.com/contents/hydralazine-plus-nitrate-therapy-in-patients-with-heart-failure-with-reduced-ejection-fraction>
- Coman, O., Paunescu, H., Ghita, I., Coman, L., Badararu, A., & Fulga, I. (2009). Beta 3 adrenergic receptors: molecular, histological, functional and pharmacological approaches. *Romanian Journal of Morphology and Embryology*, 169-179.

- Communal, C., Singh, K., Sawyer, D., & Colucci, W. (1999). Opposing effects of beta(1)- and beta(2)-adrenergic receptors on cardiac myocyte apoptosis : role of a pertussis toxin-sensitive G protein. *Circulation*(22), 2210-2212.
- Communal, C., Singh, K., Sawyer, D., & Colucci, W. (1999). Opposing effects of beta(1)- and beta(2)-adrenergic receptors on cardiac myocyte apoptosis: role of a pertussis toxin-sensitive G protein. *Circulation*, 2210-2212.
- Cong, M., Perry, S., Hu, L., Hanson, P., Claing, A., & Lefkowitz, R. (2001). Binding of the beta 2 adrenergic receptor to N ethylmaleimide-sensitive factor regulates receptor recycling. *J Biol Chem*(276), 45145-41152.
- Conway, B., Minor, L., Xu, J., Gunnet, J., DeBiasio, R., D'Andrea, M., . . . Demarest, K. (1999). Quantification of G-Protein Coupled Receptor Internalization Using G-Protein Coupled Receptor-Green Fluorescent Protein Conjugates with the ArrayScantrade mark High-Content Screening System. *J Biomol Screen*(4), 75-86.
- Cooper, G. (2000). Protein Degradation. In G. Cooper (Ed.), *The Cell: A Molecular Approach*. Sunderland: Sinauer Associates.
- Cowie, M., Lacey, L., & Tabberer, M. (2005). Heart Failure After Myocardial Infarction: A Neglected Problem? *British Journal of Cardiology* (12), 205-208.
- Craig, T., Anderson, D., Evans, A., Girach, F., & Henley, J. (2015). SUMOylation of Syntaxin1A regulates presynaptic endocytosis. *Scientific Reports* (5), 1-11.
- Crick, S., Sheppard, M., Ho, S., Gebstein, L., & Anderson, R. (1998). Anatomy of the pig heart : comparisons with normal human cardiac structure. *J Anat*(193), 105-119.
- Daaka, Y., Luttrell, L., & Leflowitz, R. (1997). Switching of the coupling of the adrenergic receptor to different G-proteins by protein kinase A. *Nature*(390), 88-91.
- Day, S., Westfall, M., & Metzger, J. (2007). Tuning cardiac performance in ischemic heart disease and failure by modulating myofilament function. *Mol Med*(9), 911-921.
- De Lean, A., Stadel, J., & Lefkowitz, R. (1980). A ternary complex model explains the agonist specific binding properties of the adenylate cyclase coupled beta adrenergic receptor. *J Biol Chem*(255), 7108-7117.
- deAlmeida, A., van Oort, R., & Wehrens, X. (2010). Transverse Aortic Constriction in Mice. *J Vis Exp*(38), 1729-1734.
- del Monte, F., Kaumann, A., Poole-Wilson, P., Wynne, D., Pepper, J., & Harding, S. (1993). Coexistence of functioning beta 1- and beta 2-adrenoceptors in single myocytes from human ventricle. *Circulation*(88), 854-863.
- Demarque, M., Naverddine, K., Neyret-Kahn, H., Andrieux, A., Danenberg, E., Jouvion, G., . . . Dejean, A. (2011). Sumoylation by Ubc9 regulates the

stem cell compartment and structure and function of the intestinal epithelium in mice. *Gastroenterology*(140), 286-296.

- Denolin, H., Kuhn, H., Krayenbuehl, H., Loogen, F., & Reale, A. (1983). The definition of heart failure. *European Heart Journal*(4), 445-448.
- Desterro, J., Rodriguez, M. K., & R.T, H. (1999). Identification of the enzyme required for the activation of the small ubiquitin like proteon SUMO-1. *J Biol Chem*(274), 10618-10624.
- Desterro, J., Rodriguez, M., & Hay, R. (1998). SUMO-1 modification of IkkappaBalpha inhibits NF-kappaB activation. *Mol Cell*(2), 233-239.
- Desterro, J., Thomson, J., & Hay, R. (1997). Ubch9 conjugates SUMO but not ubiquitin . *FEBS letters*(417), 297-300.
- DeWire, S., Ahn, S., Lefkowitz, R., & Shenoy, S. (2007). β -arrestins and cell signaling. *Annu Rev Physiol*(69), 483-510.
- Diagnostics, N. (2004). <http://ehs.psu.edu>. Retrieved March 16, 2017, from http://ehs.psu.edu/sites/ehs/files/lsc_theory_of_operation_part_1.pdf
- Dickstein, K., Cohen-Solal, A., Filippatos, G., McMurray, J., Ponikowski, P., Poole-Wilson, P., . . . Swedberg, K. (2008). ESC guidelines for the diagnosis and treatment of acute and chronic heart failure 2008. *European Society of Cardiology* (29), 2388-2442.
- Diez, J., Lopez, B., Gonzalez, A., & Querejeta, R. (2007). The role of myocardial collagen network in hypertensive heart disease. *Curr Hyperten Rev*(3), 1-7.
- Djurovic, S., Iversen, N., Jeansson, S., Hoover, F., & Christensen, G. (2004). Comparison of nonviral transfection and adeno-associated viral transduction on cardiomyocytes. *Mol Biotechnol*(28), 21-32.
- Doerks, T., Copley, R., Schultz, J., Ponting, C., & Bork, P. (2002). Systematic identification of novel proten domain families associated with nuclear functions. *Genome Res*(12), 47-56.
- Dorn, G., Tepe, N., Lorenz, J., Koch, W., & Liggett, S. (1999). Low- and high-level transgenic expression of beta2-adrenergic receptors differentially affect cardiac hypertrophy and function in Galphaq-overexpressing mice. *PNAS*(11), 6400-6405.
- Dorval, V., & Fraser, P. (2006). Small ubiquitin-like modifier (SUMO) modification of natively unfolded proteins tau and α -synuclein. *Journal of Biological Chemistry*(281), 9919-9924.
- Downes, G., & Gautam, N. (1999). The G protein subunit gene families . *Genomics*(62), 544-552.
- Dumitru, I. (2016, January 11). *Heart Failure Treatment & Management*. Retrieved April 14, 2017, from <http://emedicine.medscape.com/article/163062-treatment#d1>

- Dutting, E., Schroder-Kress, N., Sticht, H., & Enz, R. (2011). SUMO E3 ligases are expressed in the retina and regulate SUMOylation of the metabotropic glutamate receptor 8b. *BioChem J*(435), 365-371.
- Duval, D., Duval, G., Kedinger, C., Poch, O., & Boeuf, H. (2003). The 'PINIT' motif, of a newly identified conserved domain of the PIAS protein family, is essential for nuclear retention of PIAS3L. *FEBS Letters*(554), 111-118.
- Eisner, D., & Trafford, A. (2002). Heart Failure and the Ryanodine Receptor. *Circ Res*(91), 979-981.
- Engelhardt, S., Hein, L., Wiesmann, F., & Lohse, M. (1999). Progressive hypertrophy and heart failure in beta1-adrenergic receptor transgenic mice. *PNAS*(12), 7059-7064.
- Espinoza-Fonesca, L., Autry, J., & Thomas, D. (2015). Sarcolipin and phospholamban inhibit the calcium pump by populating a similar metal ion-free intermediate state. *Biochem Biophys Res Commun.* (463), 37-41.
- Fajardo, G., Zhao, M., Urashima, T., Kobilka, B., & Bernstein, D. (2007). β -adrenergic receptor subtypes mediate a temporal switch between cardiotoxic and cardioprotective signaling in doxorubicin cardiomyopathy. *Pediatr Res*, abstract.
- Fan, G., Shumay, E., Wang, H., & Malbon, C. (2001). The scaffold protein gravin (cAMP dependent protein kinase anchoring protein 250) binds the beta 2 adrenergic receptor via the receptor cytoplasmic Arg-329 to Leu-413 domain and provides a mobile scaffold during desensitisation. *J Biol Chem*(276), 24005-24014.
- Felce, J., Knox, R., & Davis, S. (2014). Type-3 BRET, an improved competition-based bioluminescence resonance energy transfer assay. *Biophys J*(12), L41-L43.
- Feldman, A., Cates, A., Veazey, W., Hershberger, R., Bristow, M., Baughman, K., . . . Van Dop, C. (1988). Increase of the 40,000-mol wt pertussis toxin substrate (G protein) in the failing human heart. *J Clin Invest*, 189-197.
- Felgner, P., Gadek, T., Holm, M., Roman, R., Chan, H., Wenz, M., . . . Danielsen, M. (1987). Lipofection: a highly efficient, lipid-mediated DNA-transfection procedure. *PNAS*(84), 7413-7417.
- Ferguson, S., Downey, W., Colapietro, A., Barak, L., Menard, L., & Caron, M. (1996). Role of beta arrestin in mediating agonist promoted G protein coupled receptor internalisation. *Science*(271), 363-366.
- Ferrandon, S., Feinstein, T., Castro, M., Wang, B., Bouley, R., Potts, J., . . . Vilardaga, J. (2009). Sustained cyclic AMP production by parathyroid hormone receptor endocytosis. *Nature Chemical Biology*, 734-742.
- Fischmeister, R., Castro, L., Abi-Gerges, A., Rochais, F., Jurevicius, J., Leroy, J., & Vandecasteele, G. (2006). Compartmentation of cyclic nucleotide signaling in the heart: the role of cyclic nucleotide phosphodiesterases. *Circ Res*(99), 816-828.

- Francis, G., McDonald, K., Chu, C., & Cohn, J. (1995). Pathophysiologic aspects of endstage heart failure. *Am J Cardiol*(75), 11A-16A.
- Frank, R. (2002). The SPOT-synthesis technique. Synthetic peptide arrays on membrane supports--principles and applications. *J Immunol Methods*(267), 13-26.
- Fraser, C., & Venter, J. (1980). Regulation of beta adrenergic receptors density in the control of adrenergic responsiveness. *Prog Clin Biol Res*(42), 127-144.
- Freedman, N., & Lefkowitz, R. (1996). Desensitization of G protein-coupled receptors. *Recent Prog Horm Res*(51), 319-351.
- Fuhs, S., & Insel, P. (2011). Caveolin-3 undergoes SUMOylation by the SUMO E3 ligase PIASy: sumoylation affects G-protein-coupled receptor desensitization. *J Biol Chem*(286), 14830-14841.
- Furst, J., Sutton, R., Chen, J., Brunger, A., & Grigorieff, N. (2003). Electron cryomicroscopy structure of N-ethyl maleimide sensitive factor at 11 Å resolution. *The EMBO Journal*(17), 4365-4374.
- Futter, C., Pearse, A., Hewlett, L., & Hopkins. (1996). Multivesicular endosomes containing internalized EGF-EGF receptor complexes mature and then fuse directly with lysosomes. *The Journal of Cell Biology* (132), 1011-1023.
- Gagnon, A., Kalla, L., & Benovic, J. (1998). Role of clathrin mediated endocytosis in agonist induced down regulation of the beta 2 adrenergic receptor. *J Biol Chem*(273), 6976-6981.
- Gareau, J., & Lima, C. (2010). The SUMO pathway: emerging mechanisms that shape specificity, conjugation and recognition. *Nat Rev Mol Cell Biol*(11), 861-871.
- Gareau, J., Reverter, D., & Lima, C. (2012). Determinants of small ubiquitin-like modifier 1 (SUMO1) protein specificity, E3 ligase, and SUMO-RanGAP1 binding activities of nucleoporin RanBP2. *Journal of Biological Chemistry*(287), 4740-4751.
- GEHealthcare. (2014). <http://www.gelifesciences.com>. Retrieved February 3, 2017, from [/webapp/wcs/stores/swww.gelifesciences.comervlet/CategoryDisplay?categoryId=3301626&catalogId=126109&productId=&top=Y&storeId=12751&langId=-1](http://webapp/wcs/stores/swww.gelifesciences.comervlet/CategoryDisplay?categoryId=3301626&catalogId=126109&productId=&top=Y&storeId=12751&langId=-1)
- Gocke, C., Yu, H., & Kang, J. (2005). Systematic identification and analysis of mammalian small ubiquitin-like modifier substrates. *Journal of Biological Chemistry*(280), 5004-5012.
- Gomez, A., Valdivia, H., Cheng, H., Lederer, M., Santana, L., Cannell, M., . . . Lederer, W. (1997). Defective excitation contraction coupling in experimental cardiac hypertrophy and heart failure . *Science*(276), 800-806.

- Gong, L., Millas, S., Maul, G., & Yeh, E. (2000). Differential regulation of sentrinized proteins by a novel sentrin specific proteases. *J Biol Chem*(275), 3355-3359.
- Goodman, O. J., Krupnick, J., Santini, F., Gurevich, V., Penn, R., Gagnon, A., . . . Benovic, J. (1996). Beta arrestin acts as a clathrin adaptor in endocytosis of the beta 2 adrenergic receptor. *Nature*(383), 447-450.
- Gowran, A., Murphy, C., & Campbell, V. (2009). Δ^9 - Tetrahydrocannabinol regulates the p53 post - translational modifiers Murine double minute 2 and the Small Ubiquitin MOdifier protein in the rat brain. *FEBS letters*(583), 3412-3418.
- Graham, F., Smiley, J., Russel, W., & Nairu, R. (1977). Characteristics of a human cell line transformed by DNA from human adenovirus type 5. *J Gen Virol*(36), 59-72.
- Green, S., Cole, G., Jacinto, M., Innis, M., & Liggett, S. (1993). A polymorphism of the human beta 2 adrenergic receptor within the fourth transmembrane domain alters ligand binding and functional properties of the receptor. *J Biol Chem*(268), 23116-23121.
- Green, S., Turki, J., Bejarano, P., Hall, I., & Liggett, S. (1995). Influence of beta 2 adrenergic receptor genotypes on signal transduction in human airway smooth muscle cells. *Am Respir Cell Mol Biol*(13), 25-33.
- Green, S., Turki, J., Innis, M., & Liggett, S. (1994). Amino terminal polymorphisms of the human beta 2 adrenergic receptor impact distinct agonist promoted regulatory properties . *Biochemistry*(33), 9414-9419.
- Greenberg, B., Butler, J., Felker, G., Ponikowski, P., Voors, A., Desai, A., . . . Zsebo, K. (2016). Calcium upregulation by percutaneous administration of gene therapy in patients with cardiac disease (CUPID 2): a randomised, multinational, double-blind, placebo-controlled, phase 2b trial. *LANCET*(387), 1178-1186.
- Greenberg, B., Yaroshinsky, A., Zsebo, K., Butler, J., Felker, G., Voors, A., . . . Hajjar, R. (2014). Design of a phase 2b trial of intracoronary administration of AAV1/SERCA2a in patients with advanced heart failure: the CUPID 2 trial (calcium up-regulation by percutaneous administration of gene therapy in cardiac disease phase 2b). *JACC Heart Failure*(1), 84-92.
- Gunasekaran, K., Tsai, C., Kumar, S., Zanuy, D., & Nussinov, R. (2003). Extended disordered proteins: targeting function with less scaffold. *Trends Biochem Sci*(2), 81-85.
- Guo, X., Wang, X., Wang, Z., Banerjee, S., Yang, J., Huang, L., & Dixon, J. (2016). Site-specific Proteasome Phosphorylation Controls Cell Proliferation and Tumorigenesis. *Nat Cell Biol*, 202-212.
- Gupta, M., McLendon, P., Gulick, J., James, J., Khalili, K., & Robbins, J. (2016). UBC9-Mediated Sumoylation Favorably Impacts Cardiac Function in Compromised Hearts. *Circ Res*(118), 1894-1905.

- Gurevich, V., & Gurevich, E. (2003). The new face of active receptor bound arrestin attracts new partners. *Structure*(11), 1037-1042.
- Haberland, M., Montgomery, R., & Olson, E. (2009). The many roles of histone deacetylases in development and physiology: implications for disease and therapy. *Nature Reviews Genetics* (10), 32-42.
- Hadcock, J., Wang, H., & Malbon, C. (1989). Agonist induced destabilisation of beta adrenergic receptor mRNA. Attenuation of glucocorticoid induced up regulation of beta adrenergic receptors. *J Biol Chem*(264), 19928-19933.
- Hajjar, R., Kang, J., Gwathmey, J., & Rosenzweig, A. (1997). Physiological Effects of Adenoviral Gene Transfer of Sarcoplasmic Reticulum Calcium ATPase in Isolated Rat Myocytes. *Circulation*(95), 423-429.
- Hamm, H. (1998). The many faces of G protein signaling. *J Biol Chem*(273), 669-672.
- Hannoun, Z., Greenhough, S., Jaffray, E., Hay, R., & Hay, D. (2010). Post-translational modification by SUMO. *Toxicology* (278), 288-293.
- Hartz, P. (2005). *TOPOISOMERASE I-BINDING ARGININE/SERINE-RICH PROTEIN; TOPORS* . Retrieved April 20, 2017, from <http://www.omim.org/entry/609507>
- Hasenfuss, G., Schilinger, W., Lehnart, S., Preuss, M., Pieske, B., Maier, L., . . . Just, H. (1999). Relationship between Na⁺-Ca²⁺-exchanger protein levels and diastolic function of failing human myocardium. *Circulation*(99), 641-648.
- Hattori, M., & Ozawa, T. (2015). Bioluminescent tools for the analysis of G-protein-coupled receptor and arrestin interactions. *Royal Society of Chemistry Advances*(5), 12655-12663.
- Hattori, T., Taft, J., Swist, K., Luo, H., Witt, H., Slattery, M., . . . Koide, S. (2013). Recombinant antibodies to histone post-translational modifications. *Nature Methods*(10), 992-995.
- Hausdorff, W., Bouvier, M., O'Dowd, B., Irons, G., Caron, M., & Lefkowitz, R. (1989). Phosphorylation sites on two domains of the beta 2-adrenergic receptor are involved in distinct pathways of receptor desensitization. *J Biol Chem*(264), 12657-12665.
- Hawkins, G., Tantisira, K., Meyers, D., Ampleford, E., Moore, W., Klanerman, B., . . . Bleeker, E. (2006). Sequence, haplotype and association analysis of ADRB2 in a multiethnic asthma case control study. *Am J Respir Crit Care Med*(174), 1101-1109.
- Hay, R. (2005). SUMO: a history of modification . *Molecular Cell*(18), 1-12.
- Hay, R. (2013). Decoding the SUMO signal. *Biochemical Society Transactions*(41), 463-473.

- Hayashi, T., Seki, M., Maeda, D., Wang, W., Kawabe, Y., Seki, T., . . . Enomoto, T. (2002). Ubc9 is essential for viability of higher eukaryotic cells. *Exp Cell Res*(280), 212-221.
- Hebert, T., Moffett, S., Morello, J., Loisel, T., Bichet, D., Barret, C., & Bouvier, M. (1996). a peptide derived from a beta 2 adrenergic receptor transmembrane domain inhibits both receptor dimerisation and activation. *J Biol Chem*(271), 16384-16392.
- Hedaya, M., Mahmoudi, M., Rose, N., & Rezaei, N. (2010). Proinflammatory cytokines in heart failure: double-edged swords. *Heart Fail Rev*(15), 543-562.
- Hein, P., Michel, M., Leineweber, K., Wieland, T., Wettschureck, N., & Offermanns, S. (2005). *Practical Methods in Cardiovascular Research: Receptor and binding studies* (Dhein, S; Mohr, F; Delmar, M ed.). Berlin: Springer.
- Hein, P., Rochais, F., Hoffmann, C., Dorsch, S., Nikolaev, V., Enfelhardt, S., . . . Bunemann, M. (2006). GS Activation Is Time-limiting in Initiating Receptor-mediated Signaling. *The Journal of Biological Chemistry*(281), 33345-33351.
- Heineke, J., & Molkentin, J. (2006). Regulation of cardiac hypertrophy by intracellular signaling pathways. *Nat. Rev. Mol. Cell. Biol.* (7), 589-600.
- Henley, J., Craig, T., & Wilkinson, K. (2014). Neuronal SUMOylation mechanisms, physiology and roles in neuronal dysfunction. *Physiological reviews*(94), 1249-1285.
- Hertel, C., & Staehelin, M. (1983). Reappearance of beta-adrenergic receptors after isoproterenol treatment in intact C6-cells. *The Journal of Cell Biology* (216), 1538-1543.
- Heusch, G., Skychally, A., & Schulz, R. (2011). The in-situ pig heart with regional ischemia/reperfusion - ready for translation. *J Mol Cell Cardiol*(50), 951-963.
- Heyman, S., Schroen, B., Vermeersch, P., Milting, H., Gao, F., Kassner, A., . . . Janssens, S. (2005). Increased cardiac expression of tissue inhibitor of metalloproteinase-1 and tissue inhibitor of metalloproteinase-2 is related to cardiac fibrosis and dysfunction in the chronic pressure-overloaded human heart. *Circulation*(112), 1136-1144.
- Hickey, C., Wilson, N., & Hochstrasser, M. (2012). Function and regulation of SUMO proteases. *Nature Reviews Molecular Cell Biology*(13), 755-766.
- Hietakangas, V., Ahlskog, J., Jakobsson, A., Hellesuo, M., Sahlberg, N., Holmberg, C., . . . Sistonen, L. (2003). Phosphorylation of serine 303 is a prerequisite for the stress-inducible SUMO modification of heat shock factor 1. *Mol Cell Biol*(23), 2953-2968.

- Hill, S., Ganellin, C., Timmerman, H., Schwartz, J., Shankley, N., Young, J., . . . Haas, H. (1997). International Union of Pharmacology. XIII. Classification of histamine receptors. *Pharmacological Reviews*(49), 253-278.
- Hjelm, H., Hjelm, K., & Sjoquist, J. (1972). Protein A from *Staphylococcus aureus*. Its isolation by affinity chromatography and its use as an immunosorbent for isolation of immunoglobulins. *FEBS Lett*(28), 73-76.
- Hochstrasser, M. (2001). SP-RING for SUMO. New Functions Bloom for a Ubiquitin-like Protein. *Cell*(107), 5-8.
- Hochstrasser, M. (2001). SP-RING for SUMO: new functions bloom for a ubiquitin-like protein. *Cell*(107), 5-8.
- Hoegge, C., Pfander, B., Moldovan, G., Pyrowolakis, G., & Jentsch, S. (2002). RAD6-dependent DNA repair is linked to modification of PCNA by ubiquitin and SUMO. *Nature*(419), 135-141.
- Houser, S., Marguiles, K., Murphy, A., Spinale, F., Francis, G., Prabhu, S., . . . Koch, W. (2012). Animal Models of Heart Failure. *Circulation Research*(111), 131-150.
- Huang, T., Wuerzberger-Davis, S., Wu, Z., & Miyamoto, S. (2003). Sequential modification of NEMO/IKK γ by SUMO-1 and ubiquitin mediates NF- κ B activation by genotoxic stress. *Cell*(115), 565-576.
- Hunt, S., Abraham, W., Chin, M., Feldman, A., Francis, G., Ganiats, T., . . . al, e. (2005). ACC/AHA 2005 Guideline Update for the Diagnosis and Management of Chronic Heart Failure in the Adult. *Circulation*(112), e154-e235.
- i-base.info. (2017, August 17). *appendix-3-list-of-amino-acids-and-their-abbreviations*. Retrieved from <http://i-base.info: http://i-base.info/appendix-3-list-of-amino-acids-and-their-abbreviations/>
- Ibrahaim, M., Masri, A., Navaratnarajah, M., Siedlecka, U., Soppa, G., Moshkov, A., . . . Terraciano, C. (2010). Prolonged mechanical unloading affects cardiomyocyte excitation-contraction coupling, transverse-tubule structure, and the cell surface. *FASEB*(9), 3321-3329.
- Ikonnikov, G., & Yelle, D. (2016). *Physiology of cardiac conduction and contractility*. Retrieved June 20, 2017, from <http://www.pathophys.org/physiology-of-cardiac-conduction-and-contractility/>
- Impens, F., Radoshevich, L., Cossart, P., & Ribet, D. (2014). Mapping of SUMO sites and analysis of SUMOylation changes induced by external stimuli. *PNAS*(111), 12432-12437.
- Impens, F., Radoshevich, L., Cossart, P., & Ribet, D. (2014). Mapping of SUMO sites and analysis of SUMOylation changes induced by external stimuli. *PNAS*(111), 12432-12437.
- Irannejad, R., & Von Zastrow, M. (2014). GPCR signaling along the endocytic pathway. *Current Opinion in Cell Biology*, 109-116.

- Irannejad, R., Tomshine, J., Tomshine, J., Chevalier, M., Mahoney, J., Steyaert, J., . . . von Zastrow, M. (2013). Conformational biosensors reveal GPCR signalling from endosomes. *Nature*, 534-538.
- Izumo, S., Lompre, A., Matsuoka, R., Koren, G., Schwartz, K., Nadal-Ginard, B., & Mahdavi, V. (1987). Myosin heavy chain mRNA and protein isoform transitions during cardiac hypertrophy. Interaction between haemodynamic and thyroid hormone-induced signals. *J Clin Invest*(79), 970-977.
- Januzzi, J., Filippatos, G., Nieminen, M., & Gheorghiade, M. (2012). Troponin Elevation in Patients With Heart Failure. *European Heart Journal*(33), 2265-2271.
- Jaski, B., Jessup, M., Mancini, D., Cappola, T., Pauly, D., Greenberg, B., . . . Hajjar, R. (2009). Calcium Upregulation by Percutaneous Administration of Gene Therapy in Cardiac Disease (CUPID Trial), a First-in-Human Phase 1/2 Clinical Trial. *Journal of Cardiac Failure*(15), 170-181.
- Jensen, C., Swigart, P., De Marco, T., Hoopes, C., & Simpson, P. (2009). α 1-Adrenergic receptor subtypes in nonfailing and failing human myocardium. *Circ Heart Fail*, 654-663.
- Johnson, E., & Blobel, G. (1997). Ubc9p is the conjugating enzyme for the ubiquitin like protein Smt3p. *Journal of biological chemistry*(272), 26799-26802.
- Johnson, M. (1998). The Beta Adrenoceptor. *Am J Respir Crit Care Med*(158), S146-S153.
- Jones, D., Crowe, E., Stevens, T., & Candido, E. (2002). Functional and phylogenetic analysis of the ubiquitylation system in caenorhabditis elegans: ubiquitin conjugating enzymes, ubiquitin activating enzymes, and ubiquitin like proteins. *Genome Biol*(3), 1-0002.
- Joseph, J., Tan, S., Karpova, T., McNally, J., & Dasso, M. (2002). SUMO-1 targets RanGAP1 to kinetochores and mitotic spindles. *J Cell Biol*(156), 595-602.
- Kadambi, V., & Kranias, E. (1997). Phospholamban: a protein coming of age. *Biochem Biophys Res Commun*(239), 1-5.
- Kallal, L., Gagnon, A., Penn, R., & Benovic, J. (1998). Visualization of agonist-induced sequestration and down-regulation of a green fluorescent protein-tagged β 2-adrenergic receptor. *J. Biol. Chem.*(273), 322-328.
- Katragadda, M., Maciejewski, M., & Yeagle, P. (2004). Structural studies of the putative helix 8 in the human β 2 adrenergic receptor: an NMR study. *Biochim Biophys Acta*(1663), 74-81.
- Katritch, V., Reynolds, K., Cherezov, V., Hanson, M., Roth, C., Yeager, M., & Abagyan, R. (2009). Analysis of Full and Partial Agonists Binding to β 2-Adrenergic Receptor Suggests a Role of Transmembrane Helix V in Agonist-Specific Conformational Changes. *J Mol Recognit*, 307-318.

- Kaumann, A., Bartel, S., Molenaar, P., Sanders, L., Burrell, K., Vetter, D., . . . Krause, E. (1999). Activation of beta 2 adrenergic receptors hastes relaxation and mediates phosphorylation of phospholamban, troponin I, and C-protein in ventricular myocardium from patients with terminal heart failure . *Circulation*(99), 65-72.
- Kaur, K., Park, H., Pandey, N., Azuma, Y., & Guzman, R. (2017). Identification of a New SUMO-Interacting Motif in PIASy. *JBC*, 1-18.
- Kawaguchi, M., Takahashi, M., Hata, T., Kashima, Y., Usui, F., Morimoto, H., . . . Ikeda, U. (2011). Inflammasome activation of cardiac fibroblasts is essential for myocardial ischemia/reperfusion injury. *Circulation*(123), 594-604.
- Kawano, K., Yano, Y., Omae, K., Matsuzaki, S., & Matsuzaki, K. (2013). Stoichiometric analysis of oligomerization of membrane proteins on living cells using coiled-coil labeling and spectral imaging. *Anal Chem*(85), 3454-3461.
- Kawase, Y., & Hajjar, R. (2008). The cardiac sarcoplasmic/endoplasmic reticulum calcium ATPase: a potent target for cardiovascular diseases. *Nature Clinical Practice Cardiovascular Medicine*(5), 554-565.
- Keith, M., Geranmayegan, A., Sole, M., Kurian, R., Robinson, A., Omran, A., & Jeejeebhoy, K. (1998). Increased Oxidative Stress in Patients With Congestive Heart Failure. *Journal of American Cardiology*, 1352-1356.
- Kerscher, O. (2007). SUMO junction-what's your function? New insights through SUMO-interacting motifs. *EMBO Rep*(8), 550-555.
- Kessler, J., Kahle, K., Sun, T., Meerbrey, K., Schlabach, M., Schmitt, E., . . . al, e. (2012). A SUMOylation-dependent transcriptional subprogram is required for Myc-driven tumorigenesis. *Science*(335), 348-353.
- Kho, C., Lee, A. J., Oh, J., Gorski, P., Fish, K., Sanchez, R., . . . Hajjar, R. (2015). Small-molecule activation of SERCA2a SUMOylation for the treatment of heart failure. *Nature Communications*(6), 1-11.
- Kho, C., Lee, A., Jeong, D., Oh, J., Chaanine, A., Kizana, E., . . . Hajjar, R. (2011). SUMO-1 dependent modulation of SERCA2a in heart failure. *Nature*(477), 601-605.
- Kho, C., Lee, A., Jeong, D., Oh, J., Chaanine, A., Kizana, E., . . . Hajjar, R. (2011). SUMO1-dependent modulation of SERCA2a in heart failure. *Nature*(477), 601-605.
- Kim, M., Chia, I., & Constantini, F. (2008). SUMOylation target sites at the C terminus protect Axin from ubiquitination and confer protein stability. *FASEB J*(11), 3785-3794.
- Kobilka, B., Dixon, R., Friella, H., Dohlman, M., Bolanowski, I., & Sigal, I. (1987). cDNA for the human B2 adrenergic receptor: a protein with multiple spanning domains and encoded by a gene whose chromosomal

- location is shared with that of a receptor for platelet growth factor. *Proc Natl Acad Sci U S A*(84), 46-50.
- Kociol, R., Pang, P., Gheorghide, M., Fonarow, G., O'Connor, C., & Felker, G. (2010). Troponin elevation in heart failure prevalence, mechanisms, and clinical implications. *J Am Coll Cardiol* (56), 1071-1078.
- Kohout, T. L., Perry, S., Conner, D., & Lefkowitz, R. (2001). Beta arrestin 1 and 2 differentially regulate heptahelical receptor signalling and traficking. *Proc Natl Acad Sci*(98), 1601-1606.
- Komander, D. (2009). The emerging complexity of protein ubiquitination. *Biochem Soc Trans*, 937-953.
- Konerman, M., & Hummel, S. (2014). Sodium Restriction in Heart Failure: Benefit or Harm? *Curr Treat Options Cardiovasc Med*(16), 286-288.
- Konturek, S., Konteruk, J., Pawlik, T., & Brzozowski, T. (2004). Brain gut axis and its role in the control of food intake. *Journal of Physiology and Pharmacology*, 137-154.
- Koss, K., & Kranias, E. (1996). Phospholamban: a prominent regulator of myocardial contractility. *Circ Res*(79), 1059-1063.
- Kotaja, N., Karvonen, U., Janne, O., & Palvimo, J. (2002). PIAS proteins modulate transcription factors by functioning as SUMO-1 ligases. *Mol Cell Biol*(22), 5222-5234.
- Koudstaal, S., Jansen of Lorkeers, S., Gho, J., van Hout, G., Jansen, M., Grunderman, P., . . . Chamuleau, S. (2014). Myocardial Infarction and Functional Outcome Assessment in Pigs. *J Vis Exp*(86), 51269-51279.
- Kovesdi, I., & Hedley, S. (2010). Adenoviral Producer Cells. *Viruses*(8), 1681-1703.
- Kranias, E. (1985). Regulation of calcium transport by protein phosphatase activity associated with cardiac sarcoplasmic reticulum. *J Biol Chem*(260), 11006-11010.
- Kranias, E., & Solaro, R. (1982). Phosphorylation of troponin I and phospholamban during catecholamine stimulation of rabbit heart. *Nature*(298), 182-184.
- Krasel, C., Bunemann, M., Lorenz, K., & Lohse, M. (2005). Beta arrestin binding to the beta 2 adrenergic receptor requires both receptor phosphorylation and receptor activation. *J Biol Chem*(280), 9528-9535.
- Krayenbuehl, H., Hess, O., Monrad, E., Schneider, J., Mall, G., & Turina, M. (1989). Left ventricular myocardial structure in aortic valve disease before, intermediate, and late after aortic valve replacement. *Circulation*(79), 744-755.
- Krueger, K., Daaka, Y., Pitcher, J., & Lefkowitz, R. (1997). The role of sequestration in G protein coupled receptor resensitisation. Regulation of

- beta 2 adrenergic receptor dephosphorylation by vesicular acidification. *J Biol Chem*(272), 5-8.
- Lan, T., Liu, Q., Li, C., Wu, G., Steyaert, J., & Lambert, N. (2015). BRET evidence that β 2 adrenergic receptors do not oligomerize in cells. *Scientific Reports* (5), 1-12.
- Laporte, S., Oakley, R., Holt, J., Barak, L., & Caron, M. (2000). The interaction of beta arrestin with the AP-2 adaptor is required for the clustering of beta 2 adrenergic receptor into clathrin coated pits. *J Biol Chem*(275), 23120-23126.
- Lavoie, C., Mercier, J., Salahpour, A., Umapathy, D., Breit, A., Villeneuve, L., . . . Hebert, T. (2002). Beta 1/Beta 2 adrenergic receptor heterodimerisation regulates beta 2 adrenergic receptor internalisation and ERK signaling efficacy. *J Biol Chem*(277), 35402-35410.
- Le Peuch, C., Guilleux, J., & Demaille, J. (1980). Phospholamban phosphorylation in the perfused rat heart is not solely dependent on beta-adrenergic stimulation. *FEBS Letter*(114), 165-168.
- Lee, A., Dongtak, J., Shinichi, M., Gyun, O., Lifan, L., Yoshiyuki, I., . . . Kho, C. (2014). The Role of SUMO-1 in Cardiac Oxidative Stress and Hypertrophy . *Antioxidants & Redox Signaling*(21), 1986-2001.
- Lee, J., & Thorgeirsson, S. (2004). Genome-scale profiling of gene expression in hepatocellular carcinoma: classification, survival prediction, and identification of therapeutic targets. *Gastroenterology*(127), S51-S55.
- Lefkowitz, R., & Shenoy, S. (2005). Transduction of receptor signals by beta-arrestins. *Science*(308), 512-517.
- Lefkowitz, R., Rajagopal, K., & Whalen, E. (2006). New Roles for β -Arrestins in Cell Signaling: Not Just for Seven-Transmembrane Receptors. *Molecular Cell*(5), 643-652.
- Leight, E., D, G., & Kornfeld, K. (2005). Sumoylation of LIN-1 promotes transcriptional repression and inhibition of vulval cell fates. *Development*(132), 1047-1056.
- Li, H., Niu, H., Peng, Y., Wang, J., & He, P. (2013). Ubc9 promotes invasion and metastasis of lung cancer cells. *Oncology Reports*(29), 1588-1594.
- Li, Q., & Muma, N. (2013). Estradiol potentiates 8-OH-DPAT-induced sumoylation of 5-HT 1A receptor: Characterization and subcellular distribution of sumoylated 5-HT 1A receptors. *Psychoneuroendocrinology*(38), 2542-2553.
- Li, X., Vadrevu, S., Dunlop, A., Day, J., Advant, N., Troeger, J., . . . Baillie, G. (2010). Selective SUMO modification of cAMP-specific phosphodiesterase-4D5 (PDE4D5) regulates the functional consequences of phosphorylation by PKA and ERK. *Biochem J*(428), 55-65.
- Li, X., Zhou, M., Huang, W., & Yang, H. (2017). N-glycosylation of the β 2AR regulates receptor function by modulating dimerisation. *FEBS*(10), 1-15.

- Liggett, S. (2002). Update on current concepts of the molecular basis of B2-adrenergic receptor signalling. *J Allergy Clin Immunol*(110), S223-S228.
- Lin, D., Tatham, M., Yu, B., Kim, S., Hay, R., & Chen, Y. (2002). Identification of a substrate recognition site on UBC9. *J Biol Chem*(277), 21740-21748.
- Litalien, C., & Beaulieu, P. (2011). Molecular Mechanisms of Drug Actions: From Receptors to Effectors. In B. Fuhrman, J. Zimmerman, J. Carcillo, R. Clark, M. Relvas, A. Rotta, . . . J. Tobias, *Pediatric Critical Care* (pp. 1553-1568). Philadelphia: Elsevier.
- Liu, Y., Lagowski, J., Gao, S., Raymond, J., White, C., & Kulesz-Martin, M. (2010). Regulation of psoriatic chemokine CCL20 by E3 ligases Trim32 and Piasy in keratinocytes. *J Invest Dermatol*(130), 1384-1390.
- Lokuta, A., Rogers, T., Lederer, W., & Valdivia, H. (1995). Modulation of cardiac ryanodine receptors of swine and rabbit by a phosphorylation-dephosphorylation mechanism. *J Physiol (Lond)*(487), 609-622.
- Lompre, A. S., d'Albis, A., Lacombe, G., Thiem, N., & Swynghedauw, B. (1979). Myosin isoenzyme redistribution in chronic heart overload. *Nature*(282), 105-107.
- Lorenz, W., McCann, R., Longiaru, M., & Cormier, M. (1991). Isolation and expression of a cDNA encoding Renilla reniformis luciferase. *Proc Natl Acad Sci USA*, 88, 4438-4442.
- Lorton, D., Lubahn, C., Molinaro, C., & Bellinger, D. (2017). Beta2-Adrenergic Receptor Regulates Inflammation in Autoimmune Arthritis: Inhibit or Promote? - Depends on Timing, Immune Organ and Posttranslational Receptor Modifications. *FASEB Journal*, 31, 1.
- Louch, W., Sheehan, K., & Wolska, B. (2011). Methods in Cardiomyocyte Isolation, Culture, and Gene Transfer. *J Mol Cell Cardiol*(51), 288-298.
- Louis, N., Evelgh, C., & Graham, F. (1997). Cloning and sequencing of the cellular-viral junctions from the human adenovirus type 5 transformed 293 cell line. *Virology*(233), 423-429.
- Lu, Z., Xu, X., Hu, X., Fassett, J., Zhu, G., Tao, Y., . . . Chen, Y. (2010). PGC-1 α regulates expression of myocardial mitochondrial antioxidants and myocardial oxidative stress after chronic systolic overload. *Antioxid Redox Signal*(13), 1011-1022.
- Lu, Z., Xu, X., Hu, X., Lee, S., Traverse, J., Zhu, G., . . . Chen, Y. (2010). Oxidative stress regulates left ventricular PDE5 expression in the failing heart. *Circulation*(121), 1474-1483.
- Luttrell, L., & Gesty-Palmer, D. (2010). Beyond desensitization: Physiological relevance of arrestin-dependent signaling. *Pharmacol Rev*(62), 305-330.
- Luttrell, L., Ferguson, S., Daaka, Y., Miller, W., Maudsley, S., Rocca, D., . . . Lefkowitz, R. (1999). Beta-arrestin-dependent formation of beta2 adrenergic receptor-Src protein kinase complexes. *Science*(29), 655-661.

- Lyon, A., MacLeod, K., Zhang, Y., Garcia, E., Kanda, G., Lab, M., . . . Gorelik, J. (2009). Loss of T-tubules and other changes to surface topography in ventricular myocytes from failing human and rat heart. *PNAS*(106), 6854-6859.
- MacLannan, D., & Kranias, E. (2003). Phospholamban: a crucial regulator of cardiac contractility. *Nature* (4), 565-577.
- Macon, B., Yu, W., & Reed-Guy, L. (2015). *Healthline*. Retrieved December 1, 2016, from <http://www.healthline.com/health/acute-myocardial-infarction#Overview1>
- Madamanchi, A. (2007). β -Adrenergic receptor signaling in cardiac function and heart failure. *McGill Journal of Medicine*(10), 99-104.
- Mahan, L., & Insel, P. (1986). Expression of beta adrenergic receptors in synchronous and asynchronous S49 lymphoma cell. Receptor metabolism after irreversible blockade of receptors in cells transversing the cell division cycle. *Mol Pharm*(29), 7-15.
- Mahmood, T., & Yang, P. (2012). Western Blot: Technique, Theory, and Trouble Shooting. *N Am J Med Sci*(9), 429-434.
- Mak, J., Hisada, T., Salmon, M., Barnes, P., & Chung, K. (2002). Glucocorticoids reverse IL-1 beta induced impairment of beta adrenoceptor mediated relaxation and up regulation of G protein coupled receptor kinases . *Br J Pharmacol*(135), 987-996.
- Malave, H., Taylor, A., Nattama, J., Deswal, A., & Mann, D. (2003). Circulating levels of tumour necrosis factor correlate with indexes of depressed heart rate variability: a study in patients with mild to moderate heart failure. *Chest*(123), 716-724.
- Manurung, D., & Trisnohadi, H. (2007). Beta Blockers for Congestive Heart Failure. *Acta Med Indones-Indones J Intern Med*, 44-48.
- Marantz, P., Tobin, J., Wassertheil-Smoller, S., Steingart, R., Wexler, J., Budner, N., . . . Wachspress, J. (1988). The relationship between left ventricular systolic function and congestive heart failure diagnosed by clinical criteria. *Circulation*(77), 607-612.
- Marks, A. (2000). Cardiac intracellular calcium release channels: role in heart failure. *Circ Res*(87), 8-11.
- Martin, T., Robinson, E., Harvey, A., MacDonald, M., Grieve, D., Paul, A., & Currie, S. (2012). Surgical optimization and characterization of a minimally invasive aortic banding procedure to induce cardiac hypertrophy in mice. *Experimental Physiology*(97), 822-832.
- Marvin, H. (1964). Diseases of the heart and blood vessels: Nomenclature and criteria for diagnosis. *Arch Intern Med*(113), 906-907.
- Matic, I., Schimmel, J., Hendriks, I. v., van de Rijke, F., van Dam, H., Gnad, F., . . . Vertegaal, A. (2010). Site-specific identification of SUMO-2 targets

in cells reveals an inverted SUMOylation motif and a hydrophobic cluster SUMOylation motif. *Mol Cell*(39), 641-652.

- Matic, I., van Hagen, M., Schimmel, J., Macek, B., Ogg, S., Tatham, M., . . . Vetegaal, A. (2008). In vivo identification of human small ubiquitin like modifier polymerisation sites by high accuracy mass spectrometry and an in vitro in vivo strategy. *Mol. Cell. Proteomics* (7), 132-144.
- Matsuzaki, K., Minami, T., Tojo, M., Honda, Y., Uchimara, Y., Saitoh, H., . . . Nakao, M. (2003). Serum response factor is modulated by the SUMO-1 conjugation system. *Biochem Biophys Res Commun*(306), 32-38.
- McDonald, P., Chow, C., Miller, W., LaPorte, S., Field, M., Lin, F. D., & Lefkowitz, R. (2000). B-arrestin 2: A receptor-regulated MAPK scaffold for the activation of JNK3. *Science*(290), 1574-1577.
- McGraw, D., Forbes, S., Kramer, L., & Liggett, S. (1998). Polymorphisms of the 5' leader cistron of the human beta 2 adrenergic receptor regulate receptor expression. *J Clin Invest*(102), 1927-1932.
- McGraw, D., Mihbachler, K., Schwarb, M., Rahman, F., Small, K., & Liggett, S. (2006). Airway smooth muscle prostaglandin-Ep1 receptors directly modulate beta 2 adrenergic receptors within a unique heterodimeric complex. *J Clin Invest*(116), 1400-1409.
- McLean, A., & Milligan, G. (2000). Ligand regulation of green fluorescent protein-tagged forms of the human beta(1)- and beta(2)-adrenoceptors; comparisons with the unmodified receptors. *Br J Pharmacol*(130), 1825-1832.
- McLean, A., Bevan, N., Rees, S., & Milligan, G. (1999). Visualizing Differences in Ligand Regulation of Wild-Type and Constitutively Active Mutant B2-Adrenoceptor-Green Fluorescent Protein Fusion Proteins. *Molecular Pharmacology* (56), 1182-1191.
- Meek, D., & Knippschild, U. (2003). Post-translational modification of MDM2. *Mol Cancer Research*(1), 1017-1026.
- Mercadier, J., Lompre, A., Wisnewsky, C., Samuel, J., Bercovici, J., Swynghedauw, B., & Schwartz, K. (1981). Myosin isoenzymic changes in several models of rat cardiac hypertrophy. *Circ Res*(49), 525-532.
- Mercier, J., Salahpour, A., Angers, S., Breit, A., & Bouvier, M. (2002). quantitative assessment of B1 and B2 adrenergic receptor homo and heterodimerisation by bioluminescence resonance energy transfer. *J Biol Chem*(277), 44925-44931.
- Mercier, J., Salahpour, A., Angers, S., Breit, A., & Bouvier, M. (2002). Quantitative assessment of beta 1- and beta 2-adrenergic receptor homo and heterodimerization by bioluminescence resonance energy transfer. *J Biol Chem*(47), 44925-44931.

- Metzger, J., & Westfall, M. (2004). Covalent and noncovalent modification of thin filament action: the essential role of troponin in cardiac muscle regulation. *Circ Res*(94), 146-158.
- Meulmeester, E., Kunze, M., Hsiao, H., Urlaub, H., & Melchior, F. (2008). Mechanism and consequences for paralog-specific sumoylation of ubiquitin-specific protease 25. *Mol Cell*(30), 610-619.
- Mialet-Perez, J., Green, S., Miller, W., & Liggett, S. (2004). A primate dominant third glycosylation site of the beta 2 adrenergic receptor routes receptors to degradation during agonist regulation. *J Biol Chem*(279), 38603-38607.
- Miller-Davis, C., Marden, S., & Leidy, N. (2006). The New York Heart Association. Classes and functional status: What are we really measuring? *Heart and Lung: The Journal of Acute and Critical Care*(35), 217-224.
- Millman, E., Rosenfield, J., Vaughan, D., Nguyen, J., Dai, W., Alpizar-Foster, E., . . . Knoll, B. M. (2004). Endosome sorting of β_2 -adrenoceptors is GRK5 independent. *Brit Journal Pharmacol*(141), 277-284.
- Miyamoto, M., del Monte, F., Schmidt, U., DiSalvo, T., Kang, Z., Matsui, T., . . . Hajjar, R. (2000). Adenoviral gene transfer of SERCA2a improves left-ventricular function in aortic-banded rats in transition to heart failure. *Proc Natl Acad Sci USA*(97), 793-798.
- Moffett, S., Rousseau, G., Lagace, M., & Bouvier, M. (2001). The palmitoylation state of the β_2 AR regulates the synergistic action of cyclic AMP dependent protein kinase and BARK involved in its phosphorylation and desensitisation. *Journal of neurochemistry*(76), 269-279.
- Mohideen, F., Capili, A., Bilimoria, P., Yamada, T., Bonni, A., & Lima, C. (2009). A molecular basis for phosphorylation-dependent SUMO conjugation by the E2 UBC9. *Nat Struc Mol Biol*(16), 945-952.
- Molinoff, P. (1984). Alpha- and beta-adrenergic receptor subtypes properties, distribution and regulation. *Drugs*, 1-15.
- Monrad, E., Hess, O., Murakami, T., Nonogi, H., Corin, W., & Krayenbuehl, H. (1988). Time course of regression of left ventricular hypertrophy after aortic valve replacement. *Circulation*(77), 1345-1355.
- Mooney, S., Grande, J., Salisbury, J., & Janknecht, R. (2010). Sumoylation of p68 and p72 RNA helicases affects protein stability and transactivation potential. *Biochemistry*(49), 1-10.
- Moore, R., Tuffana, A., Millman, E., Dai, W., Hall, H., Dickey, B., & Knoll, B. (1999). Agonist induced sorting of human beta 2 adrenergic receptors to lysosomes during down regulation. *J Cell Sci*(112), 329-338.
- Morrison, K., Moore, R., Carsrud, N., Trial, J., Millman, E., Tuvim, M., . . . Knoll, B. (1996). Repetitive endocytosis and recycling of the beta 2-adrenergic receptor during agonist-induced steady state redistribution. *Molecular Pharmacology*(50), 692-699.

- Mukhopadhyay, D., Ayaydin, F., Koli, N., Tan, S., Anan, T., Kametaka, A., . . . Dasso, M. (2006). SUSP1 antagonizes formation of highly SUMO2/3-conjugated species. *J Cell Biol*(174), 939-949.
- Murakami, P., Pungor, E., Files, J., Do, L., van Rijnsoever, R., Vogels, R., . . . McCaman, M. (2002). A single short stretch of homology between adenoviral vector and packaging cell line can give rise to cytopathic effect-inducing, helper-dependent E1-positive particles. *Hum Gene Ther*(13), 909-920.
- Naujokat, C., & Hoffman, S. (2002). Role and Function of the 26S Proteasome in Proliferation and Apoptosis. *Nature Lab Invest*(82), 965-980.
- NHS. (2016). *Treatments for heart failure*. Retrieved April 14, 2017, from <http://www.nhs.uk/Conditions/Heart-failure/Pages/Treatment.aspx>
- Ni, Y., Zhao, X., Bao, G., Zou, L., Teng, L., Wang, Z., . . . Pei, G. (2006). Activation of β_2 -adrenergic receptor stimulates γ -secretase activity and accelerates amyloid plaque formation. *Nature Medicine*, 1390-1396.
- NIH. (2011). *Your Heart's Electrical System*. Retrieved April 19, 2017, from <https://www.nhlbi.nih.gov/health/health-topics/topics/hhw/electrical>
- Nikolaev, V., Bunemann, M., Schmitteckert, E., Lohse, M., & Egelhardt, S. (2006). Cyclic AMP imaging in adult cardiac myocytes reveals far-reaching beta1-adrenergic but locally confined beta2-adrenergic receptor-mediated signaling. *Circ Res*(10), 1084-1091.
- Nikolaev, V., Moshkov, A., Lyon, A., Miragoli, M., Novak, P., Paur, H., . . . Gorelik, J. (2010). Beta2-adrenergic receptor redistribution in heart failure changes cAMP compartmentation. *Science*(327), 1653-1657.
- Nishida, T., & Yasuda, H. (2002). PIAS1 and PIAS α function as SUMO-E3 ligases toward androgen receptor and repress androgen receptor-dependent transcription. *Journal of Biological Chemistry*(277), 41311-41317.
- Nistico, R., Ferraina, C., Marconi, V., Blandini, F., Negri, L., Egebjerg, J., & Feligioni, M. (2014). Age-related changes of protein SUMOylation balance in the ABPP Tg2576 mouse model of Alzheimer's disease. *Frontiers Pharmacology*(5), 1-9.
- Nobles, K., Xiao, K., Ahn, S., Shukla, A., Lam, C., Rajagopal, S., . . . Lefkowitz, R. (2011). Distinct phosphorylation sites on the β_2 -adrenergic receptor establish a barcode that encodes differential functions of β -arrestin. *Sci Signal*(4), 1-22.
- Oakley, R., Laporte, S., Holt, J., Caron, M., & Barak, L. (2000). Differential Affinities of Visual Arrestin, β Arrestin1, and β Arrestin2 for G Protein-coupled Receptors Delineate Two Major Classes of Receptors. *The Journal of Biological Chemistry*(275), 17201-17210.
- O'Dowd, B., Hnatowich, M., Caron, M., Lefkowitz, R., & Bouvier, M. (1989). Palmitoylation of the human β_2 -adrenergic receptor. Mutation of Cys341

in the carboxyl tail leads to an uncoupled non palmitoylated form of the receptor. *J Biol Chem*(264), 7564-7569.

- O'Dowd, B., Hnatowich, M., Regan, J., Leader, W., Caron, M., & Lefkowitz, R. (1988). Site directed mutagenesis of the cytoplasmic domains of the human beta 2 adrenergic receptor. Localisation of regions involved in G protein receptor coupling. *J Biol Chem*(263), 15986-15992.
- Olesen, C., Sorensen, T., Nielsen, R., Moller, J., & Nissen, P. (2004). Dephosphorylation of the calcium pump coupled to counterion occlusion. *Science*(306), 2251-2255.
- Ostrom, R., Post, S., & Insel, P. (2000). Stoichiometry and compartmentalisation in G protein coupled receptor signaling: implications for therapeutic interventions involving Gs. *Perspectives in Pharmacol*(294), 407-412.
- Ovchinnikov, Y., Abdulaev, N., & Bogachuk, A. (1988). Two adjacent cysteine residues in the C terminal cytoplasmic fragment of bovine rhodopsin are palmitoylated . *FEBS Letters*(230), 1-5.
- Pai, R., & Hetherington, M. (2015, February 20). *Beta-Blockers for Heart Failure*. Retrieved April 14, 2017, from <http://www.webmd.com/heart-disease/heart-failure/beta-blockers-for-heart-failure>
- Palczewski, K., Kumasaka, T., Hori, T., Behnke, C., Motoshima, H., Fox, B., . . . Miyano, M. (2000). Crystal structure of rhodopsin: a G protein coupled receptor. *Science*(289), 739-945.
- Pandey, D., Chen, F., Patel, A., Patel, V., Rudic, D., Wang, C., . . . Fulton, D. (2011). SUMOylation of NADPH Oxidases Negatively Regulates Reactive Oxygen Species Production. *The FASEB Journal*(25), 1093-1094.
- Park-Sarge, O., & Sarge, K. (2005). Detection of Sumoylated Proteins. *Methods Mol Biol*, 329-338.
- Parmar, V., Grinde, E., Mazurkiewicz, J., & Herrick-Davis, K. (2016). Beta2-adrenergic receptor homodimers: Role of transmembrane domain 1 and helix 8 in dimerization and cell surface expression. *Biochimica et Biophysica Acta (BBA) - Biomembranes*(12), 1-11.
- Pathak, A., del Monte, F., Zhao, W., Schultz, J., Lorenz, J., Bodi, I., . . . Kranias, E. (2005). Enhancement of Cardiac Function and Suppression of Heart Failure Progression By Inhibition of Protein Phosphatase 1. *Circulation*(96), 756-766.
- Pelaia, G., & Marsico, S. (1994). Regulation of beta 2-adrenergic receptors and the implications for bronchial asthma: an update. *Monaldi Arch Chest Dis*(49), 125-130.
- Perry, J., Tainer, J., & Boddy, M. (2008). A SIM-ultaneous role for SUMO and ubiquitin. *Trends Biochem Sci*(33), 201-208.
- Perry, S., Baillie, G., Kohout, T., McPhee, I., Magiera, M., Ang, K., . . . Lefkowitz, R. (2002). Targeting of cyclic AMP degradation to beta 2-adrenergic receptors by beta-arrestins. *Science*(298), 834-836.

- Perry, S., Baillie, G., Kohout, T., McPhee, I., Magiera, M., Ang, K., . . . Leflowitz, R. (2002). Targetting of cyclic AMP degradation to beta 2 adrenergic receptors by beta-arrestins. *Science*(298), 834-836.
- Peske, B. (2004). Reverse remodeling in heart failure - fact or fiction? *Eur Heart J Suppl*(5), 66-78.
- Pichler, A., & Melchior, F. (2002). Ubiquitin-related modifier SUMO1 and nucleocytoplasmic transport. *Traffic*(3), 381-387.
- Pipping, S., Andexinger, S., & Lohse, M. (1995). Sequestration and recycling of beta 2-adrenergic receptors permit receptor resensitization. *Molecular Pharmacology*(47), 666-676.
- Qing, F., Rahman, S., Rhodes, C., Hayes, M., & Ind, P. H. (1997). B-adrenergic receptors in vivo and lung function in drug-free asthmatic subjects. *Am J Respir Crit Care Med*(155), A885.
- Rabe, K., Tenor, H., Dent, G., Schudt, C., Liebig, S., & Magnussen, H. (1993). Phosphodiesterase isoenzymes modulating inherent tone in human airways: identification and characterisation. *Am J Physiol Lung Cell Mol Physiol*(264), L458-L464.
- Rands, E., Candelore, M., Cheung, A., Hill, W., Strader, C., & Dixon, R. (1990). Mutational analysis of beta adrenergic receptor glycosylation. *Journal of Biological Chemistry*(265), 10759-10764.
- Rasmussen, S., Choi, H., Fung, J., Pardon, E., Casarosa, P., Chae, P., . . . Kobilka, B. (2011). Structure of a nanobody-stabilized active state of the B(2) adrenoceptor. *Nature*(469), 175-180.
- Rasmussen, S., Choi, H., Rosenbaum, D., Kobilka, T., Thian, F., Edwards, P., . . . Kobilka, B. (2007). Crystal structure of the human beta2 adrenergic G-protein-coupled receptor. *Nature*(450), 383-387.
- Rasmussen, S., DeVree, B., Zou, Y., Kruse, A., Chung, K., Kobilka, T., . . . Kobilka, B. (2011). Crystal structure of the b2 adrenergic receptor-Gs protein complex. *Nature*(477), 1-9.
- Rasmussen, S., Devree, B., Zou, Y., Kruse, A., Chung, K., Kobilka, T., . . . Sunahara, R. e. (2011). Crystal structure of the B2 adrenergic receptor-Gs protein complex. *Nature*(477), 549-555.
- Raul, A., Baker, A., & Nicklin, S. (2012). Vector Systems for Prenatal Gene Therapy: Principles of Adenovirus Design and Production. In C. C. Waddington (Ed.), *Methods in Molecular Biology* (pp. 1-32). New York: Springer Science+Business Media.
- Reihause, E., Innis, M., MacIntyre, N., & Liggett, S. (1993). Mutations in the gene encoding for the beta 2 adrenergic receptor in normal and asthamtic subjects. *Am J Respir Cell Mol Biol*(8), 334-339.
- Renwick, J., Kerr, C., McTaggart, R., & Yeung, J. (1993). Cardiac electrophysiology and conduction pathway ablation. *Can J Anaesth*(40), 1053-1064.

- Reverter, D., & Lima, C. (2005). Insights into E3 ligase activity revealed by a SUMO-RanGAP1-Ubc9-Nup358 complex. *Nature*(435), 687-692.
- Ribet, D., Hamon, M., Gouin, E., Nahori, M., Impens, F., Neyret-Kahn, H., . . . Cossart, P. (2010). *Listeria monocytogenes* impairs SUMOylation for efficient infection . *Nature*(464), 1192-1195.
- Riobi, N., & Manning, D. (2005). Receptors coupled to heterotrimeric G proteins of the G12 family. *Trends Pharm Sci*(26), 146-154.
- Rissanen, T., & Yla-Herttuala, S. (2007). Current status of cardiovascular gene therapy. *Mol Ther*(15), 1233-1247.
- Rockland-Inc. (2017, February 20). *Post-Translational Modification (PTM) Antibodies*. Retrieved from [www.rockland-inc.com](http://www.rockland-inc.com/post-translational-modification-antibodies.aspx):
<http://www.rockland-inc.com/post-translational-modification-antibodies.aspx>
- Rodriguez, M., Dargemont, C., & Hay, R. (2001). SUMO-1 conjugation in vivo requires both a consensus modification motif and nuclear targetting. *J Biol Chem*(276), 12654-12659.
- Roger, V. (2013). Epidemiology of heart failure. *Circulation Research*, 646-659(113).
- Rogers, R., Horvath, C., & Matunis, M. (2003). SUMO modification of STAT1 and its role in PIAS-mediated inhibition of gene activation. *Journal of Biological Chemistry*(278), 30091-30097.
- Rosas, P., Liu, Y., Abdalla, M., Thomas, C., Kidwell, D., Dusio, G., . . . Tong, C. (2015). Phosphorylation of Cardiac Myosin-Binding Protein-C Is a Critical Mediator of Diastolic Function. *Circulation Heart Failure*(8), 582-594.
- Rosenbaum, D., Cherezov, V., Hanson, M., Rasmussen, S., Thian, F., Kobilka, T., . . . Kobilka, B. (2007). GPCR engineering yields high-resolution structural insights into beta2-adrenergic receptor function. *Science*(5854), 1266-1273.
- Sachdev, S., Bruhn, L., Sieber, H., Pichler, A., Melchior, F., & Grosschedl, R. (2001). PIASy, a nuclear matrix-associated SUMO E3 ligase, represses LEF1 activity by sequestration into nuclear bodies. *Genes and Development*(15), 3088-3103.
- Sachdev, S., Bruhn, L., Sieber, H., Pichler, A., Melchoir, F., & Grosschedl, R. (2001). PIASy, a nuclear matrix-associated SUMO E3 ligase, represses LEF1 activity by sequestration into nuclear bodies. *Genes Dev*(15), 3088-3103.
- Sadeghi, H., & Birnbaumer, M. (1999). O-Glycosylation of the V2 vasopressin receptor. *Glycobiology*(9), 731-737.
- Saitoh, H., & Hinchey, J. (2000). Functional heterogeneity of small ubiquitin related protein modifiers SUMO-1 versus SUMO-2/3. *J. Biol. Chem*(275), 6252-6258.

- Saitoh, H., & Hinchev, J. (2000). Functional heterogeneity of small ubiquitin related protein modifiers SUMO-1 versus SUMO-2/3. *J Biol Chem*(275), 6252-6258.
- Salahpour, A., Angers, S., Mercier, J., Lagace, M., Marullo, S., & Bouvier, M. (2004). Homodimerisation of the beta 2 adrenergic receptor as a prerequisite for cell surface targetting . *J Biol Chem*(279), 33390-33397.
- Sampson, D., Wang, M., & Matunis, M. (2001). The small ubiquitin like modifier (SUMO-1) consensus sequence mediates UBC9 binding and is essential for SUMO-1 modification. *J Biol Chem*(276), 21664-21669.
- Sarangi, P., & Zhao, X. (2015). SUMO-mediated regulation of DNA damage repair and responses. *Trends Biochem Sci*(40), 233-242.
- Savio-Gamilberti, E., Frank, J., Inoue, M., Goldhaber, J., Cannell, M. B., Bridge, J., & Sachse, F. (2008). Novel features of the rabbittransverse tubular system revealed by quantitative analysis of three-dimensional reconstructions from confocal images. *Biophys J*(95), 2053-2062.
- Scherer, W., Syverton, J., Gey, G., & Syverton, G. (1953). Studies on the propagation in vitro of poliomyelitis viruses IV. Viral multiplication in a stable strain of human malignant epithelial cells (strain HeLa) derived from an epidermoid carcinoma of the cervix. *J Exp Med*(97), 695-710.
- Schmidt, U., Hajjar, R., Helm, P., Kim, C., Doye, A., & Gwathmey, J. (1998). Contribution of Abnormal Sarcoplasmic Reticulum ATPase Activity to Systolic and Diastolic Dysfunction in Human Heart Failure . *Journal of Molecular and Cellular Cardiology*(30), 1929-1937.
- Schrier, R. (1990). Body fluid volume regulation in health and disease: A unifying hypothesis. *Ann Intern Med*(113), 155-159.
- Schroder, F., Handrock, R., Beuckelmann, D., Hirt, S., Hullin, R., Priebe, L., . . . Herzig, S. (1998). Increased Availability and Open Probability of Single L-Type Calcium Channels From Failing Compared With Nonfailing Human Ventricle. *Circulation*(98), 969-976.
- Schwinger, R., Bohm, M., Schmidt, U., Karczewski, P., Bavendiek, U., Flesch, M., . . . Erdmann, E. (1995). Unchanged protein levels of SERCA II and phospholamban but reduced Ca²⁺ uptake and Ca(2+)-ATPase activity of cardiac sarcoplasmic reticulum from dilated cardiomyopathy patients compared with patients with nonfailing hearts. *Circulation*(92), 3220-3228.
- Seeler, J., & Dejean, A. (2003). Nuclear and unclear functions of SUMO. *Nature Reviews Molecular Cell Biology*(4), 690-699.
- Seeler, J., & Dejean, A. (2003). Nuclear and unclear functions of SUMO. *Nature Reviews Molecular Cell Biology*(4), 690-699.
- Seidah, N., & Prat, A. (2012). The biology and therapeutic targeting of the proprotein convertases. *Nature Reviews Drug Discovery* (11), 367-383.

- Selektor, Y., & Weber, K. (2008). The salt-avid state of congestive heart failure revisited. *Am J Med Sci*(335), 209-218.
- Shannon, T., & Bers, D. (2004). Integrated Ca²⁺ management in cardiac myocytes. *Ann N Y Acad Sci*(1015), 28-38.
- Shen, L., Dong, C., Liu, H., Naismith, J., & Hay, R. (2006). The structure of SENP1-SUMO-2 complex suggests a structural basis for discrimination between SUMO paralogues during processing. *Biochem J*(397), 279-288.
- Shen, L., Geoffroy, M., Jaffray, E., & Hay, R. (2009). Characterisation of SENP7, a SUMO-2/4 specific isopeptidase. *Biochem J*(421), 223-230.
- Shenoy, S., Drake, M., Nelson, C., Houtz, D., Xiao, K., Madabushi, S., . . . Lefkowitz, R. (2006). β -Arrestin-dependent, G Protein-independent ERK1/2 Activation by the β 2 Adrenergic Receptor. *The Journal of Biological Chemistry*, 1261-1273.
- Shenoy, S., McDonald, P., Kohout, T., & Lefkowitz, R. (2001). Regulation of receptor fate by ubiquitination of activated beta 2 adrenergic receptor and beta arrestin. *Science*(294), 1307-1313.
- Shenoy, S., Xiao, K., Venkataramanan, V., Snyder, P., Freedman, N., & Weissman, A. (2008). Nedd4 Mediates Agonist-dependent Ubiquitination, Lysosomal Targeting, and Degradation of the β 2-Adrenergic Receptor. *The Journal of Biological Chemistry*(283), 22166-22176.
- Shuai, K., & Liu, B. (2005). Regulation of gene-activation pathways by PIAS proteins in the immune system. *Nature Reviews Immunology*(5), 593-605.
- SigmaAldrich. (2017). www.sigmaaldrich.com. Retrieved April 10, 2017, from <http://www.sigmaaldrich.com/life-science/custom-oligos/custom-peptides/learning-center/solid-phase-synthesis.html>
- Silva, G., Finley, D., & Vogel, C. (2015). K63 polyubiquitination is a new modulator of the oxidative stress response. *Nat Struct Mol Biol*, 116-123.
- Simmerman, H., Collins, J., Theibert, J., Wegener, A., & Jones, L. (1986). Sequence analysis of phospholamban. Identification of phosphorylation sites and two major structural domains. *J Biol Chem*(261), 13333-13334.
- Simonis, G., Strasser, R., & Ebner, B. (2012). Reperfusion injury in acute myocardial infarction. *Critical Care*(16), A22-A27.
- Singh, M., & Anderson, M. (2011). Is CaMKII a link between inflammation and hypertrophy in heart? *J Mol Med*(89), 537-543.
- Sivaramakrishnan, S., & Spudich, J. (2011). Systematic control of protein interaction using a modular ER/K α -helix linker. *Proc. Natl. Acad. Sci. U.S.A.*(108), 20467-20472.
- Skychally, A., van Caster, P., Iliodromitis, E., Schulz, R., Kremastinos, D., & Heusch, G. (2009). Ischemic postconditioning: experimental models and protocol algorithms. *Basic Res Cardiol*(104), 469-483.

- Smith, C. (2013, January 3). *Stable vs. Transient Transfection of Eukaryotic Cells*. Retrieved April 10, 2017, from www.biocompare.com: <http://www.biocompare.com/Editorial-Articles/126324-Transfection/>
- Song, J., Zhang, Z., Hu, W., & Chen, Y. (2005). Small ubiquitin-like modifier (SUMO) recognition of a SUMO binding motif: a reversal of the bound orientation. *J Biol Chem*(280), 40122-40129.
- Stewart, S., MacIntyre, K., MacLeod, M., Bailey, A., Capewell, S., & McMurray, J. (2001). Trends in hospitalization for heart failure in Scotland, 1990-1996 An epidemic that has reached its peak? *European Journal of Heart Failure*(22), 209-217.
- Strader, C., Candelore, M., Hill, W., Sigal, I., & Dixon, R. (1989). Identification of two serine residues involved in agonist activation of the β -adrenergic receptor. *J Biol Chem*(264), 13572-13578.
- Strader, C., Sigal, I., Candelore, M., Rands, E., Hill, W., & Dixon, R. (1988). Conserved aspartic acid residues 79 and 113 of the β -adrenergic receptor have different roles in receptor function. *J Biol Chem*(263), 10267-10271.
- Strosberg, A. (1993). Structure, function, and regulation. *Protein Science*, 1198-1209.
- Strulovici, B., Cerione, R., Kilpatrick, B., Caron, M., & Lefkowitz, R. (1984). Direct demonstration of impaired functionality of a purified desensitized beta-adrenergic receptor in a reconstituted system. *Science*(225), 837-840.
- Stubhan, M., Markert, M., Mayer, K., Trautmann, T., Klumpp, A., Henke, J., & Guth, B. (2008). Evaluation of cardiovascular and ECG parameters in the normal, freely moving Göttingen Minipig. *Journal of Pharmacological and Toxicological Methods*(57), 202-211.
- Subramaniam, S., Sixt, K., Barrow, R., & Snyder, S. (2009). Rhes, a striatal specific protein, mediates mutant-huntingtin cytotoxicity. *Science*(324), 1327-1330.
- Takimoto, E., Champion, H., Li, M., Belardi, D., Ren, S., Rodriguez, E., . . . Kass, D. (2005). Chronic inhibition of cyclic GMP phosphodiesterase 5A prevents and reverses cardiac hypertrophy. *Nat Med*(11), 214-222.
- Tang, W., & Gilman, A. (1992). Adenylyl Cyclases. *Cell*(70), 869-872.
- Tang, Z., El Far, O., Betz, H., & Scheschonka, A. (2005). Pias1 interaction and sumoylation of metabotropic glutamate receptor 8. *J Biol Chem*(280), 38153-38159.
- Tank, A., & Wong, D. (2015). Peripheral and central effects of circulating catecholamines. *Comprehensive Physiology*, 1-15.
- Tankou, S., Ishii, K., Elliott, C., Yalla, K., Day, J., Furukori, K., . . . Sawa, A. (2016). SUMOylation of DISC1: A Potential Role in Neural Progenitor Proliferation in the Developing Cortex. *Molecular Neuropsychiatry*(2), 20-27.

- Tatham, M., Jaffray, E., Vaughan, O., Desterro, J., Botting, C., Naismith, J., & Hay, R. (2001). Polymeric chains of SUMO-2 and SUMO-3 are conjugated to protein substrates by SAE1/SAE2 and UBC9. *J. Biol. Chem*(276), 35368-35374.
- Tesmer, J., Sunahara, R., Gilman, A., & Sprang, S. (1997). Crystal structure of the catalytic domains of adenylyl cyclase in a complex with G α :GTP γ S. *Science*(278), 1907-1916.
- Tesmer, J., Sunahara, R., Gilman, A., & Sprang, S. (1997). Crystal structure of the catalytic domains of adenylyl cyclases in a complex with G α :GTP γ S. *Science*(278), 1907-1916.
- Thakar, K., Niedenthal, R., Okaz, E., Franken, S., Jakobs, A., Gupta, S., . . . Dietz, F. (2008). SUMOylation of the hepatoma-derived growth factor negatively influences its binding to chromatin. *FEBS*(7), 1411-1426.
- ThermoFisherScientific. (2017, April 10). *HA Tag Antibodies*. Retrieved April 10, 2017, from [www.thermofisher.com: https://www.thermofisher.com/uk/en/home/life-science/antibodies/primary-antibodies/epitope-tag-antibodies/ha-tag-antibodies.html#](https://www.thermofisher.com/uk/en/home/life-science/antibodies/primary-antibodies/epitope-tag-antibodies/ha-tag-antibodies.html#)
- Thorp, A., & Schlaich, M. (2015). Relevance of sympathetic nervous system activation in obesity and metabolic syndrome. *Journal of Diabetic Research*, 1155-1163.
- Thygesen, K., Alpert, J., & White, H. (2007). Universal Definition of Myocardial Infarction. *Journal of the American College of Cardiology* (22), 2173-2195.
- Tilemann, L., Lee, A., Ishikawa, K., Agüero, J., Rapti, K., Santos-Gallego, C., . . . Hajjar, R. (2013). SUMO-1 Gene Transfer Improves Cardiac Function in a Large-Animal Model of Heart Failure. *Sci Transl Med*(211), 211ra159.
- Tomko, R., Xu, R., & Philipson, L. (1997). HCAR and MCAR: the human and mouse cellular receptors for subgroup C adenoviruses and group B coxsackieviruses. *PNAS*(94), 3352-3356.
- Tong, C., Stelzer, J., Greaser, M., Powers, P., & Moss, R. (2008). Acceleration of crossbridge kinetics by protein kinase A phosphorylation of cardiac myosin binding protein C modulates cardiac function. *Circ Res*(103), 974-982.
- Toyoshima, C., & Mizutani, T. (2004). Crystal structure of the calcium pump with a bound ATP analogue. *Nature*(430), 529-535.
- Toyoshima, C., Nakasako, M., Nomura, H., & Ogawa, H. (2000). Crystal structure of the calcium pump of sarcoplasmic reticulum at 2.6 Å resolution. *Nature*(405), 647-655.
- Tran, T., Friedman, J., Qunaidi, E., Baameur, F., Moore, R., & Clark, R. (2004). Characterization of agonist stimulation of cAMP-dependent protein kinase and G protein-coupled receptor kinase phosphorylation of the B2-

- adrenergic receptor using phosphoserine-specific antibodies. *Mol Pharmacol*(65), 196-206.
- Trester-Zedlitz, M., Burlingame, A., Kobilka, B., & von Zastrow, M. (2005). Mass spectrometric analysis of agonist effects on posttranslational modifications of the β_2 -adrenoceptor in mammalian cells. *Biochemistry*(44), 6133-6143.
- Tsukamoto, Y., Mano, T., Sakata, Y., Ohtani, T., Takeda, Y., Tamaki, S., . . . Komuru, I. (2013). A novel heart failure mice model of hypertensive heart disease by angiotensin II infusion, nephrectomy, and salt loading. *Am J Physiol Heart Circ Physiol*(305), 1658-1667.
- Tuteja, N. (2009). Signaling through G protein coupled receptors. *Plant Signal Behav*(10), 942-947.
- Uberti, M., Hague, C., Oller, H., Minneman, K., & Hall, R. (2005). Heterodimerisation with beta 2 adrenergic receptors promotes surface expression and functional activity of alpha 1D adrenergic receptors. *J Pharm Exp Ther*(313), 16-23.
- Uhlen, M., & Ponten, F. (2005). Antibody-based Proteomics for Human Tissue Profiling. *Molecular and Cellular Proteomics*(4), 384-393.
- Ulrich, H. (2008). The fast growing business of SUMO chains. *Molecular Cell*(32), 301-305.
- Varadaraj, A., Mattoscio, D., & Chiocca, S. (2014). SUMO Ubc9 enzyme as a viral target. *IUBMB Life*(66), 27-33.
- Vaughan, D., Millman, E., Godines, V., Friedman, J., Tran, T., Dai, W., . . . Moore, R. (2006). Role of the G protein coupled receptor kinase site serine cluster in beta 2 adrenergic receptor internalisation, desensitisation and beta arrestin translocation. *J Biol Chem*(281), 7684-7692.
- Vertegaal, A., Andersen, J., Ogg, S., Hay, R., Mann, M., & Lamond, A. (2006). Distinct and overlapping sets of SUMO-1 and SUMO-2 target proteins revealed by quantitative proteomics. *Mol. Cell Proteomics* (5), 2298-2310.
- Violin, J., DiPilato, L., Yildirim, N., Elston, T., Zhang, J., & Lefkowitz, R. (2008). β_2 -Adrenergic Receptor Signaling and Desensitization Elucidated by Quantitative Modeling of Real Time cAMP Dynamics. *The Journal of Biological Chemistry*(283), 2949-2961.
- Violin, J., Ren, X., & Lefkowitz, R. (2006). G protein coupled receptor kinase specificity for beta arrestin recruitment to the beta 2 adrenergic receptor revealed by fluorescence resonance energy transfer. *J Biol Chem*(281), 20577-20588.
- Wang, H., Tao, J., Shumay, E., & Malbon, C. (2006). G protein coupled receptor associated A kinase anchoring proteins: AKAP79 and AKAP250 (gravin). *Eur J Cell Biol*(85), 643-650.

- Wang, J., & Schwartz, R. (2010). Sumoylation and regulation of cardiac gene expression. *Circ Research*(107), 19-29.
- Wang, P., Gao, H., Ni, Y., Wang, B., Wu, Y., Ji, L., . . . Pei, G. (2003). β -Arrestin 2 Functions as a G-Protein-coupled Receptor-activated Regulator of Oncoprotein Mdm2. *The Journal of Biological Chemistry*(278), 6363-6370.
- Wang, Y., & Dasso, M. (2009). SUMOylation and deSUMOylation at a glance. *J. Cell. Sci*(122), 4249-4252.
- Ward, R., Alvarez-Curto, E., & Milligan, G. (2011). Using the Flp-In™ T-Rex™ System to Regulate. In *Receptor Signal Transduction Protocols: Third Edition* (pp. 21-37). Springer.
- Ward, W., & Cormier, M. (1979). An energy transfer protein in coelenterate bioluminescence. Characterization of the Renilla green-fluorescent protein. *The Journal of biological chemistry*(254), 781-788.
- Warne, T., Serrano-Vega, M., Baker, J., Moukhametzianov, R., Edwards, P., Henderson, R., . . . Schertler, G. (2008). Structure of a β 1-adrenergic G protein-coupled receptor. *Nature*(454), 486-491.
- Watari, K., Nakaya, M., & Kurose, H. (2014). Multiple functions of G protein-coupled receptor kinases. *J Mol Signal*(9), 1-10.
- Wenger, N., & Greenbaum, L. (1984). From adrenoceptor mechanisms to clinical therapeutics: Raymond Ahlquist, Ph.D., 1914-1983. *Journal of the American College of Cardiology*, 419-421.
- Wettersten, N., & Maisel, A. (2015). Role of Cardiac Troponin Levels in Acute Heart Failure. *CFR*(2), 102-106.
- Wieland, K., Zuurmond, H., Krasel, C., Izjerman, A., & Lohse, M. (1996). Involvement of Asn-293 in stereospecific agonist recognition and in activation of the β 2-adrenergic receptor. *Proc Natl Acad Sci USA*(93), 9276-9281.
- Wilkinson, K., & Henley, J. (2011). Analysis of metabotropic glutamate receptor 7 as a potential substrate for SUMOylation. *Neuroscience letters*(491), 181-186.
- Wold, W., Tollefson, A., & Hermiston, T. (1993). E3 transcription unit of adenovirus. In P. Bohm, & W. Doerfler (Eds.), *The Molecular Repertoire of Adenoviruses* (pp. 237-278). Berlin: Springer-Verlag.
- Wright, P., & Dyson, J. (2015). Intrinsically Disordered Proteins in Cellular Signaling and Regulation. *Nat Rev Mol Cell Biol*(16), 18-29.
- www.hopkinsmedicine.org. (2017). <http://www.hopkinsmedicine.org>. Retrieved March 31, 2017, from <http://www.hopkinsmedicine.org/healthlibrary/GetImage.aspx?ImageId=322243>

- Xiao, N., Li, H., Mei, W., & Cheng, J. (2015). SUMOylation Attenuates Human β -Arrestin 2 Inhibition of IL-1R/TRAF6 Signaling. *The Journal of Biological Chemistry*(290), 1927-1935.
- Xiao, R. (2001). Beta-adrenergic signaling in the heart: dual coupling of the beta2-adrenergic receptor to G(s) and G(i) proteins. *Sci STKE*(104), 1-15.
- Xu, D., Guo, H., Xu, X., Lu, Z., Fassett, J., Hu, X., . . . Chen, Y. (2011). Exacerbated pulmonary arterial hypertension and right ventricular hypertrophy in animals with loss of function of extracellular superoxide dismutase. *Hypertension*(58), 303-309.
- Yang, S., Galanis, A., Witty, J., & Sharrocks, A. (2006). An extended consensus motif enhances the specificity of substrate modification by SUMO. *EMBO J*(25), 5083-5093.
- Yang, S., Jaffray, E., Hay, R., & Sharrocks, A. (2003). Dynamic interplay of the SUMO and ERK pathways in regulating Elk-1 transcriptional activity. *Mol Cell*(12), 63-74.
- Yang, X., & Chiang, C. (2013). Sumoylation in gene regulation, human disease, and therapeutic action. *F1000Prime Rep*(5), 5-45.
- Yao, X., Parnot, C., Deupi, X., Ratnala, V., Swaminath, G., Farrens, D., & Kobilka, B. (2006). Coupling ligand structure to specific conformational switches in the β 2-adrenoceptor. *Nature Chemical Biology*(2), 417-422.
- Yu, A., & Malek, T. (2000). The Proteasome Regulates Receptor-mediated Endocytosis of Interleukin-2. *The Journal of Biological Chemistry*, 381-385.
- Yuan, N., Friedman, J., Whaley, B., & Clark, R. (1994). cAMPdependent protein kinase and protein kinase C consensus site mutations of the β -adrenergic receptor. Effect on desensitization and stimulation of adenylyl cyclase. *J Biol Chem*(269), 23032-23038.
- Yunus, A., & Lima, C. (2009). Structure of the Siz/PIAS SUMO E3 ligase Siz1 and determinants required for SUMO modification of PCNA. *Molecular Cell*(35), 669-682.
- Zaccolo, M., De Giorgi, F., Cho, C., Feng, L., Knapp, T., Negulescu, P., . . . Pozzan, T. (2000). A genetically encoded, fluorescent indicator for cyclic AMP in living cells. *Nature Cell Biology*(2), 25-29.
- Zakhary, D., Moravec, C., & Bond, M. (2000). Regulation of PKA binding to AKAPs in the heart: alterations in human heart failure. *Circulation*(12), 1459-1464.
- Zhang, J., Barak, L., Winkler, K., Caron, M., & Ferguson, S. (1997). A Central Role for β -Arrestins and Clathrin-coated Vesicle-mediated Endocytosis in β 2-Adrenergic Receptor Resensitization. *The Journal of Biological Chemistry*(272), 27005-27014.

- Zhang, J., Liu, Y., Jiang, K., & Jia, J. (2017). SUMO regulates the activity of Smoothed and Costal-2 in Drosophila Hedgehog signaling. *Scientific Reports* (7), 4279-4285.
- Zhang, X., Goeres, J., Zhang, H., Yen, T., Porter, A., & Matunis, M. (2008). SUMO-2/3 modification and binding regulate the association of CENP-E with kinetochores and progression through mitosis. *Mol. Cell.* (29), 729-741.
- Zheng, M., Zhu, W., Han, Q., & Xiao, R. (2005). Emerging concepts and therapeutic implications of beta-adrenergic receptor subtype signaling. *Pharmacol Therapy*, 257-268.
- Zhou, W., Ryan, J., & Zhou, H. (2004). Global analyses of SUMOylated proteins in *saccharomyces cerevisiae*. Induction of protein SUMOylation by cellular stresses. *J Biol Chem*(279), 32262-32268.
- Zhu, W., Wang, S., Chakir, K., Yang, D., Zhang, T., Brown, J., . . . Xiao, R. (2003). Linkage of beta1-adrenergic stimulation to apoptotic heart cell death through protein kinase A-independent activation of Ca²⁺/calmodulin kinase II. *J Clin Invest*, 617-625.
- Zhu, W., Zheng, M., Koch, W., Lefkowitz, R., Kobilka, B., & Xiao, R. (2001). Dual modulation of cell survival and cell death by beta(2)-adrenergic signaling in adult mouse cardiac myocytes. *Proc Natl Acad Sci USA*, 1607-1612.